CATION-EXCHANGED ZEOLITES AS NOVEL STORAGE MATERIALS OF NITRIC OXIDE: THERAPEUTIC POTENTIAL IN BIOMEDICAL APPLICATIONS.

SARAH FOX

Presented for Ph.D

February 2008

Declaration.

I hereby declare that the data published in this thesis are the result of my own work, carried out under the supervision of Professors Adriano Rossi and Ian Megson at the University of Edinburgh, and that this thesis has been completed entirely by myself and has not previously been submitted for any other degree or qualification.

Sarah Fox

Acknowledgements.

There are numerous thanks due for academic, moral and financial support given to me throughout the making of this thesis.

I am very grateful for the academic support of my supervisors Professors Adriano Rossi and Ian Megson. To Adriano, thank you for believing in me enough to keep me around for another few years. Ian, thanks for not forgetting about me when you moved to Teuchter land. I couldn't have asked for two better supervisors.

I also have many colleagues to thank for both technical assistance and friendship over the years. Pete, Jillian, Nikki R, Nick, Tom and Tara for help with laborious bug spreading experiments. To the CVS lot; Fiona, Neil, Amie, Katie, Danielle, Nikki L, Phil, Graeme, Mark, Caroline, Robert, Catriona, Helen, Nick, Sara, Gillian, Yuri, Rudolph, Danny and Ross, without whom the lab would be a boring place. A special mention to Katie who always took time to show me the ropes and looked out for me when things were tough. To the CIR lot; Jillian, Nikki, Sarah, Tara, Hsin-Ni, Pete, Aisleen, Paula, Sylwia, Lynsey, Sandra, Rodger, Stelios, Irini, Tom, Shonna, Kev and Mark for supplying PRP and neutrophils as well as more than a few crazy CIR nights out. A special mention to Jillian who made a CIR girl out of me and who was always eager to help and to Shonna for making flow cytometry a whole lot easier.

I would like to acknowledge the EPSRC for their generous funding of this PhD project. A very big thanks is owed to our collaborators at St Andrews, Paul, Bo,

Russell and Tony for the unenviable task of synthesising hundreds and hundreds of zeolite discs and for interesting chats and discussions.

To my best bud Gillian, thank you for always having faith in me and telling me so whenever I needed a boost.

Thanks to my wonderful and talented mother for always believing in me and helping me financially when I needed. I would not be where I am today without her hard work and ambition rubbing off on me over the years. I am truly my mother's daughter.

Finally to Peter, my verbal thesaurus. Without his enthusiasm for science, eagerness to help, unfaltering moral support, love and head rubs over the past year, completing this thesis would have been much harder. He has been my 'Times' reader in a world where 'the Sun' has reigned supreme.

Abstract.

The discovery of nitric oxide (NO) as the endothelium derived relaxing factor (EDRF) in the late 1980s has sparked a breadth of research focussed around the effects of this molecule in many aspects of mammalian biology. NO is implicated in many processes in the body including vasodilation, the prevention of platelet aggregation and thrombus formation, neurotransmission, wound repair and immunomodulatory effect. The multifaceted properties of NO hold tremendous possibilities for its use in prophylactic and therapeutic processes, especially in the development of biocompatible coatings for medical devices.

This thesis presents a novel method to store and deliver NO at biologically relevant amounts in a targeted manner through the use of cation-exchanged zeolite materials. Zeolites are microporous materials that are extensively used for gas adsorption, due to the high surface area available for chemical reactions. Zeolites are widely available, cheaply produced and are easily manipulated to produce materials with varying NO storage and release capacities, achieved through alteration of the cation exchanged in the structure and composition of zeolite in the polymer binder. NO is liberated from these structures on contact with an aqueous environment, making them ideal candidates for the development of biocompatible coatings on medical devices.

The first experimental chapter examines the effects of two cation-exchanged zeolites (Co^{2+} and Zn^{2+}) and the ability to inhibit collagen-induced platelet aggregation of human platelets *ex vivo*. The primary optimisation of zeolite design was carried out by comparing the effects of several compositions of Co^{2+} and Zn^{2+} zeolites in different polymer binders (PTFE and PDMS) using NO electrode measurements, platelet aggregation studies and fixed wire myography. Previous reports of sGC-independent mechanisms of NO in platelets was also addressed in the platelet

aggregation experiments through the use of specific inhibitors of sGC and by comparison with other NO donors, DEA/NO and SNP, which have well characterised mechanisms of anti-platelet action. These studies indicated that Zn^{2+} and Co^{2+} exchanged zeolites at high compositions of zeolite to the polymer binder had potent anti-platelet effects that were associated with high concentrations of NO released for approximately one hour. The anti-platelet effects lasted for up to 2 hours in platelet rich plasma and washed platelets and were shown to be largely sGC-independent. NO-release profiles varied considerably depending on several aspects of zeolite design and the aqueous environment surrounding the zeolite. This is highlighted in the study of whole-blood aggregation, which shows dramatically reduced anti-thrombotic potential of NO-loaded zeolites compared to that seen in PRP. Results from this chapter conclude that the 50% Zn^{2+}-exchanged zeolite in a PTFE binder had the most promising NO release characteristics for further investigation in different biological assays. Cytotoxicity was assessed using this zeolite by measuring lactate dehydrogenase (LDH) release from platelets following zeolite incubation and suggested no significant adverse effects of zeolite exposure on platelet viability.

Chapter 4 focuses on the effects of 50% Zn^{2+} exchanged zeolites on neutrophil activation through the effect of exposure of zeolites on neutrophil activation markers in isolated human neutrophils *in vitro*. Flow cytometric analyses of fluorescently labelled conjugates of antibodies against neutrophil surface markers were investigated in the absence and presence of the neutrophil activator, formyl Met-Leu-Phe (fMLP). The results revealed a concentration dependent 'priming' effect of NO on neutrophil activation, indicating that high concentrations of NO have a pro-inflammatory effect in this assay. Cell viability was assessed in parallel with the above experiment using Annexin V/Propidium iodide staining. This revealed a small concentration-

dependent, up-regulation in necrotic cell changes in neutrophils exposed to NO released from these zeolites.

Chapter 5 investigates the anti-bacterial effects of the 50% Zn^{2+} zeolites against common strains of Gram-negative and Gram-positive bacteria that are commonly found in nosocomial infections caused by medical devices. The colony forming unit assay was used to assess bacterial growth in the presence of the zeolites over several time-points. Results revealed impressive anti-bacterial properties of NO-loaded zeolites against all strains of bacteria studied over relatively short time-spans. The bactericidal effect was concentration dependent and showed an interesting temporal effect in one strain. Possible Zn^{2+} leaching from the NO-free zeolite control showed bacteriostatic effects in Gram-positive bacteria, adding an extra dimension to the use of these materials as *ex vivo* anti-bacterial agents.

The salient finding of this study is the success of NO-releasing zeolites to produce effects in a number of different biological assays, which show promise for the use of these material as anti-thrombotic and anti-infective coatings for medical devices. Further optimisation of zeolite design is required to produce longer duration NO-release materials and this thesis provides evidence of several ways in which this can be easily achieved to produce further advancements in this field.

Publications and Presentations.

Full papers:

Wheatley P.S, Butler A.R, Crane M.S, Fox S, Xiao, B, Rossi, A.G, Megson I.L, Morris R.E. (2006). NO-releasing zeolites and their antithrombotic properties. *Journal of the American Chemical Society*, **128,** 502-9.

Xiao B, Wheatley P.S, Zhao X, Fletcher A.J, Fox S, Rossi A.G, Megson I.L, Bordiga S, Regli L, Thomas KM, Morris R.E. (2007). High capacity hydrogen and nitric oxide adsorption and storage in a metal organic framework. *Journal of the American Chemical Society,* **129(5),** 1203-9.

Fox S, Wheatley P.S, Xiao B, Morris R.E, Megson I.L, Rossi A.G. (2008).The effect of a novel NO-releasing material on neutrophil function; the potential for development of biocompatible coatings for medical devices. *In preparation.*

Fox S, Wilkinson, T.S, Wheatley P.S, Butler A.R, Morris R.E. Xiao B, Megson I.L, Rossi A.G (2008). The Anti-Bacterial Properties of Zn^{2+}-Exchanged Zeolites; potential as anti-bacterial coatings for medical devices. *In preparation.*

Abstracts:

Fox S, Wheatley P.S, Morris R.E, Butler A.R, Rossi A.G, Megson I.L (2005). Nitric-oxide loaded Co^{2+} and Zn^{2+}-exchanged zeolites have powerful anti-aggregatory properties in human platelets. pA2 online.

Presentation (oral):

BPS Winter Meeting 2005. London "Nitric-oxide loaded $Co^{2=}$ and Zn^{2+}-exchanged zeolites have powerful anti-aggregatory properties in human platelets".

NO Forum 2006. University of Hertfordshire, St Albans. "Nitric Oxide-loaded Zn^{2+}zeolites as potential anti-bacterial agents".

Presentations (poster):

2nd annual Adhesion meeting 2005, Edinburgh. "Nitric oxide-loaded zeolites are powerful inhibitors of platelet activation: temporal and mechanistic studies for formulation of suitable anti-thrombotic coatings."

NO forum 2005, London, "Nitric oxide-loaded Co^{2+} and Zn^{2+}-exchanged zeolites have powerful anti-aggregatory properties in human platelets".

Biosciences meeting 2006, Glasgow. "Nitric oxide-loaded zeolites are powerful inhibitors of platelet activation: potential in anti-thrombotic coatings."

Cardiovascular Science Symposium 2006, Edinburgh. "Nitric oxide-loaded zeolites are powerful inhibitors of platelet activation: temporal and mechanistic studies for formulation of suitable anti-thrombotic coatings."

Contents.

Figure Index

Chapter One – Introduction

Chapter Two. Materials and Methods.

Chapter Three. Optimisation of Zeolite design; potential in anti-thrombotic coatings for medical devices.

Chapter Four. The Effect of Zn^{2+}-exchanged Zeolites on Human Neutrophil Function.

Chapter Five; The Anti-bacterial Properties of Zn^{2+}-exchanged Zeolites.

Chapter Six; General Discussion.

Abbreviations.

Abbreviation	Definition
ADMA	Assymetric dimethylarginine
BH_4	Tetrahydrobiopterin
Ca^{2+}	Calcium ion
CaM	Calmodulin
CFU	Colony forming unit
Co^{2+}	Cobalt ion
Cu^{1+}	Copper (I) ion
Cu^{2+}	Copper (II) ion
cGMP	Cyclic guanosine- 3',5'- monophosphate
CNS	Central nervous system
CVS	Cardiovascular system
DEA/NO	Diethylamine diazeniumdiolate
DES	Drug eluting stent
DETA/NO	(Z)-1-[2-(2-aminoethy)-N-(2-ammonioethy)amino] diazeniumdiolate
EDRF	Endothelium derived relaxing factor
EPSRC	Engineering and physical sciences research council
eNOS	Endothelial nitric oxide synthase
FAD	Flavin adenine dinucleotide
Fe^{2+}	Ferrous
Fe^{3+}	Ferric
FITC	Fluorescein isothiocyanate
fMLP	*N*- formylmethionyl- leucyl -phenylalanine
FMN	Flavin mononucleotide
FS	Forward scatter
GTN	Glyceryl trinitate
GTP	Guanosine 5'-triphosphate
Hb	Haemoglobin
His	Histidine
ICAM-1	Intracellualr adhesion molecule-1
IFN-γ	Interferon-gamma
Ig	Immunoglobulin
IL	Interleukin
iNOS	Inducible nitric oxide synthase
IP_3	Inositol triphosphate
ISDN	Isosorbide dinitrate
L-Arg	L-Arginine
LB	Luria Bertani
LDH	Lactate dehydrogenase
L-NAME	N- (G) nitro-L-arginine methyl ester
LTA	Linde Type A
MRSA	Methicillin resistant *Staphylococcus aereus*
MSSA	Methicillin sensitive *Staphylococcus aereus*
NADPH	Nicotinamide adenine dinucleotide
NANC	Non-adrenergic, non-cholenergic

NFκB	Nuclear transcription factor kappa-B
NO	Nitric oxide
NO^+	Nitrosonium
NO^-	Nitroxyl
NO_x	NO-related species
NO_2^-	Nitrite
NO_3^-	Nitrate
NO_2	Nitrogen dioxide
N_2O_3	Dinitrogen trioxide
N_2O_4	Dinitrogen tetraoxide
NONOate	Diazeniumdiolate
nNOS	Neuronal nitric oxide synthaase
O_2^-	Superoxide anion
ODQ	1-*H*-[1,2,4]oxodiazolo[4,3-a]quinoxalin-1-one
·OH	Hydroxyl radica;
$ONOO^-$	Peroxynitrite
ONOOH	Peroxynitrous acid
PA01	*Psuedomonas aeruginosa* strain 01
PAF	Platelet activating factor
PBS	Phosphate buffered saline
PDE	Phosphodiesterase
PDMS	Polydimethylsiloxane
PE	Phenylephrine
PE (CD62L)	Phycoerythrin
PGI_2	Prostaglandin I_2
PI	Propidium iodide
PKA	Protein kinase A
PKG	Protein kinase G
PLC	Phospholipase C
PPP	Platelet poor plasma
PRP	Platelet rich plasma
PTFE	Polytetrafluoroethylene
PS	Phosphatidyserine
PSS	Physiological saline solution
ROS	Reactive oxygen species
R-SH	Thiol (reduced)
R-SNO	S-nitrosothiol
S.E.M	Standard error of the mean
sGC	Soluble guanylate cyclase
Ser	Serine
SERCA	Sarco-endoplasmic reticulum Ca^{2+} ATPase
SIN-1	3-morpholinosydnonomine
SNAP	S-nitroso-*N*-acetyl-D,L-penicillamine
SNP	Sodium nitroprusside
SNVP	S-nitroso-*N*-valeryl-D,L-penicillamine
SOD	Superoxide dismutase
SS	Side scatter
TNF-α	Tumour necrosis factor alpha

Tyr	Tyrosine
VASP	Vasodilator-stimulated phosphoprotein
WP	Washed platelets
Zn^{2+}	Zinc ion

CHAPTER ONE- INTRODUCTION

1 Introduction

Nitric oxide (NO), an endogenously produced free radical signalling molecule, is involved in a plethora of physiological and pathophysiological processes. Interest in NO biology has resulted in over 80,000 research papers since its discovery as the endothelium derived relaxing factor (EDRF) in the late 1980s (Moncada & Higgs, 2006). NO is now known to be important for vascular haemostasis, due to its intimate involvement in vasodilation, smooth muscle proliferation and the inhibition of platelet activation and adhesion (Moncada *et al.*, 1988; Palmer *et al.*, 1987; Radomski *et al.*, 1987b, d). NO also plays an integral role in various aspects of immune function and regulation, including inflammatory cell activation, adhesion, apoptosis and microbial killing (Albina & Reichner, 1998; Bogdan, 1997; Kubes *et al.*, 1991). The impressive array of effects is further expanded by the capacity of NO to act as both a neurotransmitter and an adjuvant to wound healing (Sanders & Ward, 1992; Shabani *et al.*, 1996). The dysfunction of NO production and signalling is implicated in a wide range of diseases, such as hypertension, hypercholesterolemia, diabetes and septic shock, yet NO-based therapeutics remain under-represented in clinical treatment options (Kojda & Harrison, 1999; Megson & Webb, 2002). The multifaceted effects of NO are both its greatest strength and its greatest weakness when it comes to harnessing its potential in drug therapies. The production of widespread vasodilation upon systemic delivery of NO-donor compounds is potentially dangerous for most clinical applications. The localised delivery of NO to specific areas of need would avoid the detrimental effects of untargeted therapy. The multifaceted properties of NO hold tremendous possibilities for its use in

prophylactic and therapeutic processes, especially in the development of biocompatible coatings for medical devices. For example, the release of NO from the surface of vascular stents would not only inhibit thrombus formation at the surface, but could also aid in the prevention of neointimal thickening; a major cause of restenosis of vessels following stent placement (Petrovic & Peterlin, 2005). Additionally, biocompatibility of medical device coatings could also benefit from the anti-microbial actions of NO to aid in the prevention of nosocomial infections associated with medical device usage. NO-releasing polymers have produced promising results in the production of materials with improved biocompatibility. These polymers incorporate NO-donor molecules, which then release their NO moiety upon contact with an aqueous environment. Potential drawbacks to the use of these materials are the limited NO reservoir loaded into the polymer matrix, duration and concentration of NO released and the leaching of potentially toxic donor molecule by-products.

NO-loaded cation-exchanged zeolites are microporous materials with high capacity gas storage properties due to the large surface area available for chemical reaction. These materials liberate stores of $NO_{(g)}$ on contact with an aqueous environment and don't require molecular adducts to stabilise NO prior to release making them ideal candidates for development as biocompatible surface coatings. Moreover, these materials have tunable NO storage and release properties, achieved through modulation of various aspects of zeolite design and subsequently offer the potential to tailor NO-release to specific requirements, an attractive feature given the complexity of NO signalling in the body. The biological efficacy of these NO-

releasing materials was investigated in this thesis, with respect to modulation of platelet aggregation, neutrophil activation and bacterial growth responses to evaluate the potential of these materials in a variety of biomedical applications. NO-loaded zeolite materials also provide unique tools with which to investigate various aspects of NO biology with particular emphasis on localised delivery of pure NO.

The aim of this thesis is to characterise the biological efficacy of these novel NO-releasing zeolite materials, with respect to their pharmacological potential in the development of biocompatible coatings and as unique tools to aid in the further understanding the physiology and pharmacology of locally delivered NO.

1.1 NITRIC OXIDE

The discovery of NO as the endothelium derived relaxing factor (EDRF) over 25 years ago lead the way in determining the importance of NO in the body. The stimulation of isolated smooth muscle preparations with various agonists including acetylcholine, bradykinin and thrombin produced vascular relaxation, but importantly this was only evident when the endothelium was present (Furchgott *et al.*, 1987; Furchgott & Zawadzki, 1980; Ignarro, 1987; Ignarro *et al.*, 1987c; Moncada *et al.*, 1988; Palmer *et al.*, 1988; Palmer *et al.*, 1987). An unknown factor released from the endothelium, termed EDRF was shown to be responsible for the relaxation of vascular smooth muscle and it was simultaneously shown that EDRF was also a potent inhibitor of platelet aggregation and adhesion (Bhardwaj *et al.*,

1988; Busse *et al.*, 1987; Hogan *et al.*, 1988; Macdonald *et al.*, 1988; Radomski *et al.*, 1987c). The search for the elusive factor concluded when EDRF was shown to be pharmacologically and chemically indistinguishable from NO (Ignarro *et al.*, 1987a; Ignarro *et al.*, 1987b; Ignarro *et al.*, 1988; Palmer *et al.*, 1987; Radomski *et al.*, 1987a). It is now apparent that this inorganic, free radical molecule is involved in a wide range of physiological and pathophysiological processes including modulation of vascular tone (Moncada & Palmer, 1991; Radomski, 1995) , inhibition of platelet (Hogan *et al.*, 1988; Radomski *et al.*, 1987b, c, d; Vane *et al.*, 1990) and inflammatory cell activation (Granger & Kubes, 1994; Kubes *et al.*, 1993), modulation of immune responses (Albina & Reichner, 1998; MacMicking *et al.*, 1997; Nicotera *et al.*, 1995) and as a neurotransmitter in non-adrenergic non-cholinergic (NANC) synapses (Berdeaux, 1993; Grozdanovic *et al.*, 1994; Rand, 1992; Sanders & Ward, 1992). The importance of the key discovery of NO was recognised when the Nobel Prize in Physiology and Medicine was awarded to Furchgott, Ignarro and Murad in 1998. Research involving NO is now a major theme producing over 80,000 publications to date from a diverse range of disciplines.

1.1.1 SYNTHESIS OF NO

NO is synthesised in the body by three isoforms of the enzyme NO Synthase (NOS). NOS isoenzymes are cytochrome-P450-related type enzymes that catalyze the formation of NO and L-Citrulline (L-Cit) from L-Arginine (L-Arg) and molecular oxygen (O_2) (Bredt *et al.*, 1991b). The three isoforms of NOS were first isolated and described in a range of studies from the early 1990s. They are named endothelial

NOS (eNOS or NOSIII), neuronal NOS (nNOS or NOSI) and inducible NOS (iNOS or NOSII). These enzymes differ in their localisation and in the case of iNOS, by the mechanism of regulation. eNOS is predominantly found in the endothelium and platelets where it is constitutively active, producing low (pM-nM) concentrations of NO important for vascular haemostasis (Forstermann *et al.*, 1991a; Forstermann *et al.*, 1991b; Marsden *et al.*, 1992; Nishida *et al.*, 1992; Pollock *et al.*, 1991). eNOS is activated by several agonists, including thrombin, bradykinin and acetylcholine and can also be stimulated by mechanical forces such as shear stress. nNOS is also constitutively expressed and is found in non-adrenergic, non-cholinergic (NANC) neurones where NO is produced at low concentrations (pM) and functions as a neurotransmitter (Bredt *et al.*, 1991a; Bredt *et al.*, 1990; Sheng *et al.*, 1992). The activity of eNOS and nNOS is dependent on the increase in Ca^{2+} concentrations and the subsequent binding of calmodulin (CaM) which promotes electron flow necessary for the oxidation of L-Arg to NO (Schmidt *et al.*, 1992a; Schmidt *et al.*, 1992b). The inducible isoform of NOS is usually expressed in inflammatory cells such as macrophages and neutrophils (Ahn *et al.*, 1994; Kadota *et al.*, 1991; Yui *et al.*, 1991a; Yui *et al.*, 1991b). The enzyme is activated in response to various inflammatory cytokines and bacterial endotoxins, where it generates high local concentrations of NO (nM-μM) important for the immune response to infection (Moncada & Palmer, 1991). iNOS has Ca^{2+}/CaM permanently bound within the structure and therefore functions independently of changes in Ca^{2+} concentration (Yui *et al.*, 1991b).

1.1.2 NOS CATALYTIC MECHANISM

NOS enzymes exist as homodimers, each monomer has a bidomain structure consisting of a N-terminal oxygenase domain and a C-terminal reductase domain linked by a Ca^{2+}/calmodulin-binding region. The oxygenase domain contains the binding sites for the co-factor, tetrahydrobiopterin (BH_4), L-Arg and a haem prosthetic group. The reductase domain contains the biding sites for flavin mononucleotide (FMN), flavin adenine dinucleotide (FAD), and nicotinamide adenine dinucletide (NADPH). Electrons donated from NADPH flow via flavins in the reductase domain to the haem group of the oxygenase domain where they reduce ferric (Fe^{3+}) haem to the ferrous (Fe^{2+}) form thereby allowing O_2 to bind.

The electron flow then stimulates the next step in NO synthesis through oxidation of L-Arg to the intermediate N^{ω} - hydroxy-L-arginine (NHA) and then NO. The co-factor BH_4 is thought to be necessary for the synthesis of NO by NOS, as studies have indicated that lack of BH_4 can lead to uncoupling of the NADPH enzyme and subsequent superoxide (O_2^-) formation (Vasquez-Vivar *et al.*, 2003; Vasquez-Vivar *et al.*, 1998). BH_4 is therefore thought to act as redox electron acceptor important for the successful coupling of NADPH oxidation and NO synthesis and thereby inhibiting the formation of the potent oxidant O_2^- (Vasquez-Vivar *et al.*, 1999; Vasquez-Vivar *et al.*, 2003; Vasquez-Vivar *et al.*, 1998; Vasquez-Vivar *et al.*, 2002). Uncoupling of enzymes such as NADPH and xanthine oxidase, which subsequently leads to O_2^- production is now known to be an important contributor to oxidative stress. Oxidative stress is a condition occurring when the balance of oxidant formation exceeds the capacity of endogenous anti-oxidants such as superoxide

dismutase (SOD). The increased presence of O_2^- can mask the beneficial effects of NO due to the high reactivity of NO with O_2^-, leading to formation of the potent oxidant peroxynitrite ($ONOO^-$; see section 1.1.5.1). Oxidative stress has been linked with many pathophysiological states including atherosclerosis, hypertension and diabetes (Brune *et al.*, 2003; Giugliano *et al.*, 1996; Loscalzo, 2003).

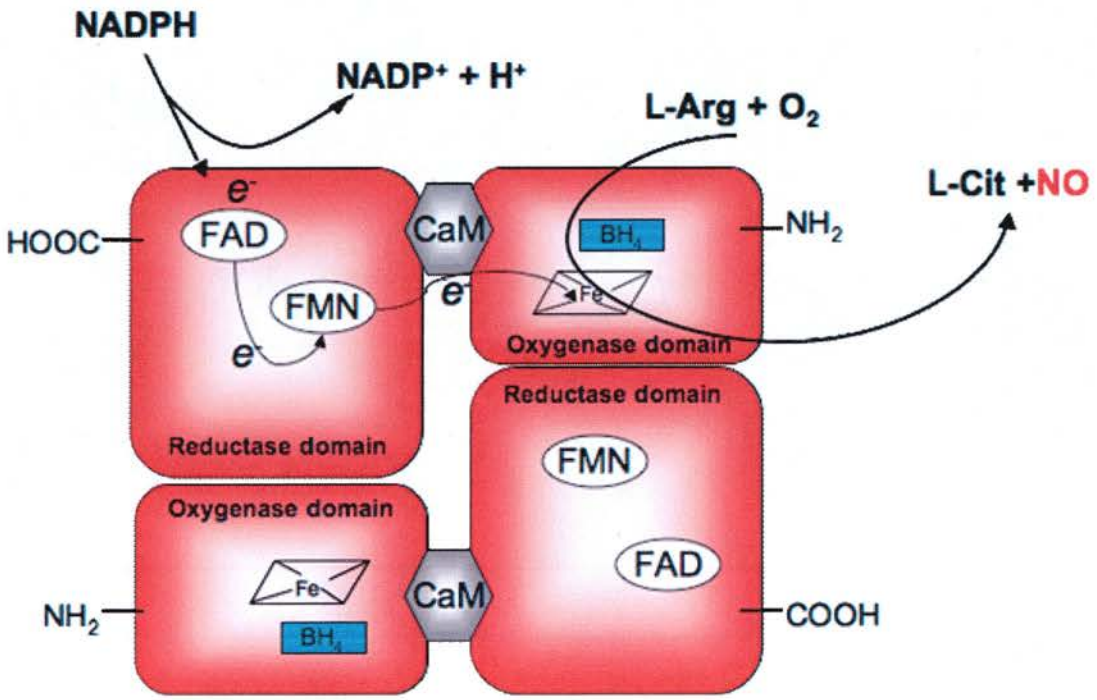

Figure 1.1. Schematic Representation of the Structure of NOS.

The electron is donated from the reduction of NADPH to $NADP^+ + H^+$. The flow of electrons (e^-) passes through the flavins (FAD and FMN) of the reductase domain of one subunit and is passed, via calmodulin (CaM) to the haem-group of the oxygenase domain in the second subunit. Tetrahydrobiopterin (BH_4) acts as a co-factor in the oxidation of L-Arg to L-Cit and NO. Adapted from Alderton et al. (2001).

1.1.3 NO:sGC:cGMP PATHWAY

NO has a high affinity for haem-containing enzymes especially soluble guanylate cyclase (sGC), the enzyme generally regarded as the intracellular NO 'receptor'. The majority of the effects of NO are mediated through the activation of sGC and the subsequent conversion of guanosine 5'-triphosphate (GTP) to the 3', 5'-cyclic guanosine monophosphate (cGMP) (Schmidt *et al.*, 1993). The production of cGMP triggers downstream signalling events through protein kinase G (PKG), phosphodiesterases (PDEs) and ion channels.

1.1.3.1 SOLUBLE GUANYLATE CYCLASE

The sGC enzyme exists as a heterodimer of α and β monomer subunits each with a 3 domain structure consisting of a C-terminal catalytic domain, a N-terminal haem binding domain joined by a central dimerisation domain (figure 1.2; Garbers, 1990; Hobbs, 1997; Koesling, 1999; Wedel *et al.*, 1995). Two isoforms of the heterodimer have been described ($\alpha_1\beta_1$ and $\alpha_2\beta_1$) which are functionally indistinguishable. The β_1 subunit is ubiquitously expressed, whereas the expression of the two isoforms of the α subunit has distinct localizations. The $\alpha_2\beta_1$ heterodimer occurs mainly in the brain and the $\alpha_1\beta_1$ isoform is expressed in a much broader range of tissues and forms the predominantly expressed isoform of sGC activated by NO (Gibb & Garthwaite, 2001; Hobbs, 1997; Koesling *et al.*, 2004).

NO diffuses from the site of synthesis to activate sGC present in the cytosol. The haem domain is important for the successful activation of sGC by NO. Several amino acids in the β subunit have shown to be integral to the function of the enzyme

through modulation of the haem-binding domain. Of these, the His 105 residue has been shown to be essential for the activation of sGC by NO. It is the rupture of the axial ligand between haem and sGC at His 105 upon NO binding which promotes the increase in enzymatic activity (Bellamy *et al.*, 2002; Hobbs, 1997; Wedel *et al.*, 1995). Other residues, including Cys 78 & 214 (Friebe *et al.,* 1997) and Tyr 125 and Arg 139 (Schmidt *et al.*, 2004) have also been shown to be important for haem binding to sGC. NO binds to the haem to form a nitrosyl-haem complex, which acts to increase the enzymatic activity of sGC by up to 400 fold (Stone & Marletta, 1995). The active enzyme also shows a reduction in the K_m for GTP, most likely through the exposure of high affinity binding regions for GTP in the catalytic domain, thereby increasing the conversion of GTP to cGMP (Hobbs, 1997). The functional diversity of cGMP production by sGC in different cell types may account for the equally diverse actions of NO in the body. It has been shown that many factors can affect the desensitisation rate of sGC. These include the presence of GTP, oxy-haemoglobin and thiols, which are thought to increase the rate of deactivation of NO-sGC signalling. Thus, the half-life of sGC signalling varies depending on cell type and is far more rapid than the determined rate of deactivation of purified nitosyl-sGC, which is between 5 s and 3 min (Kharitonov *et al.*, 1997). The rapid desensitisation of sGC in intact cells, including human platelets has been estimated to occur within seconds with recovery taking place in minutes (Bellamy *et al,* 2000). This demonstrates that sGC is capable of rapidly responding to transient NO concentrations and subsequently can produce functionally dynamic concentrations of cGMP.

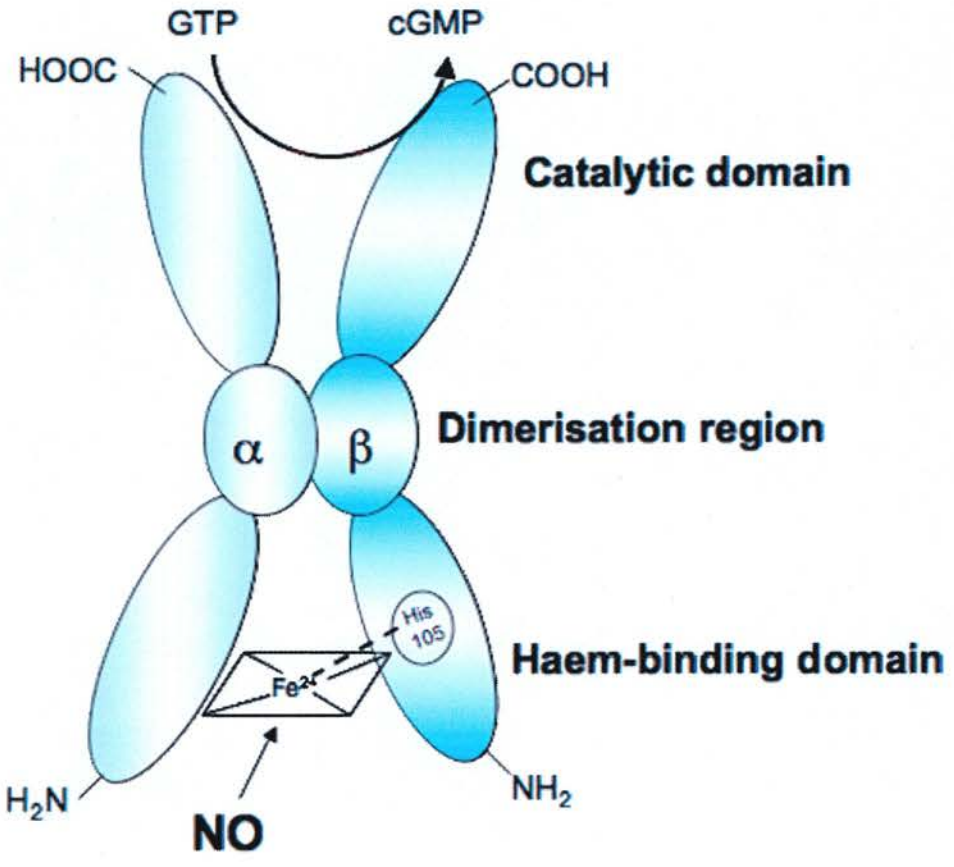

Figure 1.2. Schematic Representation of the Structure of sGC.

The structure of sGC consisits of 3 domains as indicated which show the binding of NO and the catalytic conversion of GTP to cGMP. The Histidine residue at location 105 on the β subunit is represented as important for the binding of NO to the haem prosthetic group. Adapted from Hobbs (1997).

1.1.3.2 TARGETS FOR cGMP

An increase in cGMP production triggers signalling principally through high affinity PKG and PDE pathways. PKG, of which there are 2 isoforms (PKG I and PKG II; (Jarchau *et al.*, 1994; Pohler *et al.*, 1995; Smolenski *et al.*, 1998) is a serine/threonine protein kinase which acts to inhibit Ca^{2+} signalling through triggering a reduction in

intracellular Ca^{2+} concentrations $[Ca^{2+}]_i$ in platelets and smooth muscle. The decrease in $[Ca^{2+}]_i$ is potentiated through the phosphorylation of a serine residue on the inositol triphosphate (IP_3) receptor on the sarcoplasmic reticulum which prevents the efflux of Ca^{2+} into the cytoplasm (Komalavilas & Lincoln, 1994). The IP_3 pathway of Ca^{2+} mobilisation is further inhibited via the inhibition of phospholipase C (PLC), the enzyme involved in IP_3 production (Carvajal *et al.*, 2000; Lincoln & Cornwell, 1993). In smooth muscle, cGMP also can affect Ca^{2+} concentrations via direct interactions with Ca^{2+} channels and transporters (Carrier *et al.*, 1997; Nara *et al.*, 2000). The involvement of PKG in the phosphorylation of other proteins involved in the inhibition of platelet activation and smooth muscle relaxation include heat shock proteins (Hsp; (Carvajal *et al.*, 2000) and vasodilator-stimulated phosphoprotein (VASP) in platelets (Butt *et al.*, 1994; Halbrugge *et al.*, 1990). VASP is involved in the organisation of the cytoskeleton through the regulation of actin polymerisation (Reinhard *et al.*, 1995; Reinhard *et al.*, 2001). Phosphorylation of VASP by PKG results in the inability of VASP to interact with actin filaments (Wang *et al.*, 2006). This correlates with platelet GPIIb/IIIa receptor inhibition (Horstrup *et al.*, 1994).

PDEs catalyse the hydrolysis of cGMP and cAMP to their corresponding inactive 5'-nucleotides, thereby altering the levels of cGMP in the intracellular environment. There are a large family of PDE isoforms that exist in mammals (Beavo *et al.*, 1994; Soderling & Beavo, 2000), with representative isoforms expressed in different cells (Kuthe *et al.*, 2001). The PDE-V isoform has received much attention following the discovery that selective inhibitors of this enzyme, tested for cardiovascular purposes,

had impressive side-effects on male penile erection (Moreland *et al.*, 1998; Uckert *et al.*, 2001). As a result, these drugs are now primarily marketed to treat erectile dysfunction, where inhibition of PDE-V in the corpus cavernosum results in the accumulation of cGMP, thereby prolonging vessel dilation to aid in penile erection (Corbin *et al.*, 2002; Doh *et al.*, 2002; Kuthe *et al.*, 2002).

1.1.4 NO MEDIATED cGMP-INDEPENDENT MECHANISMS

It is now evident that NO can produce effects via cGMP-independent mechanisms. The involvement of cGMP-independent pathways is particularly evident in the anti-platelet activity of select NO-donors (Crane *et al.*, 2005; Sogo *et al.*, 2000a; Ward *et al.*, 2000) and the regulation of inflammatory cell apoptosis (Ward *et al.*, 2000). The contribution of sGC-independent effects have also been described in the smooth muscle relaxing properties of NO (Bellamy *et al.*, 2002; Bradley *et al.*, 1998; Miller *et al.*, 2004). Despite the known involvement of NO-mediated sGC-independent effects, little is known regarding the pathway through which NO exerts its effects in the absence of active sGC. However, it has been postulated that these sGC-independent effects are linked to situations where high concentrations of NO are present in the extracellular environment (Crane *et al.*, 2005). The relative lack of sGC-independent anti-platelet effects in the presence of peroxynitrite donating compounds (eg SIN-1; see section 1.1.8.4) or S-nitrosothiols (eg. SNAP; see section 1.1.8.2) suggests an exclusive effect of NO in these responses (Sogo *et al.*, 2000a). The activation of ion channels and/or transporters have been implicated as a possible mechanism of sGC-independent effects in some tissues (Bolotina *et al.*, 1994;

Bradley *et al.*, 1998; Gupta *et al.*, 1994; Homer & Wanstall, 2002; Plane *et al.*, 1996) possibly through the nitrosation of critical protein residues on the cell membrane (Crane *et al.*, 2005). $OONO^-$ is a potent nitrating species capable of nitrating protein residues critical for cell signalling, and has been linked with the production of sGC-independent induction of apoptosis in neutrophils (Ward *et al.*, 2000).

The use of the specific inhibitor of sGC, 1-*H*-[1,2,4]oxadizolo[4,3-*a*]quinoxalin-1-one (ODQ; figure 1.3) has been pivotal in the discovery and the advancement of our understanding of cGMP-independent effects of NO. ODQ rapidly oxidises the ferrous haem of sGC to the ferric form thereby effectively reducing the capacity for NO to bind and stimulate the enzyme in an irreversible manner (Feelisch *et al.*, 1999; Zhao *et al.*, 2000). ODQ has benefits over previously used inhibitors, methylene blue and LY 83583 (6-anilino-5,8-quinolinequinone), which can generate superoxide anion (O_2^-) and interfere with prostanoid synthesis (Gryglewski *et al.*, 1986; Hasegawa *et al.*, 2004; Marczin *et al.*, 1992; Wolin *et al.*, 1990). ODQ has been described by many as a selective inhibitor of sGC (Garthwaite *et al.*, 1995; Schrammel *et al.*, 1996), but evidence suggests that ODQ can interfere with other heme protein-dependent processes in vascular tissue, including NOS activity at ODQ concentrations $\geq$ 30μM (Feelisch *et al.*, 1999). Thus, careful consideration is required when interpreting results using ODQ mediated inhibition of sGC.

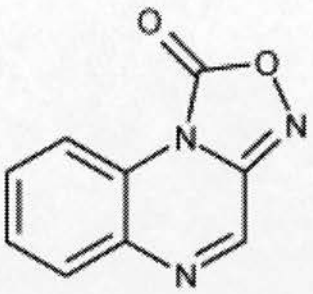

Figure 1.3. The Structure of ODQ.

1.1.5 NO BIOCHEMISTRY

The biochemistry of NO is complex due to the diversity of the reactions involving this radical species. NO can rapidly react with a number of molecules resulting in the production of a variety NO-related species, which can exert biological effects on their own. The array of NO-related products produced by the many reactions of NO goes some way in explaining the 'double edged sword' paradox associated with NO in the body. The concentration of NO and the relative presence of each biological species in particular tissues and organs determines the eventual signalling pathway of NO. The redox environment can be dramatically altered in several physiological and pathophysiological conditions, resulting in pro and anti-oxidant outcomes for NO. The most physiologically relevant reactions of NO in the body are those with superoxide, haem, molecular oxygen, thiols and tyrosine.

1.1.5.1 REACTION WITH SUPEROXIDE

Superoxide (O_2^-) is a reactive oxygen species (ROS) generated in mammals through several enzymes including xanthine oxidases, NADPH oxidases, NOS, cycloxygenases and enzymes of the respiratory chain (Forman & Torres, 2002; Nohl

et al., 2003; Souza *et al.*, 2002; Terada *et al.*, 1991; Vasquez-Vivar & Kalyanaraman, 2000; Zhang *et al.*, 1998). The body removes O_2^- via the action of the enzyme superoxide dismutase (SOD) and catalase to produce oxygen and water (equation 1). This process is important to regulate the potent oxidant effects of O_2^-, however increased production of O_2^- can overcome these regulatory mechanisms and reduce the bioavailabilty of NO. O_2^- reacts with NO at almost diffusion limited rates (rate constant - 6.7 x $10^9 M^{-1}$ s^{-1}) (Huie & Padmaja, 1993) to produce peroxynitrite ($ONOO^-$; equation 2). This preferential reaction of NO for O_2^- masks the beneficial effects of NO by reducing NO bioavailablility, and is increasingly associated with disease pathology (Cuzzocrea, 2006; Kojda & Harrison, 1999; Loscalzo, 2003; Miller *et al.*, 1998; Thomas *et al.*, 2006).

$$2O_2^- + 2H^+ \xrightarrow{SOD} O_2 + H_2O_2 \xrightarrow{catalase} 2O_2 + H_2O \quad (1)$$

$$NO + O_2^- \longrightarrow ONOO^- \quad (2)$$

$ONOO^-$ is a potent oxidising agent, which may be responsible for the cytotoxic effects associated with high concentrations of NO in a number of cell types and immune responses (Bartosz, 1996; Virag *et al.*, 2003). It is rapidly decomposed via peroxynitrous acid (equation 3) to form NO_2 and hydroxyl radicals (•OH; equation 4).

$$ONOO^- + H^+ \longrightarrow ONOOH \quad (3)$$

$$ONOOH \longrightarrow NO_2 + \bullet OH \quad (4)$$

1.1.5.2 REACTION WITH HAEM

The reaction of NO with haem constitutes the majority of the physiological effects of NO. The haem containing enzyme sGC (see section 1.1.3.1) is the main effector for NO signalling, which catalyses production of cGMP upon activation. Other haem containing enzymes are also important in NO biology. These include oxy and deoxy-haemoglobin which bind NO to form methaemoglobin and nitrate (NO_3^-) or iron-nitrosyl-haemoglobin respectively. Oxy-haemoglobin is generally considered as an NO scavenger and the likely route of NO inactivation (Kosaka *et al.*, 1989; Schechter & Gladwin, 2003). However, evidence suggests that deoxy-haemoglobin can act to prolong NO bioactivity of NO via the formation of S-nitosohaemoglobin. To this end, the formation of intermediate S-nitrosohaemoglobin and other S-nitroso-protein adducts also act as NO transporters, enabling the effects of NO to occur far from the site of synthesis (Hobbs *et al.*, 2002; Jia *et al.*, 1996; Kosaka *et al.*, 1989; Rassaf *et al.*, 2005). The high affinity of NO for haem results in the interaction of NO with several other haemoproteins including COX, NOS and cytochrome P450 (Buga *et al.*, 1993; Goodwin *et al.*, 1998; Khatsenko *et al.*, 1993; Wink *et al.*, 1993). The conformational change associated with NO-haem interactions confers inhibitory actions on their catalytic activities.

1.1.5.3 REACTION WITH MOLECULAR OXYGEN

NO is oxidised by molecular oxygen (O_2) to yield nitrogen dioxide (NO_2; equation 5). This reaction is relevant for both O_2 in gaseous and aqueous phases and thus describes the reaction pathway through which NO_2, a prominent air pollutant, is

formed from internal combustion engines. In physiological solutions the reaction between NO and O_2 is relatively slow (approx 4 x 10^6 M^{-1} s^{-1}). NO_2 will react with H_2O to form nitrite (NO_2^-) and nitrate (NO_3^-; equation 6; Butler *et al.*, 1995) but the reaction with NO to form N_2O_3 occurs in preference to this (equation 7). N_2O_3 is an important physiological NO-species due to the potent thiol nitrosating properties of this molecule (section 1.1.5.4). N_2O_3 will also react with H_2O to form NO_2^- and H^+ (equation 8).

$$NO + O_2 \longrightarrow NO_2 \quad (5)$$

$$2NO_2 + H_2O \longrightarrow NO_2^- + NO_3^- + 2H^+ \quad (6)$$

$$NO_2 + NO \longrightarrow N_2O_3 \quad (7)$$

$$N_2O_3 + H_2O \longrightarrow 2NO_2^- + 2H^+ \quad (8)$$

1.1.5.4 REACTION WITH THIOLS

The potent nitrosating species in the body is N_2O_3, which reacts with thiols (general formula R-SH) to form S-nitrosothiol species (general formula RSNO; equation 9).

$$N_2O_3 + RSH \longrightarrow R\text{-}S\text{-}N{=}O + H^+ + NO_2^- \quad (9)$$

The NO moiety of S-nitrosated species is nitrosonium (NO^+), which can be transferred to other thiols via transnitrosation reactions (equation 10).

$$R_1\text{-}S\text{-}N{=}O + R_2SH \longrightarrow R_1SH + R_2S\text{-}N{=}O \quad (10)$$

The mechanism by through which S-nitrosothiols are activated to liberate NO is unclear although decomposition is accelerated in the presence of Cu^+ and can be susceptible to light (equation 7).

$$2R\text{-}S\text{-}N{=}O \xrightarrow[+\ light]{+\ Cu^+} 2RSSR + 2NO \qquad (11)$$

Storage of NO in S-nitrosothiol forms is now recognised to an important physiological process and associated with the formation of intermediates that can prolong NO bioactivity in the body (Crane *et al.*, 2002; Stamler *et al.*, 1992a; Stamler *et al.*, 1992b; Stamler *et al.*, 1992c). Furthermore, the storage and transfer of nitrosonium species occurs without the release the NO radical and is therefore not subjected to the same potent scavenging and redox reactions. Thus, formation of RSNO provides functional explanation as to how NO can exert effects in environments containing high concentrations of scavengers such as haemoglobin (Rassaf *et al.*, 2005).

1.1.5.5 REACTION WITH TYROSINE

The NO-related species $ONOO^-$ is a potent nitrating species, reacting at sites of electron density, such as aromatic rings, to transfer an NO_2^+ moiety. Tyrosine residues are common sites of nitration by $ONOO^-$. Nitration of critical tyrosine residues, especially those involved in cell signalling phosphorylation events, is implicated with effects associated with $ONOO^-$, including inhibition of platelet aggregation. Formation of nitrotyrosine is also used as a marker of nitrative-stress

associated with the progression of diseases such as Parkinson's disease, atherosclerosis, arthritis, Alzheimer's and multiple sclerosis (Ischiropoulos, 1998; Kamat, 2006; Nakazawa *et al.*, 2000; Radi, 2004).

1.1.6 NO PHYSIOLOGY AND PATHOPHYSIOLOGY.

The ubiquitous presence of NO in the body means that it is has far-reaching roles in the cardiovascular, immune and nervous systems. The physiological and pathophysiological impact of NO in these systems is dependent upon relative concentrations of NO produced, the target cell type and the surrounding biological milieu. Reduced NO bioavailability is recognised as a significant risk factor in many disease states including atherosclerosis, diabetes, hypertension and neurodegenerative disorders (Li & Forstermann, 2000; Llorens & Nava, 2003). Bioavailability of NO can be reduced in a number of ways including reduction of NO synthesis by substrate or co-factor deficiencies, enzyme uncoupling, endothelial injury or increases in NOS inhibitor asymmetric dimethylarginine (ADMA) (Boger *et al.*, 1998; Cooke, 1998; Kennedy *et al.*, 2004; Kielstein *et al.*, 2001; Rengasamy & Johns, 1993; Vasquez-Vivar *et al.*, 2003; Vasquez-Vivar *et al.*, 1998). NO bioavailability is also significantly impacted by changes in the redox environment. The diffusion limited reaction of NO with O_2^- results in $ONOO^-$ production (section 1.1.5.1), preventing NO from reaching its target while having potent nitrating effects often associated with NO-mediated cytotoxicity (Miller *et al.*, 1998; Pacher *et al.*, 2007).

1.1.6.1 CARDIOVASCULAR SYSTEM

The synthesis of NO from vascular endothelium is integral in the maintenance of vascular haemostasis through both modulation of vascular tone and inhibition of platelet activation and adhesion. Reduced bioavailability of endothelial derived NO is one of the main factors involved in endothelial dysfunction, a disorder implicated in the progression of numerous diseases including athereosclerosis, hypertension and diabetes (Cosentino & Luscher, 1998; Luscher, 1994; Wennmalm, 1994). Models of eNOS deficiency demonstrate decreased vascular reactivity, hypertension, atherosclerosis and increased injury following ischemic events (Bonthu *et al.*, 1997; Faraci *et al.*, 1998; Huang *et al.*, 1996; Jones *et al.*, 1999; Knowles *et al.*, 2000). Platelet-derived NO is also important in modulating platelet responses following stimulation of aggregation, through prevention of further platelet recruitment (Freedman & Keaney, 1999; Freedman *et al.*, 1997; Freedman *et al.*, 1998). Dysfunction in platelet NO production has been linked with increased thrombotic risk in patients with angina and acute coronary syndromes (Freedman & Loscalzo, 2003; Freedman *et al.*, 1998; Tanus-Santos *et al.*, 2002).

The expression of all isoforms of NOS can be found in the heart (Balligand & Cannon, 1997; Balligand *et al.*, 1994; Takimoto *et al.*, 2000). Here, NO is important for modulation of force and rate of contraction through interactions with Ca^{2+}-channel function and changes in cardiac preload and afterload through its vasoactive properties (Balligand *et al.*, 1993; Choate *et al.*, 2001).

1.1.6.2 IMMUNE SYSTEM

The inflammatory response is a fundamental process for host defence against infection and for mediating tissue repair. The inflammatory reaction involves the recruitment of inflammatory cells to the site of injury or infection in response to noxious chemical stimuli or microbial toxins (Driscoll *et al.*, 1997). The identification of foreign substances in the body is essential for the rapid and successful clearance of infection, however, when the formidable array of inflammatory effector molecules is targeted inappropriately, such as in chronic inflammatory diseases and medical device placement, the resulting damage to host tissue is harmful and potentially fatal.

1.1.6.2.1 RECRUITMENT OF INFLAMMATORY CELLS

NO is involved in many stages of the inflammatory response (Guzik *et al.*, 2003). Constitutively active eNOS produces low concentrations of NO released from the vascular endothelium and platelets to inhibit platelet and inflammatory cell adhesion (Granger & Kubes, 1994; Kubes *et al.*, 1993; Thom *et al.*, 1994). Here, NO is involved in the modulation of leukocyte and endothelial adhesion molecule expression to prevent inflammatory cell recruitment from the blood stream into the tissue. Rolling leukocyte/endothelial interactions are important for the "capture" of inflammatory cells at the vessel wall, prior to firm adhesion and migration into the tissue (Frenette & Wagner, 1997; Tedder *et al.*, 1995). Adhesion is initiated by L-selectin (CD62L), a leukocyte surface glycoprotein, which is shed upon exposure with various ligands on the vessel surface to promote leukocyte rolling adhesive

interactions (Hafezi-Moghadam *et al.*, 2001; von Andrian & Arfors, 1993). Release of NO from vascular endothelium prevents leukocyte rolling through inhibition of CD62L shedding (Benjamim *et al.*, 2002). Firm adhesion is partly mediated via the leukocyte β_2-integrin adhesion molecule CD11b (Mac-1; figure 1.4), which is up-regulated at the leukocyte surface due to translocation from intracellular storage pools during degranulation (Hughes *et al.*, 1992). Inhibition of NOS by L-NAME has been shown to increase the adhesion of leukocytes to the endothelium through increased expression of leukocyte adhesion molecule, CD11b/CD18 confirming the role of NO in inhibiting inflammatory cell adhesion to the endothelium and maintaining vascular haemostasis (Kubes *et al.*, 1991; Ma *et al.*, 1993). Inappropriate recruitment of inflammatory cells into tissue can occur at sites of endothelial dysfunction or injury, where endothelial production of NO is compromised. Endothelial dysfunction is a common risk factor associated with many diseases including atherosclerosis (Guerra *et al.*, 1989; Napoli, 2002). Infiltration of inflammatory cells into atherosclerotic plaques contributes to disease pathogenesis in several ways; by promoting plaque progression through accumulation of macrophage-derived foam cells, the non-discriminate attack of inflammatory cell exudates on host tissues and by increasing the risk of plaque rupture through pro-apoptotic effects on smooth muscle cells (Eriksson *et al.*, 2001; Shaw *et al.*, 2005).

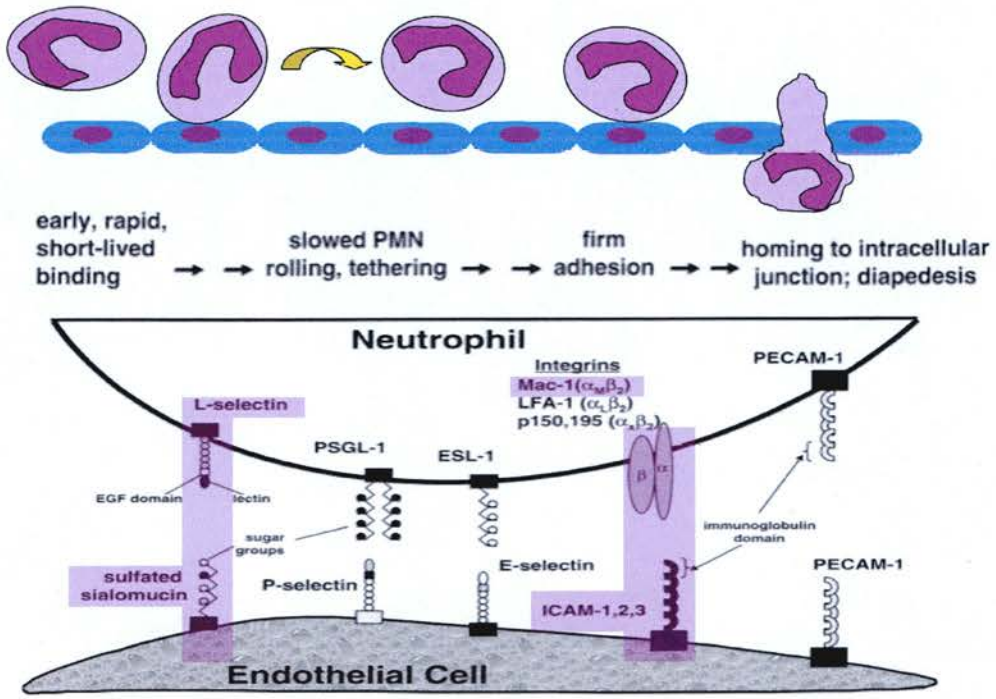

Figure 1.4. Neutrophil/endothelial cell interactions.

A representation of the stages of neutrophil adhesion to endothelium prior to migration (diapedesis) and the receptor/ligands involved. The highlighted sections represent the neutrophil adhesion markers L-selectin (CD62L) and Mac-1 (CD11b) and their corresponding endothelial ligands. Adapted from Wagner and Roth, 2000.

1.1.6.2.2 MICROBIAL DEFENCE

High concentrations of NO are released by inflammatory cells, via activation of iNOS in response to various inflammatory mediators and bacterial products (Moncada & Palmer, 1991). During the response to injury or infection, NO is important for the clearance of infecting pathogens (Bogdan, 1997) and for promoting tissue repair (Stallmeyer *et al.*, 1999). Murine iNOS knock-out models highlight the importance of NO synthesis during microbial infection as these mice show increased susceptibility to infection (MacMicking *et al.*, 1995). Furthermore, reduced

expression of iNOS has been associated with the pathophysiology of cystic fibrosis, a condition associated with increased susceptibility to bacterial lung infection (Kelley & Drumm, 1998; Meng *et al.*, 1998). The involvement of NO in endogenous microbial defence has increased the interest in NO-donors as antimicrobial agents, particularly in wound healing, where risk of infection is high. NO-donors have exhibited inhibitory actions against a variety of bacteria, fungi, viruses and parasites (Ascenzi *et al.*, 2003; Coban *et al.*, 2003; Karupiah & Harris, 1995; Rementeria *et al.*, 1995). The mechanism by which NO exerts its anti-microbial actions are both dependent upon the species of NO produced and the pathogen. For example, anti-parasitic actions of NO have been related to the S-nitrosylation of cysteine proteases (Ascenzi *et al.*, 2003) and candidacidal activity has implicated the potent nitrating species, $OONO^-$ (Vazquez-Torres *et al.*, 1996). In addition, differences in susceptibility to NO and NO-related species varies between strains of the same microbial group. NO has greater anti-bacterial properties than $OONO^-$ against *Leishmania major* and *Giardia lamblia* (Assreuy *et al.*, 1994; Fernandes & Assreuy, 1997) whereas *Salmonella typhimurium* was more sensitive to $OONO^-$ and S-nitrosothiol species and demonstrated no adverse effects from NO *per se* (De Groote et al., 1995). Differences in the anti-microbial actions of NO has been attributed to the huge variety of microbial defenses including expression of stress regulons, scavengers, detoxifying enzymes, repair systems and strategies to subvert or avoid host phagocytes (Fang, 1997). Gram-positive and Gram-negative bacteria differ fundamentally in the make-up of their membranes (see figure 1.5), which has previously been shown to determine the sensitivity of bacteria to oxidant stress (Dahl

et al., 1989). Gram-negative bacteria have a greater chance of oxidation of membrane lipids and proteins and therefore show greater sensitivity to singlet oxygen than Gram-positive bacteria that allow passage of singlet oxygen through to the cytoplasm where it is inactivated (Dahl *et al.*, 1989).

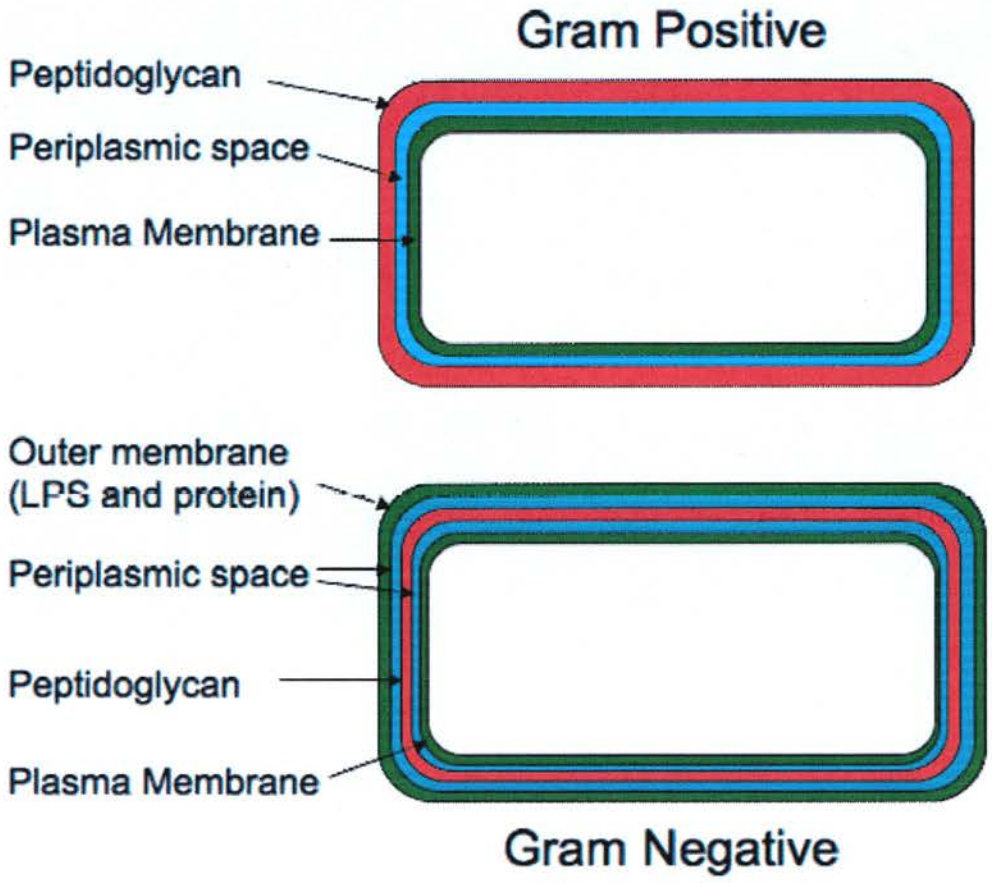

Figure 1.5. Schematic Representation of the Structure of Gram Positive and Gram Negative Bacterial Membranes.

Although iNOS expression is undoubtedly important in immune defence mechanisms, the over expression of this enzyme has also been associated with detrimental immune responses, in particular, septic shock (Thiemermann, 1997). Septic shock is a severe condition resulting in vascular collapse and potential death. Murine iNOS and eNOS knock-out models demonstrate increased survival upon

challenge with concentrations of LPS, highlighting a detrimental role for NOS derived NO in this condition (Connelly *et al.*, 2005; MacMicking *et al.*, 1997; MacMicking *et al.*, 1995; Mashimo & Goyal, 1999).

1.1.6.2.3 APOPTOSIS

NO has a paradoxical role in the regulation of inflammatory cell apoptosis, demonstrating both anti and pro- apoptotic effects (Albina & Reichner, 1998; Brune *et al.*, 1998; Mannick *et al.*, 1997; Nicotera *et al.*, 1995). Apoptosis is a highly regulated, cell death process that is critical for the resolution of the inflammatory response (Haslett *et al.*, 1994; Savill, 1997). Regulation of apoptosis occurs through a number of pro- and anti-apoptotic signaling pathways. The balance between these two pathways determines the fate of the inflammatory cell in a cell specific manner. The dual effect of NO in apoptosis can be attributed to both the ability of NO to form a variety of species depending on the redox environment and the ability of these species to interfere with pro- or anti-apoptotic cell machinery. Anti-apoptotic responses have been linked with low concentrations of NO that promote cell survival through cGMP-dependent mechanisms and by direct S-nitrosylation of protein thiols (Brune *et al.*, 1998; Yoshioka *et al.*, 2006). Pro-apoptotic effects are linked with release of high concentrations of NO and in particular, the formation of $OONO^-$ from the interaction of NO with O_2^-, which can induce apoptosis through cGMP-independent mechanisms. Caspase cleavage, upregulation in Bcl-2 family protein expression, inhibition of survival pathway signalling and release of mitochondrial

cytochrome c of have all been implicated in the pro-apoptoic effects of NO and related speices (Taylor *et al.*, 2003; Tejedo *et al.*, 1999; Ward *et al.*, 2000).

Neutrophils are the most abundant cell type recruited to sites of injury or infection in response to inflammatory mediators. When they reach the site, they kill and clear pathogenic organisms or cell debris through release of histotoxic granule contents and the production of ROS. The neutrophil then remains *in situ,* where it rapidly undergoes apoptosis, characterised by cytoplasmic blebbing, chromatin condensation, exposure of membrane phosphatidylserine residues and DNA fragmentation (Haslett *et al.*, 1994; Kerr *et al.*, 1972; Ward *et al.*, 1999a; Wyllie *et al.*, 1980). During apoptosis, the neutrophil membrane is maintained, allowing the retention of the histotoxic contents before clearance by phagocytes (Savill, 1997). In contrast, neutrophil necrosis is a death process in which the cell swells and the membrane ruptures, allowing release of the histotoxic contents and resulting in the exacerbation of the inflammatory response (Haslett, 1997). In conditions characterised by chronic inflammatory reactions such as arthritis, the successful resolution of the inflammatory response is often inhibited, leading to sustained pain and swelling (Wong & Lord, 2004). Agents that promote the resolution of the inflammatory response via the induction of apoptosis are highly sought after as treatments for chronic inflammatory conditions, which are not adequately controlled by conventional anti-inflammatory drugs (Marshall *et al.*, 2007; Rossi *et al.*, 2006; Ward *et al.*, 1999b). The role of NO on the induction of neutrophil apoptosis and in macrophage clearance of apoptotic cells has been one such avenue explored in this regard (Savill, 1997; Shaw *et al.*, 2005; Taylor *et al.*, 2003; Ward *et al.*, 2000). The

complex interactions of NO on apoptotic cell machinery limit the use of NO as pro- or anti-apoptotic therapeutics to promote resolution of inflammation due to the lack of cell-specific apoptotic responses. This need is particularly important in the resolution of inflammation in atherosclerotic plaques, which requires inflammatory cell specific responses to avoid apoptosis of the smooth muscle, which could weaken the fibrous plaque cap and increase the risk of rupture and thrombosis (Shaw *et al.*, 2005).

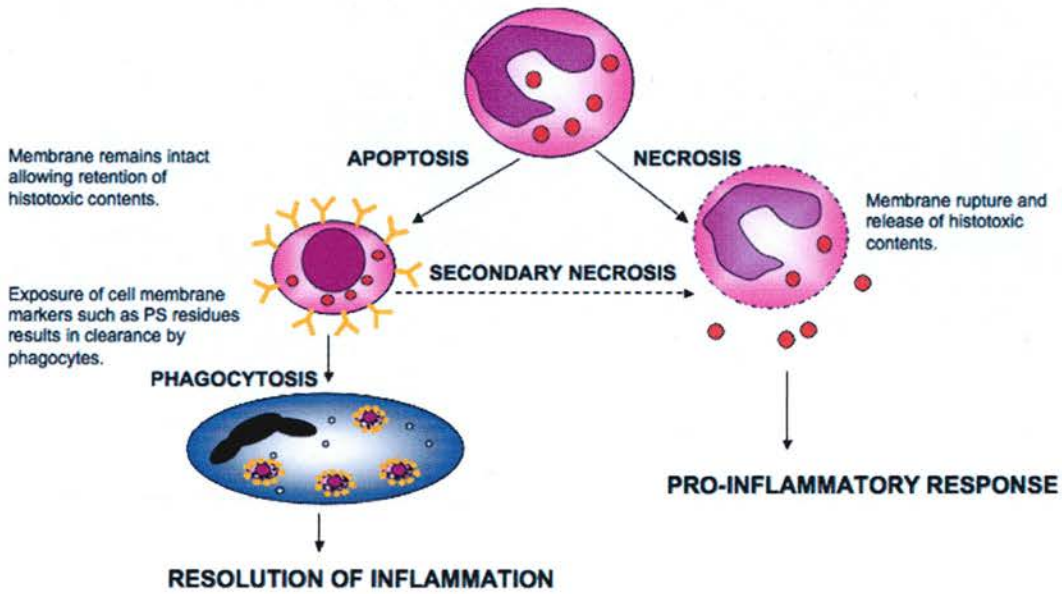

Figure 1.6. Apoptotic and Necrotic death of the Neutrophil.

Necrotic cell death results in rupture of the cell membrane and release of histotoxic contents into the surrounding environment and is thus a pro-inflammatory pathway. Apoptotic cell death allows the retention of histotoxic contents and the clearance of cells by phagocytosis thereby resolving the inflammatory response. When phagocytes are overwhelmed or not present, apoptotic cells will undergo secondary necrosis, releasing the histotoxic contents and further stimulating a pro-inflammatory response.

1.1.6.3 WOUND HEALING.

The wound healing properties of NO are linked with many processes including decreasing bacterial load, angiogenesis, inflammation, collagen formation and cell proliferation (Burrow *et al.*, 2007; Hsu *et al.*, 2007; Luo & Chen, 2005). Murine models deficient in NOS demonstrate a reduced capacity for wound healing demonstrating the importance of NO in this process (Lee *et al.*, 1999; Stallmeyer *et al.*, 2002; Stallmeyer *et al.*, 1999). Systemic and topical therapy with NO-donors has shown improved healing responses in diabetic ulcers (Masters *et al.*, 2002; Schaffer *et al.*, 2007) and burn wounds (Ghaffari *et al.*, 2007; Zhu *et al.*, 2007), highlighting a possible role for NO in the treatment of wounds in patient subgroups that have healing deficiencies and wounds that are not readily accessible to systemic wound healing agents. Furthermore, NO could provide an alternative to conventional antibiotic treatments, which are becoming less therapeutically viable due to increased antibiotic resistant bacterial strains.

1.1.6.4 NERVOUS SYSTEM

NO synthesised by nNOS acts as a neurotransmitter in the peripheral and central nervous system, where it contributes to the activity of both excitatory and inhibitory NANC neurones The induction of inhibitory NANC neurone activity by NO in the peripheral nervous system produces smooth muscle relaxation in blood vessels (Bennett, 1997; Gumusel *et al.*, 2001), the gastrointestinal tract (Van Geldre & Lefebvre, 2004) and penile tissue (Andersson & Holmquist, 1994; Toda *et al.*, 2005). Expression of nNOS in the CNS is high within the brain, especially the

cerebellum, where NO is suggested to contribute to long-term potentiation and memory formation (Hopper & Garthwaite, 2006; Lee, 2000). The hypothalamus also expresses high levels of nNOS, where NO is implicated in central cardiovascular control functions (Zanzinger, 1999). Many of the effects produced by NO in the nervous system are linked to increases in cGMP through stimulation of sGC, although NO-related species can also stimulate neurotransmission through direct modulations of ion-channels (Ahern *et al.*, 2002; Hare, 2003). Expression of the inducible form of NOS (iNOS) is found in astrocytes, which is suggested to be important for defence against pathogens in the nervous system (Sparrow, 1994).

1.1.7 NO THERAPY

Therapy involving NO can be achieved through manipulation of the NOS;NO;sGC;cGMP signalling pathway. Supplementation of L-Arg increases the substrate for NOS dependent conversion to NO and has improved outcomes in pathologies which are generally associated with decreased NO bioavailability (Boger & Ron, 2005; De Nicola *et al.*, 1997; Wu & Meininger, 2000). NO-independent therapies include sGC stimulators, such as YC-1 and BAY-41-2272 and cGMP analogues (8-bromo-cGMP) that can mimic the effects of NO in platelets and smooth muscle and have therefore been investigated as potential therapeutics for a range of conditions (Boerrigter & Burnett, 2007; Doggrell, 2005; King *et al.*, 1998; Teng *et al.*, 1997). Downstream inhibitors of the PDE enzymes, which prolong the effects of

cGMP, have been successful in the treatment of erectile dysfunction (Corbin *et al.*, 2002; Doh *et al.*, 2002; Kuthe *et al.*, 2002).

Increased NO-production via iNOS implicated in the pathophysiology of septic shock has resulted in the search for specific inhibitors of the iNOS enzyme for potential clinical treatment of septic shock (Cobb, 2001; Rosselet *et al.*, 1998; Salerno *et al.*, 2002).

The addition of an NO-moiety to commonly used drugs to enhance their activity or counteract detrimental side effects associated with their use is an interesting area of NO-based research. NO-aspirins incorporate the NO-moiety through ester linkage with the aspirin molecule and are able to retain their COX inhibiting actions while having the added benefits of reducing gastric ulceration due to release of NO (Turnbull *et al.*, 2006b; Velazquez *et al.*, 2005). The potential for other NO-hybrid drugs include NO linked ACE inhibitors and beta-blockers that could result in more efficient reduction of blood pressure due to the direct anti-platelet and vasorelaxant effects of NO (Martelli *et al.*, 2006). The furoxan derivatives are often utilised in the development of NO-hybrid drugs which require biological activation by plasma components, similar to the organic nitrates and could therefore encounter problems with tolerance (Feelisch *et al.*, 1992; Mu *et al.*, 2000; Turnbull *et al.*, 2006a).

1.1.8 NO DONORS

The discovery of NO in a wide range of physiological processes and the association of reduced NO bioavailability in a number of disease states, held great hopes for the use of NO-based therapies in the treatment of a variety of ailments. However,

clinical treatment options using NO as a therapeutic agent are limited, despite massive research efforts to this end. The major consideration when determining the therapeutic value of NO is delivery. The multifaceted targets of NO mean that obtaining a specific effect for therapeutic benefit is difficult. Furthermore, stablising this labile molecule until it is required for release in the body has also produced challenges. Donors that require activation by tissue factors, help in achieving biological activation, however this method of NO delivery is often associated with tolerance, thereby limiting the therapeutic potential of such agents. Despite this, the use of a variety of structurally diverse classes of NO donating compounds has proved to be invaluable as investigative tools with which to further our understanding of NO physiology and pharmacology. A new generation of NO-releasing materials show promise in offering localised NO delivery for a variety of biomedical applications providing a catalyst for advancement of NO-based therapies in the clinic.

1.1.8.1 ORGANIC NITRATES

Organic nitrates, such as glyceryltrinitrate and isosorbide dinitrate (GTN and ISDN; figure 1.7) have been used for centuries to provide relief from pain associated with angina, however these NO-based therapeutics have significant drawbacks due to the development of tolerance. These drugs cause smooth muscle relaxation, through release of NO moieties in an sGC-dependant mechanism. The mechanism by which organic nitrates are activated is still not fully understood but is known to require biological factors. There have been many candidate molecules implicated in the activation of organic nitrate *in vivo* including cytochrome P450 and glutathione-S-

transferase (McGuire *et al.*, 1998; Simon *et al.*, 1996). More recent data has implicated the mitochondrial aldehyde dehydrogenase (mtADH) enzyme, as a suitable candidate, fulfilling most of the criteria of the physiological GTN-activating enzyme (Chen *et al.*, 2002). Furthermore, inhibition of this enzyme and the subsequent increased generation of O_2^- in mitochondria have also been implicated in the development of tolerance associated with nitrate use (Chen *et al.*, 2002). The oxidative stress concept of nitroglycerin tolerance is becoming more accepted as the central factor predisposing the development of tolerance, as antioxidants, such as folate have produced beneficial effects in regards to alleviating tolerance (Leopold & Loscalzo, 2003; Munzel *et al.*, 2005). Furthermore, increased oxidant stress impacts regulation of down-stream targets of nitrates such as cGMP-degrading PDEs, previously implicated in the development of tolerance (Kim *et al.*, 2001; Munzel *et al.*, 2005).

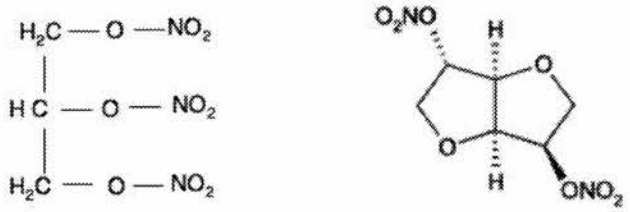

GTN ISDN

Figure 1.7. The structures of GTN and ISDN.

1.1.8.2 S-NITROSOTHIOLS

S-nitrosothiols are compounds with the general formula RS-N=O. These compounds are found endogenously where they are formed from the nitrosation (transfer of NO^+) of reduced thiols. GSNO is an example of an endogenous S-nitrosothiol (figure 1.8), formed from the nitrosation of glutathione (GSH). S-nitrosothiols can transfer the NO^+ moiety to reduced tissue thiols in transnitrosation reactions, a mechanism by which S-nitrosothiols can be transported from extracellular sources into intracellular stores (Zhang & Hogg, 2004). Furthermore, the transfer of NO^+ occurs without the release of NO radical thereby avoiding rapid oxidation or scavenging of NO and prolonging the bioavailablilty of NO. Indeed, the formation of significant pools of S-nitrosylated proteins, such as S-nitrosoalbumin and S-nitrosohaemoglobin has been implicated in prolonged vasodilatory and anti-platelet actions of NO (Crane *et al.*, 2002; Jourd'heuil *et al.*, 2000; Rassaf *et al.*, 2005). Moreover, the circulation of S-nitrosothiols allow for the effects of NO to occur distant from the site of NO production. The mechanism of decomposition of S-nitrosothiol species to release free NO is not well understood, although it is evident that the release of NO is catalysed in the presence of Cu^{2+} (section 1.1.5.4).

Synthetic S-nitrosothiol compounds, such as S-nitroso-N-acetylpenicillamine (SNAP; figure 1.8) and S-nitroso-N-valeryl-D,L-penicillamine (SNVP; figure 1.8) have provided promising therapeutic potential due to the selectivity of these compounds for certain tissues. For example, the vasodilatory actions of these agents *in vitro* have shown selectivity for tissues denuded of endothelium (Megson *et al.*, 1997; Megson *et al.*, 1999; Sogo *et al.*, 2000b). Furthermore, SNVP reduced

adhesion of radiolabelled platelets to areas of endothelial damage in rabbit vessels following balloon angioplasty, without affecting systemic blood pressure (Miller *et al.*, 2003). Thus, these compounds have the potential to target NO therapy to areas of where normal endothelial synthesis of NO is compromised.

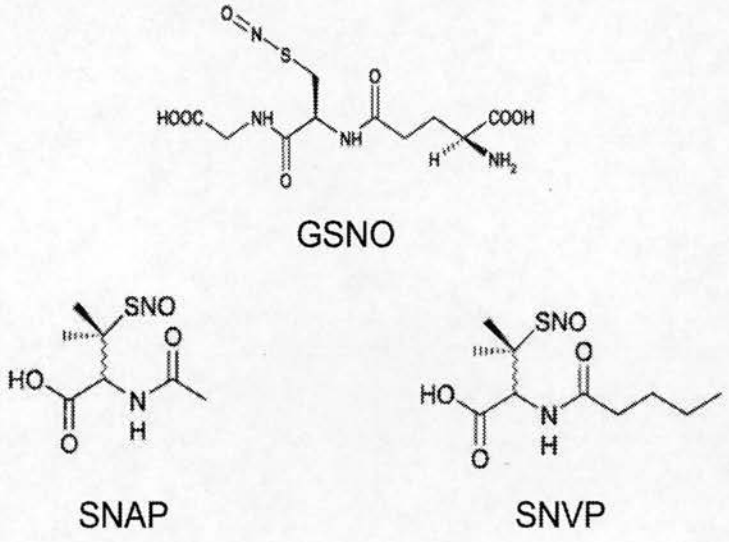

Figure 1.8. The structures of GSNO, SNAP and SNVP.

1.1.8.3 SODIUM NITROPRUSSIDE

Sodium nitroprusside (SNP; figure 1.9) releases it's NO moiety intracellularly upon activation by biological factors (Rochelle *et al.*, 1994). The mechanism of action of SNP in platelets is exclusively dependent upon cGMP formation as inhibition of sGC by ODQ has shown to abolish the functional responses produced by this drug (Sogo *et al.*, 2000a). Clinical use of SNP is limited due difficulties with dose titration and the risk of cyanide poisoning (Friederich & Butterworth, 1995; Papapetropoulos *et al.*, 1996; Wilcox *et al.*, 1990; Zhang *et al.*, 1993).

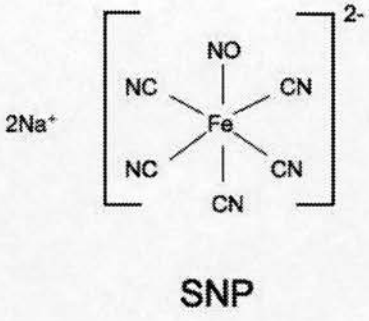

SNP

Figure 1.9. The structure of SNP.

1.1.8.4 SYDNONOMINES AND MESOIONIC OXATRIAZOLES

Sydnonomines and mesoionic oxatriazole derivatives are closely related classes of compounds with similar chemical properties. The active metabolite of the molsidomine precursor, 3-morpholinosydnonomine (SIN-1; figure1.10) was discovered to generate O_2^- concomitantly with NO, resulting in this drug being regarded as an $ONOO^-$ donor rather than a NO donor due to the near instantaneous reaction of O_2^- and NO to form $ONOO^-$ (Feelisch *et al.*, 1989; Noack & Feelisch, 1989). The structurally similar mesoionic 3-aryl-substituted oxatriazole-5-amine derivative, GEA-3162 (figure 1.10), previously considered to be a pure NO donor, has also shown clear evidence that this compound is in fact $ONOO^-$ donor (Taylor *et al.*, 2004). The generation of $ONOO^-$ holds tremendous significance when considering the therapeutic potential of such agents due to the detrimental effects associated with this potent oxidant, especially in inflammatory conditions where $ONOO^-$ has significant modulatory and cytotoxic effects in inflammatory cells (Szabo, 2003; Taylor *et al.*, 2004; Ward *et al.*, 2000).

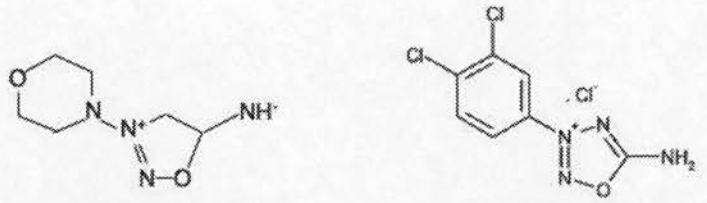

SIN-1 GEA-3162

Figure 1.10. The structures of SIN-1 and GEA-3162

1.1.8.5 DIAZENIUMDIOLATES

The diazeniumdiolate compounds are nucleophile adducts, onto which 2 molar equivalents of NO are bound, hence the acronym, "NONOates". These compounds decompose spontaneously at physiological temperature and pH, thereby bypassing the need for biological cleavage mechanisms and the associated development of tolerance. The rate of NO release occurs following first order kinetics, however, duration of NO release can be altered by varying the nucleophile adduct (Davies *et al.*, 2001; Maragos *et al.*, 1991). A diverse range of compounds exist from short-acting compounds such as diethylamine diazeniumdiolate (DEA/NO; figure 1.11) which has a half-life of approx 2 min, to much longer acting compounds, for example (Z)-1-[2-(2-aminoethyl)-N-(2-ammonioethyl)amino]diazen-1-ium-1,2-diolate (DETA/NO; figure 1.11) which has a half-life of approx 20 hrs. The spontaneous yet predictable rate of decomposition of NONOates in physiological solutions has provided researchers with excellent tools with which to investigate NO physiology and pharmacology. However, there are still significant barriers to their use in the clinical setting, due to the non-specific targets of NO delivered in this

fashion. Untargeted NO therapy is inappropriate for most conditions due to significant reduction in blood pressure caused by widespread vasodilation. Localised NO delivery systems, including incorporation of tissue specific activators (Chakrapani *et al.*, 2007a; Chakrapani *et al.*, 2007b) or the tethering of NONOates onto medical grade materials have significant potential in achieving clinically viable NO based therapeutics (Reynolds *et al.*, 2006; Smith *et al.*, 1996).

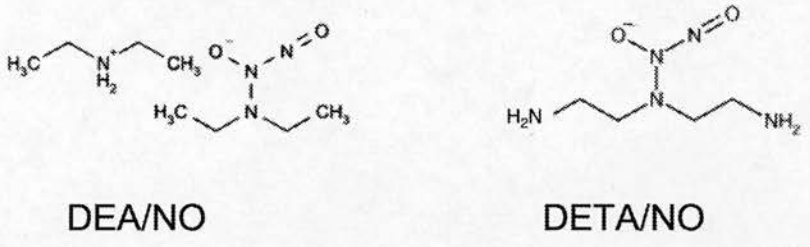

Figure 1.11. The structures of DEA/NO and DETA/NO.

1.1.9 NO-RELEASING MATERIALS

The development of new NO donating therapies relies on the ability to localise the effects of NO to areas of need. The recent development of NO-releasing materials shows exceptional promise in overcoming the barrier to the successful use of NO in biology and medicine.

1.1.9.1 N-DIAZENIUMDIOLATE BASED NO-RELEASING POLYMERS

Many varieties of NO-releasing polymers have been developed, most of which incorporate well-known NO donors such as the NONOates or S-nitrosothiols. The diazeniumdiolates in particular have been the main types of NO donor utilized in the

development of NO-releasing materials (Annich *et al.*, 2000; Jun *et al.*, 2005; Keefer, 2005; Reynolds *et al.*, 2006; Shin *et al.*, 2004; Shin & Schoenfisch, 2006; Smith *et al.*, 1996; Zhang *et al.*, 2002; Zhang *et al.*, 2003; Zhou & Meyerhoff, 2005). The spontaneous decomposition of these compounds in physiological conditions makes them an attractive candidate. Many species of NONOate have been used, each with different, yet predictable rates of NO release, allowing for the optimisation of NO release capacities. The method of incorporating the donor compound can be achieved in a number of ways, and the fundamental differences in these methods impacts on the NO release properties of these polymers. This provides another variable for the adjustment and optimisation of NO release from these materials. Smith and co workers were the first to demonstrate the incorporation of NONOates into polymers through 3 different methods described; (1) low molecular weight donor compounds dispersed into the polymer structure (2) donor molecules attached to the polymer backbone using lipophilic polymer pendant side-chains and (3) the amine group of the donor covalently bound directly onto the polymer backbone (Smith *et al.*, 1996; figure 1.12). The covalent attachment of the donor results in the amine by-product of the NONOate decomposition to remain bound to the polymer, an attractive result considering the potential carcinogenic effects of some nitrosoamine by-products (Mowery *et al.*, 2000; Ward *et al.*, 2000). However, the diffusion of the full donor molecule into the local area, as seen with methods 1 and 2, may also prove beneficial in circumstances where NO therapy requires deeper penetration of tissues. The use of diazeniumdiolate substrates, which are benign if nitrosated, are a potential solution to the use of diffusible NO donors in these

materials and the PROLI/NO compound is one such example that uses proline, a common amino acid residue, as the nucleophile adduct. The use of pendant side chains that vary in length and can incorporate 'protecting' groups that are required to be conformationally changed to allow release of the NO moiety. Such methods have been shown to alter the availability of the NO donor compound for reaction and this subsequently influences the NO release kinetics. For example, the release of NO from a diazeniumdiolated poly(vinyl chloride) (PVC) synthesised using the O(2)-alkylated diazeniumdiolate of piperazine as a linker, was shown to be very slow due to the slow rate of hydrolysis of the O(2)-protecting group (Frost *et al.*, 2005). As well as the method of preparation, the variety of polymer used can also impact NO storage and release capacities. There are hundreds of commonly used polymers with ranging porosity and/or hydrophobicity which can be utilised to develop materials that release NO for a wide range of time periods. Biodegradable polymers have also been considered (Chaux *et al.*, 1998). Polymer filler particles, such as polyethyleneimine (PEI) microspheres and fumed silica particles that can be entrapped in the pores of the polymer have also been used as carriers of diazeniumdiolate compounds (Pulfer *et al.*, 1997; Zhang *et al.*, 2003). The investigation of a diverse range of materials with an equally diverse range of NO releasing capacities provides promising avenues of research for the outcome of providing the long-awaited, successful use of diazeniumdiolates in a clinical setting.

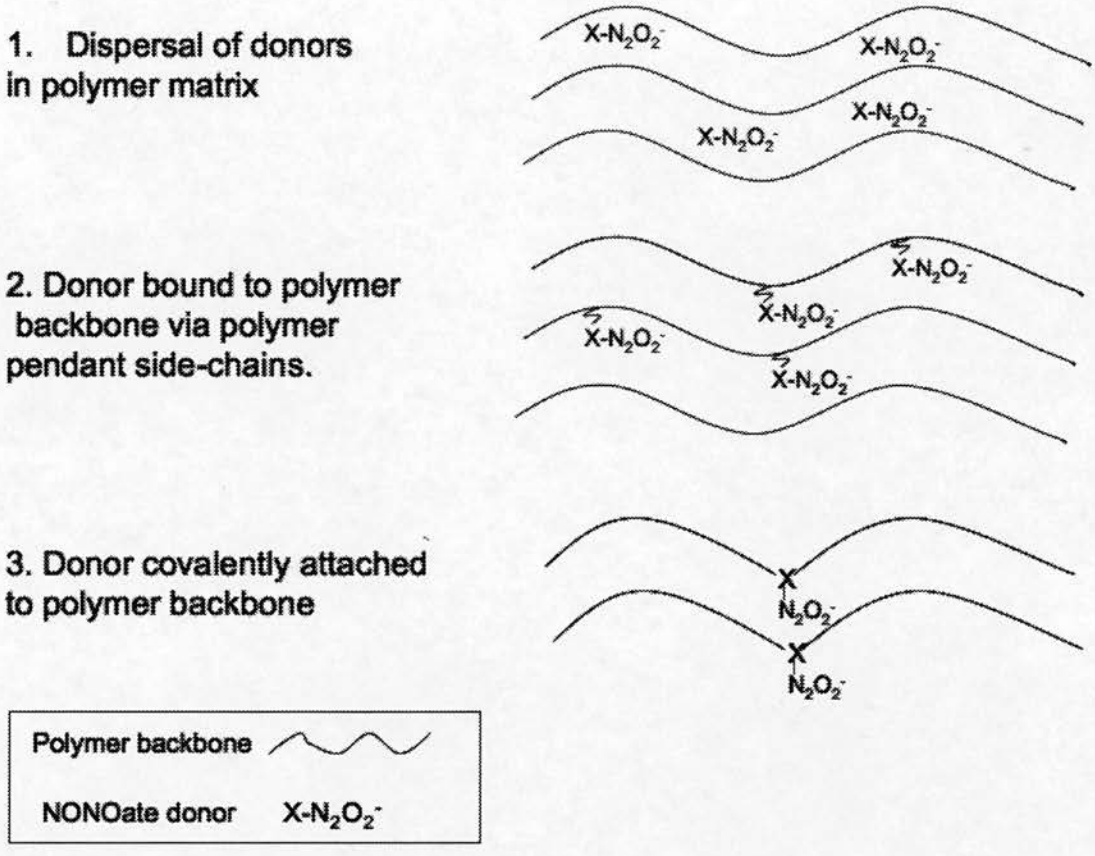

Figure 1.12. Representation of the different methods NONOate compounds can be incorporated into polymer matrices. Adapted from Smith et al. 1996.

1.1.9.2 S-NITROSOTHIOL BASED NO-RELEASING POLYMERS

S-nitrosothiol based NO-releasing polymers release their NO-moiety via 3 different mechanisms. Copper mediated decomposition requires Cu(II) to be reduced to Cu(I), which then reacts with the S-nitrosothiol to release the NO moiety. The endogenous presence of ascorbate and free thiolate in the body is sufficient to reduce Cu(II) to catalyse the decomposition of S-nitrosothiols, however the reaction of S-nitrosothiols with high mM concentrations of the reducing agent ascorbate can directly release NO with the formation of free thiol and dehydoascorbate. The third mechanism is homolytic cleavage of the S-NO bond by light, releasing NO and

producing disulphide bonds from the substrate thiols (Seabra *et al.*, 2005). The light capable of producing this effect is in the range of 330-350nm and 550-600nm. Several polymers have been developed which incorporate covalently linked S-nitrosthiol compounds to the polymer backbone to prevent leaching of the donor or its by-products (Shishido & de Oliveira, 2000; Shishido *et al.*, 2003). The S-nitrosothiol compounds can also be blended into the polymer matrix or, like the diazeniumdiolates, can be tethered to surface of polymer fillers (Frost & Meyerhoff, 2005). The fundamental limitation of the development of non-covalently linked S-nitrosothiol based polymers, is the potential leaching of the water-soluble S-nitrosothiol or its by-products, a situation that would be exacerbated under physiological flow conditions. As with the diazeniumdiolate-based polymers, the ability to produce a range of materials with a range of NO release capacities exists. The light sensitivity of S-nitrosothiol decomposition provides a unique approach to the regulation and activation of NO release from these polymeric materials. Work by Etchenique et al demonstrated a photoinitiated release of NO from monolayers of nitrosated dithiothreitol attached to gold surfaces (Frost *et al.*, 2005). The flux of NO could be increased with the use of increasing power of the light illuminating the surface. The desirable temporal and spatial control of NO release was limited in this study due to the small initial reservoir of NO available in the monolayers. Indeed, the initial NO reservoir is the major limiting factor for the development of all NO releasing materials which at present can only sustain NO fluxes for hours to days. More durable and longer lasting NO release capacities are required for more permanent fixtures such as vascular grafts and stents which would benefit from NO

release throughout the life-time of the device (weeks to years). The potential answer to this lies in utilising endogenous nitrite or S-nitrosothiol in the blood for catalytic reduction to NO through contact with copper complexes embedded in lipophilic materials (Oh & Meyerhoff, 2004, 2003). These materials rely on sufficiently high, endogenous levels of reducing agents such as ascorbic acid, cysteine or glutathione for the catalytic reduction of Cu(II) to Cu(I). Ascorbic acid is readily given in Vitamin C supplements and could easily be used in parallel with such materials to aid in the continual reduction of Cu(II) and continual production of NO from the surface of the materials. Free thiols immobilised in polymers have also been shown to generate NO through exchange reactions with circulating nitrosothiols such as S-nitrosoalbumin, which then spontaneously decomposes to release NO (Duan & Lewis, 2002; Gappa-Fahlenkamp *et al.*, 2004; Gappa-Fahlenkamp & Lewis, 2005). The decomposition of the S-nitrosothiol at the surface of the material leaves behind the original immobilised thiol, which can go through the same reaction, thereby producing NO indefinitely. An L-cysteine immobilised on the surface of such a material has shown to release physiologically relevant levels of NO capable of inhibiting platelet adhesion *in vitro* (Duan & Lewis, 2002).

1.1.10 BIOLOGICAL APPLICATIONS OF NO-RELEASING MATERIALS.

The controlled, localised delivery of NO might constitute the magic bullet in the development of NO based therapeutic for some applications. The diverse targets of NO in the body and the development of materials with wide-ranging NO release

capacities has potential for use in many biological applications. Such applications for these materials include; anti-thrombotic surfaces for blood contacting medical devices, wound healing promoters/dressings and antimicrobial agents.

1.1.10.1 BIOCOMPATIBLE COATINGS FOR MEDICAL DEVICES

Medical devices that come into contact with blood (cannulae, catheters, coronary artery and vascular stents, vascular grafts, extracorporeal loops and renal dialysis equipment) can promote thrombus formation at the surface that can both interfere with the working of the instrument and have the potential to cause severe complications for the patient. There is a current requirement for aggressive systemic anti-coagulant treatments in patients undergoing interventional procedures, however the use of such agents comes with risks, especially haemorrhage, which can be fatal. The production of biocompatible coatings that can bypass the need for systemic anti-coagulants, and are able to resist thrombus formation are a very desirable prospect. The potent anti-platelet effects of NO make it a good candidate for anti-thrombotic coatings, as does its short half life *in vivo,* which provides an unrivalled localised action and should avoid unwanted systemic side effects. Further to this, the beneficial effects of NO on inhibition of inflammatory cell activation and smooth muscle proliferation make it even more attractive for use on deices, which are associated with vascular insult. Vessel damage caused by balloon angioplasty is known to trigger smooth muscle proliferation and result in narrowing of vessels caused from neointimal hyperplasia (Holmes, 2001). Restenosis of vessels following this procedure is a significant problem, with 20-30% of all stent implant sites

showing stenosis with the need for repeat angioplasty treatment within 1 year (Pearce & McKinsey, 2003). The mechanisms of restenosis and subsequent stent failure are related to smooth muscle proliferation and migration occluding the lumen of the vessel (Hamon *et al.*, 1998). Current drug-eluting stents (DES), which incorporate drugs into the stent coating, have shown to be successful at reducing restenosis compared to bare metal stents (Cheng-Lai & Frishman, 2004; Htay & Liu, 2005; Thanigaraj *et al.*, 2006; Young, 2007). However, the long-term efficacy of these stents is unknown. Late adverse effects include aneurysm formation and hypersensitivity reactions, as well as subacute and late stent thrombosis requiring compliance with anti-platelet therapy for extended periods of time (Gurbel *et al.*, 2007; Stabile *et al.*, 2004; Virmani *et al.*, 2004). It is suggested that DES, which inhibit smooth muscle cell proliferation and migration also inhibit the long-term re-endothelialisation of the surface of the material which reduces its biocompatibility compared to bare metal stents in longer time-scales (Luscher *et al.*, 2007). NO-releasing polymers have been proposed as suitable candidates for stent-based therapies, which inhibit thrombosis, neointimal hyperplasia and promote re-endothelialisation (Sarkar *et al.*, 2006). Animal models of stent based NO-delivery has already shown to be effective at reducing the incidence of neointimal hyperplasia in a pig carotid artery overstretch model (Hou *et al.*, 2005; Yoon *et al.*, 2002), reducing thrombus formation in a sheep model of arteriovenous bridge grafts (Fleser *et al.*, 2004) and limiting restenosis in a rabbit model (Do *et al.*, 2004).

1.1.10.2 ANTI-MICROBIAL AGENTS

Medical devices, especially urinary catheters, contribute to a large proportion of nosocomial infections, which are a significant cause of morbidity and mortality within immuno-compromised, hospitalised patients (Karchmer *et al.*, 2000; Warren, 2001). Furthermore, infections acquired due to device placement increases the duration of hospitilisation and therefore impact unfavourably on healthcare budgets (Plumridge & Golledge, 1996).

The liberation of NO from polymer materials has shown to increase biocompatibility of medical devices as anti-infective coatings. A range of experiments has demonstrated reduced bacterial adhesion onto NO-releasing polymer materials compared to the NO-free controls (Nablo *et al.*, 2001; Nablo *et al.*, 2005a; Nablo *et al.*, 2005b; Nablo & Schoenfisch, 2004). Susceptibility to the anti-adhesive properties of NO-releasing polymers varies considerably between different strains of bacteria. Furthermore, the anti-adhesive properties of NO-releasing polymers, although significant, have not shown complete resistance to colonisation by any bacterial strain studied. The reduced ability to adhere is not the only factor in bacterial virulence. Many device-associated infections result from the introduction of pathogens from external sources, which can migrate to tissues independent from the area of device placements (Pittet *et al.*, 1999). Thus, a direct bactericidal effect would be more favourable, especially when considering the limited NO reservoirs stored by polymer materials, which when exhausted, provide no protection against bacterial colonisation. Currently, device-associated bacterial infections are treated with antibiotics. Given the worrying increase in antibiotic resistant strains of

bacteria, particularly within hospital environments, alternative protocols are urgently required to manage device-associated infections. NO and NO-related species have demonstrated microbicidal effects against various pathogenic organisms (Ascenzi *et al.*, 2003; Coban *et al.*, 2003; Karupiah & Harris, 1995; McMullin *et al.*, 2005; Rementeria *et al.*, 1995). Current NO-release polymers have not demonstrated microbicidal effects most likely due to low fluxes of NO that are in the picomolar range. Thus, higher capacity NO-releasing materials may provide better protection against device-associated infections, although NO-related toxicity to host tissue would be a concern (Nablo & Schoenfisch, 2005).

1.1.10.3 WOUND HEALING PROMOTORS

NO has been proposed to be involved in wound healing (see section 1.1.6.3). The use of NO in wound dressing to promote healing has become possible using NO-releasing polymers and gels, which deliver NO topically at the site of the wound. Accelerated wound repair was demonstrated in rat cutaneous wounds using an S-nitrosoglutathione-containing hydrogel material and polymers incorporating NONOate compounds (Amadeu *et al.*, 2007; Shabani *et al.*, 1996) Topical NO-release for diabetic wound healing has received particular attention due to the difficulty associated with skin healing in these patients. Animal models of impaired healing have also shown benefits from NO-supplementation from engineered dressings (Masters *et al.*, 2002). Promising results from animal models have resulted in recent human trials using NO-releasing dermal patches for the treatment of diabetic foot ulcers (Silva *et al.*, 2007).

1.2 ZEOLITES

Zeolites are naturally occurring and synthetic aluminosilicate crystalline structures endowed with unique adsorptive, ion exchange, gas storage and catalytic properties that have multiple uses in industrial, agricultural and medical applications. Hundreds of zeolite structures exist, with unique pore sizes and physiochemical properties. These materials are often referred to as "molecular sieves" due their ability to separate molecules depending on their size, shape or isoelectric point (pI). The ion exchange properties of these materials are most notable in the washing powder detergent industry where the act to soften the water through the release of zeolite bound alkali metals, such as potassium or sodium in exchange for "hard" ions such as calcium and magnesium from the water. It is in this arena that zeolites are produced in 1M tonne quantities annually. Ion-exchange properties of zeolites have also been utilised to clean-up polluting metal ions and nuclear isotopes from industrial waste effluent and fall-out (Hui et al., 2005; Mumpton, 1999). The adsorptive properties of zeolites are further utilised for environmental benefit in the removal of atmospheric pollutants (eg $NO_{(x)}$) from exhaust fumes (Gomez-Garcia et al., 2005; Rudolf et al., 2002; Sultana et al., 2000). The catalytic properties of zeolites also have indirect benefits on the environment due to their ability to improve energy efficiency of chemical reactions, for example in petroleum refining (Mumpton, 1999). Indeed, the majority of zeolite applications have been spawned from environmental concerns. Currently, the hydrogen gas storage abilities of these structures are being investigated in an attempt to provide more environmentally

friendly energy sources to replace wasteful and toxic electrochemical fuel cells (Li & Yang, 2006; Regli et al., 2005; Rosi et al., 2003).

In this thesis, the zeolite structure Linde Type A (LTA; figure 1.13) has been chosen for modification to produce NO-storing and release materials for use in biological settings. Cations are exchanged in to the structure to replace sodium so as to increase the storage capacity for NO, a technique employed to increase the absorption capacity of zeolites for toxic NO_x from exhaust fumes (Sultana et al., 2000).

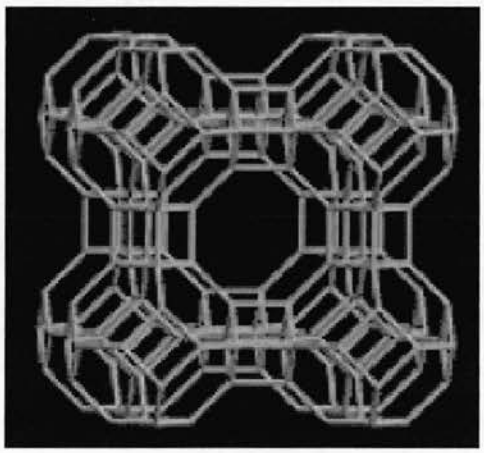

Figure 1.13. Structural representation of zeolite Linde Type-A (LTA).
Figure from the database of zeolite structures. http://www.iza-structure.org/databases/

1.2.1 ZEOLITES IN MEDICINE

Several applications for zeolites exist in the medical arena. These molecular sieves are used in filtration systems for anaesthesia to capture exhaled anaesthetic and provide protection from the potent effects of these drugs to surrounding surgical personnel (Boranic, 2000; Doyle *et al.*, 2002; Janchen *et al.*, 1998). Zeolites are also incorporated into dialysis systems as filtration materials and as contrast materials in NMR imaging (Boranic, 2000). Zeolites are also utililised as hemostatic agents in

emergency field medicine. The success of these materials has resulted in the FDA approval of Quikclot®, a zeolite incorporating hemostatic dressing, which improves the coagulability of wounds due to the filtration of water molecules from the blood, leaving the larger platelets and clotting factors at the wound site in concentrated amounts (Gurdeep *et al.*, 2006). However, similar dressing have resulted in thermal injury due to the exothermic reaction related to the powerful desorption of water at the wound site (McManus *et al.*, 2007; Wright *et al.*, 2004).

As well as the external uses, zeolites have potential in internal therapies as delivery agents. Vitamins (Boranic, 2000) , antioxidants (Ivkovic *et al.*, 2004) and drugs have been loaded into encapsulated zeolite materials for delivery in the gastrointestinal tract. Anthelmintic drugs have shown improved efficacy in animal models due to slow release kinetics achieved from drug-loaded zeolite materials (Dyer *et al.*, 2000). The low solubility of these materials at physiological pH means that internal delivery would be on a par with clay-eating, a commonly used therapy (Boranic, 2000). However, potential detrimental side effects from ion exchange, including changes in pH, effects on bacterial flora and possible cytokine release needs better characterisation in animal models. Interestingly, the immune stimulatory effects of zeolite powders have shown anti-metastatic effects in cancer cell lines and animal models of cancer. This has been attributed to the ability of the powder to stimulate expression of tumor suppressor proteins and inhibit protein kinase pathways, thereby limiting tumor growth (Pavelic *et al.*, 2001). The applications described involve the use of pure zeolite materials, most commonly found in powdered form. The tethering of zeolites onto medical grade devices as a mixture with commonly used

polymers might therefore bypass the stimulation of inflammatory responses seen with powdered formulations and provide a unique method for the use of zeolites in a clinical setting.

1.2.2 NO-LOADED ZEOLITES

The use of zeolites as NO gas storage materials requires the structure to contain transition metal ions, which have a high affinity for NO. The structure is such that one molecule of NO can bind to each metal ion within the structure. This capacity for NO storage in these zeolites is remarkable at up to 1mmols of NO per mg of zeolite (Wheatley *et al.*, 2006). The delivery of NO from zeolite structures occurs on contact with aqueous media through the displacement of NO by H_2O. Thus, zeolites provide a simple mechanism for NO delivery, which does not require chemical decomposition or the presence of reducing compounds such as thiols. Furthermore, zeolites are highly tunable compounds with the scope to optimise NO storage and release properties through very easy adjustments to various aspects of zeolite design. For example, the transition metal exchanged in the structure has an impact on the amount of NO stored, likely due to alterations in pore size through electrochemical interactions of the ions with the zeolite structure as well as the chemical attraction of the metal for NO itself. Zeolites used in this thesis are bound in a polymer to make a more robust structure for use in biomedical applications. The choice of polymer, of which there are many, may also have an impact on NO storage and release. The hydrophobicity of the polymer material may limit the H_2O reaching the zeolite thereby acting to limit and prolong the release of NO from the structure, particularly

beneficial for applications that require small fluxes of NO release over long periods of time such as stent coatings. To this end, changing the composition of zeolite with the polymer binder also provides an easy way to manipulate the amount of NO present in the original reservoir and therefore limit or increase the total amount of NO released. The production of NO-loaded zeolites has benefits over similar NO-releasing materials, which require multi-step processes involving high pressures, high temperatures or a low pH environment for the efficient loading of NO to the structure. The stability of zeolites at room temperature also holds benefits over other NO releasing materials which not only require argon storage but freezing temperatures to remain stable (Robbins *et al.*, 2004). Thus, zeolites provide an affordable, dynamic and simple means by which NO can be stored and released for a wide range of biological applications.

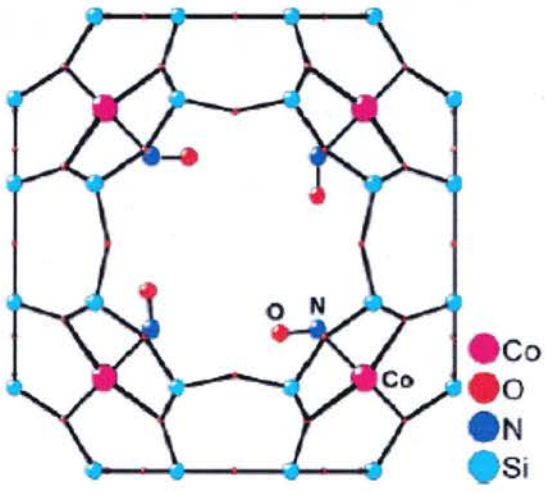

Figure 1.14. Structural representation of NO-storing Co^{2+}-exchanged zeolite. Wheatley *et al.* 2006.

Structure of the cobalt-NO complex in LTA zeolite. The cobalt is bound to three oxygen atoms of a six-ring unit in the zeolite framework and bond to nitrogen of a bent mononitrosyl ligand. Wheatley *et al.* 2006.

1.3 PROJECT AIMS AND HYPOTHESES

The aim of this thesis is to characterise and optimise the first prototype NO-loaded zeolite designs in biological experiments that assess the functional activity of these materials in *in vitro* assays relevant to the development of zeolites as biocompatible coatings for medical devices. Assays include platelet aggregation, neutrophil activation and bacterial growth to assess the potential anti-thrombotic, anti-inflammatory and microbicidal properties of NO released from zeolite materials. In concert with these experiments, NO-loaded zeolites were investigated as novel tools with which to investigate various aspects of the mechanism of action of NO.

Thus, the hypotheses for this study are as follows:

1. NO-loaded zeolites are high capacity storage materials of NO with tunable properties that allow NO-storage capacities to be easily altered.
2. NO-loaded zeolites are powerful inhibitors of collagen-induced platelet aggregation in human platelet samples and are thus, suitable candidates for the development of anti-thrombotic coatings for medical devices.
3. NO-loaded zeolites will stimulate NO-mediated sGC-independent mechanisms in platelets and smooth muscle due to release of high concentrations of NO into the extracellular environment.
4. NO-loaded zeolites will produce either pro or anti-inflammatory actions in human neutrophils is dependent on the concentration of NO exposed and activation status of the neutrophil.

5. NO-loaded zeolites can induce bacterial killing in Gram-negative and Gram-positive bacterial strains due to release of high concentrations of NO and are thus suitable candidates for the development of anti-infective coatings for medical devices.

CHAPTER TWO

Materials and Methods

2. Methods

2.1 Platelet Aggregation Studies.

2.1.1 Preparation of Platelet Rich Plasma (PRP)

Peripheral venous blood was drawn from the antecubital fossa of healthy human volunteers aged 18-64. All volunteers were non-smokers and had not taken any NSAIDs or other drugs known to affect platelet function within the past 10 days. Blood was collected in 50ml polypropylene (BD Falcon) tubes with sodium citrate (final concentration 0.38%). Platelet rich plasma (PRP) was separated from the erythrocyte/leukocyte layer by centrifugation (300*g*; 25 min) and was carefully aspirated into polypropylene tubes (BD Falcon). Platelet poor plasma (PPP) was obtained by further centrifugation of the PRP (1200*g*; 10 min) to pellet the platelets. The PPP was aspirated from the platelet pellet. The platelet count in PRP samples was determined using a Coulter Ac.T8 Haematology Analyzer (Coulter Electronics, Luton, U.K) and standardised to 250 x 10^9 /l *via* dilution with PPP.

2.1.2 Preparation of Washed Platelets (WP).

PRP was obtained as described above. The platelets were washed by centrifugation (1200*g*; 10 min) in the presence of 300ng/ml prostacyclin to prevent aggregation. The plasma supernatant was aspirated from the platelet pellet and the platelets were re-suspended in Tyrodes buffer (137mM NaCl, 2.7mM KCl, 1.05mM $MgSO_4$, 0.4mM NaH_2PO_4, 12.5mM $NaHCO_3$, 5.6mM Glucose, 10mM HEPES in H_2O at pH 7.4). A further centrifugation (1200g; 10 min) was performed, again in the presence of 300ng/ml prostacyclin. The supernatant was aspirated to remove any remaining

traces of plasma and the platelets were finally re-suspended in Tyrodes buffer with calcium (137mM NaCl, 2.7mM KCl, 1.05mM $MgSO_4$, 0.4mM NaH_2PO_4, 12.5mM $NaHCO_3$, 5.6mM Glucose, 10mM HEPES, 0.8mM CaCl in H_2O at pH 7.4). WPs were then incubated at 37°C for approximately 10 min before use to allow the inhibition of platelet activation by prostacyclin to subside. The platelet count was determined using Coulter Ac.T 8 Haematology Analyzer (Coulter Electronics, Luton, U.K) and standardized to 250 x 10^9 /l *via* dilution with Tyrodes buffer.

2.1.3 Turbidometric Platelet Aggregometry

Platelet aggregation was performed using a 4-channel optical platelet aggregometer (Chronolog, Labmedics, Stockport, UK) and data were captured via an analogue-digital converter (Maclab 4c, AD Instruments, Sussex, U.K.). Turbidometric platelet aggregation was determined by measuring changes in light transmission through test samples (PRP/WP) compared to a reference sample (PPP/Tyrodes buffer). The equipment was calibrated such that the difference in light transmission prior to aggregation between the test and reference sample was approximately 80 mV. Platelet aggregation was stimulated in test samples (500µl; 37°C) using a supramaximal concentration of collagen (2.5µg/ml). The samples were left for 5 min with continuous stirring (1000rpm) to enable maximal aggregation to be reached. Aggregation of the platelets caused a decrease in the voltage corresponding to the increase in light transmission through the test sample compared to the reference sample. The zeolite treatments were achieved by suspending the prepared zeolite discs (see materials section 2.8.1) below the surface of the 500µl sample, ensuring not to interfere with light transmission through the sample or the mechanical stirring.

After variation of the incubation period (1-120 min; 37°C) aggregation was initiated using collagen (2.5μg/ml). Platelet aggregation in test samples was expressed as a percentage of the maximum aggregation determined by stimulation of a control sample plus the stainless steel wire device with 2.5μg/ml collagen at the corresponding time-point.

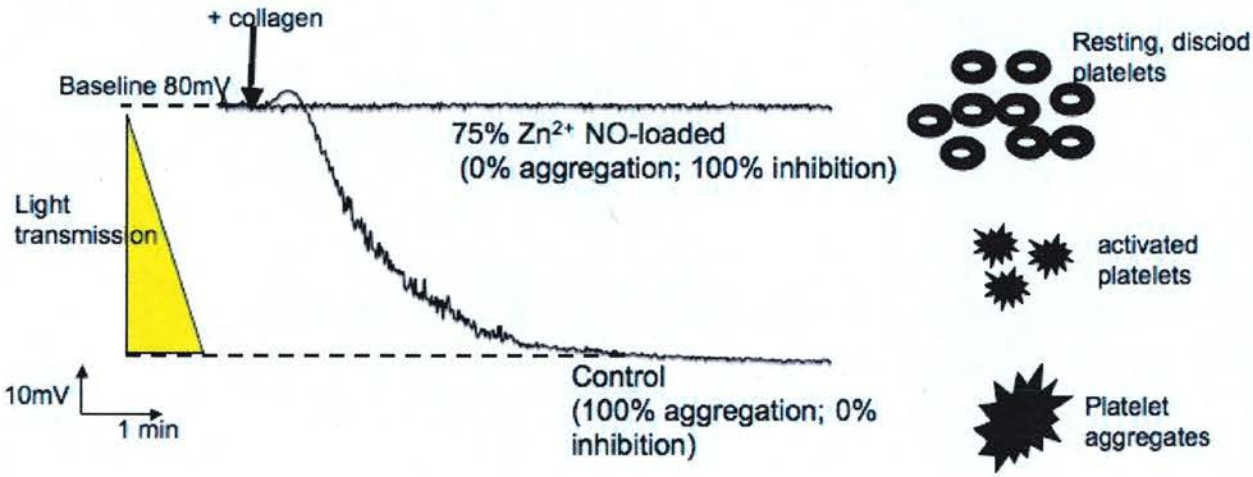

Figure 2.1. Turbidometric Platelet Aggregation.

An example of turbidometric platelet aggregation traces showing the fall from baseline mV values in control platelets (500μl; PRP) following collagen (2.5μg/ml) stimulation and the inhibition of aggregation responses in platelets treated with NO-loaded zeolite (75% Zn^{2+};1 min pre-collagen stimulation). The decrease in voltage is due to activation and aggregation of platelets allowing greater transmission of light through the samples. Maximum aggregation is reached within 5 min post collagen stimulation.

2.1.4 Whole blood aggregometry.

Peripheral venous blood was drawn *via* the antecubital fossa from healthy, non-smoking human volunteers aged 20-65. All donors had not taken any platelet active

agents in the past 10 days. Blood was collected into falcon tubes containing 10U/ml heparin and gently mixed by inverting the tubes 2-3 times. Aggregation of whole blood was investigated using a 2-channel Chronolog aggregometer (Chronolog, Labmedics, Stockport, U.K) and data captured *via* an analogue-digital converter (Maclab 4e, AD Instruments, Sussex, U.K). Aggregation was determined using an impedance electrode, which measures the change in impedance between 2 closely located metal electrodes. A small electrical current is passed between the two metal electrodes and on contact with blood, a monolayer of platelets coat the surface. When an aggregating agent is added, platelets aggregate on the monolayer increasing the impedance (electrical resistance) to the circuit. An increase in impedance is measured as an increase in voltage on the data acquisition system. The electrodes were calibrated such that maximal aggregation caused an approximate 100mV shift in baseline voltage. Aggregation was stimulated using a supramaximal concentration of collagen (2.5μg/ml). Test samples were prepared as follows; the blood was diluted 1:1 using phosphate buffered saline (PBS) and aliquoted into 1 ml samples in a cuvette containing a magnetic stir bar. Samples were incubated at 37°C with stirring (1000rpm) and the electrodes were allowed to reach a steady baseline before stimulation of aggregation. Zeolite treatments were achieved by suspending the discs in the whole blood using a stainless steel holding device and incubation times were varied (1-60 min) before initiation of aggregation by the addition of collagen. Aggregation was expressed as a percentage maximal aggregation of a control sample plus the stainless steel holding device determined after stimulation with 2.5μg/ml collagen at a corresponding time-point

2.2 *Platelet viability; Lactate dehydrogenase (LDH) assay.*

Cytotoxicity of 50% Zn^{2+} zeolites (NO loaded and NO free) to platelets in PRP was investigated using a cell viability measure (LDH) obtained from Roche Applied Sciences (Penzberg, Germany). The test measures the activity of LDH released from the cytosol of damaged cells into the supernatent using a colourimetric assay. Quantification of LDH release is measured by exploiting a two-step reaction in which LDH catalyses conversion of a tetrazolium salt to a coloured formazan salt that absorbs light at 490 nm. Therefore, absorption at 490 nm is proportional to the number of damaged cells. As the assay is colourimetric, the protocol needed to be optimised to find a concentration of platelets in the PRP that gave adequate and representative measures with positive and negative controls that were within the range of the spectrophotometer. To achieve this, several dilutions of PRP (250 $x10^9$ platelets/ml) solutions were tested using a positive control containing 2% Triton X to lyse the cells, negative controls consisted of PPP where the cells had been removed by centrifuation (1200*g*; 10 min). It was found that a 1 in 2 dilution of a 250 x 10^9 platelets/ml (i.e 125 x 10^9 platelets/ml) preparation of PRP with Tyrodes buffer contained adequate cell numbers with which to run the assay.

A 500µl sample of PRP (approx 63 x 10^9 platelets) was incubated with 50% Zn^{2+}-exchanged zeolites (NO-loaded and NO-free) at 37°C for 2 h. Aliquots (100µl) of each treatment were diluted in 100µl Tyrodes and plated in triplicate wells in a 96-well, flat-bottomed microtiter plate. Treatments included NO-loaded and NO-free zeolites, untreated PRP controls, PRP + 2% Triton X (positive controls) and PPP background samples (negative control). The assay reaction mixture was added to

each well and left for 30 min in the dark at room temperature. The plate was then read using a Dynex MRX plate reader (Dynatech Laboratories, Chantilly, V.A.) at 490 nm with prior shaking for 15 s. The absorbance values for each treatment were directly compared after subtraction of the background absorbance obtained from PPP samples.

2.3. Detection of NO

2.3.1 NO electrode

The concentration of NO released from different NO donors was investigated using a 2mm isolated NO electrode (ISO-NOP, World Precision Instruments, Stevenage, U.K) and data captured using an analogue-digital converter (Maclab 4e, AD Instruments, Sussex, U.K). The ISO-NOP electrode measures NO generation in solution *via* electrochemical detection. The electrode comprises a robust working and reference electrode within a stainless steel sleeve, which has a NO gas permeable membrane.

Prior to use each day, the electrode was calibrated by the chemical generation of NO *via* the addition of sodium nitrite (0.32-50μM) in a solution of 0.1M potassium iodide + 0.1M sulphuric acid. This method of calibration is based on the following reaction:

$$2NaNO_2 + 2KI + 2H_2SO_4 \rightarrow 2NO + I_2 + 2H_2O + K_2SO_4 + Na_2SO_4$$

A known concentration of $NaNO_2$ is added to produce NO. The KI and H_2SO_4 are present in great excess and so the limiting factor for the reaction is $NaNO_2$. Since the reaction goes to completion, the equation above states that the ratio between $NaNO_2$ and NO is 1:1. Therefore the amount of NO generated in the solution will be equal to the amount of $NaNO_2$ added.

The electrode is placed in a cuvette with the calibration solution and allowed to reach a steady baseline and then set to zero on the data acquisition system. A change in current (*p*A) is observed when NO is oxidised at the electrode producing a redox current. A calibration curve was generated *via* the cumulative addition of $NaNO_2$ (0.8μM-50μM) in 1ml of the 0.1M KI + 0.1M H_2SO_4 (figure 2.2a). A linear relationship between concentration of $NaNO_2$ and change in current amplitude was observed. These data were plotted and a straight-line equation generated from which concentrations of NO produced during experiments could be calculated (figure 2.2 B). NO electrode experiments were performed in a number of different media including PRP, PBS, 5% LB broth:PBS, WP and isolated neutrophils (see section 2.5.1; 0.5-2ml) for various times (45-120 min). NO generation was investigated by firstly allowing the electrode to reach a steady state in the media before the addition of the NO donor. In the case of the zeolite treatments, the discs were suspended in the solutions using a stainless steel holding device. Each sample was incubated at 37°C and contained a magnetic stir bar, which stirred the solution at 1000rpm for the duration of the experiment. Relevant time-points were selected for analysis and traces of NO release over time were plotted.

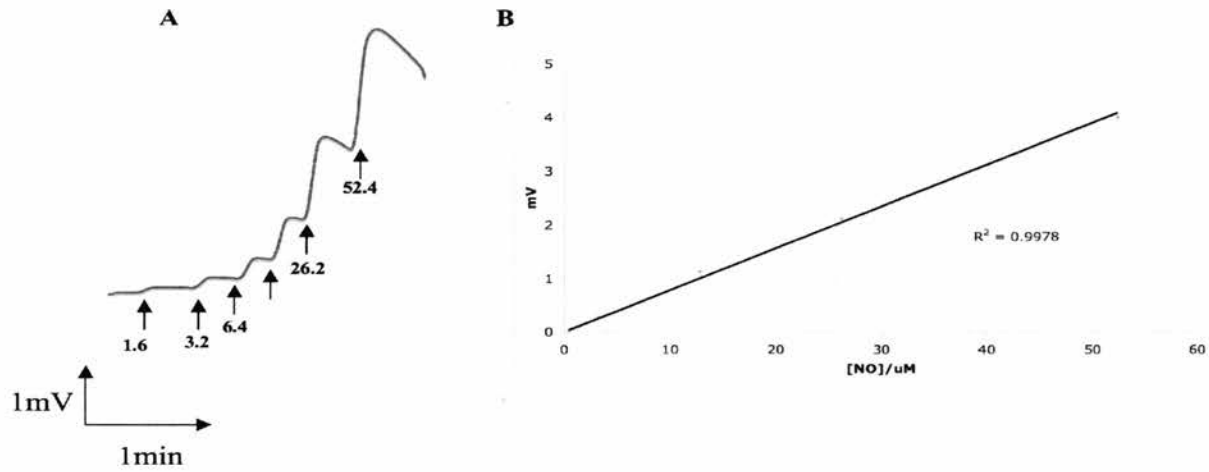

Figure 2.2 NO Electrode Calibration.

An example calibration trace (A) and the corresponding graph (B). The cumulative addition of $NaNO_2$ is indicated by the arrows (μM).

2.4. Fixed Mount Myography

2.4.1 Preparation of rat aorta rings

Male Wistar rats (Charles River laboratories, U.K.) were sacrificed by cervical dislocation and the aorta harvested into physiological buffer solution (Krebs buffer; 118.4mM NaCl, 25mM $NaCO_3$, 11mM glucose, 4.7mM KCl, 1.2mM $MgSO_4$, 1.2mM KH_2PO_4, 2.5mm $CaCl_2$). The tissue was cleaned of fat and adventitia to expose the smooth muscle and cut into ~ 4mm rings for mounting on a fixed wire myograph.

2.4.2 Fixed mount myography

Myography measures the change in smooth muscle tension through a tension transducer connected to wire mounts. The wire mounts are positioned in the lumen of the rat aorta ring and the vascular ring segments were allowed to equilibrate in standard Krebs buffer (37°C; 15 min) under no resting tension. Pre-tension was gradually applied over 30 min to 14mN. The change in smooth muscle tension through the stimulation of smooth muscle contraction or relaxation can then be detected when tension on the wire mounts is either increased or decreased. The change in tension correlates with either an increase or decrease in voltage on the data acquisition system. The myography set-up consists of 4 x 6ml heated tissue baths, containing Krebs buffer. Each bath is constantly bubbled with Carbogen gas (95% O_2; 5% CO_2) throughout the experiment.

Before use in the experiments, the vessels were left to equilibrate at 14mN tension for approximately 1 h. The buffer in the tissue bath was then replaced with Krebs solution containing 60mM of potassium chloride to contract the vessels. This was performed 3 times with a wash out using normal Krebs buffer to allow the vessels to relax back to baseline values. This step is performed to ensure the integrity of the smooth muscle in each vessel with repeats to ensure the maximum contraction is reached. All vessels were required to contract to a minimum of 9mN (~1g) before use in the experiment.

For the investigation of the smooth muscle relaxing properties of NO-loaded zeolites, a dose/response experiment was firstly carried out each day using the smooth muscle

constrictor phenylephrine (PE; 1nM -1μM) in order to calculate the EC_{80} value for the constriction (figure 2.3 A). The EC_{80} concentration of PE was then used to pre-contract the vessels before the addition of any smooth muscle relaxants (figure 2.3 B). Relaxation of the vessels following the addition of acetylcholine (ACh) to pre-contracted vessels was performed to ensure the integrity of the endothelium. Zeolites were placed into the tissue baths so that they were located at the far end of the bath, at the opposite end to the gas inlet. All vessels were pre-treated with the NOS inhibitor, N(G)-nitro-L-arginine-methyl ester (L-NAME) (100μM) to prevent endogenous production of NO. Parallel treatments using the soluble guanylate cyclase (sGC) inhibitor, 1H-[1,2,4]Oxadiazole[4,3-a]quinoxalin-1-one (ODQ; 20μM), and the NO scavenger oxyheamoglobin (Hb; 40μM) were performed to further characterise the relaxant properties of the NO-loaded zeolites. ODQ was left to incubate in the tissue bath for 15 min and Hb left for 1 min before the addition of zeolites.

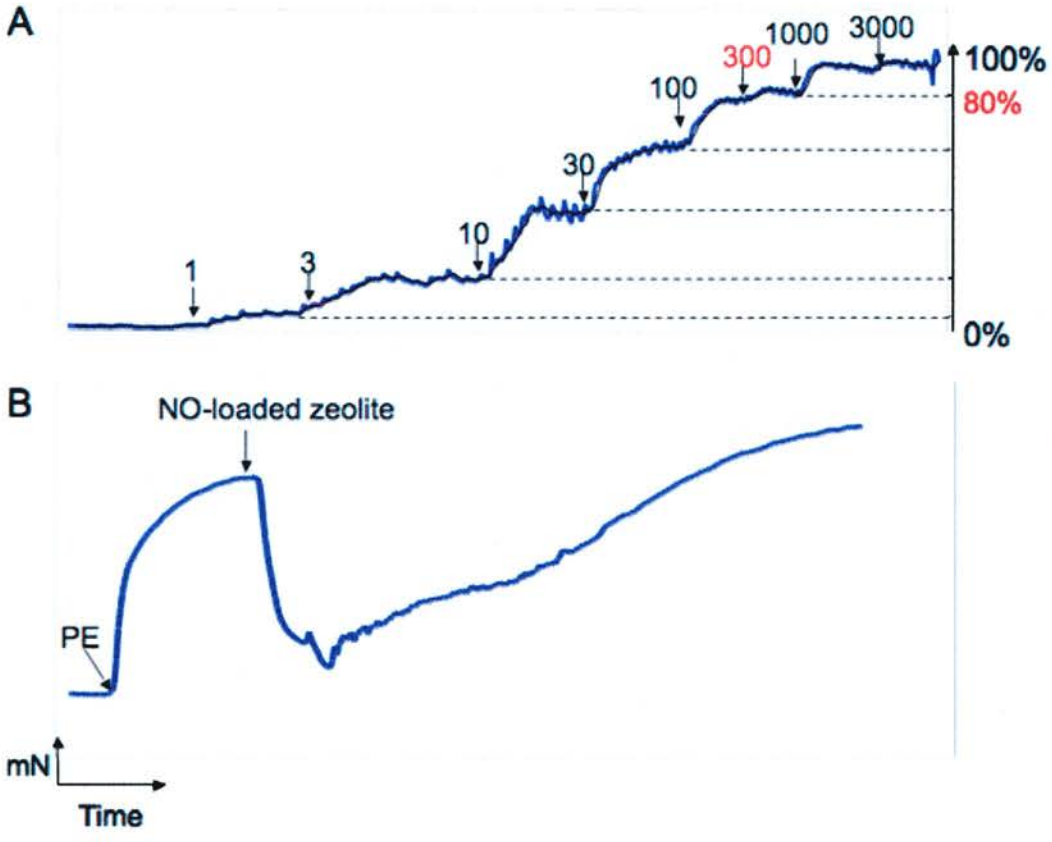

Figure 2.3. Representative myography traces; estimation of EC_{80} of PE (A) and relaxation of smooth muscle by NO-loaded zeolite (B).

The dose/response trace of smooth muscle contraction by cumulative addition of PE (A), showing the estimation of the EC_{80} concentration (red). The addition of PE (nM) is indicated by the arrows.

Trace B is a representative trace showing smooth muscle relaxation following NO-loaded zeolite suspension in a tissue bath containing a PE pre-contracted (EC_{80} concentration; approx 300nM) rat aortic ring.

2.5 Flow cytometry

2.5.1 Isolation of human neutrophils.

Human neutrophils were isolated from peripheral venous blood drawn from the antecubital fossa of healthy human volunteers aged 20-64. All volunteers were non-smokers and had not taken any NSAIDs in the past 10 days. Approximately 40ml of blood was collected into 4 separate 50ml polypropylene tubes (BD Falcon) containing sterile sodium citrate (0.38% final concentration). The PRP was separated from the whole blood by centrifugation (350*g*; 20 min) and aspirated from the leukocyte/erythrocyte-rich layer.

The leukocytes were then separated from the erythrocytes by the addition of 2.5ml of pre-warmed (37°C), Dextran T500 (6%) per 10ml blood cell suspension. Each tube was then adjusted to a 50ml volume with pre-warmed (37°C) saline solution (0.9%) and left for no longer than 30 min to allow the erythrocytes to sediment. The upper leukocyte-rich layer was then aspirated into 2 x 50ml polypropylene tubes (BD Falcon), the volume was adjusted to 50ml with pre-warmed saline (0.9%) and the cell pellet was obtained by centrifugation (350*g*; 6 min). The leukocytes were further separated into sub-populations using Percoll gradients. Isotonic Percoll solution was prepared as a 9:1 (v:v) ratio of Percoll: 10X phosphate buffered saline (PBS) without calcium (Ca^{2+}) or magnesium (Mg^{2+}). This solution was then further diluted with 1x PBS (without Ca^{2+} and Mg^{2+}) to obtain 55%, 68% and 81% isotonic Percoll solutions. Discontinuous gradients were prepared by carefully layering 3ml of 68% Percoll solution on top of 3ml of the 81% solution in a 15ml polypropylene tube (BD Falcon). The leukocyte cell pellet was combined in 3ml of the 55%

solution before being carefully pipetted on top of the 68% layer to complete the gradients. The neutrophils were separated by centrifugation of the gradients (720*g*; 20 min; acceleration and deceleration 0). Following the centrifugation, neutrophils were found at the 68:81% gradient interface and mononuclear cells were obtained from the upper 55:68% interface (figure 2.4). The cells were carefully harvested from the surrounding layers and washed twice in 1 x PBS without Ca^{2+} and Mg^{2+} by centrifugation (220*g*; 6 min).

The cell yield was estimated using a bright line haemocytometer. An aliquot (10μl) of the cell suspension was placed under the cover slip and the number of cells in the central 25 squares was counted by light microscopy (x10 magnification using x10 eye-peice). The total number of cells was then estimated by multiplying back through the appropriate dilution factors and the cells finally were washed (220*g*; 6 min) and resuspended in PBS with Ca^{2+} and Mg^{2+} at 5 million/ml for use in assays. Cell purity was assessed by flow cytometry and samples were excluded if the neutrophil purity was < 95%.

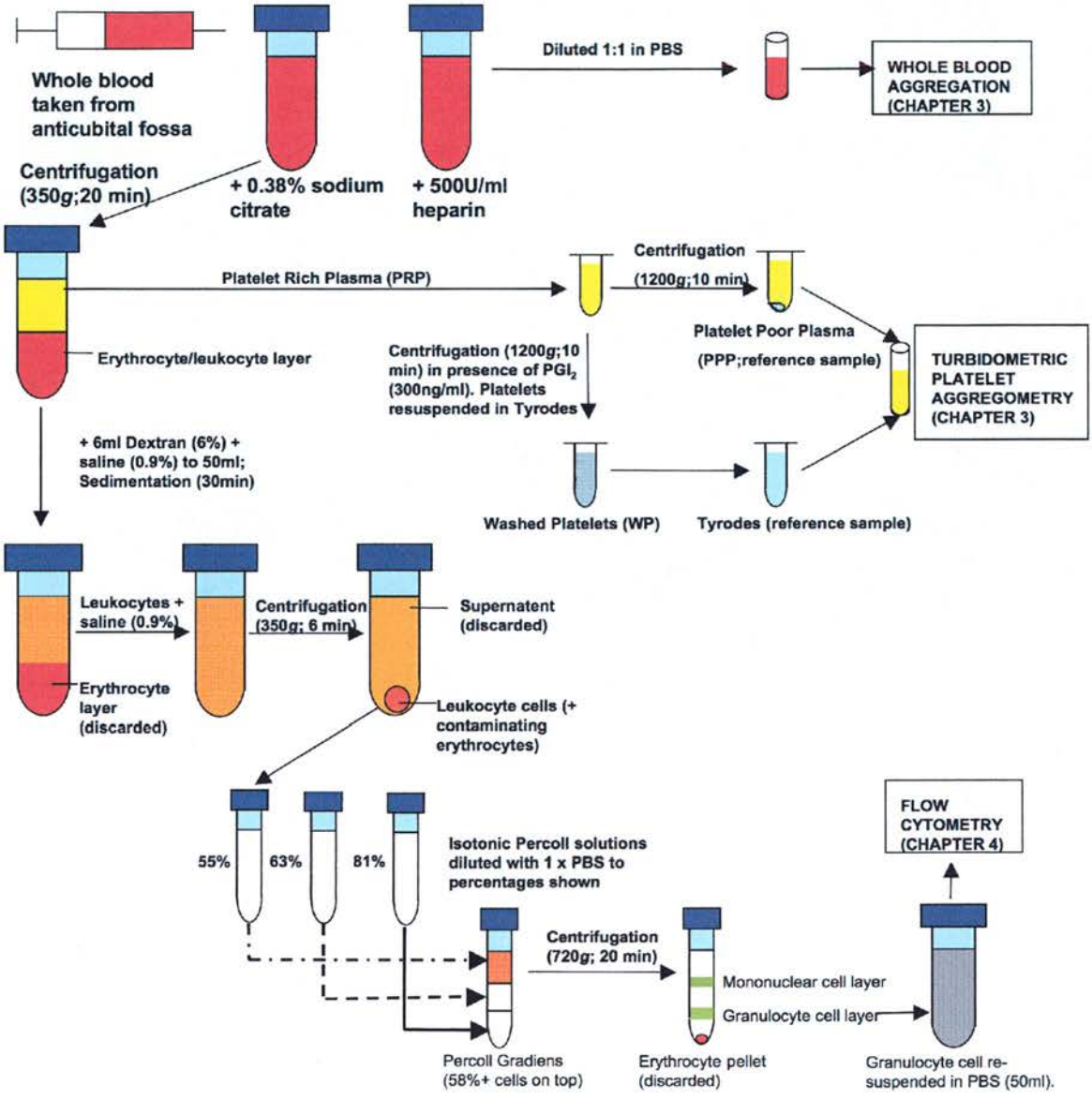

Figure 2.4. Schematic diagram of the separation and preparation of PRP, WP and isolated neutrophils from whole blood and their use within this thesis.

2.5.2 CD11b and CD62L labelled neutrophils.

The effect of NO-releasing zeolites on neutrophil activation markers was investigated using flow cytometry. Flow cytometry is a method of characterising individual cells based on their size, granularity and expression of cell markers using fluorescent agents. Cell suspensions are passed through a laser beam and cells are sorted according to the level of fluorescence and/or the resulting scatter profiles. Neutrophils have a characteristic change in forward scatter (FS) following stimulation with inflammatory mediators such as LPS or fMLP, which corresponds to the change in shape observed when neutrophils are activated. Forward scatter is therefore an indicator of cell shape and size. Side scatter (SS) is used as an indicator of granularity; the greater the side scatter profile the more granular the cell. This can be used to distinguish cell types such as the granulocytes from the mononuclear cells (see figure 4.1). Cell surface changes can be detected by labelling surface markers using fluorescent- conjugates of antibodies raised against them. In this assay, the effect of Zn^{2+}-exchanged zeolites (50% NO-loaded and NO-free) on CD62L shedding and CD11b upregulation was investigated using anti-human CD62L-PE and anti-human CD11b-FITC antibodies. The fluorescent conjugates on these antibodies, phycoerythrin (PE) and fluorescein isothiocyanate (FITC) can be detected through the FL-2 and FL-1 channels of the flow cytometer. The level of fluorescence detected is proportional to the level of surface marker labelled which is in turn dependent upon the activation status of the cell (Russell *et al.*, 1998; van Oostrom *et al.*, 2004). CD62L is involved in low affinity rolling adhesion interactions at the endothelial surface while CD11b is a marker associated with

neutrophil adhesion to endothelial cells at sites of inflammation (see section 1.1.6.2.1).

The samples for flow cytometric analysis were prepared as follows. The zeolites were incubated in 1ml of neutrophils suspended in PBS with Ca^{2+} and Mg^{2+} (5 million/ml; 37°C) for 60 min with stimulation of the cells using the formylated peptide N-formyl-MET-LEU-PHE (fMLP; 10^{-7}M) at 30 min or fMLP vehicle (PBS) for unstimulated controls. The antibodies (BD Biosciences; 6µl) were incubated in 200µl samples of the neutrophil suspension for 30 min at 4°C before analysis by flow cytometry. Flow cytometric analysis was performed using a Coulter FACSCalibur flow cytometer (Beckman Coulter, California, USA) and data were captured using EXPO^{TM} 32 *v* 2.1 analysis software (Beckman Coulter, California, USA).

2.5.3 Neutrophil viability assay; Annexin-V/Propidium iodide (PI) staining.

Flow cytometry was also used to investigate the effect of neutrophil viability after treatment with zeolites using an Annexin-V/PI assay. Annexin-V binds to externalised phosphatidylserine residues on the outer leaflet of the plasma membrane of cells undergoing apoptosis. The Annexin-V for the assay is conjugated to a FITC fluorochrome (Sigma Aldrich), which binds to exposed phosphatidylserine *via* a Ca^{2+} dependent mechanism. Apoptosis is therefore directly related to the fluorescence of the FITC-conjugate, as measured by flow cytometry through the FL-1 channel. Cell death is quantified using propidium iodide (PI) staining, a membrane impermeable

nuclear stain. Only cells with compromised plasma membranes (i.e necrotic cells) will allow the stain to reach the nucleus. PI fluorescence, measured through the FL-2 channel, together with Annexin-V positivity (FL-1 positive cells) can therefore be used to quantify cell death in a population.

The samples for Annexin-V/PI staining were prepared as follows; post zeolite treatments (see above), a 20μl sample of the neutrophil suspension (5million cells/ml in PBS with Ca^{2+} and Mg^{2+}) was taken and incubated (4°C; 10 min) in FITC-conjugated Annexin-V in PBS solution containing 5 mM $CaCl_2$. Following the 10 min incubation, the Annexin-V labelled cells were stained with PI (2μg/ml final concentration) 1 min prior to analysis by flow cytometry. Flow cytometric analysis was performed using a Coulter FACSCalibur flow cytometer (Beckman Coulter, California, USA) and data were captured using EXPO™ 32 *v* 2.1 analysis software (Beckman Coulter, California, USA). Apoptosis and necrosis was measured as a percentage of total gated cells that were Annexin-V positive (FL-1) and Annexin-V/PI positive (FL-1 and 2) respectively. Cells negative for both markers were considered healthy.

2.5.4 Cytocentrifuge Preparations

Cytospins of cell populations (figure 5.1) isolated from whole blood were prepared using 100μl of the cell suspension + 10% autologous serum. The suspension was centrifuged (300rpm; 3 min) through filters onto glass slides. The cells on the slide were allowed to dry at room temp and then stained in methanol (1 min), Quik-Diff Red® (1min) and Quik Diff-Blue® (1 min) and then washed in H_2O. Cells were

analysed for cell purity using light microscopy through an oil immersion lens (X250 magnification).

2.6. Bacterial Culture

Bacteria were cultured on a nutrient broth agar Luria-Bertani (LB) at room temperature. Bacterial suspensions were prepared by inoculating 10ml of LB broth with one colony of relevant bacteria and incubating overnight at 37°C in an orbital shaker. Bacteria were sub-cultured with a 1/100 dilution of the original bacterial suspension and incubated for 3 h to ensure experiments were conducted when bacteria were in the exponential growth phase. The bacterial killing assays required the bacteria to be suspended in a lower concentration of the nutrient broth solution to control the bacterial growth rate throughout the experiment. The bacterial suspension was washed by centrifugation (3000rpm; 15 min) and the bacterial pellet was resuspended in a 5% solution of LB broth in PBS. This step was then repeated once more to ensure adequate washing of the cells. The suspension was standardised via dilution with 5% LB:PBS to an optical density (OD) of 0.1 at 595 nm using spectrophotometry (UV1101, WPA Biochrom Ltd, Cambridge, UK). A 1 in 1000 dilution of this solution (5% LB:PBS) was used for the bacterial killing assays.

Bacterial killing was investigated in varying volumes (150-1200μl) of a 1/1 dilution of the bacterial suspension prepared above. Dilutions were done using 5% LB in PBS solution. The treatments (zeolites and control) were carried out at 37°C on a heated block with shaking at 400rpm for varying times between 2-120 min. For each treatment, the number of viable bacteria was estimated by plating out dilutions of the

bacterial suspension on LB agar plates in triplicate at 10^{-2}, and 10^{-3}. The plates were left to incubate at 37°C overnight at 5% CO_2 for approx 16 h and the number of colonies formed were counted. The number of bacteria present in the suspension post-treatments was estimated, assuming that 1 colony arises from a single bacterium. The number of bacteria at time zero was also estimated each day. Bacterial numbers from treatments were compared as a percentage of bacteria estimated at t=0.

2.7 Statistics

Data were analysed using GraphPad Prism Version 4.0b. Statistical analysis was performed using either one-way or two-way ANOVA with Bonferroni's or Dunnett's post hoc test. Where appropriate, significance was confirmed using a non-parametric Kruskall-Wallis test with Dunns post hoc test. Significance was indicated when $p < 0.05$ at a 95% confidence interval.

2.8 Materials

2.8.1 Zeolite materials.

<u>These compounds are covered by a worldwide patent No.WO 2005/003032.</u>

Zeolite discs were synthesised by Dr P.S Wheatley, Dr B Xiao and Prof. R.E Morris at the University of St. Andrews. Briefly, cations (Zn^{2+} and Co^{2+}) were exchanged into sodium-LTA zeolite using solutions of zinc or cobalt-acetate. Following filtration, the zeolite was ground with either PTFE or PDMS at various weight percentages (i.e 50% zeolite with 50% PTFE) and pressed into 5mm discs (~ 20 mg)

under 2 tons for 30s. Discs were then dehydrated and exposed to 2 atm of a mixture of NO and Helium (10% NO: 90% He) and stored under Argon in sealed Schlenk tubes. NO-free zeolite discs were not exposed to NO and were stored in tubes under normal atmospheric conditions.

2.8.2. Other reagents.

All other reagents were prepared supplied as follows;

Axxora Ltd (Nottingham, UK)

DEA/NO was diluted in 0.01M NaOH, aliquoted (10^{-2}M) and stored (-20°C). Prior to its use each day, DEA/NO was diluted in PBS ($10^{-2} - 10^{-7}$M).

BD-Biosciences (Oxford, UK)

FITC- and APC-conjugated anti-human CD11b, PE-conjugated anti-human CD62L and fluorescent isotypes (IgG1) were purchased from BD biosciences and stored (4°C). All antibodies were used at 6μg/ml final concentration.

Becton Dickinson Falcon (Oxford, UK)

50ml Falcon tubes were supplied sterile.

Bibby Sterlin Ltd (Stone, Staffs, UK)

Bug plates were supplied sterile.

British Oxygen Company (Surrey, UK)

Compressed gas (95% O_2: 5% CO_2).

Charles River (Kent, UK)

Wistar Male rats were housed and terminated according to The Animal (Scientific Procedures) Act 1986 (UK Home Office).

Fisher Scientific (Loughborough, UK)

Triton-X 100.

DMSO.

Buffer salts, EDTA, NaOH, HCl.

General plastics.

GE Healthcare (Amersham, UK)

Dextran was prepared at 6% in 0.9% NaCl and stored (4°C). Percoll was aliquoted (27ml) and stored (4°C). Gradients were prepared by diluting Percoll to 90% stock using 10X PBS and further dilution was using 1xPBS.

Labmedics (Manchester, UK).

Collagen was supplied at 1mg/ml and stored (4°C).

Aggregation and NO-electrode cuvettes and magnets.

Sigma Aldrich, Poole, Dorset

Bovine Heamoglobin (Hb). Met-hemoglobin was reduced to the ferro form by sodium dithionite and excess dithionite removed by dialysis (Martin *et al.*, 1985). Aliquots (1mM) were stored (-20°C) for less than 1 month.

SNP was diluted in PBS and aliquoted (10^{-2}M) and stored (-20°C). Stocks were diluted (10^{-5} – 10^{-7}M) with PBS prior to use each day and protected from light.

General lab solutions (PBS with and without Ca^{2+} and Mg^{2+}).

fMLP was stored (-20°C) in aliquots (10^{-2}M) diluted prior to use in PBS.

FITC-conjugated Annexin-V was stored (-20°C) in aliquots and diluted prior to use in Annexin-V binding buffer (prepared as HBSS plus 5μM $CaCl_2$).

PI was prepared (1mg/ml in H_2O) and stored (4°C) in aliquots, in light shielded containers.

General buffer reagents, KCl, NaCl, $NaCO_3$, KH_2PO_4, glucose were stored (room temperature).

$NaNO_2$ was prepared (10^{-2}- 10^{-5}M) using H_2O prior to use each day.

LB broth and agar was made up according to manufacturers instructions.

Heparin was prepared at 100U/ml in PBS and stored (4°C).

Phenylephrine hydrochloride was stored (-20°C) and diluted in PBS (10^{-2}-10^{-7}M) prior to use.

L-NAME was stored (-20°C) and diluted in PBS prior to use.

Tocris Cookson (Bristol, UK)

ODQ was diluted in DMSO, aliquoted (20mM) and stored (-20°C).

CHAPTER THREE

Optimisation of zeolite design; potential in anti-thrombotic coatings for medical devices.

Chapter 3.

Optimisation of zeolite design; potential in anti-thrombotic coatings for medical devices.

3.1. Introduction

The discovery of NO as an endothelium derived relaxing factor (EDRF) in the 1980s sparked a wealth of research focussed around the involvement of this ubiquitous molecule in a range of biological effects. It is now apparent that this inorganic, free radical is involved in a wide range of physiological and pathophysiological processes including modulation of vascular tone (Moncada & Palmer, 1991; Radomski, 1995) , inhibition of platelet (Hogan *et al.*, 1988; Radomski *et al.*, 1987a, b, c; Vane *et al.*, 1990) and inflammatory cell activation (Granger & Kubes, 1994; Kubes *et al.*, 1993), modulation of immune responses (Albina & Reichner, 1998; MacMicking *et al.*, 1997; Nicotera *et al.*, 1995) and as a neurotransmitter in non-adrenergic non-cholinergic (NANC) synapses. Despite increasing the knowledge of NO physiology and pathophysiology, the translation of massive research efforts into useful clinical therapeutics has encountered substantial barriers. The widespread targets for NO in the body mean that obtaining specific effects for therapeutic value is difficult. For example, the systemic delivery of NO donors for anti-thrombotic purposes would concurrently result in widespread vasodilation and hypotension, which can be potentially fatal. The localised delivery of NO to specific areas of need would avoid

the problem of unwanted systemic side effects as the short half-life of NO in the body ensures that effects are limited to the immediate locality of the site of release. Harnessing the reactive NO radical for localised drug delivery has proved difficult with currently available NO-donor compounds. The diazeniumdiolate NO donor compounds consist of a diolate group [N(O-)N=O] bound to a nucleophile adduct (a primary or secondary amine or polyamine) via a nitrogen atom. Many species of these 'NONOate' compounds have been developed, so called due to the release of up to 2 molar equivalents of NO per mole of compound. The NONOate compounds liberate NO spontaneously, at physiological temperature and pH, with variable, yet predictable, rates of NO release, that are dependent upon the structure of the nucleophile adduct (Keefer *et al.*, 2001). An added benefit of these NO donors is that they do not require decomposition by biological tissues, thereby avoiding development of tolerance associated with the most commonly used NO-based therapeutic, GTN (Feelisch & Kelm, 1991; Feelisch *et al.*, 1988). NONOate compounds have proved beneficial in a number of animal models of vascular diseases including pulmonary hypertension, erectile dysfunction, cerebral vasospasm, yet these compounds are not used clinically (Megson & Webb, 2002). Further characterisation of these compounds in biological systems is required in order to fully evaluate their clinical usefulness and to establish the extent of the problem posed through generation of potentially carcinogenic, nitrosamines (Maragos *et al.*, 1991). The development of NO therapy for anti-thrombotic and anti-proliferative purposes has been a major focus for NONOate and S-nitrosothiol compounds, particularly in an effort to improve outcomes following interventional

procedures such as bypass grafting, balloon angioplasty and stent placement (Keefer, 2005, 2003; Sarkar *et al.*, 2006).

The incorporation of NO donors into polymer or polymer-like matrices has gone some way to avoiding the problem of localised NO delivery. Various groups have demonstrated that the NONOate compounds can be covalently bound to a polymer backbone and NO can be liberated upon contact with aqueous solutions, with the effects persisting for hours to days (Mowery *et al.*, 2000; Parzuchowski *et al.*, 2002; Smith *et al.*, 1996). These NO-loaded polymers have proved efficacious in various biological applications and show promise in the development of coatings for a wide spectrum of blood contacting medical devices including extracorporeal loops, stents and cannulae, all of which could benefit from increased biocompatibility achieved from the inhibition of platelet and inflammatory cell activation and adhesion (Mowery *et al.*, 2000; Nablo *et al.*, 2001; Pulfer *et al.*, 1997; Schoenfisch *et al.*, 2000). In stent research, the multifaceted nature of NO has additional benefits over and above the anti-thrombotic properties due to its ability to reduce smooth muscle proliferation, a major cause of vessel restenosis following stent placement (Hou *et al.*, 2005). At present, the major drawback to the translation of NO-loaded polymers into the clinic is the duration of NO release, which would optimally be in the range of weeks to years rather than the hours to days achieved to date. Furthermore, the leaching of by-products from the polymer backbone is still a major concern. This was shown in a study by Mowery and co workers, who demonstrated measurable levels of nitrosamine following incubation of water-soluble diamine-based diazeniumdiolate incorporating polymers (Mowery *et al.*, 2000).

NO-loaded zeolites provide a novel method for storing and releasing NO for localised therapies that provides a direct source of NO radical, bypassing the requirement for intermediate activation or cleavage mechanisms associated with other NO-donating compounds (see section 1.1.8). Zeolites are micro-porous solids that have impressive gas storing characteristics and are currently utilized in catalytic converters to capture toxic oxides of nitrogen from exhaust fumes in the effort to reduce air pollution (Sultana *et al.*, 2000). The success of these zeolites as storage materials for NO sparked an interest in zeolites as NO-storing and *releasing* materials for use in biological settings. The exchange of sodium for transition metal cations in the zeolite structure greatly enhances the binding capacity of the structure for NO. The advantage of zeolites over other NO-polymers for NO storage and release is the potential to tailor NO release capacities to specific requirements by altering various aspects of zeolite design. These include changing the cation exchanged in the zeolite structure, varying the composition of NO-loaded zeolite to the polymer binder, changing the polymer binder itself and using different types of zeolite, of which there are hundreds, each with unique structures. NO-loaded zeolite materials liberate NO on contact with an aqueous solution, making them ideal candidates for the development of anti-thrombotic coatings for blood-contacting medical devices. Moreover, NO is directly displaced by H_2O to liberate it from the zeolite structure, thereby avoiding possible side-products associated with the zeolite, assuming the zeolite structure remains intact. In this chapter, the NO-release capacities, anti-platelet and smooth muscle relaxant effects of Zn^{2+} and Co^{2+}-exchanged Linde Type A (LTA) zeolites bound in various compositions of polytetrafluoroethylene (PTFE) or polydimethylsiloxane (PDMS) polymer binder

were investigated using *in vitro* techniques. These experiments will form the primary optimisation of the first prototype zeolite designs for the potential development of suitable anti-thrombotic coatings for blood-contacting medical devices. Throughout these experiments, aspects of the mechanism of the anti-platelet and smooth muscle relaxant properties of NO-loaded zeolites were investigated using ODQ, a specific inhibitor of sGC. The classical effects of NO are mostly achieved via the stimulation of sGC resulting in the up-regulation of cGMP production and the subsequent decrease in intracellular calcium concentrations. However, it is now apparent that NO can exert biological effects independent of sGC, particularly in platelets (Crane *et al.*, 2005; Sogo *et al.*, 2000). In addition to the excellent potential zeolites provide with respect to localised NO therapeutics, these materials also offer a unique pharmacological tool with which to investigate various aspects of NO physiology.

Experiments in this chapter were designed to address the following hypotheses:

- Zeolites are high capacity storage materials of NO with tunable properties.
- NO-loaded zeolites are powerful inhibitors of collagen-induced platelet aggregation in human platelet samples and are thus, suitable candidates for the development of anti-thrombotic coatings for medical devices.
- NO-loaded zeolites will stimulate NO-mediated sGC-independent mechanisms in platelets and smooth muscle in a concentration-dependent manner.

3.2. Materials and Methods

3.2.1 Zeolite materials.

Zeolite discs were synthesised by chemists at St Andrews University as described in section 2.8.1. Zn^{2+} and Co^{2+}-exchanged zeolites were used at compositions ranging from 25-75% (weight ratio) of zeolite in polymer binder. Zeolite materials were bound in PTFE polymer unless otherwise indicated. Zeolite:polymer materials were loaded with NO gas, compressed into 5mm discs and stored under Argon gas until ready for use. NO-free counterpart zeolite discs were used as zeolite controls where stated.

3.2.2. Reagents and solutions

All reagents and solutions were purchased from suppliers and prepared for use as described in section 2.8.2.

3.2.3. NO electrode

The concentration of NO released from NO-loaded zeolites (Zn^{2+} and Co^{2+}; 25-75% in PTFE polymer binder) was investigated using a 2mm isolated NO electrode (ISO-NOP, World Precision Instruments, Stevenage, U.K) and data captured using an analogue-digital converter (Maclab 4e, AD Instruments, Sussex, U.K). The electrode was calibrated prior to its use each day as described in section 2.3.1.

The electrode was left to reach equilibrium in 1ml of warmed (37°C) solution (PRP, WP, whole blood, Tyrode's, PBS) prior to the addition of the zeolite disc. The

zeolite was suspended in the cuvette via a stainless steel holding device and the NO-release was measured for 50-90 min. The solution was stirred using a magnetic stir bar at 1000rpm for the duration of the experiment. Time-points were chosen for analyses of NO concentration, which was calculated using linear regression obtained during the calibration as detailed in section 2.3.

3.2.4 Platelet aggregation studies.

Samples of whole blood, PRP or WP were obtained and prepared as described in sections 2.1.1-2.1.4.

Turbidometric platelet aggregation was carried using a 4-channel optical platelet aggregometer (Chronolog, Labmedics, Stockport, UK) and data were captured via an analogue-digital converter (Maclab 4c, AD Instruments, Sussex, U.K.). Samples of PRP and WP were obtained as described in section 2.1.1-2.1.3. Zeolites were either incubated in the platelet containing sample (PRP, WP; 500µl) for the full experimental duration or were pre-incubated in the platelet-free solution (PPP' or Tyrode's) for the appropriate time prior to transfer to PRP or WP samples for 1 min before collagen stimulation. Parallel experiments were incubated with ODQ (20µM) where appropriate for at least 15 min prior to zeolite treatments. Haemoglobin (10µM) was added 1 min prior to zeolite treatments. After variation of the zeolite incubation period (1-120 min; 37°C) aggregation was initiated using collagen (2.5µg/ml).

Whole blood, impedence aggregation was carried out using a 2-channel Chronolog aggregometer (Chronolog, Labmedics, Stockport, U.K) and data captured *via* an

analogue-digital converter (Maclab 4e, AD Instruments, Sussex, U.K). Samples of whole blood were collected and processed as described in section 2.1.4. Zeolites (50% Zn^{2+} PTFE) were suspended in the sample (1ml) using a stainless steel metal holding device and were incubated for 1-30 min prior to collagen stimulation (2.5μg/ml). Samples were stirred at 1000rpm using a magnetic stir bar for the duration of the experiment. In all cases, aggregation was allowed to proceed for 5 min following collagen stimulation. Peak aggregation responses were noted and compared as a percentage of control aggregation obtained from samples stimulated at the appropriate time in the absence of zeolite.

3.2.5 Fixed wire myography; rat aortic rings.

Fixed wire myography experimental set-up was carried out as described in section 2.4. Vessels were pre-treated with the NOS inhibitor, L-NAME (200μM) to ensure that no endogenous production of NO was involved in responses obtained. NO-loaded Co^{2+}-exchanged zeolites (75% in PTFE or PDMS polymer binder) were placed in a 6ml (Kreb's solution) tissue bath containing a phenylephrine (PE; EC_{80} concentration; see section 2.4) pre-contracted section of rat aorta. In parallel experiments, ODQ (20μM) or Hb (40μM) was incubated in the tissue baths for 15 min and 1 min respectively before addition of zeolite discs. Relaxation of the aortic ring was measured for approximately 40 min prior to zeolite suspension in the tissue bath. Time-points for analyses were chosen and the relaxation was calculated as a percentage of the EC_{80} tension response of the PE contracted vessel. The mechanistic data (ODQ, Hb and NO-free zeolite controls) were analysed for peak

relaxation responses and this value was calculated as a percentage of the pre-contracted tension response.

3.2.6 Platelet LDH release.

LDH release in PRP following 50% Zn^{2+}-exchanged zeolite treatments (NO-free and NO-loaded) was determined using a colourimetric assay as described in section 2.2. Platelets in PRP (500µl; 125 x 10^9 platelets/ml) were treated with zeolites or control (positive control-2% Triton X; negative control-PPP) for 2hrs at 37°C. Aliquots (100µl) of each treatment were diluted in 100µl Tyrode's and plated in triplicate wells in a 96-well, flat-bottomed microtiter plates. The assay reaction mixture (Roche Applied Sciences, Penzberg, Germany) was added to each well and left for 30min in the dark at room temperature. The plate was then read using a Dynex MRX plate reader (Dynatech Laboratories, Chantilly, V.A.) at 490 nm with prior shaking at for 15 s. The absorbance values for each treatment were directly compared after subtraction of the background absorbance obtained from PPP samples.

3.3 Results

3.3.1. The NO-release capacities of Zn^{2+}-exchanged zeolites.

The NO-release capacities of Zn^{2+}-exchanged zeolites of varying (25-75%) compositions of zeolite in PTFE polymer binder, suspended in PRP (1ml; 37°C), show an increase (figure 3.1 A) in NO release as the composition of NO-loaded zeolite to PTFE binder is increased. The NO release capacities do not correlate directly with the composition of zeolite as demonstrated by the NO release profile of

the 50% zeolite (AUC=386.7 +/-195.9) which is more than double than that of the NO released from the 25% zeolite composition (AUC= 42.6 +/- 12.8). The rate at which NO is released from the 50% zeolite is considerably slower than that for 75% zeolite, peaking at ~30 min following suspension, as opposed to ~10 min. NO stores are exhausted to near baseline levels by around 60min in the case of 50-75% zeolites, with the 25% zeolite composition showing undetectable levels of NO by 40 min.

The NO-release profiles of 50% Zn^{2+} zeolites in Tyrode's solution (1ml; 37°C) had a higher peak and more sustained release than that observed in PRP (AUC 673.5 +/- 83.5; figure 3.1 B; $p < 0.05$).

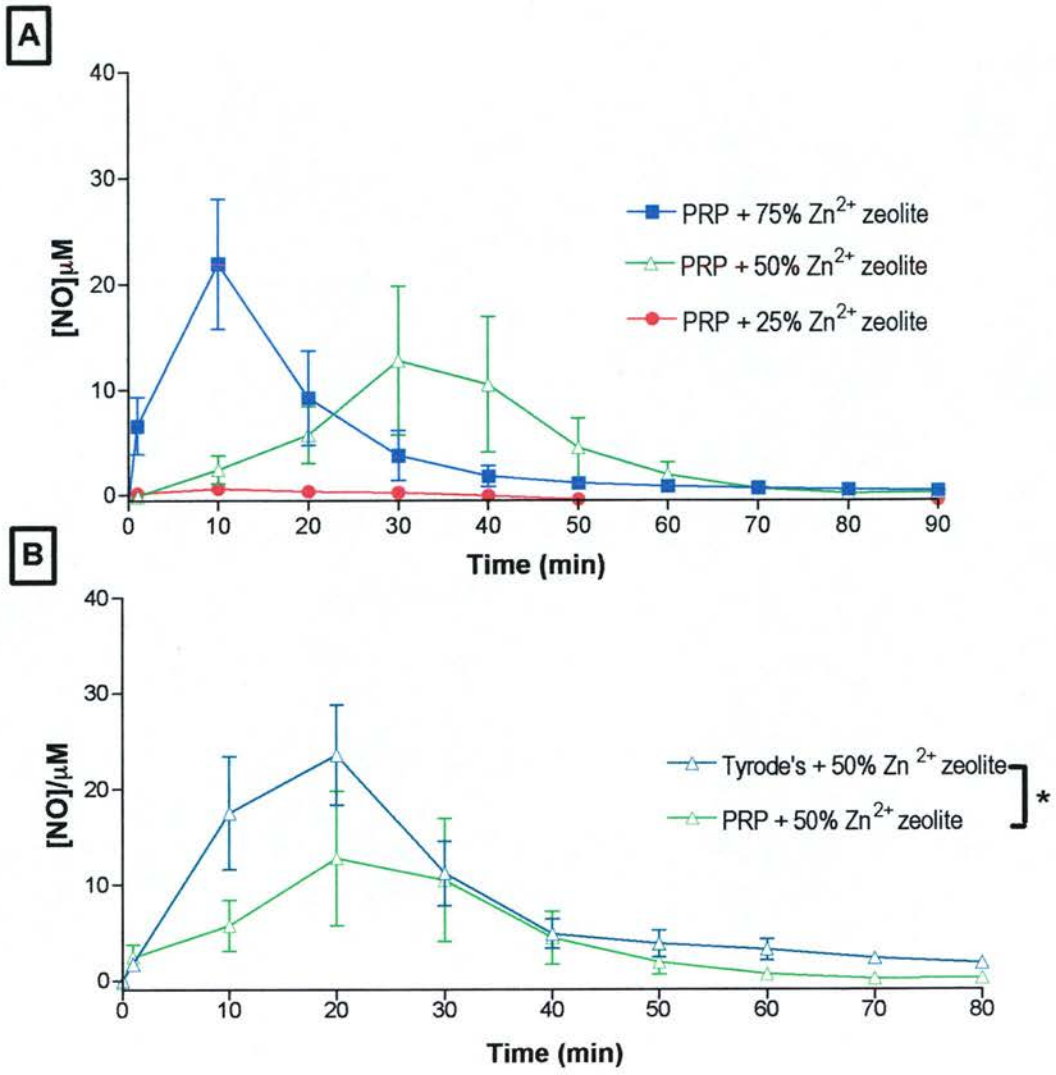

Figure 3.1 The NO-release profiles of Zn^{2+}-exchanged zeolites.

The NO-release profiles of different compositions of Zn^{2+}-exchanged zeolites;PTFE binder in PRP (A; 1ml; 37°C) incubated for 90 min (25% - red line; 50% - green line; 75% blue line) and the NO-release profiles of 50% Zn^{2+}-exchanged zeolites in PRP (light green) and Tyrode's solution (dark green) during 80 min incubations (B; 1ml; 37°C). Data points represent the mean +/- the SEM of n=5-8 independent experiments (* $p < 0.05$; Two way ANOVA).

3.3.2. The NO-release capacities of Co^{2+}-exchanged zeolites.

NO-loaded Co^{2+}-exchanged zeolites at 50 and 75% composition of zeolite to PTFE binder have dramatically different NO-release profiles in PRP (1ml; 37°C; figure 3.2 A). The peak NO concentration from 75% zeolite reaches ~30μM compared to only 5μM reached by 50%. Area under the curve analysis further underpins the difference in NO release between 50 and 75% zeolites with values of 68.3 +/- 19.6 and 599 +/- 189.2 respectively.

The suspension of the 75% zeolite disc in physiological saline solution (PSS; 1ml; 37°C; Figure 3.2 B) produced a rapid release of NO, peaking at ~ 30μM within 1 min. Peak concentrations reach around 30μM within the first few minutes. A slower release is observed in PRP with a similar peak concentration occurring after 20 min. Levels of NO are still detectable and are comparable for both solutions by 50 min. The total amount of NO released from the zeolite disc incubated in PSS is lower (AUC 368.4 +/- 125.9) over the 50 min recording period than in PRP over the same time (AUC 553.5 +/- 167.8).

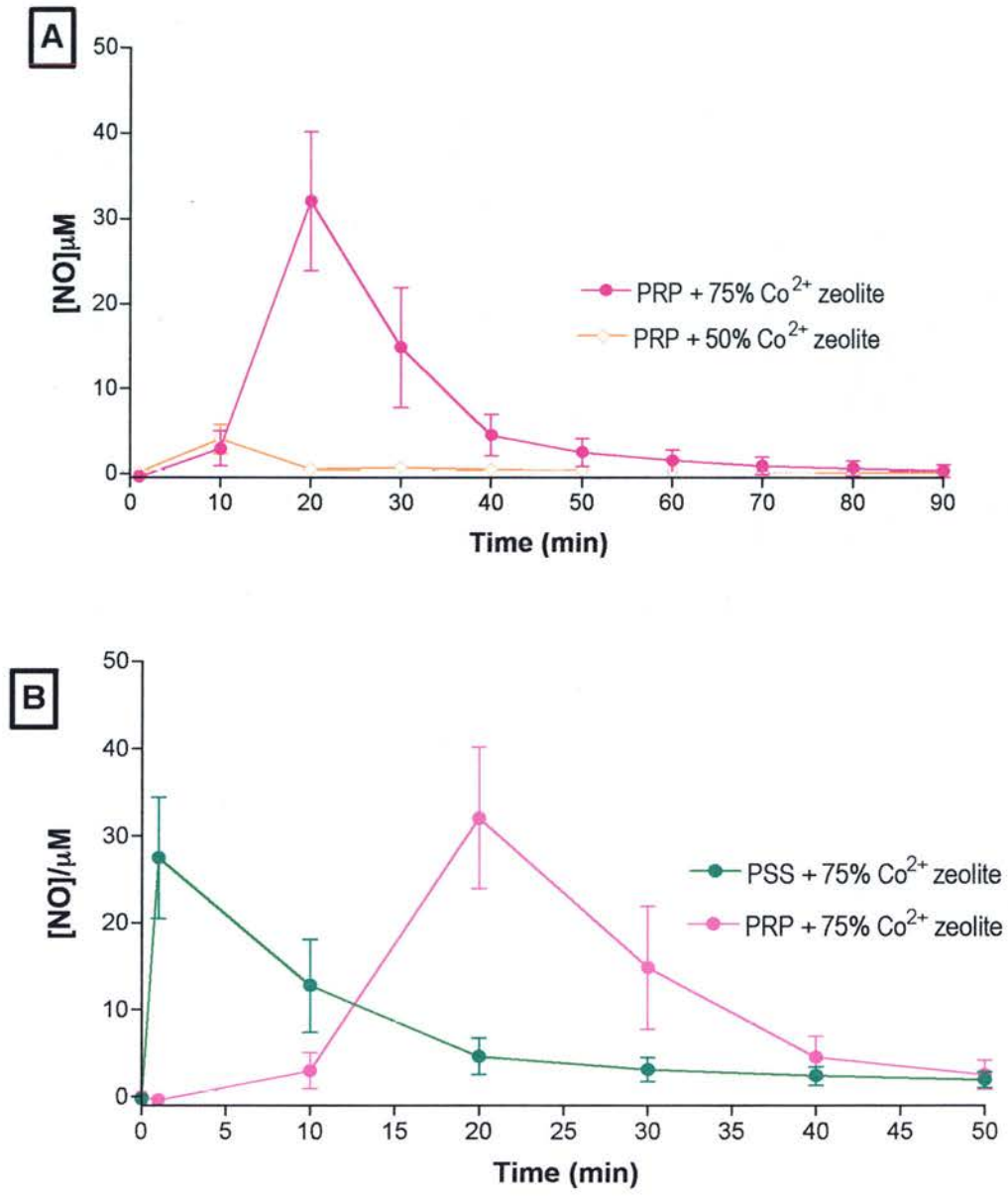

Figure 3.2 The NO-release profiles of Co^{2+}-exchanged zeolites.

The NO-release profiles of different compositions (50%-orange; 75%-pink) of Co^{2+}-exchanged PTFE bound zeolites in PRP (A; 1ml; 37°C) for 90min. Comparison of the NO-release profiles of 75% Co^{2+}-exchanged zeolites in PRP (pink) and PSS solution (dark green) for 50 min (B; 1ml; 37°C). Data points represent the mean +/- the SEM of n=5-6 independent experiments.

3.3.3. The anti-thrombotic properties of Co^{2+}-exchanged zeolites in human platelets.

Co^{2+}-exchanged zeolite discs at compositions of 50 and 75% zeolite:PTFE binder inhibited collagen-induced platelet aggregation at all time-points studied (1-120 min). The NO-free counterpart zeolite discs had no inhibitory effects on platelet aggregation (figure 3.3). Interestingly, the 75% zeolite disc has a less powerful anti-aggregating effect at 1min (approx 80% inhibition) compared to the 50% disc (100% inhibition).

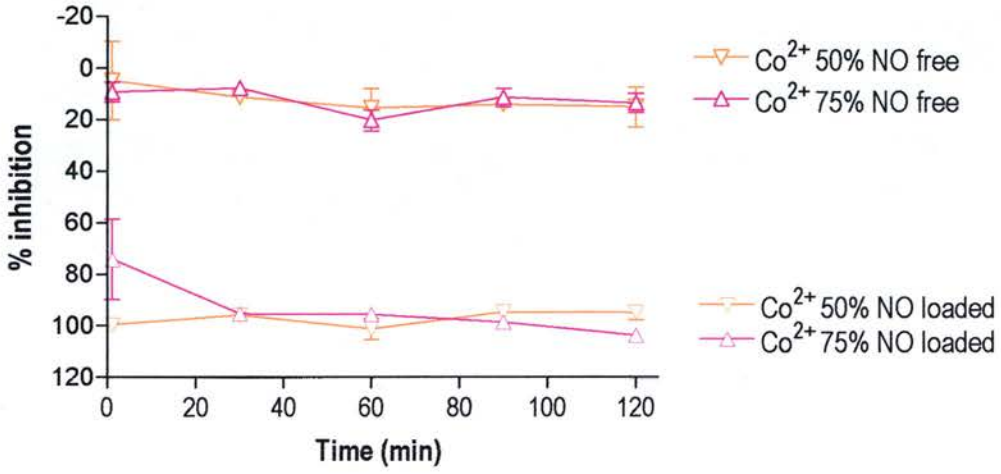

Figure 3.3. The anti-thrombotic properties of Co^{2+}-exchanged zeolites in human platelets.

The inhibition of collagen (2.5μg/ml)-induced platelet aggregation by 50% (orange) and 75% (pink) NO-loaded (filled triangles) and NO-free (empty triangles) zeolites incubated in PRP (0.5ml; 37°C) for between 1-120 min prior to collagen stimulation. Data points represent the mean +/- SEM of n=5 independent experiments.

3.3.4. The effect of two different polymer binders (PDMS and PTFE) on the smooth muscle relaxing properties of Co^{2+}-exchanged zeolites.

NO-loaded Co^{2+}-exchanged zeolites in either PTFE polymer binder (75% zeolite: 25% polymer binder) relaxed pre-contracted rat aortic rings more rapidly and potently than the same composition of zeolite in a PDMS polymer binder. Both polymer bound zeolites relaxed the rings for approximately 40 min (figure 3.4 A). The pre-incubation of the sGC-inhibitor, ODQ (20μM) had no significant effect on the relaxation responses of both polymer bound zeolites although maximum responses appear to be slightly reduced. The pre-incubation of the NO scavenger, haemoglobin (40μM) did not significantly inhibit the relaxation produced by PTFE bound zeolites but was able to significantly inhibit the response produced from PDMS bound zeolites. NO-free zeolite counterpart discs did not produce any relaxation effects in pre-contracted rat aortic rings (figure 3.4 B).

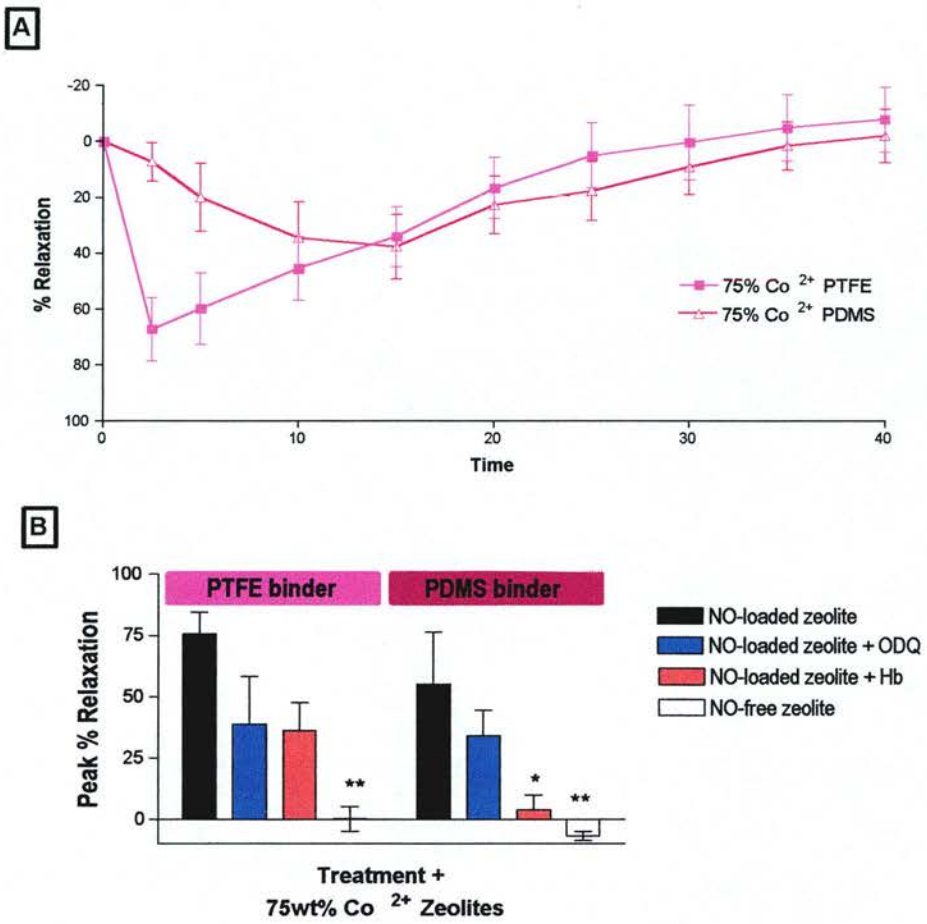

Figure 3.4. The smooth muscle relaxing properties of Co^{2+}-exchanged zeolites.

The duration of smooth muscle relaxation of PE pre-contracted rat aortic rings (A) following suspension of NO-loaded Co^{2+}-exchanged zeolites (75%:PTFE or PDMS polymer binder) into the tissue bath (6ml; oxygenated PSS; 37°C). Relaxation is expressed as a percentage of the value obtained from PE contraction of the ring and are the mean +/- SEM of n=7-8 independent experiments.

Graph B represents the maximum relaxation responses of rat aortic rings following NO-loaded zeolite treatment alone (black), in the presence of ODQ (blue; 20μM), in the presence of Hb (red; 40μM) and the NO-free zeolite control disc (white). Data are obtained using 75% Co^{2+} exchanged zeolites bound in either PTFE (pink) or PDMS (purple) polymers. Data are the mean +/- SEM of 4-6 independent experiments. Asterisks denote statistical significance from the appropriate NO-loaded zeolite treatment alone (* $p < 0.05$, ** $p < 0.01$ vs NO-loaded zeolite alone; one way ANOVA with Dunnet's post hoc).

3.3.5. The anti-thrombotic properties of Zn^{2+}-exchanged zeolites in human platelets.

NO-loaded Zn^{2+}-exchanged zeolites at compositions $\geq$ 50% inhibit collagen induced platelet aggregation for up to 80 min. The NO-free counterpart zeolites had no effect on platelet aggregation (Figure 3.5A). The 25% NO-loaded zeolite produced varying results on collagen induced platelet aggregation that correlated to two separately produced sample batches with opposing effects on the inhibition of platelet aggregation (Figure 3.5 B).

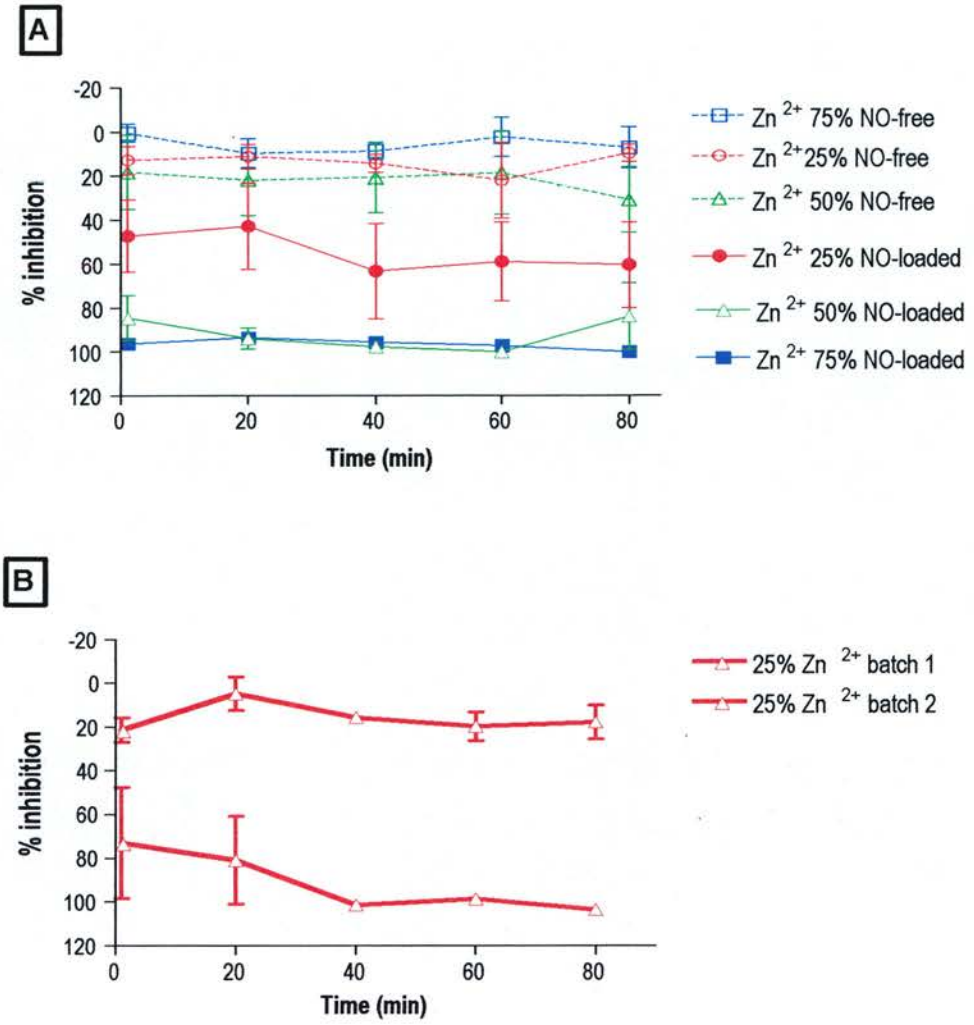

Figure 3.5. The anti-thrombotic properties of Zn^{2+}-exchanged zeolites in human platelets.

The inhibition of collagen (2.5µl/ml) induced platelet aggregation by 25% (red), 50% (green) and 75% (blue) NO-loaded (filled symbols) and NO-free (empty symbols) zeolites incubated in PRP (0.5ml; 37°C) for between 1-80 min prior to collagen stimulation. Data points represent the mean +/- the SEM for n=6 independent experiments. Graph B shows the inhibition of collagen-induced platelet aggregation by two separately produced batches of the 25% NO-loaded zeolites. The symbols indicate the mean +/- the SEM of n=3 for each batch.

3.3.6. The mechanism of anti-platelet action of NO-loaded Zn^{2+}-exchanged zeolites – inhibition of sGC by ODQ (20μM).

NO-loaded zeolites and the NO-donor compounds, DEA/NO and SNP, composition and concentration-dependently inhibit collagen-induced platelet aggregation (figure 3.7). NO-loaded Zn^{2+}-exchanged zeolites at compositions >25% inhibit collagen-induced platelet aggregation following 1min zeolite incubations (figure 3.7 A). The addition of the sGC inhibitor, ODQ (20μM) had no effect on the inhibition of platelet aggregation by 50 and 75% zeolite discs. The inhibition of platelet aggregation by DEA/NO was significantly reversed by ODQ at the mid-range of DEA/NO concentrations as indicated by the rightward shift in the log dose/response curve (figure 3.7 B). However, the inhibition of platelet aggregation by the highest concentrations of DEA/NO was not reversed by the addition of ODQ. The inhibition of platelet aggregation by SNP was severely attenuated by the addition of ODQ (figure 3.6 C).

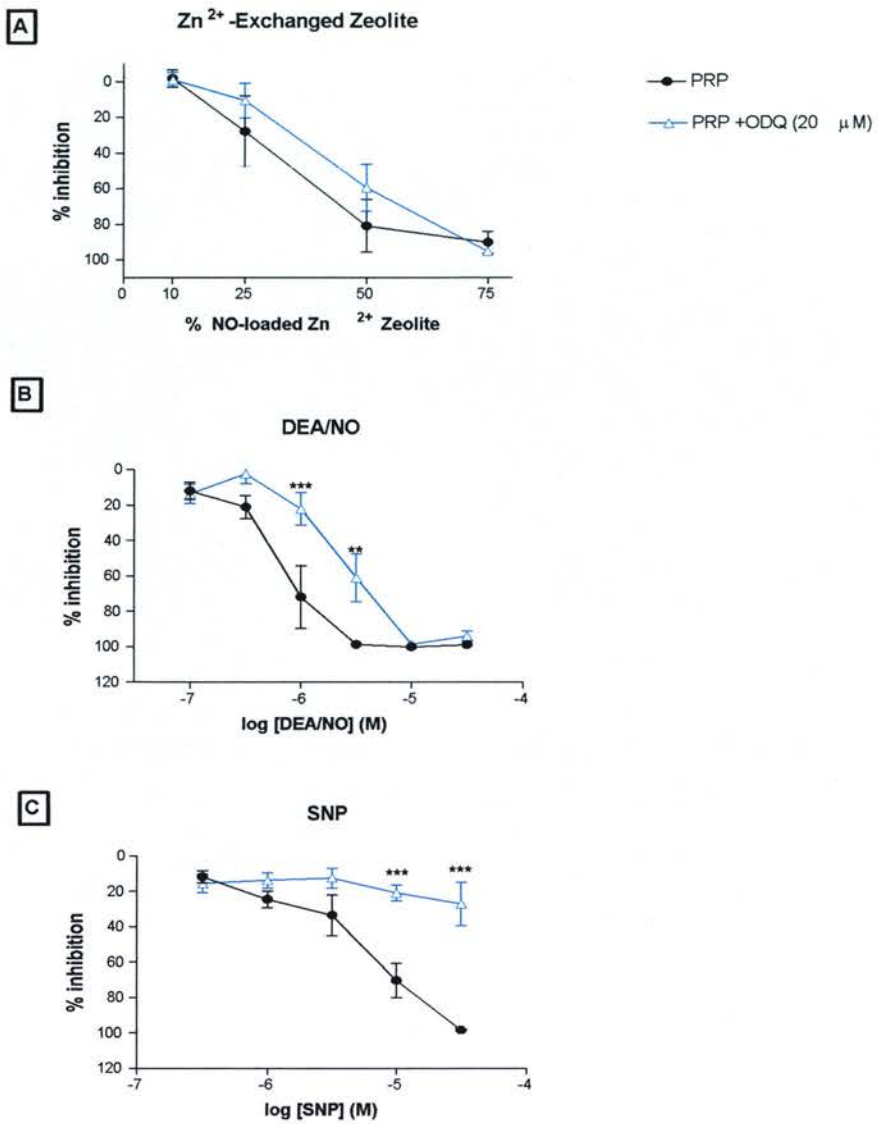

Figure 3.6. The mechanism of the anti-platelet action of NO-loaded Zn^{2+} exchanged zeolites, DEA/NO and SNP; inhibiton of sGC by ODQ (20μM).

The inhibition of collagen-induced platelet aggregation by various compositions (10-75%) of NO-loaded Zn^{2+}-exchanged zeolites (A) and log concentrations (-7 – (-)4M) of NO donors DEA/NO (B) and SNP (C), in the absence (black) and presence (blue) of ODQ (20μM). Data points represent the mean +/- SEM of n=6-8 independent experiments. Asterisks denote statistical significance from the appropriate NO-donor in the absence of ODQ (* $p < 0.05$, ** $p < 0.01$, *** $p < 0.001$; Two way ANOVA with Bonferroni's post hoc test).

3.3.7. The mechanism of anti-platelet action of NO-loaded Zn^{2+}-exchanged zeolites - scavenging of NO by Hb (10μM).

Collagen-induced platelet aggregation is significantly inhibited following incubation (1min; 37°C) of NO-loaded Zn^{2+} exchanged zeolites at compositions ≥ 50%. NO-free counterpart zeolites had no effect on inhibition of aggregation. The addition of the NO scavenger Hb, (10μM), reversed the modest inhibition of aggregation by the 25% zeolite disc and significantly reversed the inhibition by the 50% zeolite ($p < 0.05$). The addition of Hb had no effect on inhibition of aggregation by the highest composition (75%) of the NO-loaded Zn^{2+}-exchanged zeolite disc.

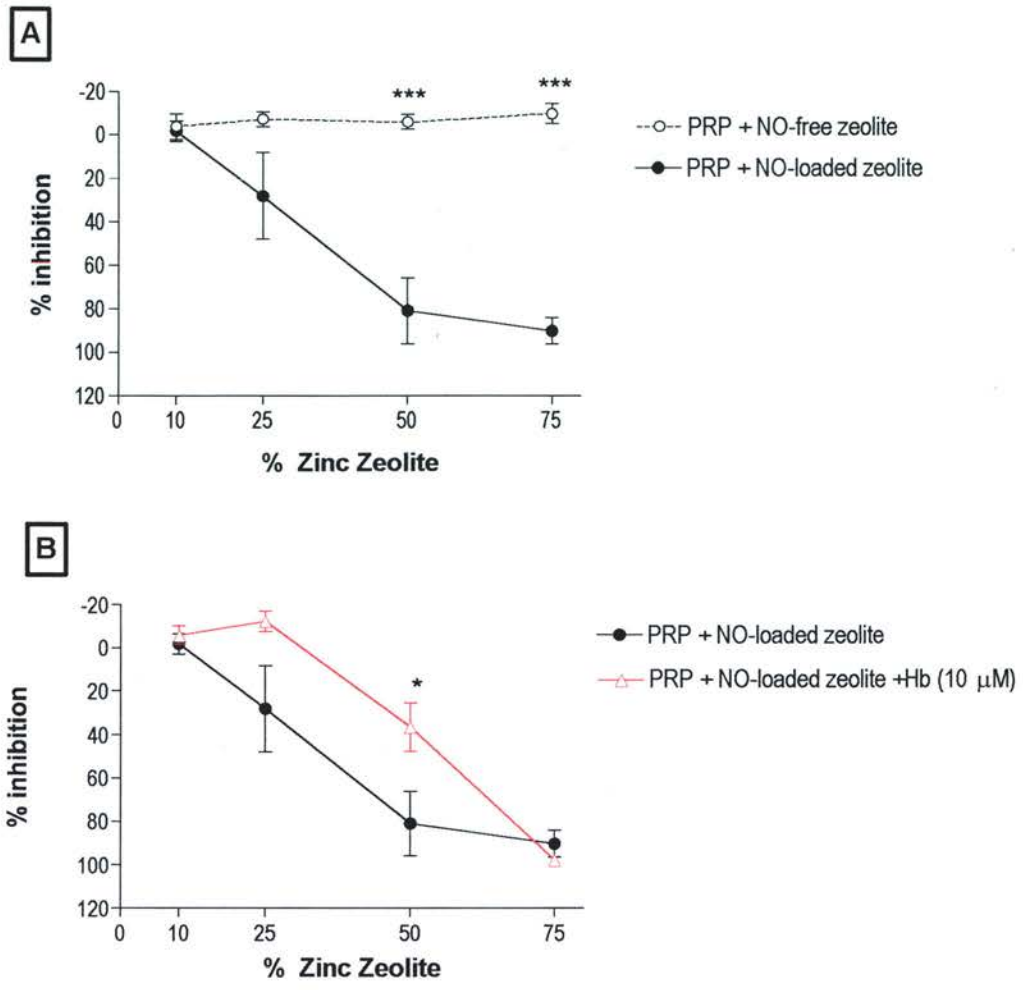

Figure 3.7. The mechanism of the anti-platelet action of NO-loaded Zn^{2+} exchanged zeolites; scavenging of NO by haemoglobin (10μM).

The inhibitions of collagen-induced platelet aggregation by various compositions (10-75%) of NO loaded (black) and NO-free (dashed;A) Zn^{2+}-exchanged zeolites in the absence and presence (red) of Hb (10μM;B). Data points represent the mean +/- SEM of n=6-8 independent experiments. Asterisks denote statistical significance from NO-loaded zeolite treatment alone at the appropriate zeolite composition (* $p < 0.05$, *** $p < 0.001$; Two way ANOVA with Bonferroni's post hoc test.)

3.3.8. The mechanism of the anti-platelet action of NO-loaded Zn^{2+} - exchanged zeolites – pre-incubation of zeolites in PPP/WP.

To investigate the potential of NO-stored plasma reservoirs on prolonged inhibition of aggregation, WP samples were used. Pre-incubation of the zeolite disc in platelet free medium, prior to the transfer of the disc to the platelet sample at the appropriate time-point was also done to minimise the likely formation of plasma stores in PRP as well as to investigate the anti-platelet effects of NO-released from the zeolites at isolated time-points. The pre-incubation (1-80min) of 50% NO-loaded Zn^{2+} zeolites in PPP or Tyrode's solution (0.5ml; 37°C) prior to transfer to PRP or WP (0.5ml; 37°C; 1min) for aggregation experiments demonstrated inhibition of collagen-induced aggregation for the duration of the experiment (80 min) in both PRP and WP (figure 3.7). The addition of the sGC inhibitor, ODQ (20μM) had no effect on the inhibition of platelet aggregation at any time-point in PRP (figure 3.8 A) but significantly reversed the inhibition of aggregation seen at the 80 min time-point only in WP ($p < 0.001$; figure 3.8 B).

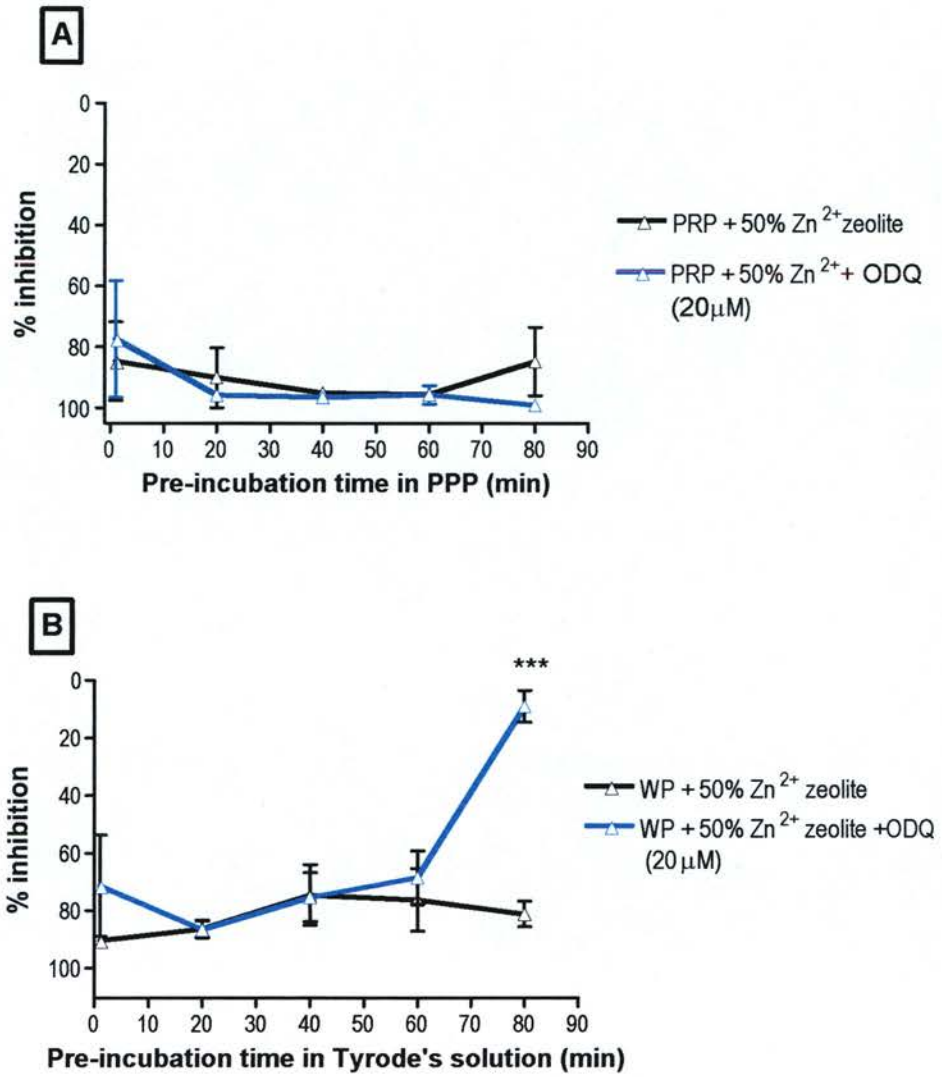

Figure 3.8. The mechanism of the anti-platelet action of NO-loaded Zn^{2+} exchanged zeolites, pre-incubation of zeolite in PPP and Tyrode's.

The inhibitions of collagen-induced (2.5μg/ml) platelet aggregation by 50% NO-loaded Zn^{2+}-exchanged zeolites in PRP (A) and WP (B) following a pre-incubation period (1-80 min) in PPP or Tyrode's respectively before transfer of the disc (1 min) prior to stimulation of aggregation in the absence (black) and presence (blue) of ODQ (20μM). Data points represent the mean +/- SEM of n=3-4 independent experiments. Asterisks denote significance from NO-loaded zeolite treatment in the absence of ODQ at the corresponding time-point (*** $p < 0.001$; Two way ANOVA with Bonferroni's post hoc test.)

3.3.9. The anti-thrombotic effects of NO-loaded 50% Zn^{2+}-exchanged zeolites in whole blood.

The inhibition of collagen-induced platelet aggregation following incubation (1ml; 37°C) of NO-loaded 50% Zn^{2+} zeolites is markedly reduced compared to that seen in PRP (figure 3.8) with a maximum of ~ 40% inhibition achieved at 1 min and subsequent time-points showing a gradual reduction of the inhibition.

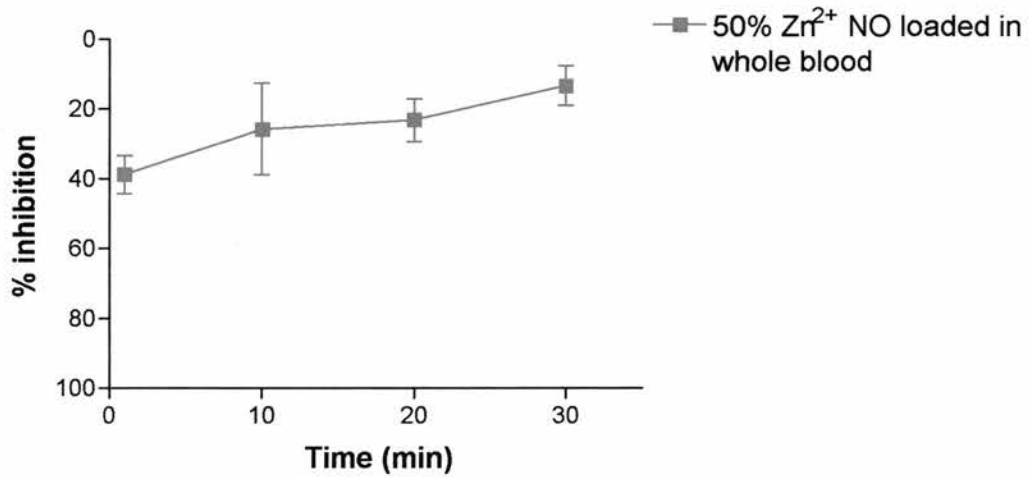

Figure 3.9. Anti-platelet properties of 50% NO-loaded Zn^{2+}-exchanged zeolites in whole blood.

The % inhibition of collagen-induced (2.5μg/ml) platelet aggregation by 50% NO-loaded Zn^{2+}-exchanged zeolites in whole blood (1ml) following disc incubations between 1-30 min. Data points represent the mean +/- SEM of n=6 independent experiments.

3.3.10. Platelet viability following treatment with 50% Zn^{2+}-exchanged zeolites; LDH release.

PRP samples (500µl; 125 x 10^9platelets/ml) treated with 50% Zn^{2+}-exchanged zeolite discs (NO-free and NO-loaded) for 2 h (37°C) caused no significant release of LDH compared to control, untreated samples (figure 3.10). Significant release of LDH can be observed upon treatment of PRP samples with the positive control (2% Triton-X; $p < 0.01$ vs control).

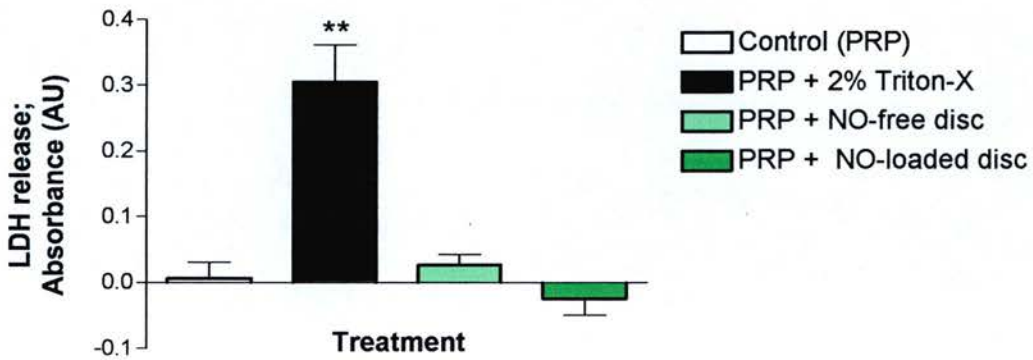

Figure 3.10. Platelet LDH release following treatment with 50% Zn^{2+}-exchanged zeolites.

Colourimetric assay determining LDH release from platelets in PRP (500µl; 125 x 10^9 platelts/ml) following control (white), 2% Triton-X (black) and NO-free (light green) and NO loaded (dark green) 50% NO-loaded Zn^{2+}-exchanged zeolte treatments for 2 h at 37°C. Absorbance was measured at 490nm. Bars represent the mean +/- SEM of n=5 independent experiments all done in triplicate. Asterisks denote significance from control (** $p < 0.01$; one way ANOVA with Dunnett's post hoc).

3.4. Discussion.

3.4.1 The tunable NO-release properties of NO-loaded zeolites.

Cation-exchanged zeolites are high capacity storage materials of NO with dynamic properties that have the potential for tailored NO-storage and release according to specific need. Results in this chapter demonstrate several ways that NO release properties of zeolites can be altered. Firstly, the type of cation exchanged in the structure was shown to impact on the amount of NO released. The NO-release profiles of Zn^{2+} and Co^{2+} exchanged zeolites differed not only in quantity of NO released but also in its rate of NO release. Furthermore, the composition of the zeolite to the polymer binding material also changed the NO-release profiles of these zeolites, which subsequently altered the biological effects produced. Low compositions (10%) of zinc exchanged zeolites failed to inhibit collagen-induced aggregation whereas high compositions (50-75%) consistently abolished platelet aggregation for up to 2h. Interestingly, changing the composition of the zeolite in the polymer did not predictably change NO-storage capacities of the materials. For example, 50% composition of Zn^{2+} zeolite contained double the amount of potential NO storing zeolite than the 25% composition, but the NO-release from 25% Zn^{2+} zeolites was almost 10 times less than that observed from the 50% zeolite. Zeolites are stored under argon until ready for use and have been shown to reliably retain their NO stores for a significant time-period (>16weeks;Wheatley *et al.*, 2006). The reason for the dramatic loss of NO release from the lower compositions is not known but it could be possible exclusion of water from the zeolite by the higher composition

of hydrophobic PTFE polymer causes a substantial hindrance on NO-release from the zeolite.

As well as duration, kinetics of release can also be important. Experiments in this chapter have demonstrated how zeolite design influences NO release kinetics but it was also evident that the surrounding media had an impact on NO release. This is most obvious with the 75% Co^{2+} exchanged zeolite, which had a lag phase before the rapid release of NO occurred at 10 min in PRP. In a physiological salt solution (PSS), there was no lag phase and peak NO-release was achieved within the first 5 min. The answer to this change is differences in constituents of the solution. PRP contains many large proteins, such as albumin, that could easily block the pores of the zeolite material thereby slowing down the diffusion of H_2O in, and NO out. The 50% Zn^{2+} zeolite did not show any lag phase in PRP compared to Tyrode's solution and rate of release was similar in each solution (figure 3.1 B). The lack of any lag phase in Zn^{2+} zeolites could be attributed to differences in pore sizes, which could differ due to changes in electrostatic forces exerted on the zeolite structure from different ions. Differences in these molecular forces may also explain the variation in storage capacities of different ion-exchaged structures. Although rate of release of NO from 50% Zn^{2+}zeolites was unaffected by change in solution, lower peak NO concentrations were released in PRP than in Tyrode's solution, providing further evidence of how the aqueous media can impact NO release. The differences observed here are most likely due to the presence of contaminating free haemoglobin in PRP, reducing the NO signal in electrode experiments. Measurement of Hb content in PRP has been done previously. This study demonstrated that

approximately 0.35μM Hb can be found in PRP (Crane *et al.*, 2005). A reduction in NO concentration was not evident with the 75% Co^{2+} zeolites in PRP compared to PSS, although the much higher NO concentration released could make any small scavenging effects appear negligible in this instance.

NO stores liberated from higher compositions of zeolite showed a great deal of variation in total NO release, determined by NO electrode measurements, suggesting that zeolite production techniques may influence the concentration of the NO reservoir stored. Problems with NO storage in the 25% Zn^{2+} zeolite were especially prominent in the functional platelet aggregation studies. Some discs were able to abolish aggregation whereas others produced no effect at all (figure 3.5 B). Standardisation of zeolite production techniques would be likely to help overcome these issues for future research.

The concentration of endogenously produced NO required to inhibit platelet aggregation in the body is very small (< nM). In our aggregation assay, the concentration of NO released is in the micromolar range, far exceeding the concentration required to produce effects in the body. However, the 50% Zn^{2+} zeolite, which was able to abolish aggregation in PRP and WP samples, showed dramatically reduced anti-thrombotic effects in whole blood where NO is likely to be quickly scavenged. There have been several groups working on different kinds of NO-releasing polymer materials for the development of anti-thrombotic coatings (Mowery *et al.*, 2000; Oh & Meyerhoff, 2004; Reynolds *et al.*, 2004; Schoenfisch *et al.*, 2000; Zhang *et al.*, 2002). Many of these polymers have demonstrated fluxes of

NO in the pico to nanomolar range that have still been capable of producing biological effects in *in vivo* models (Schoenfisch *et al.*, 2000; Zhang *et al.*, 2002). For stent or vessel graft-based materials, lower NO concentrations have been shown to produce the beneficial anti-thrombotic and anti-proliferative effects (Annich *et al.*, 2000; Fleser *et al.*, 2004; Hou *et al.*, 2005; Zhang *et al.*, 2002). Thus, although the 50% Zn^{2+} zeolite did not perform well in the whole blood aggregation study, this does not best reflect the ability of the zeolite surface to remain free from adhering platelets, the main end-point studied in NO-releasing polymer technologies. Further studies are needed to quantify the anti-adhesive properties of the zeolite surface.

At present, the duration of NO release from zeolites is insufficient for most applications on medical devices. Ideally, NO-release would last for days to weeks for most applications. At present, none of the zeolite design alterations examined in this chapter, including using different polymer binders has increased the duration of release. Despite this, many other avenues are yet to be explored, including changing the type of zeolite itself, of which there are hundreds with unique structures, or by using different cations to exchange within the structures. Interest in the use of copper (Cu) ion containing materials is increasing due to the ability of Cu^{1+} to catalyse the production of NO from nitrite (Oh & Meyerhoff, 2004, 2003). A Cu^{2+} exchanged zeolite might therefore produce a preliminary burst of NO from stored reservoirs, which would be ultimately oxidised to nitrite. The reduction of Cu^{2+} to Cu^{1+} at the zeolite surface by endogenous reducing agents, such as ascorbate, then creates the potential to recycle nitrite to NO at its surface, providing a potentially

unending source of bioavailable NO. The major drawback with this technology is the highly cytotoxic nature of Cu ions *in vivo.*

Duration of release is undoubtedly important for the development of anti-thrombotic coatings on devices used in long-term procedures although short-term NO-release from the surface of biomedical devices could also afford protection against thrombotic and proliferative responses in the perioperative period when it is needed the most. Short-term NO release could also prove useful in minor interventional procedures such as cannulation. Indeed, other NO-releasing polymers have shown effective anti-thrombotic potential in this arena, which has concomitantly led to improved working life for intravascular sensing equipment such as glucose and oxygen sensors (Oh *et al.*, 2005; Schoenfisch *et al.*, 2002; Shin *et al.*, 2004; Shin & Schoenfisch, 2006).

3.4.2 Mechanism of action of NO-loaded zeolites.

As well as the therapeutic potential of NO-loaded zeolites, these materials offer a unique tool with which to investigate the mechanism of action of NO as they liberate NO into the extracellular environment and in theory leave all potential zeolite by-products bound in the structure. Many of the classical effects of NO are produced via the sGC enzyme which, when activated, catalyses the production of cGMP from GTP (Schmidt *et al.*, 1993). The stimulation of sGC by NO results in inhibition of platelet aggregation through the modulation of Ca^{2+} levels important for initiating aggregation (Busse *et al.*, 1987; Radomski *et al.*, 1987c). There have been several reports of a sGC independent effects of NO, particularly in NO-mediated anti-

platelet actions (Crane *et al.*, 2005; Gordge *et al.*, 1998; Homer & Wanstall, 2002; Sogo *et al.*, 2000; Wanstall *et al.*, 2005). The potent inhibition of sGC can be achieved through the use of ODQ. Pre-incubating platelets with ODQ completely abolished the inhibition of platelet aggregation achieved from the NO donor SNP, whereas it had no effect on the inhibition caused by another NO donor, DEA/NO, in keeping with previous results (Crane *et al.*, 2005; Sogo *et al.*, 2000). The difference observed between these two donors has been attributed to the site of NO production (Gordge *et al.*, 1998; Wanstall *et al.*, 2005), although NO concentration cannot be ruled out. It is suggested previously that the site and concentration of NO predisposes the occurrence of sGC-independent mechanisms (Crane *et al.*, 2005; Sogo *et al.*, 2000). There is a relative lack of sGC-independent anti-platelet effects with species of NO donor that require bioactivation suggesting that liberation of NO in the intracellular environment may exclusively target sGC. SNP is an example of a bioactivated, intracellular NO donor (see section 1.1.8.3) that was only able to inhibit aggregation in the absence of ODQ, supporting this hypothesis (figure 3.7 B). DEA/NO is a spontaneous NO donor that liberates NO both in the extracellular and intracellular environment. ODQ was only partially able to reverse its effects on platelet aggregation (figure 3.7 C) indicating that the effect of DEA/NO on platelets is through both sGC-dependent and independent mechanisms. As zeolites release high concentrations of NO into the extracellular environment and do not require bioactivation to release NO, it was hypothesised that there would be an sGC-independent component to the anti-platelet effects of NO-loaded zeolites. Indeed, ODQ had no significant effect on the anti-platelet effect of 75% Zn^{2+} zeolites after 1 min zeolite incubation (figure 3.6). There was a partial reversal of the anti-platelet

effects of the 50% zeolite after 1 min incubation indicating there is a partial sGC-dependent effect at this time-point (figure 3.6). At later time-points (10-80 min), the anti-aggregatory actions of 50% Zn^{2+} zeolites were unaffected by inhibition of sGC (figure 3.8), which could be related to the presence of higher NO concentrations liberated at these time-points as indicated by NO-electrode profiles (figure 3.1 B). The modest inhibition of platelet aggregation by the 25% Zn^{2+} zeolite after 1 min was completely abolished by the ODQ, which is further evidence for the requirement of high NO concentrations in the production of sGC-independent effects. These studies support previous evidence highlighting the requirement for high concentrations of extracellular NO in the production of NO-mediated sGC-independent effects (Crane *et al.*, 2005; Sogo *et al.*, 2000). The alternative pathway stimulated by NO is not clear although it has been suggested that the nitration of surface platelet protein residues or direct modulation of Ca^{2+} ion channels and transporters can result in decreased aggregation (Crane *et al.*, 2005; Gupta *et al.*, 1994; Pernollet *et al.*, 1996; Trepakova *et al.*, 1999; Wanstall *et al.*, 2005) as well as surface thiol modifications (Gordge *et al.*, 1998). Such surface modifications would certainly be more likely with extracellular release of NO, particularly at high concentrations which would have greater nitrating or oxidising actions on surface proteins and lipids. Further to the mechanism of action in platelets, it was shown that ODQ also partially inhibited the relaxation response of rat aorta preparations by Co^{2+} zeolites, demonstrating an sGC-independent component to the relaxing mechanisms of NO in smooth muscle. These findings are in line with various others reporting NO-mediated sGC-independent effects in smooth muscle (Bellamy *et al.*, 2002; Bradley *et al.*, 1998; Miller *et al.*, 2004). Direct modulation of Ca^{2+} -

dependent K^+ channels by NO has been shown to produce relaxation in smooth muscle highlighting a possible route by which NO can exert vasorelaxation in the absence of sGC (Bolotina *et al.*, 1994). Better understanding of how NO exerts these sGC-independent effects could provide new pathways for pharmacological manipulation that have the potential to mimic the effects of NO in the body in the absence of NO itself. To this end, the results demonstrated here warrant further investigation.

The use of the NO scavenger haemoglobin had little impact on the effects observed, particularly with the high composition zeolites, which release massive concentrations of NO. This could suggest that NO was not the effector molecule and perhaps another species was producing the effects, however it is more likely that these high concentrations of NO are saturating the reaction sites for NO on Hb. NO reacts with Hb in a 4:1 ratio, thus the presence of 10μM Hb would effectively scavenge up to 40μM NO. This concentration would be very quickly reached as shown by NO-electrode experiments, more so by the 75% Zn^{2+} zeolite that has a very rapid onset of NO release (figure 3.1 A). As the platelet assay uses light transmission to measure aggregation, the Hb content, which is strongly pigmented, could not be used at high concentrations. However, a higher concentration of Hb was used in the myography experiments (40μM), which still was not sufficient to completely reverse relaxation responses induced by NO-loaded zeolite exposure. However, the marked reduction in anti-platelet effects in the whole blood aggregation experiments, demonstrates a physiological scavenging of NO by scavengers found in blood. Despite problems with effective scavenging of NO, the use of NO-free counterpart zeolites provides

the best indication of the involvement of NO. These discs had no effect in either the aggregation or the myography assays. Thus, it is fair to assume that NO *is* the major effector molecule in the observed effects.

Although the NO-release profiles of zeolites appear exhausted by approximately 1 h, the anti-thrombotic effects last over 2 h. This prolongation of effects is not evident in the smooth muscle relaxant properties of zeolites, indicating that there may be a platelet/plasma specific component to this effect. Previous work has implicated low molecular weight thiol plasma constituents in the prolongation of anti-platelet effects of NO-donors (Crane *et al.*, 2002). Low molecular weight thiols were shown to be important for the transfer of NO from protein S-nitrosothiol reservoirs that can subsequently inhibit platelet aggregation for prolonged periods of time, exceeding the observed biological half-life of NO-donors (Crane *et al.*, 2005). Washed platelet experiments were used to examine the role of plasma-borne S-nitrosothiol reservoirs in our experiment. It was shown that 50% Zn^{2+} NO-loaded zeolites were able to inhibit aggregation of washed platelets for over 90mins, still beyond the apparent NO-release time of the disc. Further time-points were not studied due to the short functional life of platelets *ex vivo.* It is important to note that the NO-release concentration in the aggregation assay may be double that seen in the electrode experiment due to differences in experimental volume. Also, the NO-electrode was at minimal sensitivity due to the high concentrations released throughout the experiments to ensure the full NO release remained on scale. It is likely that increasing the sensitivity would have produced an NO signal after 60 min in the range known to inhibit platelet aggregation. The zeolite discs were pre-incubated in

either PPP or Tyrode's solution prior to transfer to PRP or WP at the appropriate time-point. This hypothesis is further supported when considering the pre-incubation technique used (figure 3.8), which meant that the zeolites were only in contact with the platelet sample for 1 min prior to collagen stimulation following varying incubation times in the platelet free sample. This further down-plays the involvement of plasma-borne NO reservoirs in the anti-platelet effects of NO-loaded zeolites and indicates that NO released at those specific time-points was adequate to inhibit aggregation. Furthermore, the pre-incubation of ODQ in PRP had no effect on the inhibition of aggregation, suggesting the effect is sGC-independent and therefore possibly associated with high concentrations of NO in the extracellular environment. The relative lack of sGC-independent effects reported in the presence of $OONO^-$ or S-nitrosothiols (nitrosonium; Sogo *et al.*, 2000) further supports the claim that extracellular NO radical from zeolite stores are producing these effects.

The short duration of effects seen in smooth muscle is probably due to lower NO concentrations in this assay as the zeolite discs were placed in a 6ml volume. Future studies should simultaneously produce NO electrode measurements along with aggregation and myography experiments to examine the actual concentrations present producing the observed effects.

3.4.3 Toxicity of NO-loaded zeolites to human platelets.

Cytotoxicity of NO is an area with much contention within the literature. The involvement of other NO-related species, such as peroxynitrite ($ONOO^-$) has been suggested to be the major cause of death in a number of cell types (Halliwell *et al.*,

1999; Pacher *et al.*, 2007; Sies & de Groot, 1992; Virag *et al.*, 2003). $ONOO^-$ is formed through the interaction of NO with O_2^- and is a potent oxidant, resulting in lipid peroxidation, DNA fragmentation and protein nitration and oxidation (Taylor *et al.*, 2004; Virag *et al.*, 2003). LDH-release from platelets following treatment with NO-loaded zeolites for 2h was found to be comparable to control, suggesting no adverse effects of these high concentrations of NO on platelet death (figure 3.9). Platelet function was difficult to assess at later time-points due to the potent and lasting anti-platelet effects of the zeolites and the short functional life of platelets *ex vivo*. Smooth muscle contraction and relaxation responses were unaffected following zeolite treatments although the concentration of NO in this assay is lower than that used for aggregation. These results show promise in the future development of NO-loaded zeolites for *in vivo* practices, although further characterisation of NO cytotoxicity to other relevant cell types is required, particularly endothelial cell lines which would come into close proximity with many potential medical device surfaces such as stents and vascular grafts.

3.4.4 Summary and conclusions

In summary, NO-loaded zeolites provide promising tools to deliver NO locally at physiologically relevant concentrations and are potential candidates for development of anti-thrombotic coatings on medical devices. At present, the NO-release profiles are not optimal for most medical device applications, which would require longer durations of NO release to provide adequate anti-thrombotic protection throughout the working life of the device and avoid the use of prophylactic, systemic anti-thrombotic therapies. Of particular interest are the anti-thrombotic, anti-proliferative

and anti-inflammatory effects of NO in relation to vascular stent devices. These devices are currently associated with high levels of restenosis due to the remodelling of the vessel wall caused by proliferating smooth mucscle cells. Stent-based NO delivery could provide the answer to many of the burdens associated with stent failure, including platelet and inflammatory cell adhesion and aggregation, and limit these effects to a localised area, providing a clear advantage to potentially detrimental polypharmacy approaches. Indeed, NO-releasing stents have already produced promising results in various animal models (Buergler et al., 2000; Do et al., 2004; Kaposzta et al., 2002; Vermeersch et al., 2001; Yoon et al., 2002).

Temporal limitations in current NO-release characteristics of cation-exchanged zeolites have the potential to be overcome with further optimisation of zeolite design and through increased consideration of the biological surroundings. Despite these drawbacks, zeolite materials have been shown to be high capacity storage and release materials of biologically active concentrations of NO, which may be more suited to alternative clinical applications rather than long-term anti-thrombotic therapies. There are likely short-term procedures that could benefit significantly from NO release, especially when considering the potential advantage of NO-induced vessel dilatation and reduction in vasospasm in cannulation procedures (Clatterbuck *et al.*, 2005; Keefer, 2003). With this in mind, the optimal NO-releasing zeolite so far was considered to be the 50% Zn^{2+} exchanged zeolite which had a steadier, more prolonged release of NO compared to other types of zeolite. Cytotoxicity of this zeolite in platelets was investigated through measurement of LDH. It was shown that, despite high concentrations of NO being released into the platelet sample, no increase in LDH release was observed suggesting that these zeolites do not induce

cell necrosis. This zeolite was chosen for further testing in more diverse biological settings.

CHAPTER FOUR

The Effect of Zn^{2+}-Exchanged Zeolites on Human Neutrophil Function.

Chapter 4. The Effect of Zn^{2+}-Exchanged Zeolites on Human Neutrophil Function.

4.1 Introduction

The inflammatory response is a fundamental process for host defence against infection and for mediating tissue repair. The inflammatory reaction involves the recruitment of inflammatory cells to the site of injury or infection in response to noxious chemical stimuli or microbial toxins (Driscoll *et al.*, 1997). The identification of foreign substances in the body is essential for the rapid and successful clearance of infection, however, when the formidable array of inflammatory effector molecules is targeted inappropriately, such as in chronic inflammatory diseases and medical device placement, the resulting damage to host tissue is harmful and potentially fatal. Biomaterial-elicited inflammatory reactions can also interfere with the functioning of medical devices as a result of increased adhesion of inflammatory cells and platelets to the surface of the device (Shin & Schoenfisch, 2006) and the associated rise in radical species, that can increase errors in measurements from biosensing equipment (Patel *et al.*, 2007). The development of more biocompatible coatings on medical devices that actively inhibit the inflammatory response by presenting anti-inflammatory agents is one method of overcoming these issues (Chitkara *et al.*, 2006; Luscher *et al.*, 2007). Alternatively, coatings that can mimic host tissue, so as to avoid the identification of the device as foreign are also eagerly investigated. The seeding of host endothelial cells around

vascular stents have produced promising results in this field, highlighting a potential long-term solution to the inflammatory, restenotic and thrombogenic responses associated with stent failure (Consigny, 2000; Ratcliffe, 2000; Rogers *et al.*, 1996). The vascular endothelium produces numerous factors important for the maintenance of haemostasis, and NO is recognised as one factor central to the anti-thrombogenic and anti-inflammatory properties of the endothelium. Moreover, the diverse actions of NO in the body extend to inhibition of smooth muscle proliferation and anti-microbial properties, making NO a prime candidate for the development of biomaterials with superior biocompatibility. NO-releasing polymers have shown promise in reducing platelet activation and adhesion, making them potential candidates for blood contacting medical devices (Frost *et al.*, 2005). Furthermore, NO-releasing polymers that reduce bacterial adhesion have also made some headway in the development of anti-infective coatings for medical devices (Nablo *et al.*, 2005).

The use of NO as an anti-inflammatory agent is controversial due to the paradoxical effects of NO in immunomodulation. NO is involved in many stages of the inflammatory response (Guzik *et al.*, 2003). For example, constitutively active eNOS produces low concentrations of NO released from the vascular endothelium to inhibit platelet and inflammatory cell adhesion to its surface (Granger & Kubes, 1994; Kubes *et al.*, 1993). In contrast, high concentrations of NO are released by inflammatory cells, via activation of iNOS in response to various inflammatory mediators and bacterial products such as LPS (Moncada & Palmer, 1991). Here, NO is important for the clearance of infecting pathogens (Bogdan, 1997) and for

promoting tissue repair (Stallmeyer *et al.*, 1999). NO also has a paradoxical role in the regulation of inflammatory cell apoptosis (Albina & Reichner, 1998; Brune *et al.*, 1998b; Mannick *et al.*, 1997; Nicotera *et al.*, 1995). The induction and inhibition of apoptosis of inflammatory cells by NO donors have been reported in the literature (Taylor *et al.*, 2003; Ward *et al.*, 2000) This contradiction in the effects of NO is one that is mirrored in many areas of NO biology, particularly with respect to cytotoxicity (Wink *et al.*, 1995; Wink *et al.*, 1998a; Wink *et al.*, 1998b). In most cases, the explanation for the difference lies in the species and concentration of NO present (Brune *et al.*, 1998a; Dusting *et al.*, 1998; Sandau *et al.*, 1999). For example, the concentration of NO can vary considerably according to the distance of the target to the site of NO production. Moreover, a variety of effects associated with NO are produced by NO-related species, resulting from the reaction of NO with constituents of the biological milieu via redox or additive chemistry. Thus, the make-up of the biological milieu can govern the reaction pathway down which NO will proceed, thereby altering the biological effects produced. For instance, the increased production of superoxide (O_2^-) during an inflammatory response leads to increased production of the potent oxidant, peroxynitrite ($ONOO^-$) following the reaction of NO with O_2^- (Beckman & Koppenol, 1996; Koppenol *et al.*, 1992). In many situations, the increased presence of $ONOO^-$ correlates with increased cytotoxicty (Beckman & Koppenol, 1996; Nakazawa *et al.*, 2000; Szabo, 2003; Wink *et al.*, 2001). On the contrary, NO can also protect cells from injury (Sandau *et al.*, 1997; Wink *et al.*, 1993). The supplementation of NO has been shown to reduce death of cardiomyocytes following ischeamia reperfusion injury (Iwase *et al.*, 2007; Sandau *et al.*, 1997; Wink *et al.*, 1993) and at low concentrations NO has been shown to

delay apoptosis of inflammatory cells such as neutrophils (Taylor *et al.*, 2003). This, "double-edged sword" effect of NO in the body holds many barriers to the successful use of NO as a therapeutic. Careful consideration of the concentration of NO and the surrounding biological milieu is required to design NO therapeutics that can avoid adverse side effects.

During the inflammatory response, neutrophils are the most abundant type of immune cell present at sites of infection. They circulate in the blood stream from where they are recruited to sites of injury or infection in response to various inflammatory mediators and cytokines (Gompertz & Stockley, 2000). They migrate into the tissue through adhesive interactions with the vascular endothelium where they kill and clear pathogens and cell debris via phagocytosis (Quie, 1980). Neutrophils have numerous granules within the cytoplasm that contain a toxic soup of proteases and cationic peptides that kill and digest phagocytosed pathogens (Faurschou & Borregaard, 2003). Granule contents and O_2^- are also released into the local environment to aid in killing surrounding pathogens, however, the non-specific effects of these toxic agents can contribute to host tissue damage and the pathogenesis of several diseases (Kitsis & Weissmann, 1991; Wong & Lord, 2004). Consequently, the fine control of the inflammatory response is important in reducing the indiscriminate attack on host tissues whilst retaining the anti-pathogenic effects of neutrophil attack. Apoptosis, or programmed cell death, of neutrophils is a process that is crucial for the resolution of the inflammatory response (Haslett, 1999; Savill, 1997; Savill & Haslett, 1995). Neutrophil apoptosis involves a characteristic stream of events that allow for the clearance of these cells and their histotoxic

contents by phagocytes in an anti-inflammatory fashion. In the absence of apoptotic clearance, necrotic cell death occurs which is a pro-inflammatory process, causing exacerbation of inflammation due the rupture of neutrophils and the release of their histotoxic contents. Thus, the lifecycle of the neutrophil and the factors regulating apoptosis are interesting targets for the production of novel anti-inflammatory drugs (Rossi *et al.*, 2006; Ward *et al.*, 1999). The role of NO as an inducer of apoptosis has been explored, although the involvement of NO *per se* in these effects is controversial (Shaw *et al.*, 2005).

In this chapter, the effects of a novel NO-releasing zeolite on the activation status and death of human neutrophils *in vitro* was investigated with the view to their use as biocompatible coatings for medical devices. NO-releasing zeolites are high capacity storage and release materials of NO that have previously been shown to be powerful inhibitors of platelet activation (Wheatley *et al.*, 2006). The infiltration of neutrophils to the site of device placement is a common feature associated with medical device usage and so the application of NO-loaded zeolite materials *in vivo* requires the characterisation of the effects of NO on inflammatory cell function. The involvement of NO in the inhibition of inflammatory cell adhesion suggests a benefit of releasing NO from the surface of such devices. However the multifaceted relationship of NO with pro and anti-inflammatory processes can mean detrimental effects may prevail. NO-releasing zeolites have been shown in previous chapters to release high concentrations of NO over a short period of time, mirroring the profile of NO released by iNOS rather than the anti-inflammatory, low concentrations released by eNOS. This chapter investigates the potential of these materials to

promote or prevent neutrophil activation *in vitro* with respect to changes in neutrophil activation and cell death markers. Correlation of these effects with the concentration of NO exposed is also investigated in an attempt to address the associated paradox of the pro and anti-inflammatory effects of NO.

This chapter investigates the effect of a 50% Zn^{2+}-exchanged zeolite: PTFE material (NO-loaded and NO-free) on human neutrophil activation and viability in the absence and presence of the neutrophil activator fMLP (formylated-Met- Leu- Phe), a synthetic formylated peptide which mimics the bacterially derived peptides with formylated N-terminal methionine groups. These studies will form part of the primary characterisation of these novel materials as biocompatible materials for medical device coatings.

Experiments described in this chapter were designed to test the hypothesis that NO-loaded zeolites have pro or anti-inflammatory effects in human neutrophils that are dependent upon the concentration of NO exposed in the assay.

4.2 Materials and Methods

4.2.1. Isolation and purification of human neutrophils from whole blood.

Neutrophils were purified and suspended in PBS (with Ca^{2+} and Mg^{2+}) as described in section 2.5.1. Briefly, whole blood was collected and centrifuged to separate the erythrocyte/leukocyte rich layer from the platelet rich plasma. Erythrocytes were then separated from the leukocyte cell population by Dextran sedimentation. The leukocytes were isolated into purified monocyte and neutrophil populations by centrifugation of the leukocyte cell layer through discontinuous, layered Percoll gradients at 81%, 70% and 55%. Monocytes were harvested from the 55/70% interface and neutrophils were harvested from the 70/81% interface. Figure 4.1 shows representative flow profiles and microscopic pictures of the different cell populations found throughout the purification process.

4.2.2. Cytocentrifuge Preparations

Cytospins of cell populations (figure 4.1) isolated from whole blood were prepared using 100µl of the cell suspension + 10% autologous serum. The suspension was centrifuged (300rpm; 3min) through filters onto glass slides. The cells on the slide were allowed to dry at room temp and then stained in methanol (1 min), Quik-Diff Red® (1 min) and Quik Diff-Blue® (1 min) and then washed in H_2O. Cells were analysed for cell purity using light microscopy through an oil immersion lens (X250 magnification).

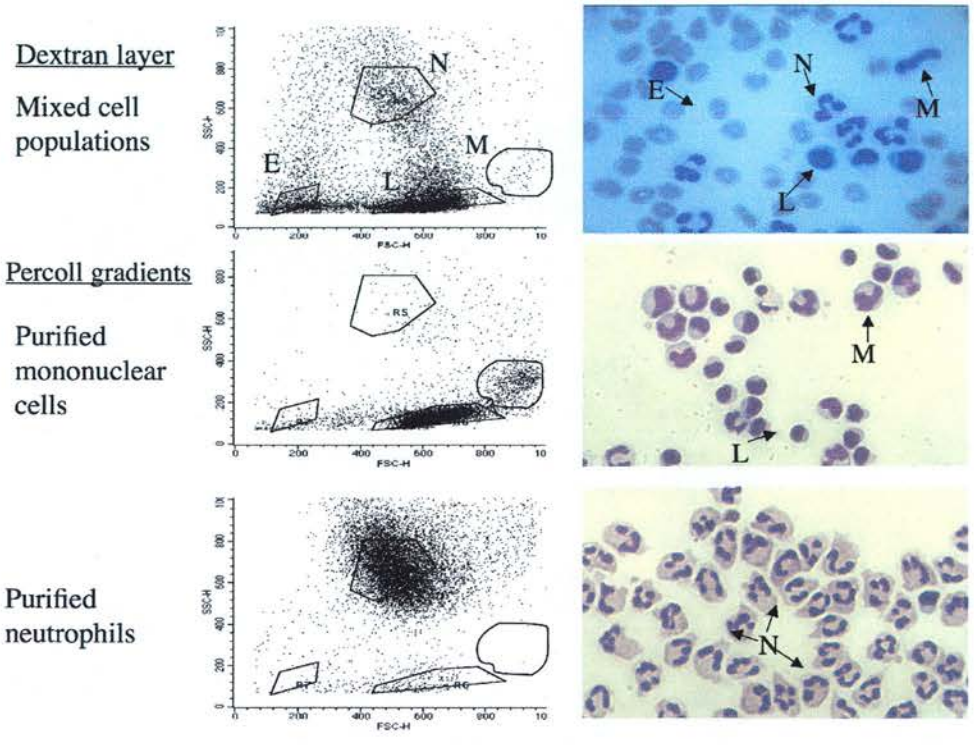

Figure 4.1 Purification of human neutrophils from whole blood.

Flow dot plots showing different gated cell populations indicated by forward scatter (FS; x-axis) and side scatter (SS; y-axis) parameters and microscopic pictures (x250 magnification) from cytocentrifuge preparations of cells at different stages of the cell purification process (following dextran sedimentation and centrifugation through Percoll gradients). The larger mononuclear cell population fall at higher forward scatter levels, whereas the highly granular neutrophils are found at high side scatter levels, allowing the gating of separate populations.

4.2.3. Neutrophil treatment with 50% Zn^{2+}-exchanged zeolites.

50% Zn^{2+}-exchanged zeolites in a PTFE polymer binder were synthesised as described in section 2.8.1. Discs were approximately 3mm diameter x1mm height. NO-loaded discs were stored in sealed Schlenk tubes containing Argon at room temperature until ready for use. Throughout these experiments zeolite treatments will be expressed in units/ml, where 1 unit = 1 zeolite disc and 0.5 units/ml is either ½ zeolite disc or 1 disc in 2ml as indicated.

Isolated neutrophils ($5x10^6$ cells/ml; PBS plus Ca^{2+} and Mg^{2+}) were incubated with zeolites (NO-loaded or NO-free) for 60min in various volumes (1-8ml; 0.125-1unit/ml) in the presence or absence of the neutrophil activator, fMLP (10^{-7}M). fMLP or vehicle (PBS) was administered at 30min of the 60min incubation period. Control samples were run in parallel to zeolite treatments both in the absence or presence of fMLP.

4.2.4 Flow cytometric analysis of neutrophil shape change and expression of activation markers, CD62L and CD11b.

Following treatments, samples were cooled on ice for 10min and 200µl aliquots from each treatment were then labelled (6µg/ml) with fluorescently labelled conjugates of antibodies against CD62L, CD11b or isotype controls (IgG-PE, IgG-FITC; or IgG-APC). The antibodies were incubated (4°C) for 30 min with gentle shaking, prior to analysis by flow cytometry. Flow cytometric analysis was performed using a Coulter FACSCalibur flow cytometer (Beckman Coulter, California, USA) and data

were captured using EXPO™ 32 *v* 2.1 analysis software (Beckman Coulter, California, USA). Fluorescence of the PE-conjugate of CD62L was measured via the FL-2 channel. Fluorescence of FITC and APC conjugates of CD11b were measured through FL-1 and FL-4 channels respectively. Shape-change was measured in parallel as changes in forward scatter (FS) profiles.

4.2.5. Flow cytometric analysis of neutrophil viability in vitro; Annexin V/Propidium Iodide (PI) staining.

Following zeolite treatments, cells were cooled for 10min on ice and then a 20μl sample of the neutrophil suspension (5million cells/ml in PBS with Ca^{2+} and Mg^{2+}) was incubated (4°C; 10min) in 180μl of FITC-conjugated Annexin-V in Annexin V-binding buffer (PBS solution containing 5mM $CaCl_2$). Following the 10 min incubation, the Annexin-V labelled cells were stained with PI (2μg/ml final concentration) 1 min prior to analysis by flow cytometry. Flow cytometric analysis was performed using a Coulter FACSCalibur flow cytometer (Beckman Coulter, California, USA) and data were captured using EXPO™ 32 *v* 2.1 analysis software (Beckman Coulter, California, USA). Apoptosis and necrosis was measured as Annexin-V positive (FL-1) and Annexin-V/PI positive (FL-1 and 2) as a percentage of total gated cells. Cells negative for both markers were considered healthy.

4.2.6 NO electrode study.

Experiments were carried out using a 2 mm isolated NO electrode (ISO-NOP, World Precision Instruments, Stevenage, U.K) and data captured using an analogue-digital converter (Maclab 4e, AD Instruments, Sussex, U.K). The electrode was calibrated as described in section *2.3.1* prior to use each day.

The electrode was placed in a cuvette containing 1ml of pre-warmed (37°C) neutrophil suspension ($5x10^6$ cells; PBS) and allowed to reach a steady baseline. The NO-loaded zeolite discs were suspended in the solution using a stainless steel wire holding device and the electrode was left to record for 60 min post-suspension of the zeolite disc. Time-points were chosen for the calculation of NO concentration released from the zeolite disc using linear regression analysis obtained from the electrode calibration.

4.2.7 Statistics.

Statistical analyses were performed using one-way or two-way analysis of variance with either Dunnet's or Bonferroni's post hoc test and confirmed using non-parametric Kruskel-Wallis with Dunn's post hoc, where appropriate. Statistical significance was assumed when $p < 0.05$ at the 95% confidence interval.

4.3 Results

4.3.1 Activation of isolated human neutrophils by fMLP (10^{-7}M).

Figure 4.2 shows the characteristic changes in neutrophil shape following activation with fMLP (10^{-7}M). Shape-change is measured by flow cytometry as a shift in forward scatter (FS). This is demonstrated by the shift in the cell population shown in the dot plot and the histogram. Approximately 60% of the neutrophils undergo shape change upon stimulation with fMLP (figure 4.2). The shedding of CD62L upon neutrophil activation is indicated by the leftward-shift in peak fluorescence of the PE conjugated antibody, measured through the FL-2 channel (figure 4.3). Up-regulation of the neutrophil adhesion marker CD11b following stimulation with fMLP is shown by the increase in fluorescence measured through channels FL-1 and FL-4, which correspond to the binding of fluorescent conjugated antibodies CD11b-FITC and CD11b-APC respectively (figure 4.4). The fluorescence profiles of the isotype-fluorescent antibodies (ISO-FITC, ISO-APC and ISO-PE) show there is no overlap with the surface marker antibodies, thereby demonstrating that the antibody isotype is not binding in a non-specific manner and that the increase in fluorescence observed is associated with antigen specific binding.

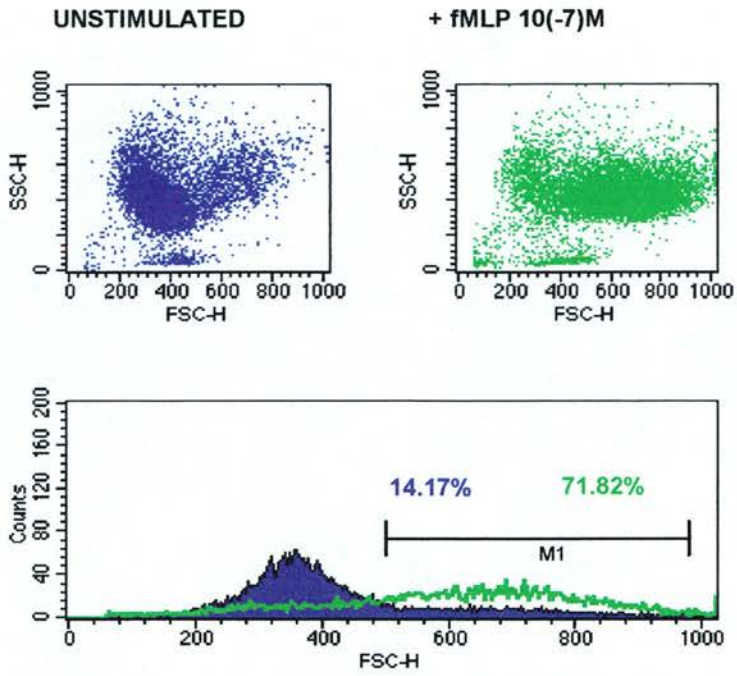

Figure 4.2. Activation of isolated human neutrophils by fMLP (10^{-7}M); neutrophil shape change.

Flow dot plots and histograms show the rightward shift in forward scatter (FS; x-axis) following stimulation of neutrophils with fMLP (10^{-7}M) indicating an increase in size of the fMLP-stimulted neutrophils. The marker M1, shows the percentage of the total neutrophil count for each treatment that falls in the marked region (purple-unstimulated; green-stimulated).

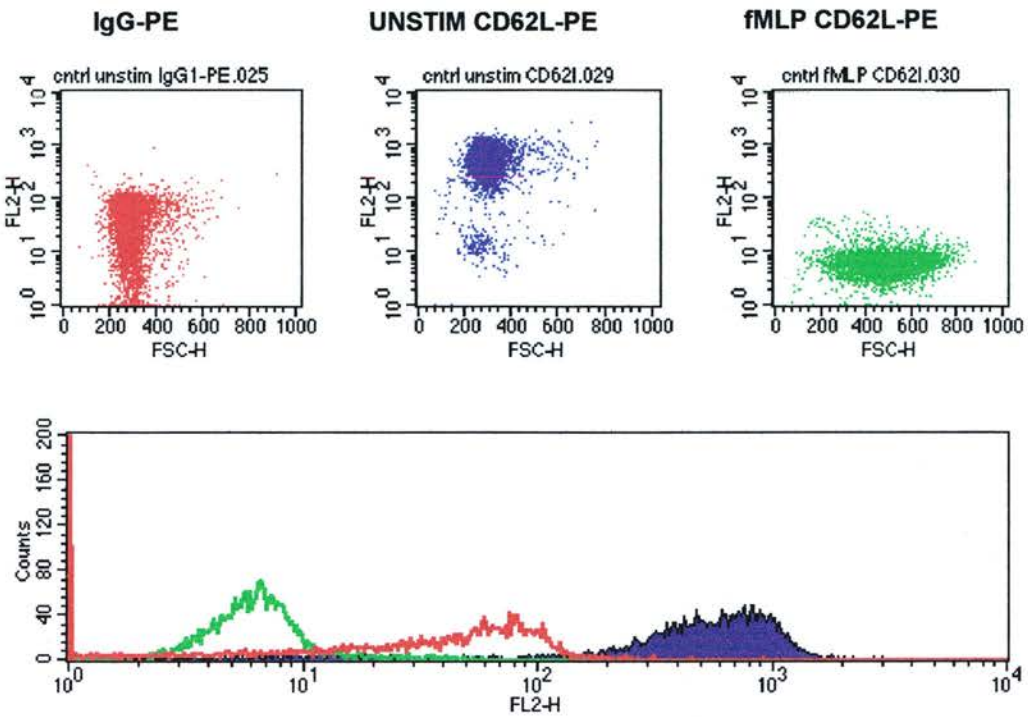

Figure 4.3. Activation of isolated human neutrophils by fMLP (10^{-7}M); shedding of CD62L.

The expression of CD62L in human neutrophil populations through measurement of fluorescent conjugates of anti-human CD62L-PE via the FL-2 channel. The levels of fluorescence (FL-2) of neutrophils labelled with isotype fluorescent conjugates (red), and fluorescent conjugates of anti-human CD62L in unstimulated (purple) and fMLP-stimulated neutrophils (green) are indicated by flow dot plots and histogram.

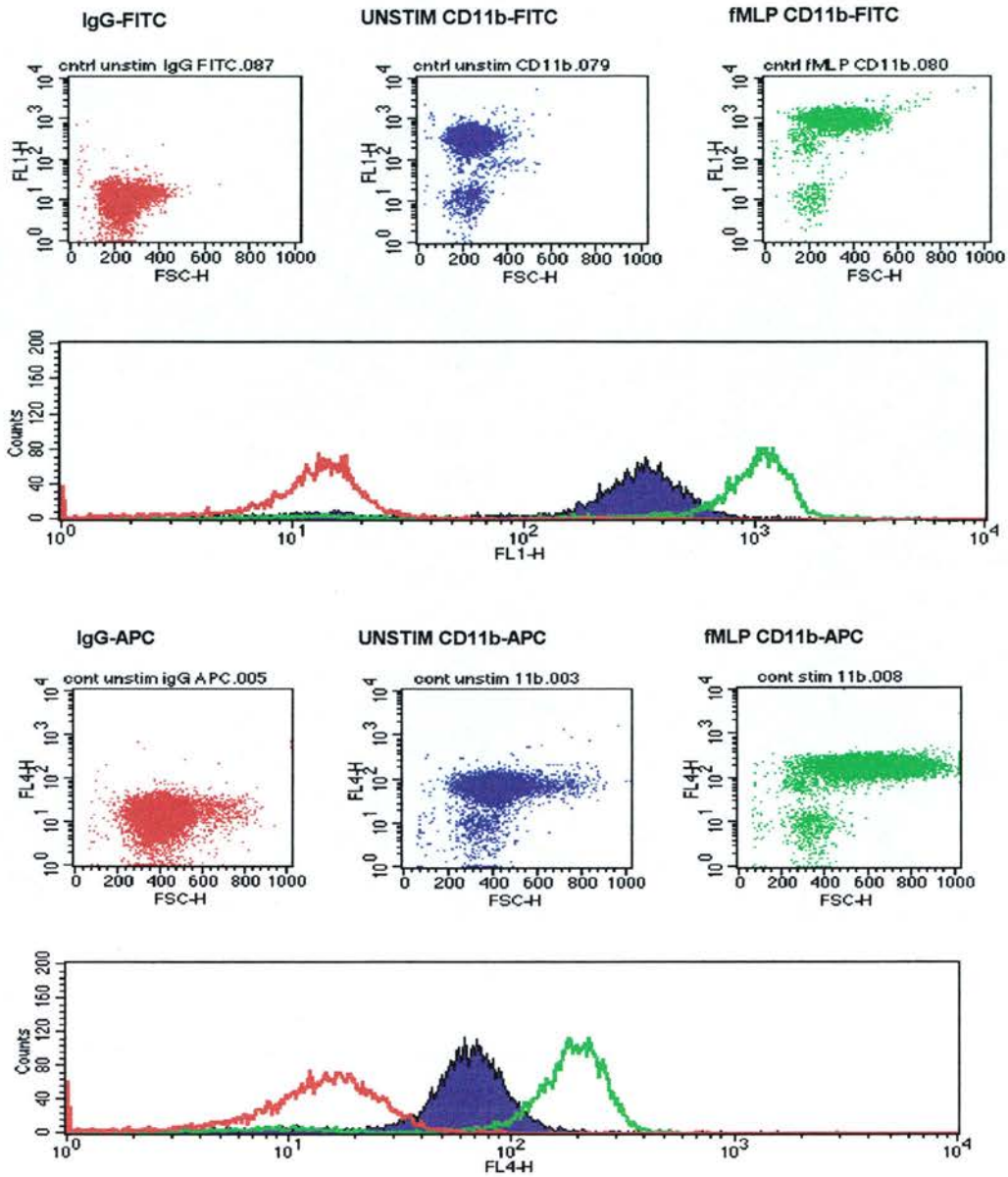

Figure 4.4. Activation of isolated human neutrophils by fMLP (10^{-7}M); up-regulation of CD11b.

The expression of CD11b in human neutrophil populations through the measurement of fluorescent conjugates of anti-human CD11b- FITC and anti-human CD11b- APC via FL-1 and FL-4 channels respectively. The levels of fluorescence (FL-1 and FL-4) of neutrophils labelled with isotype fluorescent conjugates (red), and fluorescent conjugates of anti-human CD11b in unstimulated (purple) and fMLP-stimulated neutrophils (green) are indicated by flow dot plots and histograms.

4.3.2. The effect of 50% Zn^{2+}-exchanged zeolites on neutrophil shape change.

Neutrophil stimulation with fMLP results in shape-change as indicated by the shift in forward scatter profiles of control fMLP stimulated neutrophils compared to unstimulated cells (figure 4.2 and 4.4-5). Treatment with 0.5unit/ml Zn^{2+}-zeolites (NO-free and NO-loaded) produced no apparent change in the forward scatter profiles of unstimulated and fMLP-stimulated neutrophils compared to control (figure 4.5). At 1unit/ml zeolite treatments, NO-free zeolite treatments produced comparable profiles to control in both unstimulated and fMLP-stimulated neutrophils. The NO-loaded zeolite treatment produced a shift in the forward-scatter profiles of unstimulated neutrophils, with approximately 40% more cells undergoing shape change compared to control. This augmentation of forward scatter profiles was not mirrored in fMLP-stimulated neutrophils following NO-loaded zeolite treatment, which remained similar to control (figure 4.6).

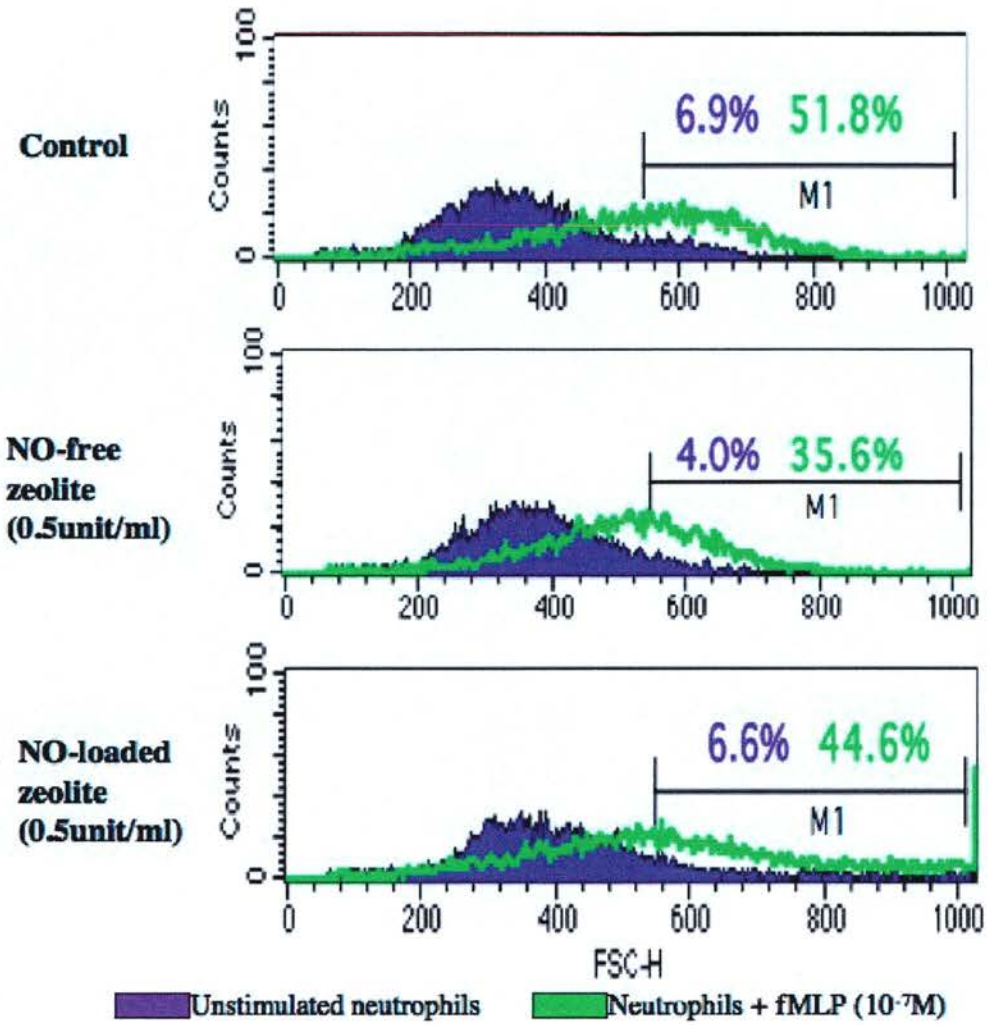

Figure 4.5. The effect of 50% Zn^{2+}-exchanged zeolites on neutrophil shape change; 0.5unit/ml zeolite treatment.

Forward-scatter (FSC; x-axis) profiles of unstimulated (purple) and fMLP-stimulated (10^{-7}M) neutrophils following control (top), NO-free (middle) and NO-loaded zeolite treatments (0.5unit/ml; 60 min). Percent of unstimulated and fMLP-treated neutrophils falling within marker range, M1 have been included for comparison between treatments.

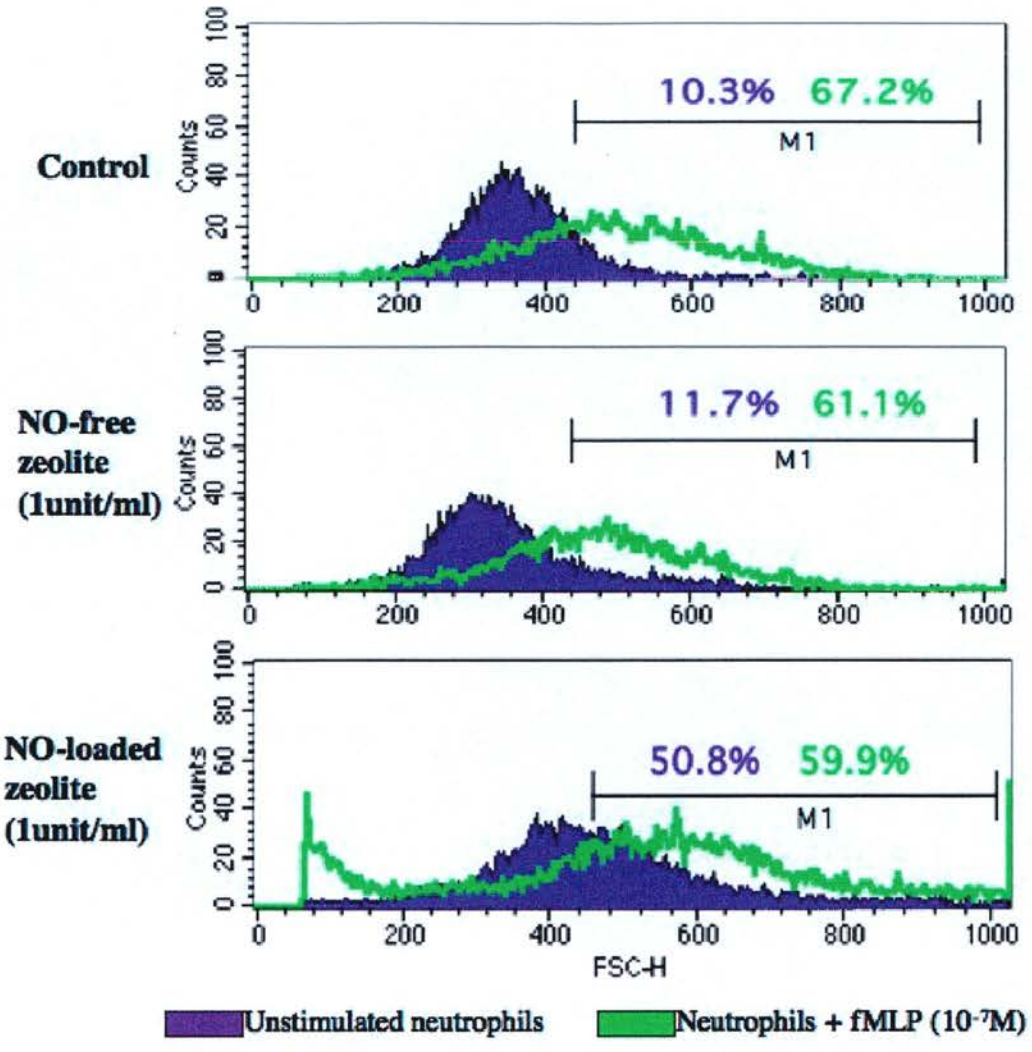

Figure 4.6. The effect of 50% Zn^{2+}-exchanged zeolites on neutrophil shape change; 1unit/ml zeolite treatment.

Forward-scatter (FSC; x-axis) profiles of unstimulated (purple) and fMLP-stimulated (10^{-7}M) neutrophils following control (top), NO-free (middle) and NO-loaded zeolite treatments (1unit/ml; 60 min). The percentage of unstimulated and fMLP-stimulated neutrophils falling within marker range, M1 have been included for comparison between treatments.

4.3.3. The effect of 50% Zn^{2+}-exchanged zeolites on neutrophil activation marker CD62L.

The shedding of CD62L following stimulation of isolated neutrophils with 10^{-7}M fMLP is demonstrated by the reduction in peak fluorescence measured through the FL-2 channel shown in the representative flow histograms. Neutrophils treated with 0.5unit/ml of the NO-free or NO-loaded zeolite discs demonstrated no significant shedding of CD62L compared to control in unstimulated or fMLP-stimulated conditions (Figure 4.7). The incubation of 1unit/ml of the NO-free zeolite disc had no significant effects whereas the NO-loaded zeolite (1unit/ml) produced significant CD62L shedding in unstimulated neutrophils (figure 4.8). The histogram shows a clear leftward shift in fluorescence (FL-1) in unstimulated (purple) neutrophils following NO-loaded zeolite treatment and lower mean fluorescence values compared to control and NO-free zeolite treatments.

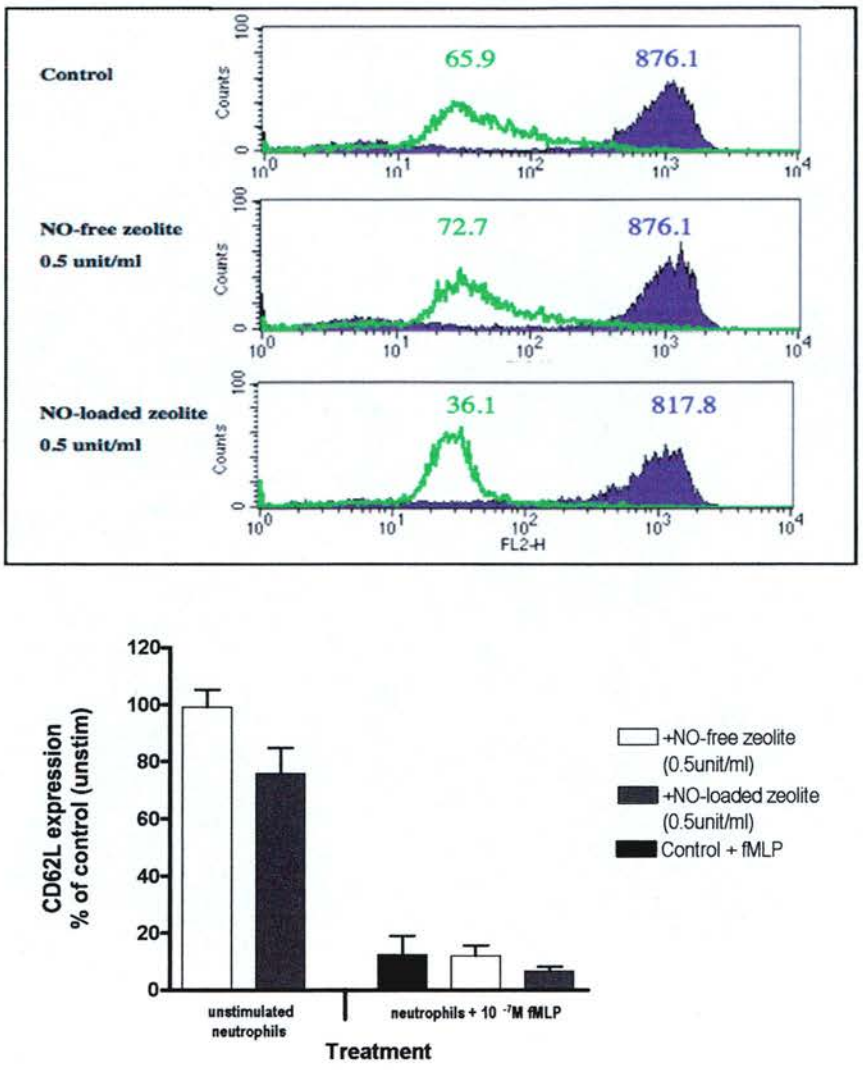

Figure 4.7. The effect of 50% Zn^{2+}-exchanged zeolites on CD62L shedding in isolated human neutrophils; 0.5unit/ml zeolite treatment.

Representative flow histograms showing fluorescence profiles and mean fluorescence values of PE-conjugated anti-human CD62L (log FL-2; x-axis) from control and zeolite (NO-free and NO-loaded; 0.5unit/ml) treated neutrophils in unstimulated (purple) and fMLP-stimulated (10^{-7}M; green) conditions. The bar graph represents the cumulative data of CD62L expression of neutrophils(5 x 10^6cells; 1ml; PBS) incubated (60 min; 37°C) with 0.5unit/ml NO-loaded zeolite disc (grey bar), 0.5unit/ml NO-free zeolite disc (white bar) or control (black) in the absence and presence of the neutrophil activator fMLP (10^{-7}M; 30 min). Data is expressed as % of control (unstimulated) values and represent the mean +/- SEM of n=5 independent experiments. Mean fluorescence (FL-2) of control (unstim) treatments was 554.0 +/- 68.9.

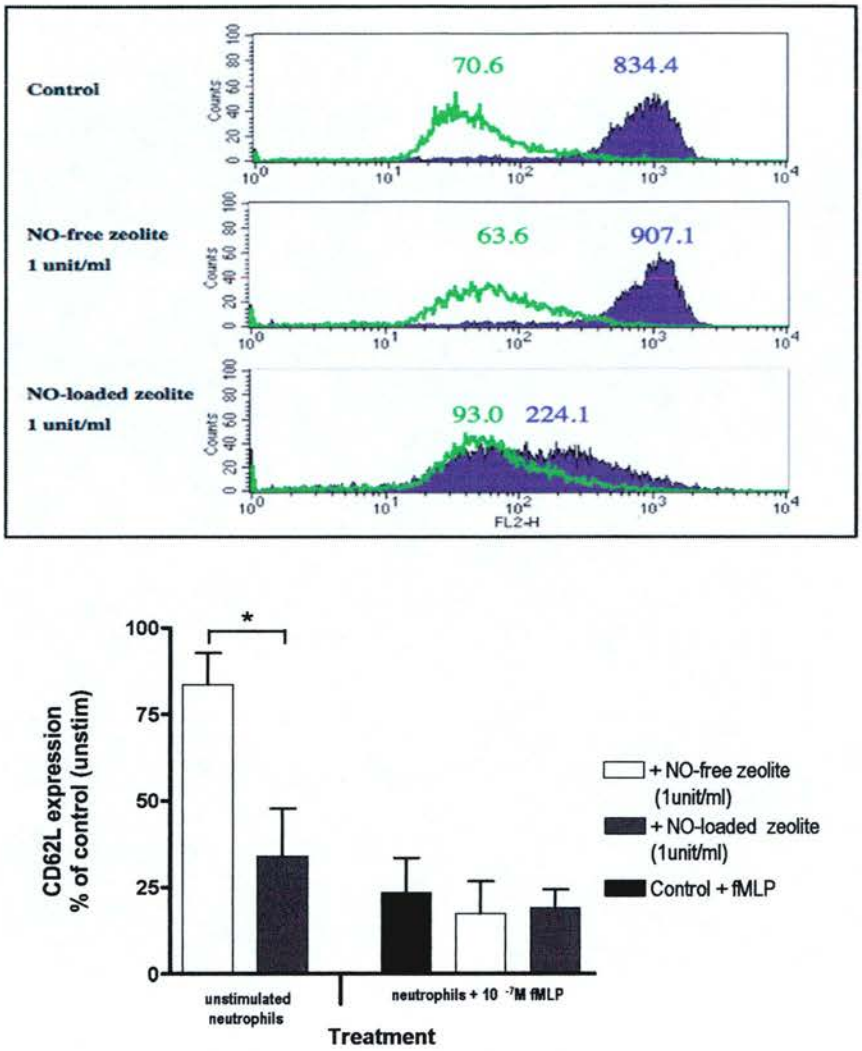

Figure 4.8. The effect of 50% Zn^{2+}-exchanged zeolites on CD62L shedding in isolated human neutrophils; 1 unit/ml zeolite treatment.

Representative flow histograms showing fluorescence profiles and mean fluorescence values of PE-conjugated anti-human CD62L (log FL-2; x-axis) from control and zeolite (NO-free and NO-loaded; 1unit/ml) treated neutrophils in unstimulated (purple) and fMLP-stimulated (10^{-7}M; green) conditions. The bar graph represents the cumulative data of CD62L expression of neutrophils (5 x 10^6cells; 1ml; PBS) incubated (60 min; 37°C) with 1unit/ml NO-loaded zeolite disc (grey bar), 1unit/ml NO-free zeolite disc (white bar) or control (black) in the absence and presence of the neutrophil activator fMLP (10^{-7}M; 30 min). Data is expressed as % of control (unstimulated) values and represent the mean +/- SEM of n=6 independent experiments. Mean fluorescence (FL-2) of control (unstim) treatments was 531.6 +/- 70.8. Asterisk denotes statistical significance compared to NO-free zeolite treatment.

4.3.4. The effect of 50% Zn^{2+}- exchanged zeolites on neutrophil activation marker CD11b.

Figure 4.9 and 4.10 show the effect of incubation (60 min; 37°C) of 0.5unit/ml and 1unit/ml of zeolite (50% Zn^{2+} NO-loaded and NO-free) in 1ml neutrophil ($5x10^6$cells) suspension respectively. Representative histograms show a rightward shift in fluorescence of fMLP-treated (10^{-7}M) neutrophils that is more pronounced following NO-loaded zeolite treatment and is confirmed by higher mean fluorescence values.

NO-free zeolite treatments produced similar levels of CD11b expression to control at both zeolite concentrations in both unstimulated and fMLP-stimulated conditions. NO-loaded zeolites had no significant effect on CD11b expression in unstimulated neutrophils but significantly enhanced expression in fMLP-stimulated neutrophils at both 0.5unit/ml and 1unit/ml zeolite treatment (figure 4.9- 4.10).

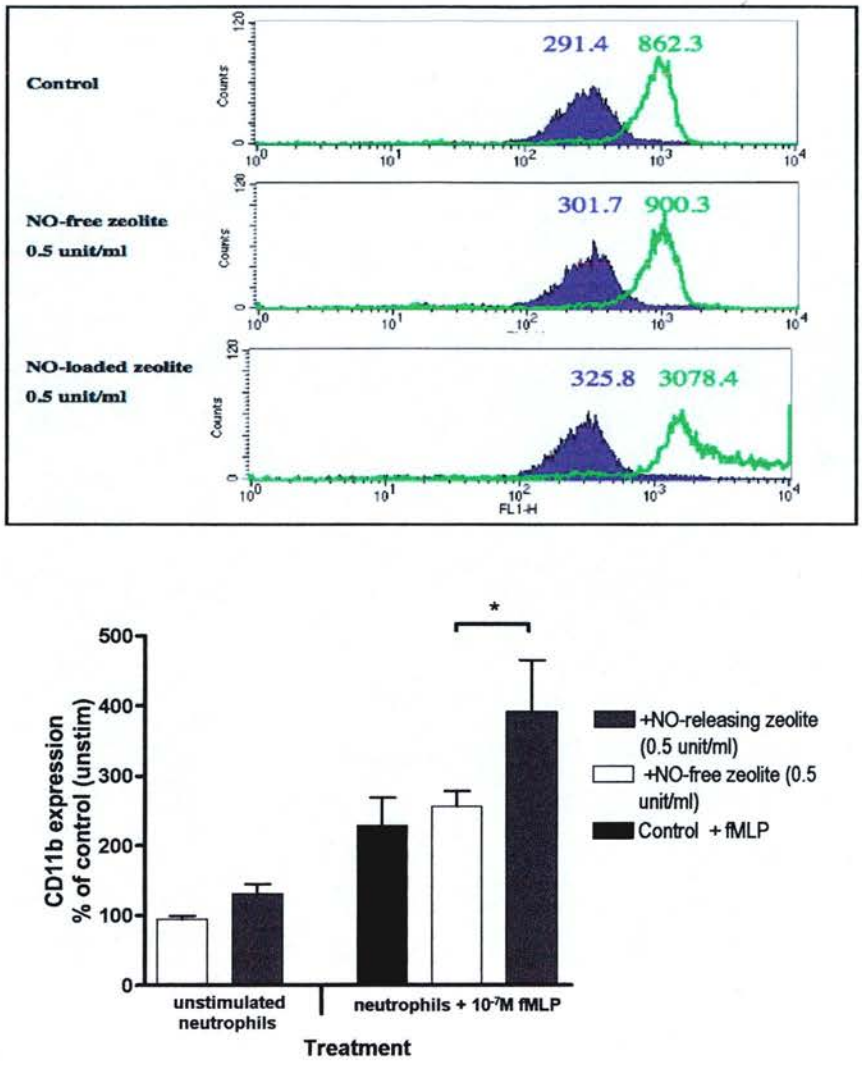

Figure 4.9. The effect of 50% Zn^{2+}-exchanged zeolites on CD11b up-regulation in isolated human neutrophils; 0.5unit/ml zeolite treatment.

Representative flow histograms showing fluorescence profiles and mean fluorescence values of FITC-conjugated anti-human CD11b (log FL-1; x-axis) from control and zeolite (NO-free and NO-loaded; 1unit/ml) treated neutrophils in unstimulated (purple) and fMLP-stimulated (10^{-7}M; green) conditions. The bar graph represents the cumulative data of CD11b expression of neutrophils (5 x 10^6cells; 1ml; PBS) incubated (60 min; 37°C) with 1unit/ml NO-loaded zeolite disc (grey bar), 1unit/ml NO-free zeolite disc (white bar) or control (black) in the absence and presence of the neutrophil activator fMLP (10^{-7}M; 30 min). Data are expressed as % of control (unstimulated) values and represent the mean +/- SEM of n=4 independent experiments. Mean fluorescence (FL-1) of control (unstim) treatments was 294.2 +/- 55.9.

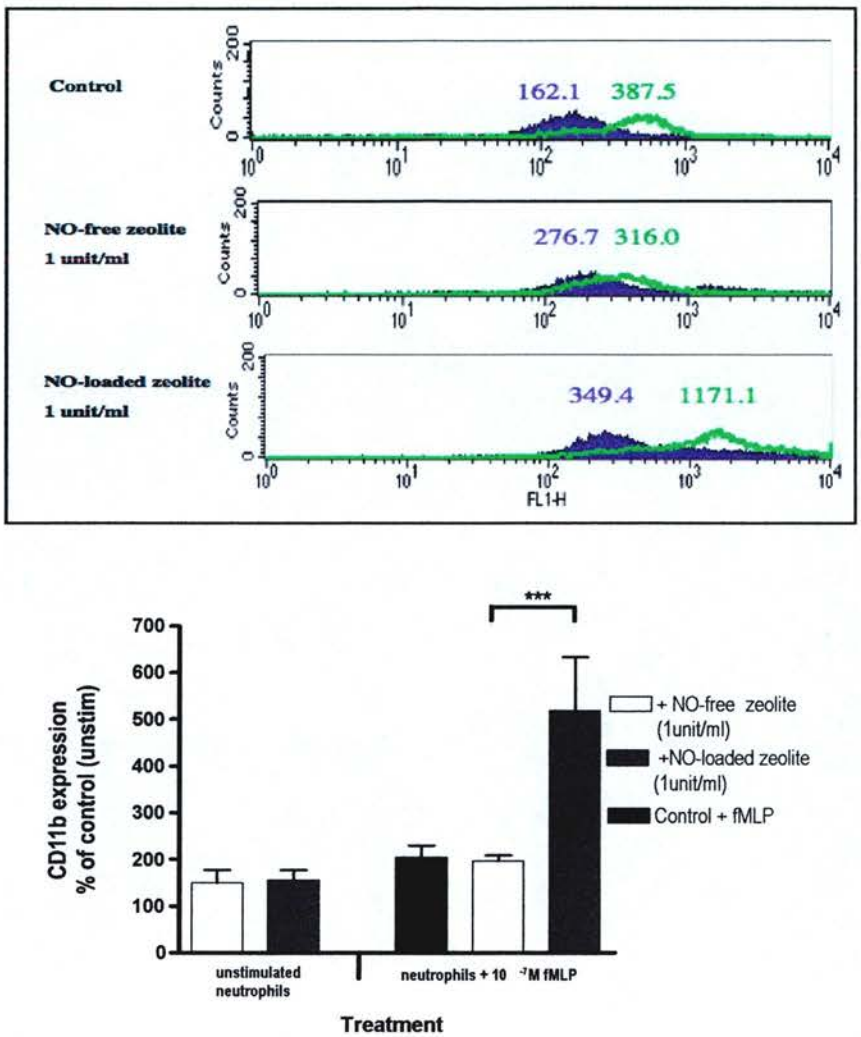

Figure 4.10. The effect of 50% Zn^{2+}-exchanged zeolites on CD11b up-regulation in isolated human neutrophils; 1unit/ml zeolite treatment.

Representative flow histograms showing fluorescence profiles and mean fluorescence values of FITC-conjugated anti-human CD11b (log FL-2; x-axis) from control and zeolite (NO-free and NO-loaded; 1unit/ml) treated neutrophils in unstimulated (purple) and fMLP-stimulated (10^{-7}M; green) conditions. The bar graph represents the cumulative data of CD11b expression of neutrophils (5 x 10^6cells; 1ml; PBS) incubated (60 min; 37°C) with 1unit/ml NO-loaded zeolite disc (grey bar), 1unit/ml NO-free zeolite disc (white bar) or control (black) in the absence and presence of the neutrophil activator fMLP (10^{-7}M; 30 min). Data are expressed as % of control (unstimulated) values and represent the mean +/- SEM of n=4 independent experiments. Mean fluorescence (FL-1) of control (unstim) treatments was 295.0 +/- 65.5. Asterisks denote significance compared to NO-free zeolite treated neutrophils (*** $p < 0.001$).

4.3.5. The concentration-dependent effect of NO-releasing zeolites on neutrophil activation markers CD62L and CD11b.

To assess the effect of lower concentrations of NO on neutrophil activation, NO-loaded zeolites discs were suspended in varying volumes (1-8ml) of the neutrophil suspension in order to dilute the concentration of NO released from the zeolite disc. Increasing the NO-loaded zeolite exposure to the neutrophil suspension ($5x10^6$ cells/ml) from 0.125unit/ml to 1unit/ml produced a decreasing trend of CD62L expression in both unstimulated and fMLP-stimulated neutrophils (figure 4.11). CD11b expression in unstimulated neutrophils was not significantly different from control at all concentrations of NO-loaded zeolite. CD11b expression in fMLP-stimulated neutrophils was markedly enhanced from control at the highest NO-loaded zeolite concentration only (1unit/ml; figure 4.12).

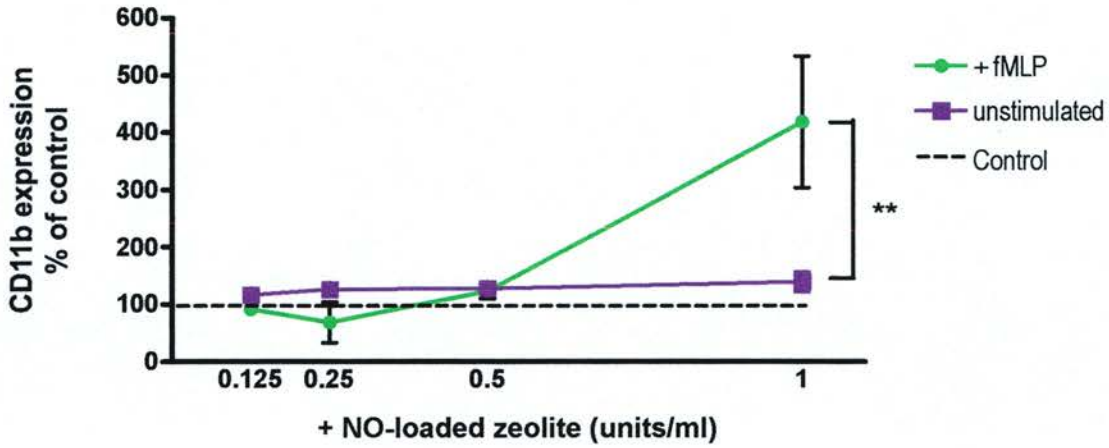

Figure 4.12. The effect of NO-loaded zeolite disc dilutions on the expression of CD11b in isolated human neutrophils.

The mean expression of CD11b-APC fluorescence measured via the FL-4 channel of neutrophils treated with increasing concentrations (0.125-1unit/ml) of NO-loaded zeolite (60min; 37°C) achieved through zeolite disc dilution in increasing volumes (1-8ml) of the neutrophil suspension ($5x10^6$ cells/ml; PBS) in untimulated (purple) and fMLP-stimulated (10^{-7}M; 30min; green) conditions. Bars represent the mean +/- SEM of n=3 independent experiments. Asterisks denote significant difference between unstimulated and fMLP stimulated neutrophils at the appropriate concentration.

4.3.6. NO-release from 50% Zn^{2+}-exchanged zeolites in isolated neutrophil suspensions.

NO-release from 50% Zn^{2+}-exchanged zeolites (NO-loaded) in a suspension (1ml) of isolated human neutrophils ($5x10^6$cells; PBS; 37°C) shows a rapid release of high concentrations (peak ~ 30μM) of NO. Peak release of NO is reached within the first 10 min and rapidly deteriorates to near baseline by 40 min (figure 4.13).

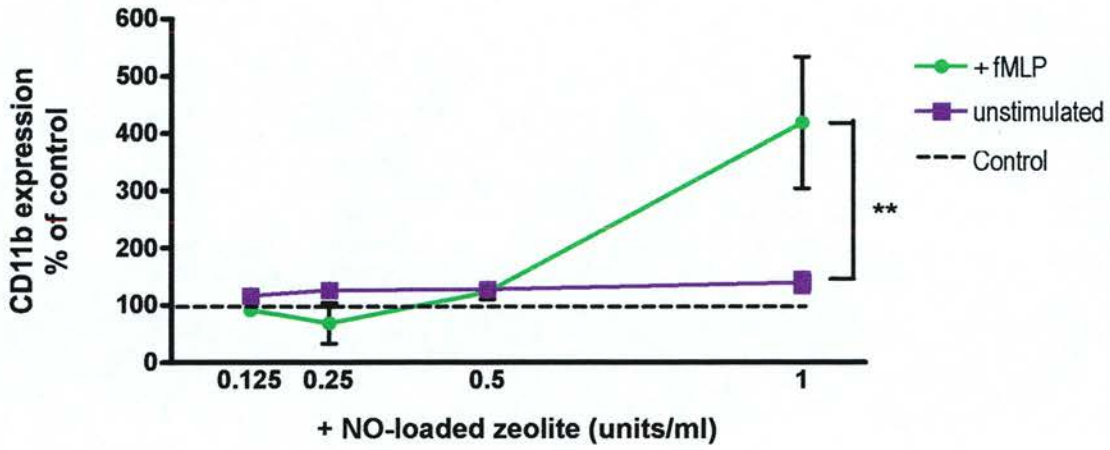

Figure 4.12. The effect of NO-loaded zeolite disc dilutions on the expression of CD11b in isolated human neutrophils.

The mean expression of CD11b-APC fluorescence measured via the FL-4 channel of neutrophils treated with increasing concentrations (0.125-1unit/ml) of NO-loaded zeolite (60min; 37°C) achieved through zeolite disc dilution in increasing volumes (1-8ml) of the neutrophil suspension ($5x10^6$ cells/ml; PBS) in untimulated (purple) and fMLP-stimulated (10^{-7}M; 30min; green) conditions. Bars represent the mean +/- SEM of n=3 independent experiments. Asterisks denote significant difference between unstimulated and fMLP stimulated neutrophils at the appropriate concentration.

4.3.6. NO-release from 50% Zn^{2+}-exchanged zeolites in isolated neutrophil suspensions.

NO-release from 50% Zn^{2+}-exchanged zeolites (NO-loaded) in a suspension (1ml) of isolated human neutrophils ($5x10^6$cells; PBS; 37°C) shows a rapid release of high concentrations (peak ~ 30μM) of NO. Peak release of NO is reached within the first 10 min and rapidly deteriorates to near baseline by 40 min (figure 4.13).

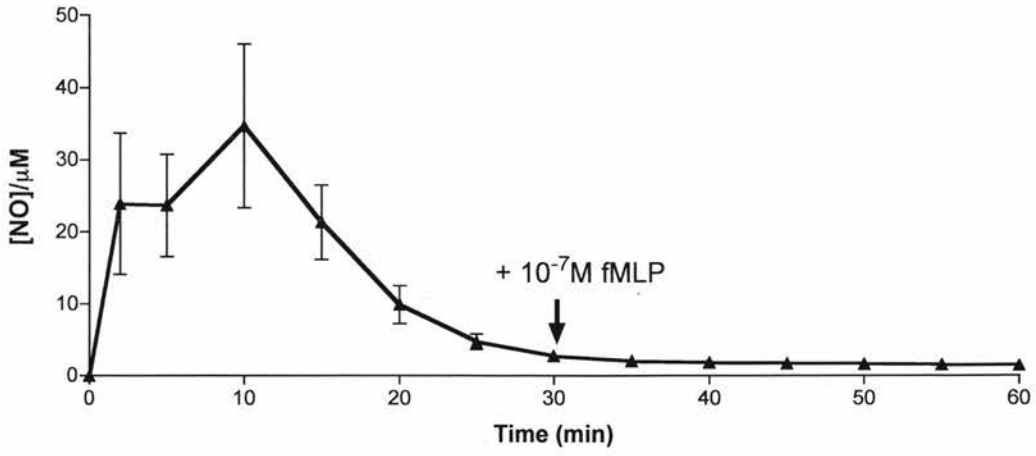

Figure 4.13. NO generation from 50% Zn^{2+}-exchanged NO-loaded zeolites in suspension with human isolated neutrophils.

NO-release profile following suspension of 50% Zn^{2+}-exchanged zeolite (NO-loaded; 1unit/ml) in isolated human neutrophils (PBS;1ml; 37°C) for 60 min. The arrow indicates the addition of fMLP (10^{-7}M) at 30min.

4.3.7. The effect of 50% Zn^{2+}-exchanged zeolites on neutrophil viability.

The incubation (60min; 37°C) of NO-free and NO-loaded zeolite disc (0.5unit/ml) in the neutrophil suspension ($5x10^6$cells; 1ml;PBS) had no significant effect on the levels of apoptosis or necrosis compared to control in unstimulated (figure 4.14) or fMLP-stimulated (figure 4.15) conditions. At 1unit/ml NO-free zeolites also had no significant effects on neutrophil apoptosis or necrosis compared to control in both unstimulated (figure 4.16) or fMLP-stimulated (figure 4.17) neutrophils. The NO-loaded disc at 1unit/ml produced a significant increase in the levels of cell necrosis compared to control in unstimulated neutrophils (figure 4.16) that was further increased in fMLP-stimulated neutrophils (figure 4.17). The increase in necrosis

following NO-loaded zeolite treatments correlated with a significant decrease in the healthy cell populations compared to control. Representative flow dot-plots demonstrate an increase in the % of cells positive for Annexin-V (FL-1) and PI (FL-2) in the upper right quadrant following NO-loaded zeolite treatment at 1unit/ml, which is indicative of necrosis. Apoptotic cell responses (Annexin V positive; lower right quadrant) were unaffected at this time-point for all treatments.

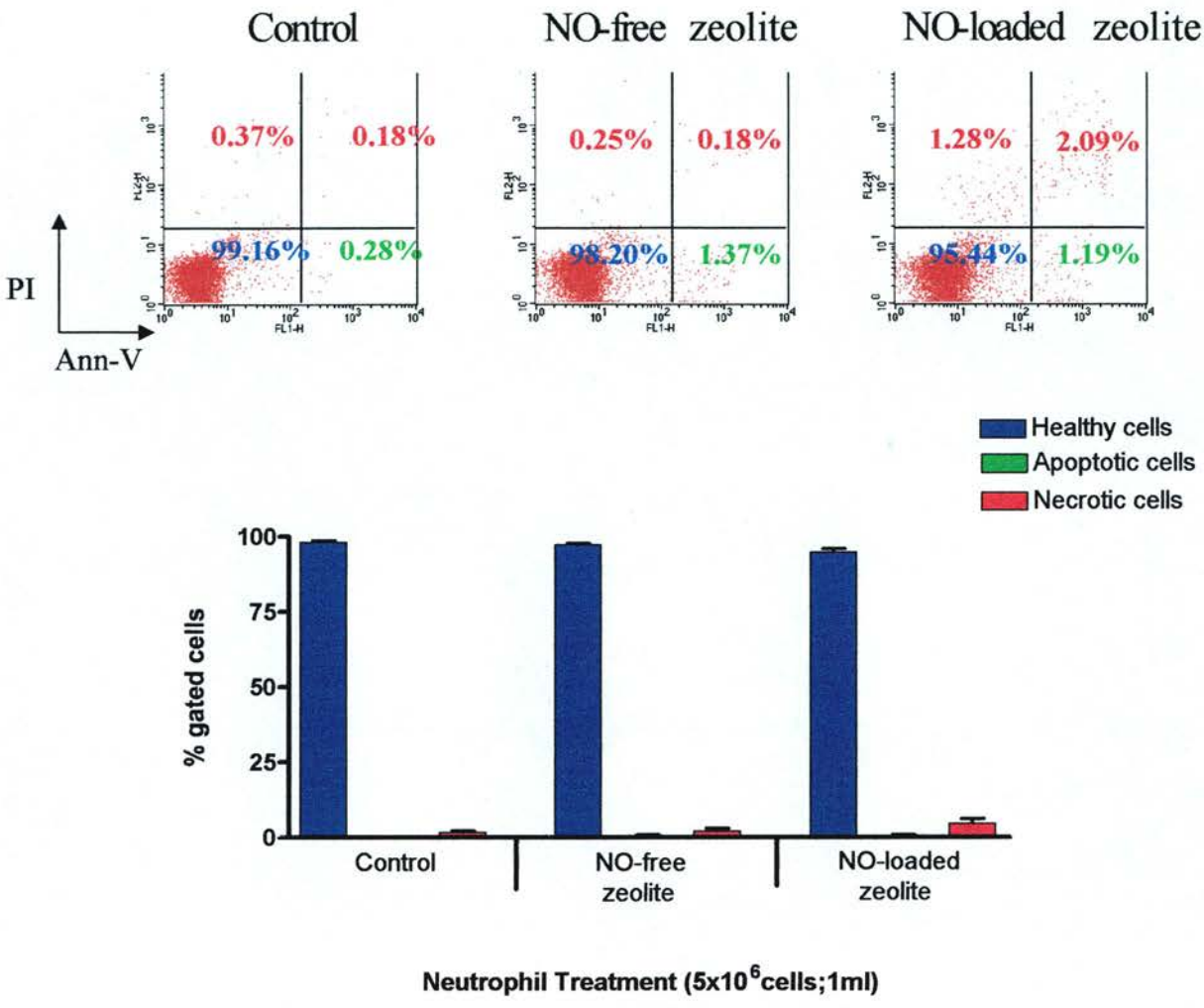

Figure 4.14. The effect of Zn^{2+}-exchanged zeolites on neutrophil viability – 0.5 unit/ml zeolite incubation.

Representative dot plots and cumulative data expression of neutrophil viability in gated populations of isolated cells using flow cytometric analysis of fluorescent cell markers. The percentage of cells considered apoptotic (green; lower right quadrant) were cells positive for the fluorescent apoptotic marker Annexin-V (FL-1; x-axis), necrotic populations (red; top quadrants) were the positive for the necrotic cell marker PI (FL-2; y-axis). Healthy cell populations (blue; bottom left quadrant) were cells that stained negative for both cell stains. Neutrophil suspensions ($5x10^6$cells; 1ml; PBS) were incubated (60 min; 37°C) with 0.5 unit/ml 50% Zn^{2+}-exchanged zeolites (NO-free and NO-loaded) in the absence of neutrophil activator, fMLP. Bars represent the mean +/- SEM for n=3 independent experiments.

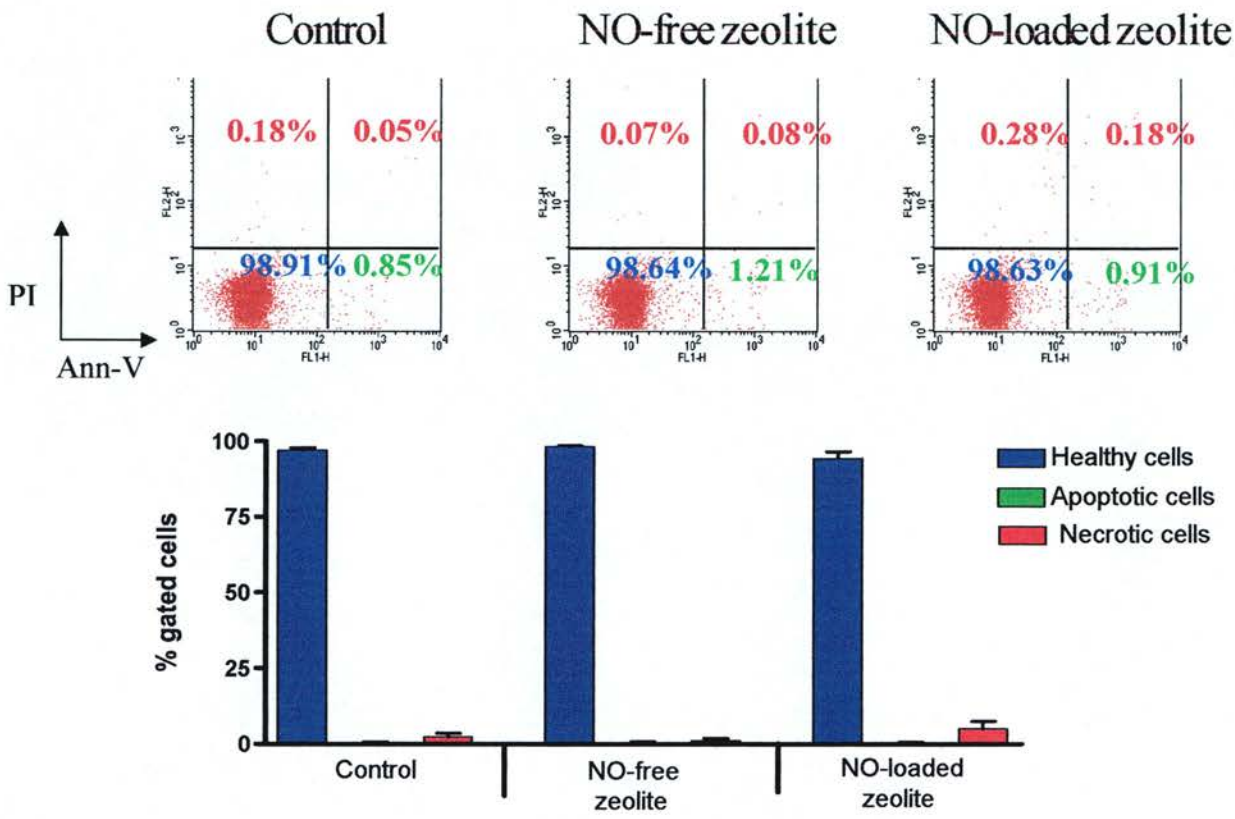

Figure 4.15. The effect of Zn^{2+}-exchanged zeolites on fMLP stimulated (10^{-7}M) neutrophil viability – 0.5 unit/ml zeolite incubation.

Representative dot plots and cumulative data expression of neutrophil viability in gated populations of isolated cells using flow cytometric analysis of fluorescent cell markers. The percentage of cells considered apoptotic (green; lower right quadrant) were cells positive for the fluorescent apoptotic marker Annexin V (FL-1; x-axis), necrotic populations (red; top quadrants) were positive for the nuclear stain PI (FL-2; y-axis). Healthy cell populations (blue; bottom left quadrant) were cells that stained negative for both cell stains. Neutrophil suspensions ($5x10^6$cells; 1ml; PBS) were incubated (60 min; 37°C) with 0.5 unit/ml 50% Zn^{2+}-exchanged zeolites (NO-free and NO-loaded) in the presence of neutrophil activator, fMLP (10^{-7}M). Bars represent the mean +/- SEM for n=3 independent experiments.

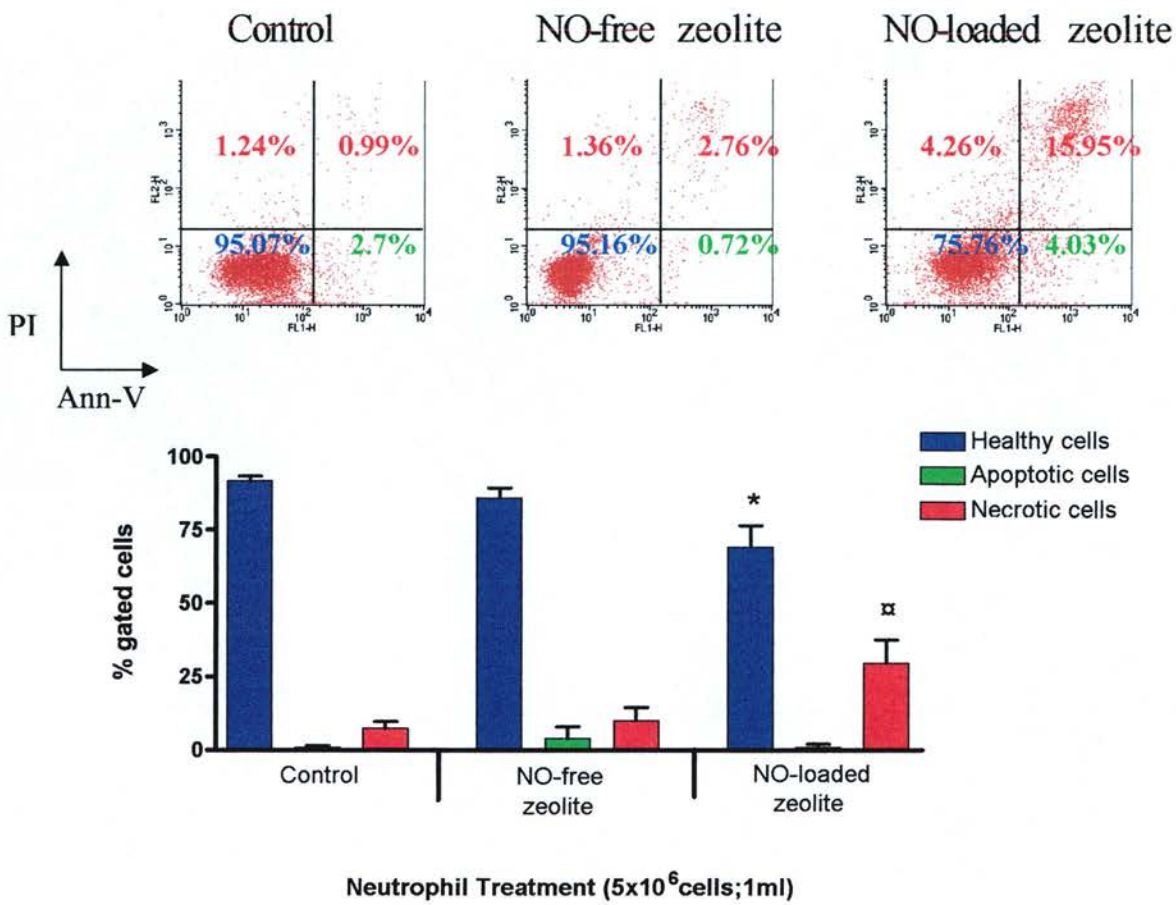

Figure 4.16. The effect of Zn^{2+}-exchanged zeolites on neutrophil viability – 1 unit/ml zeolite incubation.

The representative dot plots and cumulative data expression of neutrophil viability in gated populations of isolated cells using flow cytometric analysis of fluorescent cell markers. The percentage of cells considered apoptotic (green; lower right quadrant) were cells positive for the fluorescent apoptotic marker Annexin V (FL-1; x-axis), necrotic populations (red; upper quadrants) were the positive for the nuclear stain, PI (FL-2; y-axis). Healthy cell populations (blue; lower left quandrant) were cells that stained negative for both cell stains. Neutrophil suspensions ($5x10^6$cells; 1ml; PBS) were incubated (60 min; 37°C) with 1unit/ml 50% Zn^{2+}-exchanged zeolite (NO-free and NO-loaded) in the absence of the neutrophil activator fMLP. Bars represent the mean +/- SEM for n=4 independent experiments. * $p < 0.05$ vs control healthy; § $p < 0.05$ vs control necrotic.

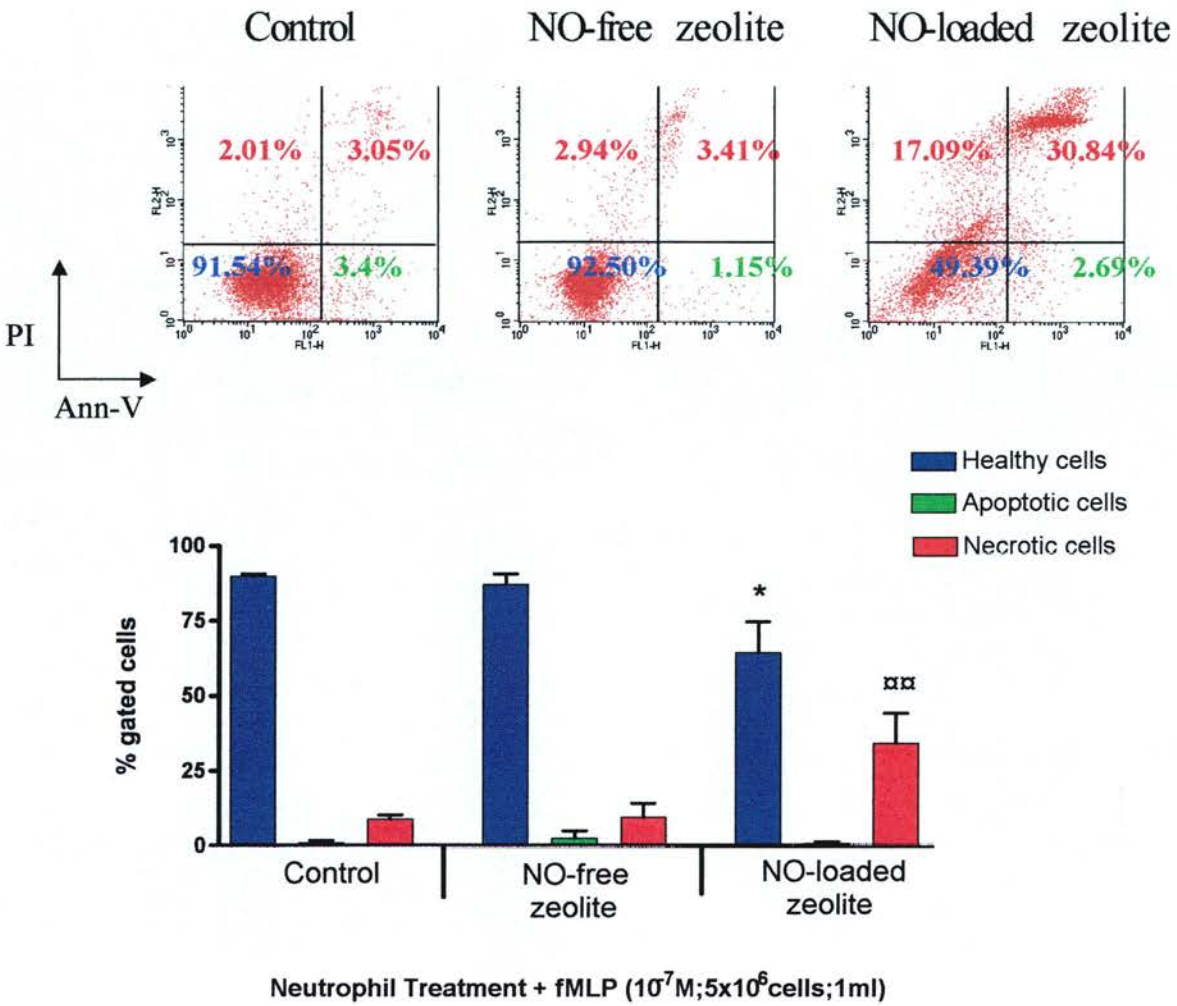

Figure 4.17. The effect of Zn^{2+}-exchanged zeolites on fMLP stimulated (10^{-7}M) neutrophil viability – 1 unit/ml zeolite incubation.

The representative dot plots and cumulative data expression of neutrophil viability in gated populations of isolated cells using flow cytometric analysis of fluorescent cell markers. The percentage of cells considered apoptotic (green; lower right quadrant) were cells positive for the fluorescent apoptotic marker Annexin V (FL-1; x-axis), necrotic populations (red; upper quadrants) were the positive for the nuclear stain, PI (FL-2; y-axis). Healthy cell populations (blue; lower left quandrant) were cells that stained negative for both cell stains. Neutrophil suspensions (5x10^6cells; 1ml; PBS) were incubated (60 min; 37°C) with 1unit/ml 50% Zn^{2+}-exchanged zeolite (NO-free and NO-loaded) in the absence of the neutrophil activator fMLP. Bars represent the mean +/- SEM for n=4 independent experiments. * $p < 0.05$ vs control healthy; § $p < 0.05$; §§ $p < 0.01$ vs control necrotic.

4.4 Discussion

The involvement of NO in neutrophil activation status is an area with much contention within the literature. The inhibition and activation of neutrophil responses has been demonstrated in numerous studies utilising effects of both endogenous and exogenous NO production. For example, exogenous application of NO donors has been shown to inhibit (Kosonen *et al.*, 1999) and increase (Okayama *et al.*, 1999) neutrophil adhesion to endothelial cells *in vitro*. Differences in the species and concentration of NO donor used in these experiments may account for the discrepancy in the effects of NO. Interestingly, the study by Kosonen *et al,* used the closely related sydnonomine and mesoionic oxatriazole species which are generally regarded as $ONOO^-$ generators due to the simultaneous generation of NO and O_2^- (Feelisch & Kelm, 1991; Hogg *et al.*, 1992; Taylor *et al.*, 2004). The inhibition of neutrophil adherence was linked to increases in cGMP, whereas the increase in neutrophil adherence by 1mM concentrations of the diazeniumdiolate compound (SPER/NO) was linked to a PKG-dependent mechanism. The inconsistencies encountered within the literature in many areas of NO biology underlies the complex interactions of NO which are dependent upon the concentration of NO and chemical species encountered by different cell types. The paradoxical effects of NO on neutrophil adherence discussed above prompted the present study into the effect of NO-releasing zeolites on neutrophil activation. The biocompatibility of materials with respect to the inflammatory response is fundamental in the successful development of such medical device coatings due to the non-specific effects of the elicited immune response on host tissues which could

result in host tissue damage as well as localised pain and swelling. To this end, we have shown that NO-releasing zeolites have the potential to significantly induce the shedding of CD62L (L-selectin) in isolated human neutrophils. This shedding was associated with high concentrations of NO released in a small volume of the neutrophil suspension and was reversed to control levels upon dilution of the zeolite in greater volumes of the neutrophil suspension, thereby indicating a concentration dependent effect of NO on L-selectin shedding. Interestingly, the shedding of L-selectin occurred in the absence of the neutrophil activator, fMLP, and was linked with concomitant changes in neutrophil shape change. This suggests that high concentrations of NO are stimulating the neutrophil inflammatory response and are consequently pro-inflammatory. In the absence of fMLP, CD11b expression was not significantly up-regulated following zeolite treatments although there does appear to be a slight enhancement, particularly at the 1unit/ml concentration. The induction of neutrophil shape change and L-selectin shedding under the same experimental conditions would suggest that this up-regulation is real and would be reflected statistically following further investigation. The expression of CD11b upon stimulation of the neutrophils with fMLP was markedly and significantly enhanced compared to the NO-free zeolite control. This effect was maintained at the lower NO concentration (0.5unit/ml) but was less marked. The enhancement of CD11b expression was reversed to control levels upon further dilution of the zeolite disc (<0.5unit/ml), suggesting this effect is dependent upon the presence of high concentrations of NO.

Neutrophil priming is achieved through treatment with priming agents, such as GM-CSF, TNF-α, PAF and IL-8 and is characterised by the enhancement of neutrophil immune responses on subsequent exposure of the primed neutrophils to an activating stimuli (Condliffe *et al.*, 1998; Kitchen *et al.*, 1996; Leino *et al.*, 1993; Partrick *et al.*, 1997). Priming is considered to be one of the regulatory mechanisms implicated in the control of neutrophil responses, allowing for an appropriate attack response related to the severity of the stimulus. The enhancement of the neutrophil respiratory burst is the most well described response of primed neutrophils (Bass *et al.*, 1988; Bauldry *et al.*, 1991; Condliffe *et al.*, 1996; Leino *et al.*, 1993), although the modulation of neutrophil cell-surface adhesion molecules, CD62L and CD11b has also been reported in priming events (Condliffe *et al.*, 1996; Partrick *et al.*, 1997) . The shedding of L-selectin and up-regulation of CD11b following NO-loaded zeolite exposure in this study suggests that these neutrophils were primed. The significant enhancement of CD11b following fMLP simulation further supports this hypothesis and is characteristic of other priming agents. NO *per se* has not been previously recognised as a priming agent, but the NO-related species, $ONOO^-$, has been shown to demonstrate priming activity, similar to that observed in this study (Rohn *et al.*, 1999). The nitration of neutrophil surface proteins is suggested to produce the majority of the priming responses observed by $ONOO^-$ (Swain *et al.*, 2002), thereby promoting degranulation and the modulation of surface adhesion markers. Neutrophil concomitantly produce NO and O_2^- when activated, thus providing the right conditions for $ONOO^-$ production. The priming effects of $ONOO^-$ add an extra dimension to the immunomodulatory effects of this molecule, beyond that of its potent oxidant and microbicidal properties. It is not clear from our experiments if

NO or $ONOO^-$ are the likely candidates of our observed effects. The expected production of the respiratory burst, and subsequent O_2^- generation following fMLP stimulation could provide the appropriate conditions for sufficient $ONOO^-$ formation and thus, could account for the marked enhancement of CD11b up-regulation following NO-loaded zeolite exposure. The shedding of CD62L occurs in the absence of fMLP stimulation and thus, in the absence of the respiratory burst, thereby down playing the role of $ONOO^-$ in favour for NO in this effect. Moreover, the concentration of $ONOO^-$ known to produce a priming effect is extremely high, at 150-300μM (Rohn *et al.*, 1999). This suggests that the rate of O_2^- generation in our assay would have to be equimolar with NO at this concentration range for $ONOO^-$ to produce the apparent priming response observed. Future investigation using a scavenger of O_2^-, such as superoxide dismutase (SOD) or $ONOO^-$ scavenger, methionine could help elucidate the effector molecule in these studies. This priming hypothesis would benefit from further characterisation through the investigation of other priming responses such as enhancement of the respiratory burst and degranulation to more fully understand this interesting finding.

NO-releasing zeolites significantly increased levels of neutrophil necrosis following 1unit/ml NO-loaded zeolite. No significant increase in neutrophil apoptosis was observed, although the 1-hour time-point used in this assay is very early to observe any modulation of normal apoptotic responses in isolated neutrophils. However, preliminary results following a 20 h zeolite incubation (data not shown) indicated that NO-treatment produced low levels of apoptosis compared to control, in favour of an enhancement of necrosis. The percentage of healthy cells remained

comparable to control. It is possible that the necrotic response at this stage is secondary necrosis following an earlier apoptotic event and further investigation using appropriate time-points could determine this. Evidence for the pro-inflammatory effects of NO in this study are 3-fold; there was increased production of necrotic cell death in neutrophils following only 1 h of NO-loaded zeolite treatment, this effect was not apparent at the 0.5unit/ml zeolite treatment suggesting a concentration dependent effect of NO on neutrophil necrosis, and finally and most importantly, the NO-free zeolite controls had no effect on neutrophil viability, further highlighting the role of NO in producing these effects.

The mechanism of NO -induced modulation of CD62L and CD11b and increase in necrosis is unknown but is likely unrelated to up-regulation of cGMP which is generally regarded as the mechanism involved with NO-mediated cell protection and inhibition of activation (Kosonen *et al.*, 1999; Wanikiat *et al.*, 1997). Previous studies describing NO-related neutrophil activation, implicate signalling pathways involving PKG, protein nitration, phosphorylation and (Okayama *et al.*, 1999, 1998) activation of nuclear transcription factor κB (NF-κB; Swain *et al.*, 2002). Measurement of nitrotyrosine residues together with inhibitors of cell signalling pathways may help to determine the mechanism involved in these effects. Confirmation of cGMP levels and inhibition of sGC should also be done to ensure these effects are mediated solely via an sGC-independent $ONOO^-$ dependent process (Brune *et al.*, 1995) although there still exists a role for high concentrations of NO in cell pathology. The inhibition of mitochondrial respiratory enzymes is one such target that has been implicated in cytotoxicity of both $ONOO^-$ and NO (Brown, 1999;

Brown *et al.*, 1998). Low concentration (nanomolar) NO inhibits the cytochrome oxidase enzyme in competition with oxygen and higher concentrations of NO inhibit a wider range of mitochondrial respiratory enzymes through thiol nitrosylation. $ONOO^-$ irreversibly inhibits numerous mitochondrial respiratory enzymes as well as causing mitochondrial damage through membrane and DNA nitration (Brown, 1999). Again, confirmation of the presence of $ONOO^-$ through co-incubation of O_2^- scavengers or $ONOO^-$ scavengers to attempt to reverse NO-loaded zeolite necrotic responses may provide insight into the significance of particular species in this effect.

The activation of neutrophils *in vivo*, occurs in response to a variety of inflammatory mediators including LPS, IL-8 and TNF-α. The bacterial peptide fMLP was one of the first chemoattractants identified as a potent activator of neutrophils (Selvatici *et al.*, 2006). This formylated tripeptide has been synthetically produced and is commonly used in the experimental investigation of neutrophil activation (Carrigan *et al.*, 2007; Saito *et al.*, 2001; Wittmann *et al.*, 2004). There are two known receptors for fMLP, called formyl peptide receptor (FPR) and FPR-like 1 (FPRL1) which are located on the neutrophil membrane and are members of the G-protein coupled receptor family (Selvatici *et al.*, 2006). The interaction of fMLP with its receptor triggers many second messenger systems involving GTP-binding protein, phospholipases, protein kinases, polyphosphoinisotide metabolism and phosphatases (Selvatici *et al.*, 2006). The non-specific triggering of many second messenger systems means that many aspects of neutrophil activation are involved in the response to fMLP. These include cytoskeletal rearrangement, degranulaton and

production of the oxidative burst which are important for the phagocytic clearance of infecting pathogens, thus making fMLP a good choice as an all-round neutrophil activator (Jesaitis & Allen, 1988). The concentration of fMLP used in our experiment is within the optimal range for neutrophil activation, however the modulation of neutrophil activation markers by fMLP at this concentration may mask any potential inhibitory effects of NO. Future work should titrate the concentration of fMLP to better investigate any inhibition of neutrophil activation. Neutrophils are activated by a number of inflammatory mediators present during different sorts of inflammatory insults. The use of other neutophil activators, such as C5a and IL-1, should be investigated to gain a better understanding of the effect of NO-releasing zeolites in different inflammatory environments.

The development of NO-loaded zeolites for medical device coatings requires consideration of the physiological conditions under which they are likely to be employed. The presence of blood derived NO-scavengers and flow conditions would reduce the bioavailabilty of NO for its targets and would therefore suggest that the high NO concentrations reached in our assay would be improbable *in vivo.* However, NO is a truly local mediator and thus, the vicinity of the targets to the site of production (ie the zeolite surface) would influence the effects produced. Neutrophil infiltration to the site of device placement occurs rapidly and therefore these cells could be subjected to the full brunt of NO release from these materials, subsequently enhancing activation and adhesion. If this scenario was true, necrotic death of neutrophils would also be enhanced at the site of device placement, possibly further exacerbating the elicited inflammatory response (see figure 4.18). Of course,

the fate of NO in the body is complex and the presence of many different factors including thiols, GSH, albumin, ROS and many more are known to contribute to the biological effects of NO, good and bad (Wink *et al.*, 1996a; Wink *et al.*, 1996b). The relative presence of these factors within the body are also subject to variation depending on internal and external stimuli and thus, the only reliable way to confirm the pro- or anti inflammatory effects of the NO-loaded 50% Zn^{2+}-exchanged zeolite is through the use of prototype zeolite-coated medical devices in animal models. However, it is important to note that the 50% Zn^{2+}-exchanged zeolite used in these experiments does not produce the optimal NO release properties ideal for use in medical devices, which would benefit from long duration, low NO concentration release characteristics, more akin to the anti-inflammatory, cytoprotective concentrations of NO described in the literature (Rauen *et al.*, 2007; Wink *et al.*, 1995). Further optimisation of zeolite design should precede *in vivo* experimentation in the search for biocompatible coatings that inhibit neutrophil adherence. Despite the lack of beneficial effects of NO-loaded zeolites on neutrophil adhesion molecule expression and viability in these experiments, high NO production via iNOS has been shown to be anti-microbial and could provide an alternative route by which current zeolite designs could increase biocompatibility of medical devices.

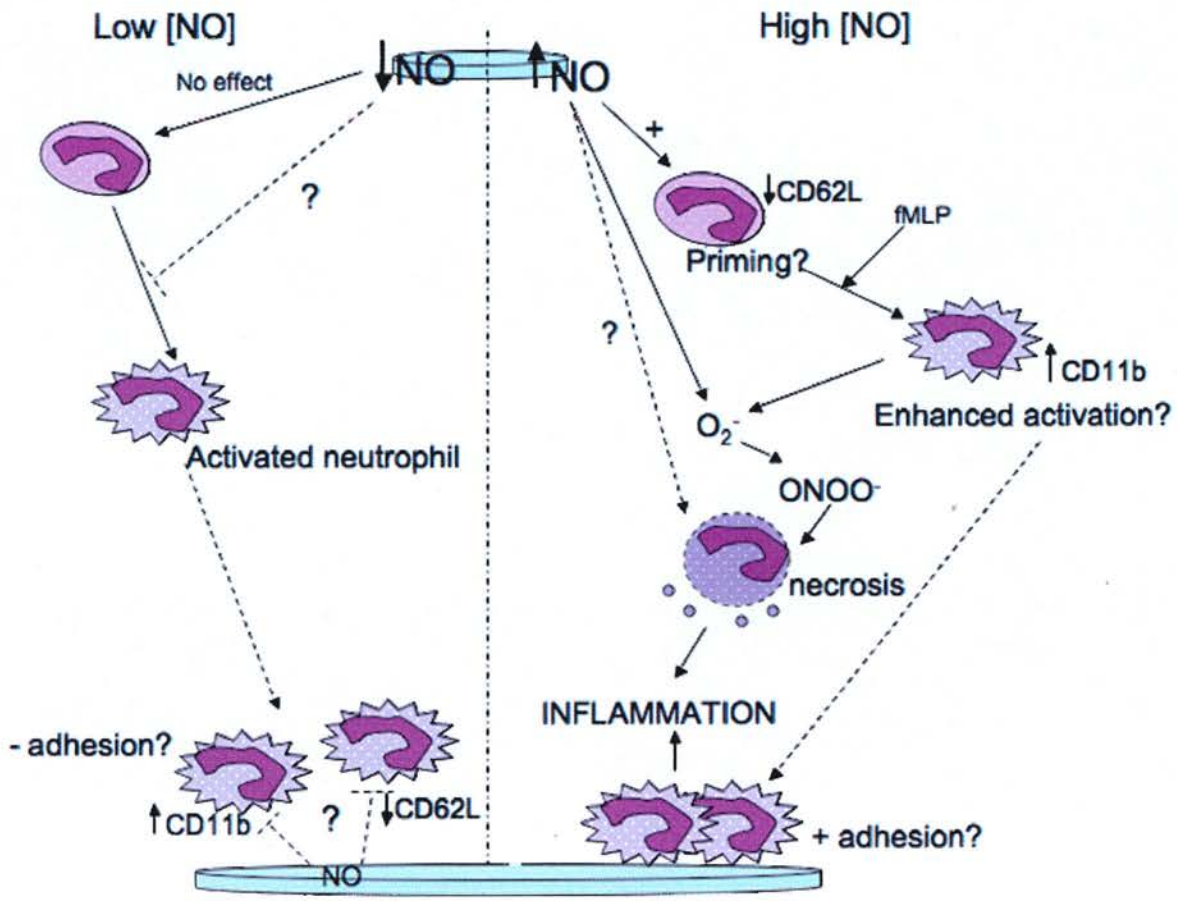

Figure 4.18. Hypothetical model of neutrophil behaviour following NO-loaded zeolite exposure; Low versus high NO concentration.

Low [NO] from zeolite dilution produced no effect on neutrophil activation in this study. However, it is possible that further lowering the concentration could have inhibited neutrophil activation and adhesion through inhibition of CD62L shedding and CD11b up-regulation. High [NO] concentrations released from zeolites promoted CD62L shedding and enhanced CD11b expression following fMLP-stimulation (10^{-7}M), suggesting these cells are primed and subsequently more likely to be adherent and pro-inflammatory. High [NO] increased necrotic cell changes, indicating high concentrations of NO are pro-inflammatory in this assay, perhaps due to increased production of $OONO^-$ following reaction with O_2^- produced by activated neutrophils.

CHAPTER 5.

The Anti-Bacterial Properties of Zn^{2+}-Exchanged Zeolites.

CHAPTER 5.

The Anti-Bacterial Properties of Zn^{2+}-Exchanged Zeolites.

5.1 Introduction

Catheter-associated urinary tract infections (CAUTIs) account for around 30-40% of all nosocomial infections (Karchmer *et al.*, 2000; Warren, 2001). The duration of hospitalisation and catheterisation significantly increases the likelihood of patients contracting a bacterial infection (Maki & Tambyah, 2001), resulting in more drug therapy and lengthier hospital stays for patients. Not only is this a significant cause of morbidity and mortality in patients, it is a greater financial burden on the healthcare system due to increased drug and hospital care costs (Plumridge & Golledge, 1996). The conventional treatment of CAUTIs involves the administration of antibiotics, which carry the inherent risk of the pathogen developing drug resistance and reducing the long-term therapeutic value of these agents. The increasing prevalence of multi-resistance bacterial strains, in particular the strain methicillin-resistant *Staphylococcus aureus* (MRSA) is a cause for concern in hospitals requiring the development of new, efficient anti-bacterial protocols.

The prevention of the incidence of CAUTIs and nosocomial infections in general, is challenging and novel therapeutics and preventative measures are required urgently. The introduction of better sterile handling techniques for hospital staff and more rigorous criteria for the application of urinary catheters has only impacted minimally on this wide-scale problem (Goldmann, 1991). The infectious agents are more likely to be already present within the patient's urinary tract. Therefore an anti-septic strategy delivered directly to the site of potential colonisation could reduce infection rates. The integration of non-antibiotic, bactericidal agents into the catheter structure provides one promising strategy to reduce the incidence of CAUTIs. It has been shown that the use of a silver-alloy/hydrogel incorporating catheter successfully reduced infections by 27-73% in a range of studies (Karchmer *et al.*, 2000; Liedberg & Lundeberg, 1990; Lundeberg, 1986; Maki & Tambyah, 2001; Rupp *et al.*, 2004). However, these catheters are expensive and the economical impact of their application is a major consideration. Nevertheless, despite their cost, it has been shown that the prevention of CAUTIs by silver alloy/hydrogel catheters is more cost-effective than the treatment of the acquired infections (Seymour, 2006). The production of cheaper and more effective bactericidal catheters could further improve the troubling infection rate and impact more favourably on healthcare budgets.

It has been demonstrated that nitric oxide (NO) has well characterised immunomodulatory effects (Albina & Reichner, 1998; Brune *et al.*, 1998; MacMicking *et al.*, 1997; Ward *et al.*, 2000) . The production of high concentrations of NO during the inflammatory response is mediated via iNOS, the inducible form of

the NO synthase enzyme. iNOS is induced by various pro-inflammatory mediators, such as TNF-α, IFN-γ, IL-1β and LPS, to produce micromolar concentrations of NO contributing to the pro-inflammatory response and microbial killing (Brandonisio *et al.*, 2001; Moncada & Palmer, 1991). The importance of NO in combating bacterial infection has been confirmed through the use of animal models, such as the murine iNOS knock-out model. Studies have shown increased susceptibility of this mouse to infection by bacterial products (MacMicking *et al.*, 1995). The suppression or dysfunction of NO production by iNOS is also linked to a number of human disease states where susceptibility to infection is common, such as cystic fibrosis (Kelley & Drumm, 1998; Meng *et al.*, 1998).

Research into the use of NO as an anti-microbial therapy has produced promising results, with studies indicating that it is cytotoxic to a large number of species of fungi, bacteria, viruses and parasites (Ascenzi *et al.*, 2003; Coban *et al.*, 2003; Karupiah & Harris, 1995; Rementeria *et al.*, 1995) . However, the multiple physiological targets of NO and the potential cytotoxicity of high NO levels to host tissue makes systemic delivery of NO using NO-donors potentially harmful and has limited the translation of these agents into the clinic. The free radical property of NO requires it to be bound to molecular carriers to stabilize it until its release is required. The diazeniumdiolate compounds are one such example of NO-donor, which incorporate NONOate groups onto stable nucleophile adducts. The rate of decomposition of NO from such species occurs spontaneously without the need for biological cleavage. This property makes these donors predictable releasers of NO, but the lack of tissue specificity upon systemic delivery means unwanted side effects,

such as systemic hypotension can be a problem. However, the use of NO as a specific anti-microbial agent has recently come closer to reality through the use of NO donor-incorporating polymers that direct NO treatment to a localised area. NO-releasing polymer materials are comprehensively researched for development of coatings for medical devices to improve the biocompatibility. Here, the uses of NO can range from inhibiting thrombus formation in blood-contacting devices (Fleser *et al.*, 2004; Mowery *et al.*, 2000; Schoenfisch *et al.*, 2000), prevention of smooth muscle proliferation in stenting (Hou *et al.*, 2005; Kaul *et al.*, 2000), prevention of vasospasm as well as the design of anti-infective surfaces for medical devices (Hetrick & Schoenfisch, 2007). A range of studies by Nablo *et al.*, demonstrate the effectiveness of a NO-releasing sol-gel derived material for reducing bacterial adhesion to the surface of sol gel/polymer based medical devices (Nablo *et al.*, 2001; Nablo *et al.*, 2005a; Nablo *et al.*, 2005b; Nablo & Schoenfisch, 2003, 2005, 2004). The ability of these materials to inhibit adhesion of a range of bacterial strains ranged from 30-95% (Nablo & Schoenfisch, 2003). The flux of NO from these materials can be tailored by altering the composition of the NO-releasing sol gel with the polymer matrix and by using NO-donor compounds with different rates of decomposition. The NONOate compounds are most commonly researched in this arena due to the existence of many types of compounds with different decomposition rates, which are dependent upon the species of the nucleophile adduct (Smith *et al.*, 1996). Careful consideration of the species of NO-donor is required to avoid adverse effects of harmful by-products leaching from the surface of the material (Fitzhugh *et al.*, 2002; Nablo & Schoenfisch, 2005). Additionally, the flux of NO obtained from the material has to be carefully engineered to ensure minimal cytotoxicity to

surrounding host tissue (Nablo & Schoenfisch, 2005). At present, the anti-adhesive properties of these materials to bacteria are impressive, however, no bactericidal effect has been established with these materials. The inhibition of bacterial adhesion is important in preventing bacterial colonisation, but due to the opportunistic nature and rapidity of multiplication of bacteria, it remains possible that the successful colonisation of just a few bacteria could lead to infection. The limited time of NO release from these materials would also mean any viable bacteria surrounding could colonise the surface when NO stores have been exhausted, reducing the therapeutic value of these materials in long-term device placements, where infection rates are most troublesome (Bissett, 2005; Huang *et al.*, 2004). A direct bactericidal effect together with the anti-adhesive properties of a NO-releasing material could serve to eliminate medical device related infections completely by eradicating all infectious agents from the surfaces surrounding the device.

In this chapter, the effectiveness of a novel, high capacity NO-storing and releasing material at reducing bacterial growth *in vitro* was assessed with the view to their potential use as anti-bacterial coatings for medical devices. As previously mentioned, the composition of zeolite to the polymer matrix and the ion exchanged within the zeolite structure can be altered to tailor the NO-release capacity of these materials, making them an attractive candidate for a variety of biocompatible medical device coatings. The release of short-lived, high concentrations of NO associated with these materials draws similarities with the kinetics of NO released by the action of iNOS during the inflammatory responses in the body, suggesting a benefit of these materials in localised clearance of infectious agents. Additionally,

anti-microbial actions of high concentrations of NO released from these materials could provide an anti-bacterial therapeutic that may avoid the development of bacterial resistance.

Thus, we hypothesised that a NO-loaded 50% Zn^{2+}-exchangd zeolite (PTFE), would possess anti-bacterial properties against bacterial strains commonly found in nosocomial device-related infections, and that the anti-bacterial properties would be dependant upon high concentrations of NO released from zeolite stores, making these materials candidates for further development as anti-infective coatings for medical devices.

The Gram-negative, *P.aeruginosa* and Gram-positive bacteria, methicillin-sensitive *Staphylococcus aureus* (MSSA) were used to assess anti-bacterial effects against these two classes of bacteria, which are chiefly differentiated by the structure of the bacterial membrane (see section 1.1.6.2.2). The use of a clinical specimen from a lung infection of *P.aeruginosa* (J1386) was investigated to ensure universal toxicity of these materials to physiologically relevant, virulent strains of bacteria. Through these experiments, aspects of the mechanism of the anti-bacterial effects of these materials were also addressed.

5.2 Methods

5.2.1 Materials

Zeolites were synthesised at St Andrews University (see section 2.8.1). Briefly, Zn^{2+}-ions were exchanged into zeolite configuration LTA. The resulting zeolite powder was loaded with NO gas under 2 atmospheres pressure and pressed into 5mm diameter discs composing 50 weight% zeolite and 50 weight% polytetrafluoroethylene (PTFE). Unless otherwise stated, 50% Zn^{2+}-exchanged zeolites were used.

The bacterial strains used in the experiments (PA01 and MSSA) were established strains used in the CIR/lung group lab. The clinical specimen, J1386, was kindly donated by Dr John Govan.

LB (Luria Bertani) broth and LB agar were purchased from Sigma (Hertfordshire, UK) was made up according to manufacturers instructions.

5.2.2 Bacterial Culture

Bacteria were cultured on a nutrient broth agar LB (Luria-Bertani) at room temperature. Bacterial suspensions were prepared by inoculating 10ml of LB broth with one colony of the relevant bacteria and incubating overnight at 37°C in an orbital shaker. Bacteria were then sub-cultured with a 1/100 dilution of the original bacterial suspension and incubated for 3 hours. The bacteria were harvested via centrifugation (1500*g*; 15 min) and re-suspended in a 5%LB:PBS solution. This step

was then repeated once more to ensure adequate washing of the cells. The suspensions were standardised each day via dilution with 5% LB broth to an optical density of 0.1 at 595nm using spectrophotometry (WPA UV 1101, Biotech Photometer). A further 1 in 1000 dilution was performed for use in the assays.

The zeolite treatments were investigated in varying volumes (150-1200μl) of a 1/1 dilution of the bacterial suspension prepared above. Dilutions were prepared using 5% LB in PBS solution. The treatments were carried out at 37°C on a heated block with shaking at 400rpm for varying times between 2-120 min.

The evaluation of bacterial growth following treatments was done using the colony forming unit (cfu) assessment. A 100μl aliquot of 10^{-2}, and 10^{-3} dilutions of the original bacterial suspension were spread onto LB agar plates in triplicate. The plates were left to incubate at 37°C overnight at 5% CO_2 for approx 16 h and the number of colonies formed were counted. The number of bacteria present in the suspension following treatments was estimated, assuming that 1 colony arises from a single bacterium and by multiplying by the dilution factors to obtain bacteria/ml. Where appropriate, treatments were compared as a percentage of the number of bacteria (cfus) at time zero (t=0).

5.2.3 NO Electrode

NO measurements were carried out using an isolated (2mm) NO electrode (ISO-NOP; World Precision Instruments, Stevenage, UK), calibrated each day prior to use with $NaNO_2$ (see chapter 2.3.1). Data were captured via an analogue-digital converter (Maclab 4e, AD Instruments, Sussex, U.K).

NO released from NO-loaded 50% Zn^{2+}-exchanged zeolites was measured in 1ml of 5% LB:PBS solution. The electrode was suspended in the solution and allowed to reach a baseline reading prior to zeolite suspension. NO measurements were recorded for approx 60min following zeolite suspension. The zeolite disc was suspended in the solution using a stainless steel holding device. Each sample was incubated at 37°C and contained a magnetic stir bar, which stirred the solution at 1000rpm for the duration of the experiment. Relevant time-points were selected for analysis and traces of NO release over time were plotted.

5.2.4 Statistics

Statistical analyses were performed using one-way or two-way analysis of variance with either Dunnet's or Bonferroni's post hoc test and confirmed using non-parametric Kruskel-Wallis with Dunn's post hoc, where appropriate. Statistical significance was assumed when $p < 0.05$ at the 95% confidence interval.

5.3 Results

5.3.1 The Effect of 50% Zn^{2+}-Exchanged Zeolites on the Growth of Gram-Negative Bacteria.

NO-loaded Zn^{2+}-exchanged zeolites at 50% composition of zeolite to PTFE binder had a significant bactericidal effect when incubated in bacterial suspensions of a laboratory (figure 5.1 A) and a clinical strain (figure 5.1 B) of *Pseudomonas aeruginosa* (PA01 and J1386 respectively). This effect was seen after a 45 min incubation of the zeolite disc in the bacterial suspension (5% LB:PBS; 150μl; 37°C). The NO-free zeolite discs had no significant effect on PA01 numbers but caused a significant reduction of J1386 bacterial numbers. Bacterial growth of the J1386 strain remained stagnant over the 45 min incubation period indicating the assay conditions were not optimal for growth of this particular bacterial strain.

Figure 5.2 shows a representative photograph of PA01 colonies grown on LB agar plates following treatments from which bacterial numbers were estimated. The lack of colonies on the agar plate following NO-loaded treatment is visible, whereas the control and NO-free zeolite treatments produced comparable numbers of colonies.

Bacterial killing was even more pronounced in the PA01 strain after 120 min zeolite incubation (150μl; 37°C), which produced zero colonies of PA01 following NO-zeolite treatment (figure 5.3).

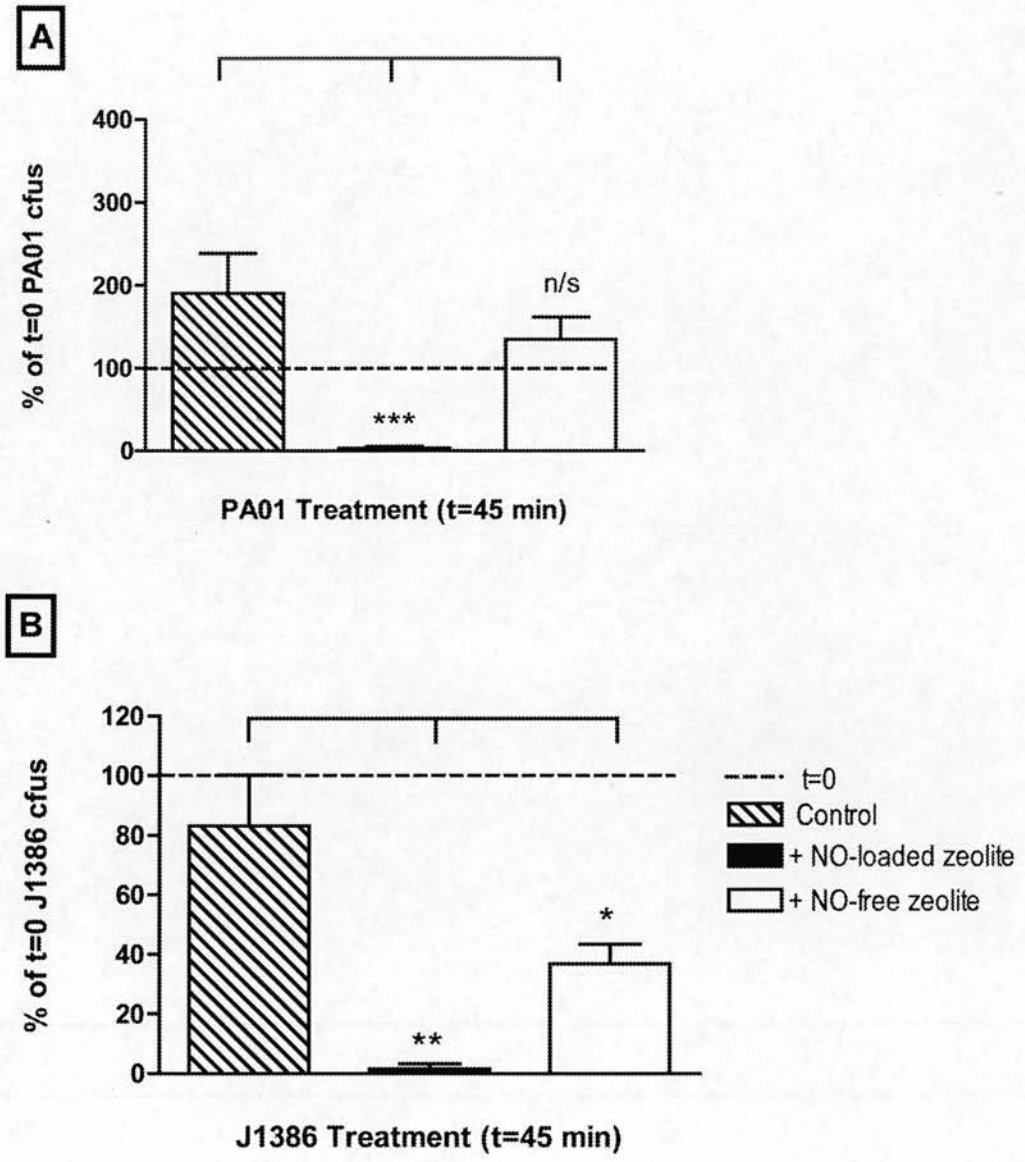

Figure 5.1- The effect of 50% Zn^{2+}-exchanged zeolites on Gram-negative bacterial growth; 45 min zeolite incubation.

Bacterial growth following NO-loaded zeolite (black bars) and NO-free zeolite (white bar) treatment (45min; 37°C) in suspensions (5% LB broth:PBS; 150μl) of a laboratory strain (A; PA01) and a clinical strain (B; J1386) of *P.aeruginosa*. Data are expressed as % of colony forming units (cfus) at t=0 (broken line). Bars indicate the mean +/- the SEM of 3-6 plates per treatment in n=6 (A) or n=4 (B) independent experiments. Asterisks denote significance from control (t=45 min; striped bar) growth. (**$p < 0.01$).

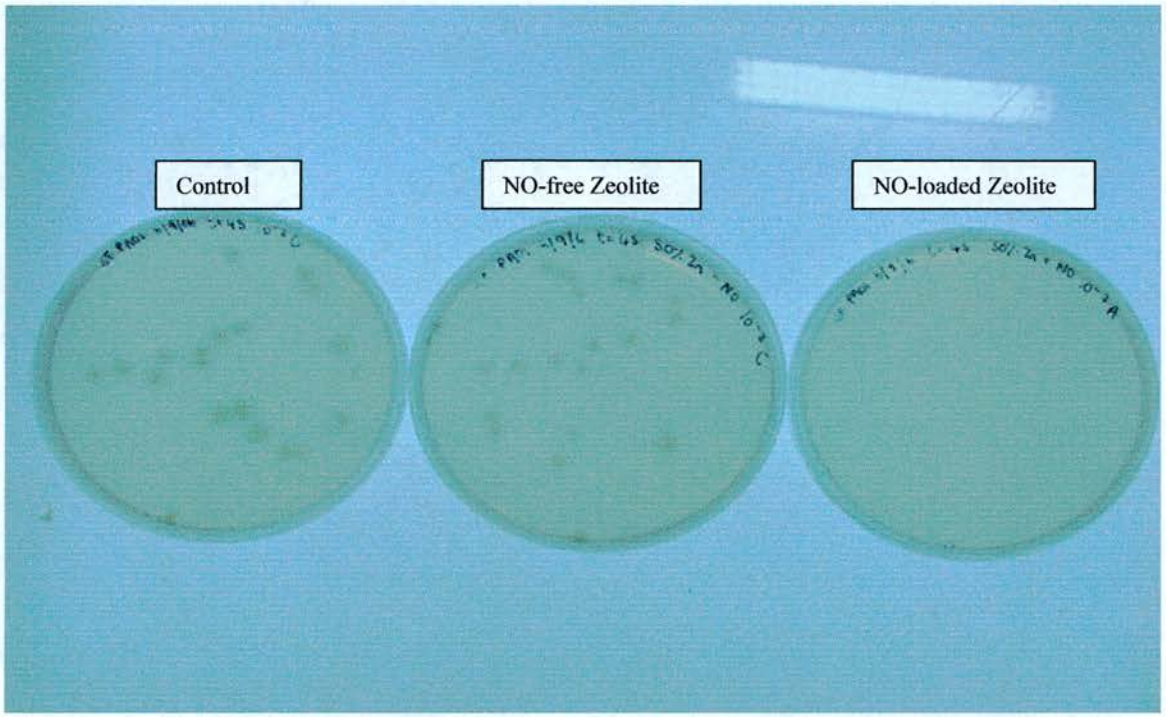

Figure 5.2 A photographic representation of PA01 colonies on LB agar plates following 50% Zn^{2+}-exchanged zeolite treatment – 45 min.

A photograph showing typical LB agar plates from which PA01 colonies were counted to estimate bacterial numbers present following the zeolite treatments (45 min). Samples from 100µl of a 10^{-2} dilution of the treated bacterial suspension were spread on LB agar plates and incubated for 16 hours (37°C; 5% CO_2) to allow colonies to form. The picture shows PA01 colonies following control (left), NO-free zeolite (middle) and NO-loaded zeolite (right) treatments.

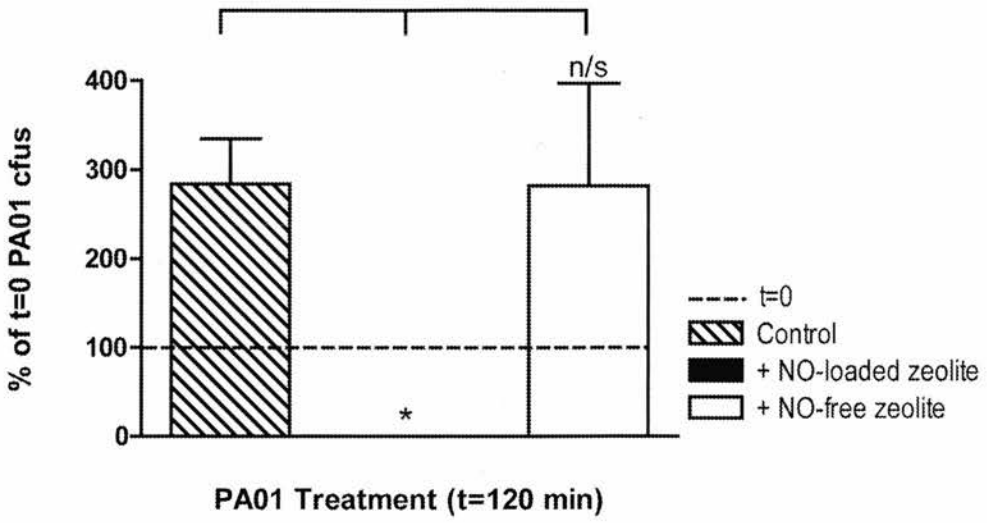

Figure 5.3. The effect of 50% Zn^{2+}-exchanged zeolites on PA01 growth – 120 min zeolite incubation.

Bacterial growth following NO-loaded zeolite (black bars) and NO-free zeolite disc (white bar) treatments (120 min; 37°C) in suspensions (5% LB broth:PBS; 150μl) of a laboratory strain (PA01) of *P.aeruginosa* . Data are expressed as % of c.olony forming units (cfus) at t=0. Bars indicate the mean +/- SEM of an average of 3-6 plates per treatment for n=3 independent experiments. Asterisks denote statistical significance from control (t=120 min; striped bar) growth (*$p < 0.05$, n/s – not significant).

5.3.2 The Effect of 50% Zn^{2+}-Exchanged Zeolites on the Growth of a Gram-positive Bacterial Strain, Methicillin-Sensitive Staphylococcus Aureus (MSSA).

The incubation of NO-loaded and NO-free zeolites in bacterial suspensions of the Gram-positive bacterial strain, MSSA, significantly reduced bacterial growth compared to control samples incubated in the same conditions (Figure 5.4). The reduction in bacterial growth by the NO-free zeolite does not appear to fall below the number of bacteria at t=0, suggesting a bacteriostatic effect of the NO-free zeolite disc. The reduction in bacterial numbers following NO-loaded zeolite treatment is more significant and below the number of bacteria present at t=0, suggesting a bactericidal effect of NO.

Figure 5.5 shows a representative photograph of MSSA colonies on LB agar following the zeolite treatments. The complete lack of colonies following NO-loaded zeolite treatment is visible, as is the reduction of the number of colonies present following NO-free zeolite treatments compared to control (t=45 min).

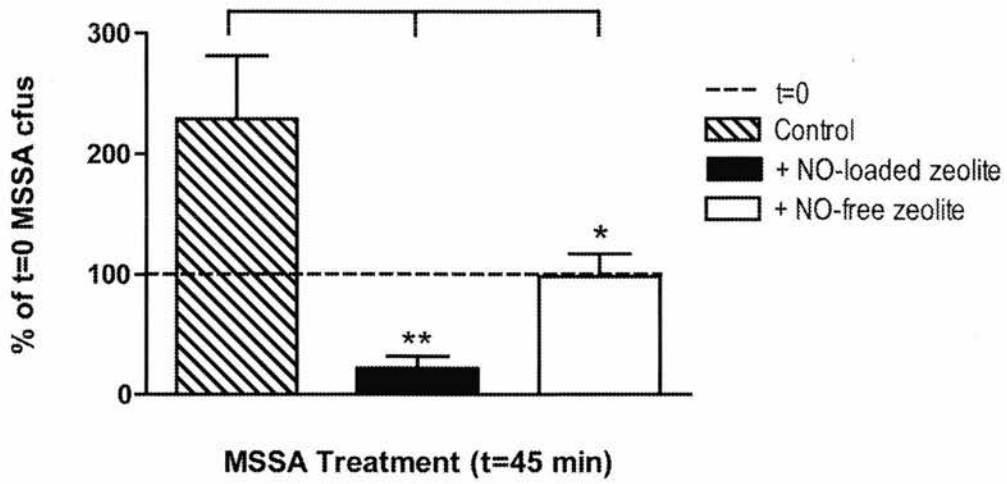

Figure 5.4 The effect of 50% Zn^{2+}-exchanged zeolites on MSSA growth.

Bacterial growth following NO-loaded zeolite (black bar) and NO-free zeolite (white bar) incubations (45 min; 37°C) in a MSSA suspension (5% LB broth:PBS; 150µl). Data are expressed as a % of colony forming units (cfus) at t=0 (broken line). Bars represent the mean +/- SEM of an average of 3-6 plates per treatment in n=6 independent experiments. Asterisks denote statistical significance from control (t=45 min) growth. (* $p < 0.05$, ** $p < 0.01$).

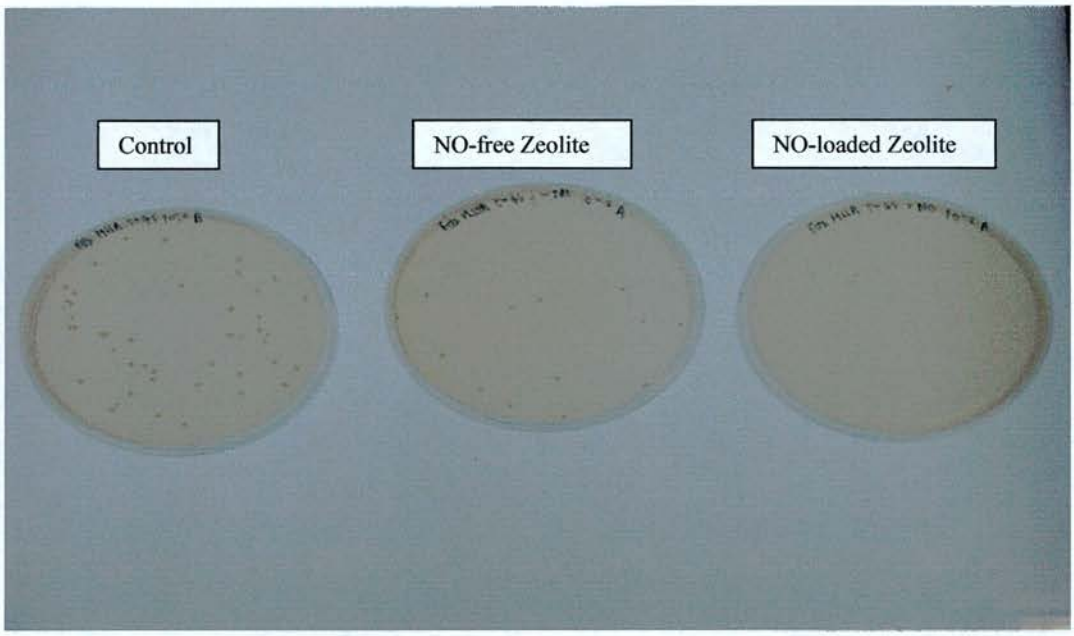

Figure 5.5. A photograph representation of MSSA colonies on LB agar plates following 50% Zn^{2+}-exchanged zeolite treatment- 45 min.

The photograph of typical LB agar plates from which MSSA colonies were counted to estimate bacterial numbers present following the zeolite treatments (45 min). Samples from 100µl of a 10^{-2} dilution of the treated bacterial suspension were spread on LB agar plates and incubated for 16 hours (37°C; 5% CO_2) to allow colonies to grow. The picture shows MSSA colonies following control (left), NO-free zeolite (middle) and NO-loaded zeolite (right) treatments.

5.3.3 The Effect of P.Aeruginosa Suspension Volume on Bacterial Killing by NO-loaded Zeolite Discs.

Zeolite discs were diluted in various volumes (150-1200μl) of *P. Aeruginosa* bacterial suspensions to assess the effect of volume, and subsequent dilution of NO concentrations, on bacterial killing. The reduction in bacterial numbers by NO-loaded zeolites was inversely related to the volume of the bacterial suspension in both the laboratory (PA01; figure 5.6 A) and the clinical (J1386; figure 5.6 B) strains of *P.Aeruginosa*. Bacterial killing by NO-loaded zeolites was significant in both PA01 and J1386, at the lowest volumes (≤300μl) when NO concentrations are likely to be highest.

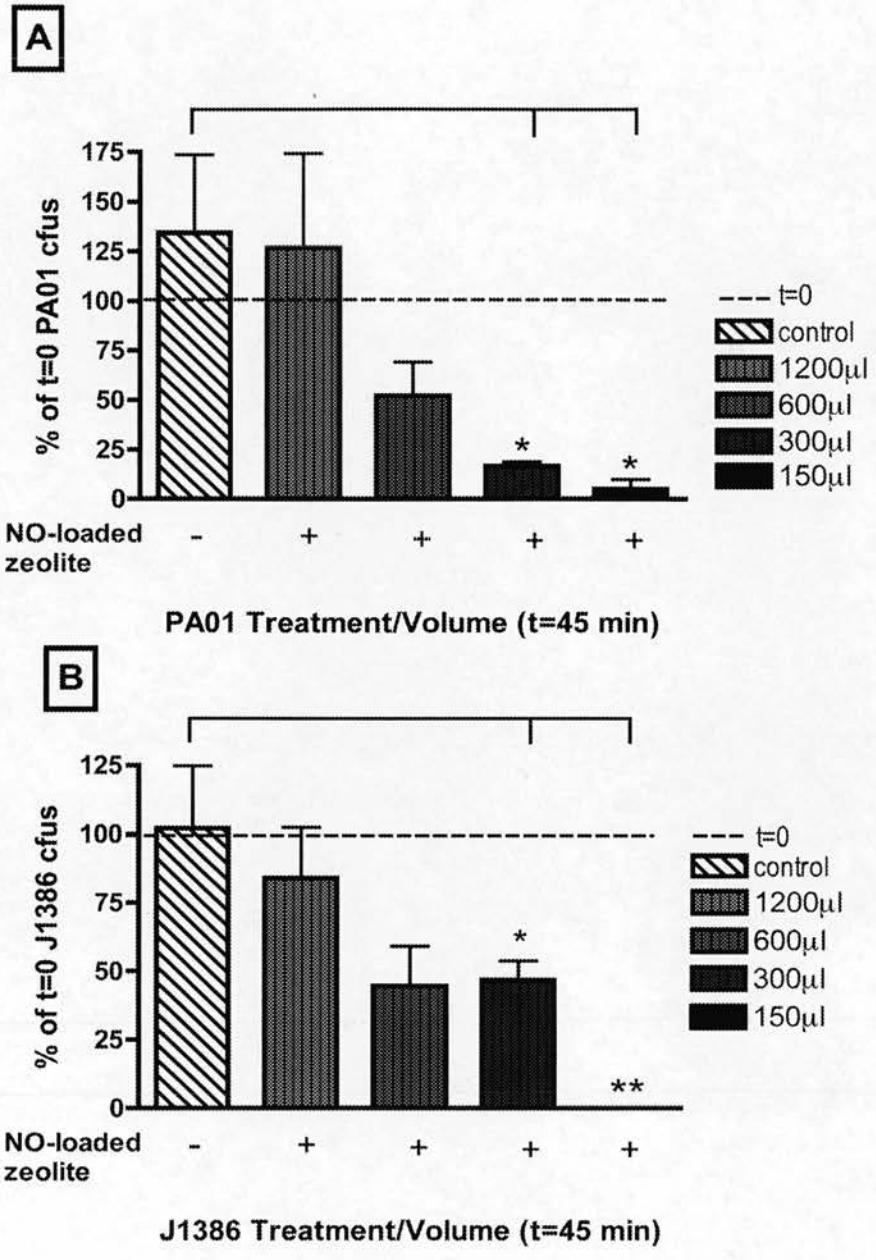

Figure 5.6 The concentration-dependent reduction of *P.aeruginosa* Growth by NO-loaded 50% Zn^{2+}-exchanged zeolites.

Bacterial growth following NO-loaded zeolite incubation (45 min;37°C) in increasing volumes (150-1200µl) of J1386 (A) and PA01 (B), optical density equalised, bacterial suspension (5% LB:PBS). Bars represent the mean +/- SEM of an average of 3-6 plates per treatment in n=3 independent experiments. Data is expressed as % of colony forming units at t=0 (dotted line). Asterisks denote statistical significance from control bacterial growth at t=45 (* $p < 0.05$, ** $p < 0.01$).

5.3.4 The Effect of MSSA Bacterial Suspension Volume on Bacterial Killing/Stasis by NO-loaded and NO-free Zeolite Discs.

The reduction of MSSA numbers by NO-loaded (figure 5.7A) and NO-free (figure 5.7B) zeolites is inhibited by increasing volumes (150-1200μl) of the MSSA suspension (5% LB broth: PBS). Significant inhibition of MSSA growth was achieved by NO-loaded discs suspended in volumes ≤ 300μl (*$p < 0.05$; **$p < 0.01$ *vs* control). The NO-free disc produces a significant reduction in MSSA growth at the lowest dilution only (150μl; $p < 0.01$ *vs* control).

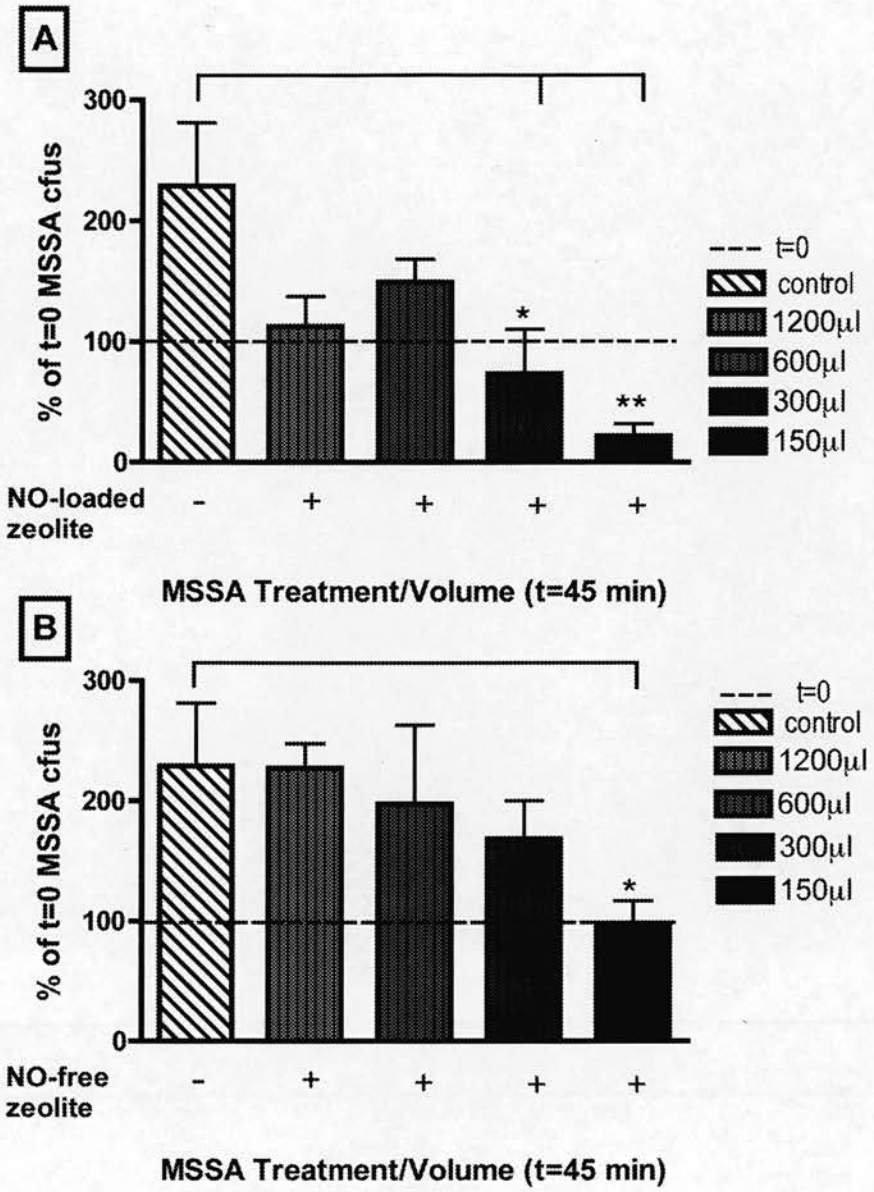

Figure 5.7. The concentration-dependent reduction of MSSA growth by NO-loaded and NO-free Zn^{2+}-exchanged zeolites.

Bacterial growth following NO-loaded zeolite (A) and NO-free zeolite (B) incubation (45 min; 37°C) in increasing volumes (150-1200µl) of MSSA, optical density equalised, bacterial suspension (5% LB:PBS). Bars represent the mean +/- SEM of an average of 3-6 plates per treatment in n=3 independent experiments. Data is expressed as % of colony forming units at t=0. Asterisks denote statistical significance from control bacterial growth at t=45 (* $p < 0.05$, ** $p < 0.01$).

5.3.5 The Effect of the Ion Exchanged in the Zeolite Structure on the Inhibition of MSSA Growth by NO-free Zeolites.

Figure 5.8 shows a photographic representation of MSSA growth on LB agar plates following treatment with 50% Zn^{2+}, Ca^{2+} and Co^{2+} -exchanged NO-free zeolite discs (150µl; 37°C, 45 min). The reduction in colonies following Zn^{2+} and Co^{2+} -exchanged zeolite treatment is visible compared to control, however the Ca^{2+}-exchanged zeolite appears to enhance growth of MSSA bacteria compared to control. The complete lack of colonies following the Co^{2+} zeolite treatment suggests that this zeolite has more cytotoxic effects on MSSA bacteria than the Zn^{2+} zeolite.

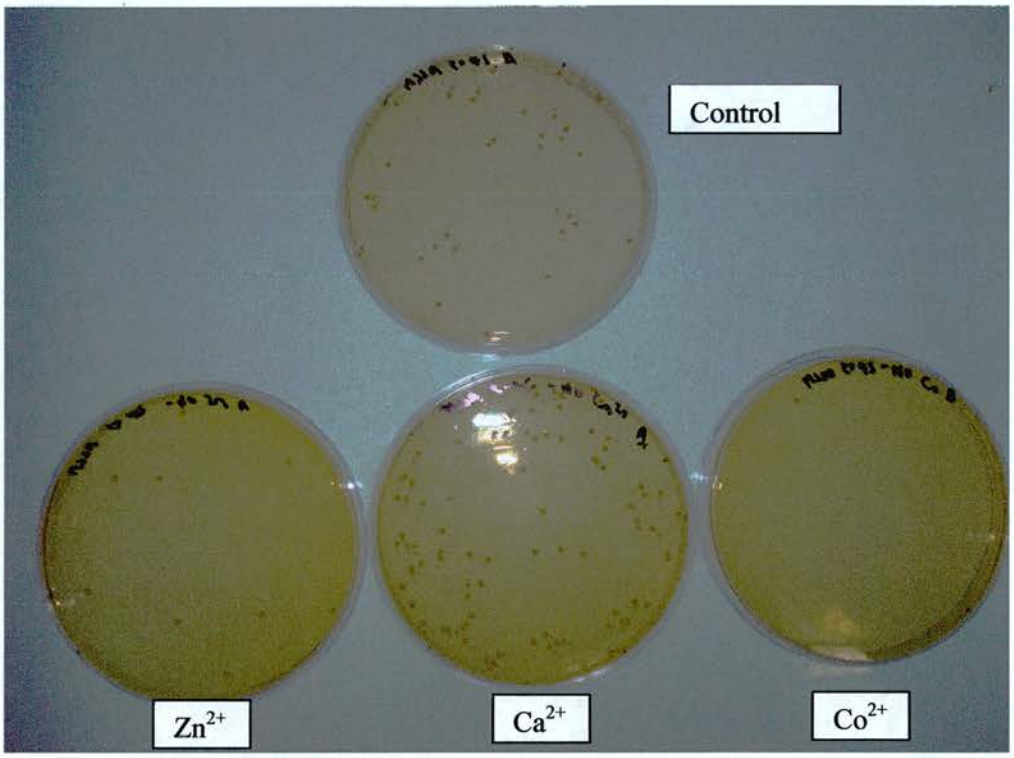

Figure 5.8 A photograph representation of MSSA colonies on LB agar plates following NO-free (50% Zn^{2+}, Ca^{2+} and Co^{2+}-exchanged) zeolite treatment.

The photo shows representative MSSA colonies grown on LB agar following control (top), 50% NO- free Zn^{2+} (bottom right), Ca^{2+} (bottom middle) and Co^{2+}-exchanged zeolite treatments in 150µl MSSA suspension (5% LB:PBS; 37°C; 45 min). Colonies were grown from 100µl of a 10^{-2} dilution of the treated bacterial sample. The plates were incubated for 16 hours (37°C; 5% CO_2) to allow colonies to form.

5.3.6 The Effect of Nitrite and Nitrate on bacterial growth of MSSA.

Addition of $NaNO_2$ or $NaNO_3$ (1mM) to MSSA suspensions (150µl; 5% LB:PBS) for 45 min (37°C) had no effect on MSSA growth and produced comparable numbers of bacteria to control untreated MSSA suspensions upon cfu analysis (figure 5.9).

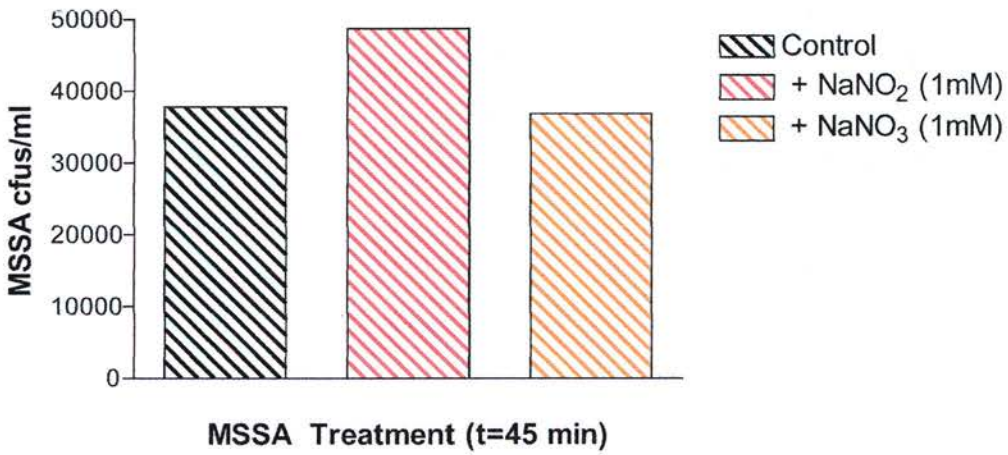

Figure 5.9. The effect of nitrite and nitrate (1mM) on MSSA growth.

MSSA bacterial suspensions (150µl; 5% LB:PBS) were treated with $NaNO_2$ (1mM; red striped bar), $NaNO_3$ (1mM; orange striped bar) or control (untreated; black striped bar) for 45 min (37°C). Data is expressed as the number of bacteria per ml, estimated using the colony forming unit assay and are the mean of n=2 experiments.

5.3.7 The Time-Dependent NO-release Reduction in PA01 Growth by NO-loaded Zeolites.

The NO release profile as measured using a NO electrode, shows a large concentration of NO (peak approx 30μM in 1ml 5% LB:PBS) released over a short time period (figure 5.10, red line). The peak NO release occurs at approx 10 min after disc suspension and the signal decomposes rapidly until NO reaches baseline by approximately 40 min.

The inhibition of PA01 growth by NO-loaded zeolites suspended in 150μl of the bacterial suspension (37°C; 5% LB:PBS) shows no significant reduction at disc incubations < 30 min. No significant inhibition of bacterial growth is apparent at the 10 and 20 min time-point although the majority of the NO has been released by this time. Significant reduction of PA01growth by NO-loaded zeolites was only evident following zeolite exposure >30 min (figure 5.10 B;*$p < 0.05$; **$p < 0.01$).

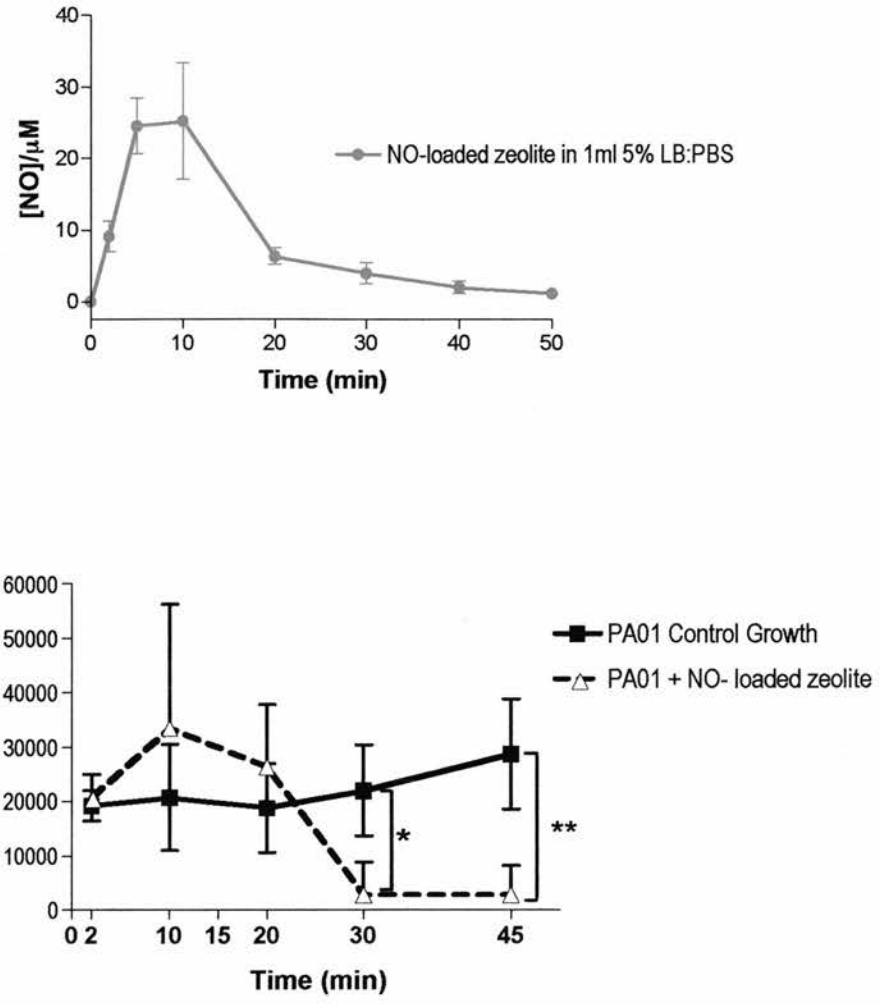

Figure 5.10. The time-dependent NO-release and reduction of *P.aeruginosa* growth by NO-loaded 50% Zn^{2+}-exchanged zeolites.

The NO release profile of NO-loaded zeolites (50% Zn^{2}; red line) measured in 5% LB:PBS media (1ml;37°C; 50 min). The [NO] was calculated at selected time-points and is the mean +/- SEM of n=5 individual experiments.

The bottom line graph shows PA01 growth following various incubation times (2-45 min) of control (black line) and NO-loaded zeolite (broken line) treated bacterial suspensions (150μl; 5% LB:PBS; 37°C). Data points represent the mean +/- SEM of an average of 3-6 plates per treatment in n=5 independent experiments. Data is expressed as the number of bacteria present per ml, estimated from the colony forming unit assay following control and zeolite treatments at each time-point. Asterisks denote significance from PA01 control growth at the appropriate time-point (*$p < 0.05$; ** $p < 0.01$).

5.4 Discussion

The colony forming unit (cfu) assay used to estimate the anti-bacterial potential of zeolite treatments is a standard technique employed in the literature to assess the antimicrobial activity of a number of agents. The reduction in bacterial numbers compared to control is a good indicator of the inhibition of bacterial growth following zeolite treatment. The estimation of the number of bacteria present at t=0 also allows the determination of a bactericidal or bacteriostatic effect of the treatments as well as the growth potential of the bacteria in experimental conditions. If the numbers of bacteria following treatments is reduced to levels < t=0, it can be considered that the bacteria are being killed, a bactericidal effect. Alternatively, a bacteriostatic response is suggested when bacterial growth fails to reach levels of the control suspensions incubated for the same time and numbers remain comparable to those estimated at t=0. In our experiments, NO-loaded zeolite treatment produced a bactericidal effect following zeolite incubation time $\geq$ 45 min against all bacterial strains investigated. This effect was significant in both Gram-negative (PA01 and J1386; figure 5.1-5.3) and Gram-positive (MSSA; figure 5.4-5.5) bacterial strains. These findings are in concordance with previous literature describing the bactericidal effect of NO (Hetrick & Schoenfisch, 2007; Hoehn *et al.*, 1998; McMullin *et al.*, 2005; Nablo & Schoenfisch, 2003). The potency of these zeolites on a wider range of bacterial strains together with potential anti-fungal and anti-viral effects remains to be investigated. However, the potency of the NO-releasing zeolites in the bacterial strains detailed, together with the rapidity of their anti-bacterial actions provides promising results for their future development.

The adhesion of bacterial cells to surfaces is central to the formation of biofilms, which are notoriously difficult to clear and are linked with the production of anti-biotic resistance (O'Neill *et al.*, 2007). It is therefore important to consider the adhesive properties of materials being developed for medical grade purposes. The polymer PTFE is commonly used in a number of medical devices due to its structural integrity and its favourable biocompatibility compared to other materials. The zeolite:PTFE material has previously been shown to inhibit platelet adhesion to its surface (Wheatley *et al.*, 2006) through the release of NO. Preliminary scanning electron micrograph images of the surface of zeolite discs following bacterial incubation indicate NO-loaded discs have similar anti-adhesive properties against bacteria (data not shown). The anti-adhesive properties of NO-releasing materials are well documented in the literature, however few of these materials have demonstrated antiseptic properties against bacteria, arguably the most important consideration in the design of anti-infective coatings. Furthermore, the resistance of current polymer based medical device coatings to bacterial adhesion is already impressive for most strains and therefore, further preventing adhesion may not improve infection rates significantly (Nablo *et al.*, 2005b). The anti-bacterial properties of NO-loaded zeolites are both bactericidal and anti-adhesive, further substantiating our proposal for the development of these materials for medical device coatings.

Small volumes of bacterial suspensions were used to suspend the zeolite discs, which subsequently concentrate the NO released from the zeolite disc. It was hypothesised

that high concentrations of NO are required to produce bactericidal effects. This hypothesis was confirmed when further dilution of the zeolite discs in increasing volumes, reversed the reduction in bacterial numbers observed at low dilution volumes (figure 5.6-7). These findings are in line with previous findings demonstrating NO-mediated reduction in bacterial viability (Coban *et al.*, 2003; Hetrick & Schoenfisch, 2007).

Differences in growth rates of control bacterial suspensions varied considerably between strains. This could be attributed to variations in metabolic activities and the biological niches in which these bacteria normally thrive. The clinical strain, J1386, is a mucoid strain isolated from the lungs of patients with cystic fibrosis, whereas the PA01 strain is a commonly used, laboratory strain isolated from skin infections. J1386 bacterial numbers remained comparable to those present at t=0 following the 45 min incubation, whereas PA01 growth almost doubled, highlighting the differences in the culture requirements for growth between these two species of *P.aeruginosa*. It is likely that J1386 requires a more nutrient-rich medium than the 5% LB medium used throughout the experiment. Interestingly, the NO-free zeolite produced a significant reduction in bacterial numbers in this strain. The reason for this reduction is unclear, but it is possibly due to leaching of Zn^{2+} from the zeolite surface. It is possible, however, that adhesion of these bacteria to the zeolite/PTFE surface could account for a reduction in bacterial numbers, as less bacteria would be left in the suspension for plating out for cfu analysis. The other Gram-negative strain, PA01 demonstrated no significant reduction of bacterial numbers following NO-free zeolite incubation, even after 120 min. It is possible that J1386 is more

prone to adherence. Further investigation using SEM to visualise the surface of the NO-free zeolite materials following exposure to J1386 would answer this.

The Gram-positive bacteria, MSSA is a strain commonly found colonising skin and nasal passages. As well as the bactericidal effect produced by the NO-loaded zeolite, the NO-free zeolite control disc also attenuated MSSA growth *in vitro*. The effects seen with the NO-free disc were bacteriostatic as the bacterial numbers present following treatments were comparable to those estimated at t=0. This finding suggests the bactericidal effect of these zeolites is due to release of NO. The bacteriostatic effect observed in MSSA could be due to the leaching of Zn^{2+} into the bacterial suspension. Attempts were made to chelate Zn^{2+} from the bacterial suspension through co-incubation of EDTA, however detrimental effects of EDTA on bacterial growth made interpretation of the implication of Zn^{2+} not possible. Future experiments could confirm of this hypothesis could be achieved through measurement of Zn^{2+} from solutions containing zeolite materials over several time-points. This could be done using flame atomic absorption spectroscopy (FAAS) or inductively coupled plasma mass spectroscopy (ICP-MS), which are techniques that can detect trace elements in biological sample through characteristic absorption wavelength or charge-mass ratio (Bolann *et al.*, 2007; Sarmiento-Gonzalez *et al.*, 2005).

Gram-positive and Gram-negative bacteria differ primarily in their membrane structure. Soderberg *et al* demonstrated a similar bacteriostatic effect in Gram-positive bacteria following zinc oxide treatment than that observed in this study. Interestingly, Gram-negative strains were generally unaffected by zinc oxide at

concentrations up to 1024μM and thus, it was speculated that the bacteriostatic effect was due to the specific binding of Zn^{2+} to components of the Gram-positive bacterial membrane, which subsequently inhibits bacterial replication (Soderberg *et al.*, 1990). No bacteriostatic effects were observed following NO-free zeolite treatments in the Gram-negative strain PA01, which supports this hypothesis and could highlight a possible mechanism for the bacteriostatic effects of NO-free zeolites in MSSA. A bactericidal effect rather than a bacteriostatic effect was observed following NO-free zeolite treatments in J1386, which implicates a different mechanism in this effect (possibly adherence) and further supports the Gram-positive bacterial susceptibility to Zn^{2+} induced bacteriostasis.

The antimicrobial effect of metal ions is best described through the use of silver ions (Ag^{+}) in wound dressings (Babu *et al.*, 2006; Bergin & Wraight, 2006; Dowsett, 2004) and antimicrobial device coatings (Bechert *et al.*, 1999; Harrison *et al.*, 2007; Kumar & Munstedt, 2005). The mechanism of the antimicrobial action is not fully understood but has been linked to a number of mechanisms including inhibition of the respiratory chain and the leakage of H^{+} through Ag^{+}-bound membrane proteins resulting in a loss of the trans-membrane proton gradient crucial for bacterial metabolism (Dibrov *et al.*, 2002; Holt & Bard, 2005). At high concentrations, the bactericidal effects of Ag^{+} is less specific, inhibiting a number of enzymatic activities and reacting with electron donor groups (Holt & Bard, 2005; Slawson *et al.*, 1992; Wells *et al.*, 1995). The mechanism of the antimicrobial action of other metal ions, including Zn^{2+} has also been reported in the literature (Aghatabay *et al.*, 2007; Silver, 1996; Soderberg *et al.*, 1990). The mechanism of their anti-bacterial

action is less well understood but is likely to target similar metabolic enzymes. The approximate composition of Zn^{2+} present within each zeolite disc is 20 μmoles, which would equate to a possible 0.13M of Zn^{2+} in the 150μl bacterial suspension in this assay. This is the very upper limit of what potentially could leach from the disc and, in practice, the concentration is likely to be much lower. However, if only 1/100 of the Zn^{2+} is displaced from the structure into the solution, the Zn^{2+} concentration would still be in the millimolar range at this dilution. Thus, it is very plausible that Zn^{2+} leaching from these zeolites could produce cytotoxic and cytostatic responses. The effects of the NO-free disc were only apparent at the lowest dilution with control growth being restored when the disc was incubated in a 300μl volume, suggesting a concentration-dependent response of bacteria to Zn^{2+}. The confirmation of the extent of the leaching is important in determining the potential of these materials for *in vivo* clinical use as toxicity to bacterial cells could translate to toxicity in host cells. Despite this, bacterial killing by Zn^{2+} within NO-loaded zeolites, could have excellent *ex vivo* prospects. For example, a simple ring of NO-loaded Zn^{2+} zeolite at the outer ends of a urinary cannula could provide protection from bacterial infections resulting from external sources, thereby bypassing the possible *in vivo* cytotoxicity of these agents to host tissue. Additionally, the use of powdered Zn^{2+} zeolites could be used as surface disinfectants. In this arena, the preliminary burst of NO could provide the powerful disinfectant effects to kill off any contaminating microbes, and once the NO reserves are exhausted, the Zn^{2+} could provide continued anti-microbial defence against susceptible strains. This is particularly attractive when considering the problems associated with the Gram-positive bacteria, MRSA. This strain is a significant cause

of morbidity and mortality within hospital environments and is diffucult to treat due to the development of antibiotic resistance in this strain (Jarvis *et al.*, 2007; Lodise & McKinnon, 2007). NO-releasing Zn^{2+} -exchanged zeolites could be a potential solution to the management of these antibiotic resistant strains, in both patient-based therapies and as novel disinfectants in hospital cleaning regimes.

Although Zn^{2+} leaching could provide additional anti-microbial protection against some strains, toxicity to host tissue remains a concern. One potential answer to the application of zeolites *in vivo* is the use of different ion exchanged zeolites. We used a Co^{2+} and a Ca^{2+} exchanged NO-free zeolite in the MSSA assay to assess the impact of the type of ion on MSSA growth. Results following incubation with the Co^{2+}-exchanged zeolite showed that it enhanced toxicity to MSSA bacteria compared to that seen with Zn^{2+}-exchanged zeolites. Preliminary experiments with the NO-free Ca^{2+}-exchanged zeolite suggested that this zeolite *enhanced* growth of MSSA compared to control. The anti-bacterial effects of the NO-loaded version of the Ca^{2+}-exchanged zeolite are yet to be investigated but are predicted to produce similar bactericidal effects to other NO-loaded zeolites as the capacity for NO storage is likely to be similar to that of Zn^{2+}. Clearly, optimisation of zeolite design is necessary to produce ion-exchanged zeolites with minimal potential toxicity while retaining the anti-microbial effects associated with the high concentrations of NO.

As well as a concentration dependent effect of NO on bacterial growth, a temporal association was also demonstrated in the inhibition of PA01 growth. Zeolite incubation times varying from 2-45min demonstrated that inhibition of PA01 growth

occurred only following at least 30 min of zeolite exposure. This was surprising because the NO release profile for these zeolites shows a rapid release of NO, reaching peak concentrations at approx 10min and returning to near baseline levels by 50min. The free radical properties of NO and related species has been suggested to produce a direct oxidative or nitrative stressing effect on cells at these concentrations. Thus, killing would be predicted to take maximal effect when peak NO concentrations are being released at 10-20 min. However, PA01 exposed to zeolite discs for these times showed absolutely no bacterial killing and bacterial numbers were comparable to control. In fact, a slight enhancement of growth at these time-points is suggestive but not significant. The direct correlation with NO concentration and degree of killing demonstrated by earlier experiments (figure 6.6 B) suggest that this temporal effect is not solely a concentration-dependent response as a similar correlation of bacterial killing should be apparent at earlier time-points when the NO concentration would be lower. It is possible therefore that NO released by zeolite discs is triggering a biological response within the PA01 bacteria, which subsequently only results in a bactericidal effect following 30-45min of NO exposure. Further investigation is required to determine if the temporal association of the bactericidal effect of NO is evident in other bacterial strains although preliminary results with MSSA suggest a similar response (data not shown). The exhaustion of bacterial defences against NO may be one explanation for the delayed killing response in PA01. Pyocyanin is a phenazine pigment produced by *Pseudomonas Aeruginosa* bacteria which has been shown to decrease the activity of NO in a number of tissues (Gryglewski *et al.*, 1992; Hussain *et al.*, 1997; Warren *et al.*, 1990). The mechanism of the inactivation of NO is not fully understood, but is

suggested to be due to the formation of nitrosylated pyocyanin species, which in turn inhibit the biological actions of NO. Bacteria can employ a number of antioxidant-like defences that vary according to the species of bacteria. Variations in the types of antioxidant produced by different bacterial strains are thought to contribute to the disparity in the susceptibility of bacteria to different species of reactive nitrogen species reported in the literature (De Groote *et al.*, 1995; Zaki *et al.*, 2005; Zhu *et al.*, 1992) . It is likely that bacteria release a deluge of defences against oxidant species, which could possibly be exhausted or overcome by the presence of high concentrations of oxidant species. In this assay, the majority of the NO is released within the first 20 minutes and if antioxidant defences were present until this stage, the subsequent release of lower concentrations of NO following this time-point would be expected to produce a less significant killing response than that observed. Previous disc dilution experiments (figure 6.6 B) demonstrated that high concentrations of NO are required to produce the level of killing in PA01 bacteria produced in the temporal assay. So, this brings us to hypothesise the involvement of a bacterial receptor interaction with NO or related species. In inflammatory cells, NO is suggested to act via a death receptor pathway to either up-regulate or down-regulate survival signals important for the prevention or initiation of programmed cell death (apoptosis) (Brune *et al.*, 1995; Brune *et al.*, 1998; Ward *et al.*, 2000). The involvement of apoptotic like signals in prokaryotes is controversial, however similar cell death phenotypes have been described in unicellular organisms including DNA fragmentation, cytoplasmic blebbing and vacuolization (Rice & Bayles, 2003). Additionally, these responses have been associated with exposure to oxidative stress (Rice & Bayles, 2003). Quorum sensing is another bacterial phenomenon that

involves the communication between bacterial cells to control virulence factors. PA01 has been described to use quorum sensing to develop biofilms. Quorum quenching involves the interference of the signalling mechanism produced from production of quorum sensing molecules and can result in the limitation of bacterial virulence. The interference of bacterial communication can also result in a mass death response in these organisms (You *et al.*, 2004) which may be a possible explanation for the dramatic reduction of bacterial numbers at a critical time-point. The interesting temporal relationship of NO and bacterial killing described in this chapter is one that has not been shown previously and is one which warrants further investigation.

The complex chemistry of NO requires one to be careful when determining the effector species of cytotoxic effects. It is suggested that NO in its pure form is not cytotoxic in a number of cell types, and that the formation of $OONO^-$ species through the interaction of NO with O_2^- is the main culprit of the majority of the cytotoxicity associated with NO (Pacher *et al.*, 2007). The upregulation of O_2^- production by immune cells during inflammatory responses together with the upregulation of NO production through iNOS provides the right conditions for significant peroxynitrite production in the inflammatory microenvironment important for microbial killing and clearance of infection *in vivo*. $OONO^-$ is a potent oxidant with multiple targets including lipid peroxidation and DNA fragmentation, which have detrimental effects on bacterial viability. The involvement of O_2^- production in our experiments is not clear and efforts to scavenge both peroxynitrite species and O_2^- in our bacterial suspensions were

fraught with difficulty due to the non-specific effects of these agents on control bacterial growth. The presence of a O_2^- generating system in this experiment is unconfirmed, however, the absence of cell types known to generate O_2^- would suggest that only background levels of O_2^- would be present, thus peroxynitrite levels could be insignificant especially compared to the levels of NO released. It still remains possible that NO itself is the cytotoxic agent given that the concentration in the bacterial suspensions is remarkably high and the non-specific effects of high concentrations of this free-radical could have detrimental effects on bacterial viability. Indeed, some strains do have greater sensitivity to the bactericidal effects of NO than $OONO^-$ (Assreuy *et al.*, 1994; Fernandes & Assreuy, 1997). Better understanding of the redox potential of bacterial products and LB broth is required to elucidate the relative presence of NO and related species. The end product of NO production, NO_2^- and NO_3^-, was not the cytotoxic species in our experiments. 1mM concentrations of the sodium salts of NO_2^- and NO_3^- failed to produce any significant effects on bacterial growth in MSSA (data not shown). Many other potential mechanisms of anti-bacterial effects of NO and related species exist including the modulation of critical bacterial proteins through interactions with sulphydryl, haem, and amine groups and aromatic residues (Fang, 1997). The elucidation of the mechanism of the anti-bacterial actions of NO is a complex procedure due to the influence of many different components on NO biochemistry. Understanding how NO produces anti-microbial actions could help harness this potential for future development of successful anti-microbials.

In summary, we have shown that 50% Zn^{2+}-exchanged zeolite:PTFE materials have potent anti-bacterial properties in Gram-negative and Gram-positive bacteria. The mechanism of the observed bactericidal effect was associated with high concentrations of NO release for over 30 minutes. The potential leaching of Zn^{2+} from the zeolite structure may contribute to the observed bacteriostatic effect of NO-free discs in Gram-positive MSSA bacteria. The potential development of these materials as anti-microbial coatings for use in medical devices requires the further characterisation of these agents in a more diverse range of bacterial and fungal strains together with a fuller understanding of the mechanism of action and cytotoxicity *in vivo* is required before these materials can be used in the clinic.

CHAPTER SIX

General Discussion

Chapter 6 - General Discussion.

6.1 Introduction

Nitric oxide (NO), the toxic by-product of combustion engines, atmospheric pollutant and widely revered biological elixir, is a major focus of scientific research spanning many disciplines. We go to great lengths to remove NO from exhaust fumes, and yet, this organic free radical has been found to be a key component in a variety of physiological and pathophysiological processes. NO is now known to be important for vascular haemostasis, due to its intimate involvement in vasodilation, smooth muscle proliferation and the inhibition of platelet activation and adhesion (Moncada *et al.*, 1988; Palmer *et al.*, 1987; Radomski *et al.*, 1987a, b). NO also plays an integral role in various aspects of immune function and regulation, including inflammatory cell activation, adhesion, apoptosis and microbial killing (Albina & Reichner, 1998; Bogdan, 1997; Kubes *et al.*, 1991). The impressive array of effects is further expanded by the capacity of NO to act as both a neurotransmitter and an adjuvant to wound healing (Sanders & Ward, 1992; Shabani *et al.*, 1996). The dysfunction of NO production and signalling is implicated in a wide range of diseases, such as hypertension, hypercholesterolemia, diabetes and septic shock, yet NO-based therapeutics remain under-represented in clinical treatment options (Kojda & Harrison, 1999; Megson & Webb, 2002). The lack of target specificity and the notoriously difficult challenge of stablising this labile molecule for localised drug delivery, has produced significant barriers to the widespread use of NO as a

therapeutic agent. However, localised NO delivery, achieved through the use of NO-donor polymer bound materials provide a promising solution to overcoming the barriers in NO therapy, avoiding the detrimental effects of untargeted, systemic release (Frost *et al.*, 2005). The supplementation of NO by liberation from polymers offers the potential in producing biocompatible surfaces for a variety of medical devices, particularly those used in interventional procedures, such as vascular grafts, extracorporeal loops and stents (Annich *et al.*, 2000; Bohl & West, 2000; Hou *et al.*, 2005; Kaul *et al.*, 2000; Kennedy *et al.*, 2003). The release of NO from the surface of vascular stents would not only inhibit thrombus formation at the surface, but could also aid in the prevention of neointimal thickening; a major cause of restenosis of vessels following stent placement (Hou *et al.*, 2005). The multifaceted effects of NO released from polymer surfaces have also been shown to have effective anti-microbial properties, highlighting a possible role for these materials in control of nosocomial infections contracted through medical device usage (Dobmeier & Schoenfisch, 2004; Nablo *et al.*, 2005; Nablo & Schoenfisch, 2003).

Cation-exchanged zeolites are microporous materials that are excellent high capacity NO gas storage materials. The large surface area allows for up to 1millimole of NO to be stored per milligram of zeolite, which is liberated upon contact of the material with aqueous media (Wheatley *et al.*, 2006). These zeolite materials provide a novel means by which to deliver NO locally, using pure NO gas as the primary source, avoiding the need for biological cleavage or by-product formation often required with other NO-donor drug bound polymers (Frost *et al.*, 2005). Furthermore, zeolite design is easily altered to produce materials with variable NO storage and release

capacities. This can be achieved through the following: careful choice of zeolite structure, of which there are hundreds of man-made and naturally occurring structures, changing the cation exchanged into the structure, the composition of the zeolite to a polymer binder and changing the polymer binder material. Thus, these zeolites provide an alternative and novel way to store and deliver NO that has dynamic properties, ideal for development of NO-releasing coatings for a wide range of biomedical applications.

6.2 Summary

Chapter 3 characterised the NO-release capacities of several zeolite "designs" of two cation-exchanged zeolites (Zn^{2+} and Co^{2+}) at various compositions of zeolite to PTFE or PDMS polymer binder, in different biological solutions. The results indicated that NO-release capacities and rate of release are impacted significantly by changes in each of the above parameters. High composition (>50%) zeolites were shown to be high capacity storage materials of NO, releasing high micromolar concentrations over approximately 1 h. Lower composition Zn^{2+}-exchanged zeolites released very small concentrations of NO that did not correlate with the reduction in NO reservoirs through changes in composition. Low composition zeolites did not display significant anti-platelet properties in collagen-induced aggregation whereas high composition zeolites had powerful anti-platelet properties, which lasted for up to 2 h and were found to be largely sGC-independent, as determined by the use of the selective inhibitor of sGC, ODQ. The anti-platelet properties of NO-loaded zeolites were indeed attributed to NO, as the NO-free counterpart zeolites did not inhibit

collagen-induced aggregation and the NO scavenger, Hb was able to partially reverse the effects seen with the 50% zeolite. The sGC-independent effects were not elucidated in this study but, as discussed, were suggested to be likely due to platelet protein modifications.

Despite several zeolite modifications, the NO-release duration of all the zeolites studied did not exceed approximately 1h although anti-platelet effects lasted for up to 2 h. This discrepancy was hypothesised to be due to the storage of NO in S-nitrosoalbumin reservoirs, which has previously been implicated in the prolongation of anti-platelet effects by short half-life NO-donor compounds (Crane *et al.*, 2002). This mechanism did not appear to contribute significantly to the anti-platelet effects of a 50% Zn^{2+}-exchanged zeolite as these zeolites retained their potent anti-platelet effects in washed platelet samples. Furthermore, this assay used pre-incubation techniques where transfer of the zeolite material occurred 1 min before collagen stimulation, compared to the previous incubation of zeolite materials in the sample for the full duration prior to collagen stimulation. This technique did not reduce the anti-platelet actions of the zeolite in PRP further downplaying the involvement of S-nitrosoalbumin stores in the prolongation of the anti-platelet effects of NO. It was concluded that these zeolites produce adequate concentrations to inhibit aggregation beyond the apparent NO-release duration measured by the NO-electrode and that the lack of NO signal at these time points was due to limitations in the sensitivity of the NO electrode.

The incubation of zeolite discs in PRP and physiological salt solutions produced varying NO release profiles, demonstrating how components of a given solution can mask NO induced effects and alter the concentration of NO reaching the target. This is further highlighted in the whole blood aggregation experiments, which show dramatically reduced anti-thrombotic potential compared to that observed in PRP. NO-released from Co^{2+}-exchanged zeolites demonstrated powerful smooth muscle relaxing effects in myography experiments that were influenced by the choice of polymer binding the zeolite. The PTFE polymer produced more favourable peak relaxation responses than a composition matched PDMS polymer bound zeolite. The experiments performed in the first chapter indicate that the 50% Zn^{2+}-exchanged zeolite in a PTFE binder has the most promising NO release characteristics with which to continue the investigation of the effects of these materials in other biological assays. However, further optimisation of zeolite design is required to produce the elusive low concentration, long-duration NO release profile ideal for development of anti-thrombotic coatings for blood-contacting medical devices.

Chapter 4 further characterises the 50% Zn^{2+}-exchanged zeolite in relation to its effects on function and viability of human neutrophils. It was shown that the NO-loaded zeolites produced concentration-dependent pro-inflammatory responses in isolated human neutrophil suspensions in the absence of the neutrophil activator fMLP. Changes in neutrophil shape were observed, together with modulation of surface adhesion molecule expression in the form of shedding of L-selectin and up-regulation of CD11b following NO-loaded zeolite incubation for only 1hour. When the neutrophils were stimulated with fMLP at 30 min of the 60 min zeolite

incubation, there was an enhancement of CD11b expression. These effects were similar to the priming activation of neutrophils by various factors including peroxynitrite ($ONOO^-$). The involvement of $ONOO^-$ in these effects is unknown although there remains a possibility that NO is involved due to the requirement for extremely high levels of O_2^- to form adequate concentrations of $ONOO^-$ known to produce the priming effect described in the literature (Rohn *et al.*, 1999). Further to this, the reduction in zeolite size and/or zeolite dilution in the neutrophil suspension quickly reversed the apparent priming response indicating that very high concentrations of NO were required, despite the likeliness that $ONOO^-$ production would still be substantial at lower dilutions, given that NO concentrations would likely still be far in excess of O_2^-. However, a role for $ONOO^-$ in these effects cannot be ruled out, especially when considering the concentration-dependent increase in neutrophil necrosis at the highest zeolite concentration. NO has a controversial role in cytotoxicity, and many studies have reported a requirement for $ONOO^-$ or H_2O_2 over NO in producing these effects (Pacher *et al.*, 2007). It cannot be discounted, in these experiments, that high concentrations of NO produced at a localised site could have cytotoxic effects against neutrophils. The lack of apparent lack of zeolite toxicity against platelets, demonstrated in the previous chapter, suggests that there may be a cell or cell suspension dependent component to the cytotoxic effects of NO. The enhancement of $ONOO^-$ production by reaction of NO with O_2^- generated by neutrophils could potentially cause increased oxidant stress in these cells. Furthermore, lack of cytotoxicity in platelet experiments may be due to 'buffering' of NO by plasma constituents.

Chapter 5 investigated the anti-bacterial properties of the 50% Zn^{2+}-exchanged zeolite against strains of bacteria commonly associated with nosocomial infections. It was shown that these zeolites are potent anti-bacterial agents that are able to significantly reduce the numbers of bacterial colony forming units after only 60 min treatments. The NO-loaded zeolite displayed bacteriocidal effects in all strains studied, as bacterial numbers were decreased to below levels estimated at the start of the experiment (t=0). The bactericidal effect of NO-loaded zeolites to a strain of the Gram-negative bacterium, Pseudomonas aeruginosa was enhanced upon longer zeolite treatment, (120 min) and bacterial numbers were completely eradicated at this time-point. Interestingly, a bacteriostatic effect of NO-free zeolites was indicated, likely due to leaching of Zn^{2+} from the zeolite structure. The bactericidal and bacteriostatic effects of the NO-loaded and NO-free zeolites were shown to be concentration dependent as dilution of the zeolite disc restored bacterial numbers. The concentration of NO required to produce bactericidal effects varied between strains but was always associated with very high concentrations of NO, released by the zeolite disc into small volumes of the bacterial suspension.

The bactericidal effect of NO-loaded zeolites had an interesting temporal component. It was shown that bacterial numbers were not reduced until after a 30 min zeolite incubation, despite peak NO-release occurring within the first 10 min. In fact, following 10 min incubation, bacterial numbers appeared slightly increased. This observation was not statistically significant although it is surprising that bacterial numbers were not reduced at this point as previous experiments showed that bacterial killing ability correlated with the concentration of NO present in the bacterial

suspension. It was suggested that perhaps NO is either temporarily scavenged by bacterial products, such as pyocyanin or that NO is triggering an unknown biological mechanism, which in turn takes 30 min to induce cytotoxic effects.

6.3 Physiological and pharmacological implications and future directions.

Cation-exchanged zeolites are high capacity storage materials of NO. NO is liberated on contact with an aqueous solution at biologically relevant amounts that have been demonstrated to have potent anti-platelet, anti-bacterial and smooth muscle relaxant properties. The effects generated are dependent upon the concentration of NO delivered from the zeolite material and the ability of NO to reach its biological target. This thesis has demonstrated how zeolite design, volume and components of biological solutions can affect NO storage and release capacities of these materials. The 50% Zn^{2+}-exchanged zeolite had the best NO-release characteristics for further investigation in this thesis, however much more zeolite optimisation is required before these materials can be considered as anti-thrombotic coatings for blood-contacting medical devices. The lack of impressive anti-thrombotic effects produced during whole blood aggregation experiments (figure 3.8) as well as the short period of NO release indicates further work is required in this area. The Cu^{2+}-exchanged zeolite or alternatively, a Cu^{2+} containing metal organic framework (another microporous material) could provide the 'magic bullet' in localised NO delivery. These materials could offer the catalytic conversion of NO from nitrite at the surface of the material upon reduction of the Cu^{2+} to Cu^{1+} (Oh &

Meyerhoff, 2004, 2003) thereby producing a constant, unending source of NO. Preliminary work is being done to this end, although leaching of toxic Cu^{2+} ions has proved problematic. Leaching of Zn^{2+}ions is suggested to have potentially produced the bacteriostatic effects described in chapter 5. Side effects of Zn^{2+}-leakage therefore must be taken into account when considering the *in vivo* application of zeolite materials although no apparent detrimental effects were seen following use of NO-free zeolites in platelet aggregation, myography or neutrophil experiments. The bacteriostatic effect of NO-free zeolites occurred in very small volumes (150µl; figure 5.4), and was insignificant upon dilution of the disc, suggesting that Zn^{2+} had to be at very high concentrations in the solution to produce any effects (figure 5.7B). These small volumes are not physiological in practice for blood-contacting medical devices, which would come into contact with large volumes of pulsatile flowing fluids and therefore the physiological impact of cation leaching from zeolites could be negligible or enhanced due to washout phenomena. The *ex vivo* application of current zeolite designs are promising, especially in anti-microbial coatings for urinary catheters, which are common risk factors associated with nosocomial infections, often acquired due to poor handling techniques during insertion (Goldmann, 1991). Here, a ring of NO-loaded zeolite material would help prevent the migration of external microbial pathogens up into the urinary tract of immuno-compromised patients. Therefore, leaching of cations from zeolite structures can be used to an advantage when engineering these materials for a number of applications. It would be beneficial to investigate the efficacy of these zeolite materials in dressings to promote wound healing and in clearing skin conditions such as acne, which has a significant bacterial component (Coenye *et al.*, 2007). Here, cations

such as Ag^{2+} and Zn^{2+} have already been shown to have beneficial effects (Babu *et al.*, 2006; Bergin & Wraight, 2006; Dowsett, 2004), further supporting the incorporation of the ion leaching zeolite designs for future investigation in these specialised areas.

The mechanism by which NO-loaded and NO-free zeolites exert their anti-microbial effects has yet to be confirmed. Anti-microbial properties of NO and NO-related species have been described in the literature. Microbial killing of NO and NO-related species have shown varying degrees of susceptibility, which are strain specific (De Groote *et al.*, 1995; Zaki *et al.*, 2005; Zhu *et al.*, 1992). Indeed, a difference in susceptibility of the bacterial strains used in chapter 5 to NO-loaded zeolite materials was evident. Harnessing any differences in susceptibility of commensal and pathogenic strains of microbes could help better design zeolite NO-release to produce strain-specific killing and avoid the detrimental effect of non-discriminate killing. It would be important to confirm the possible development of resistance to NO by bacterial strains, especially with an increase in the emergence of antibiotic resistant strains in hospitals and the community (Lodise & McKinnon, 2007). These experiments would likely involve repeated, long duration exposure of bacteria to NO-loaded zeolites to assess if bacteria subsequently developed the ability to withstand acute and prolonged exposure to NO. Further characterisation of the anti-microbial effects of NO to other pathogenic organisms, including fungi and viruses would better support the use of these materials as anti-microbial agents.

The interesting temporal association of PA01 killing and exposure to NO-loaded zeolites (figure 5.8) raised the possibility that NO is not directly inducing a lethal

oxidant stress on these prokaryotic cells and that perhaps there is a more complex biological mechanism triggered by NO or NO related species. Investigation into bacterial cell morphology, especially membrane integrity and DNA fragmentation may help to determine if these cells show signs of direct oxidative stress. If there was an alternative pathway by which NO is exerting its anti-microbial effects, such as activation or inhibition of protein kinases, immunofluoresence and Western blotting techniques could help determine the effectors in this instance.

Although there are significant drawbacks to the use of these zeolites in medical device coatings, these materials have proved to be a unique tool to investigate various aspects of NO biology. The mechanism of action of NO-loaded zeolite materials was shown to have a significant sGC-independent component in platelet aggregation and myography experiments, determined through the selective inhibition of sGC by ODQ. Similar sGC independent effects of NO have been reported in the literature, especially in regards to inhibition of platelet activation and smooth muscle relaxation. These effects were associated with high concentrations of NO released in the extracellular environment (Crane *et al.*, 2005; Miller *et al.*, 2004; Sogo *et al.*, 2000). NO-loaded zeolite materials produced sGC-independent effects similar to those observed with the NO-donor DEA/NO, which releases NO spontaneously in the extracellular environment. These effects are in contrast to those observed with the intracellular NO donor, SNP, which demonstrated no inhibition of platelet aggregation in the presence of ODQ. The sGC-independent pathway stimulated by NO has been suggested to be associated with membrane protein modifications, particularly Ca^{2+} transporting proteins, possibly through nitration of amine residues

such as tyrosine (Crane *et al.*, 2005; Eiserich *et al.*, 1998). Further investigation into protein structure modifications through measurements of nitrosotyrosine residues by liquid chromatography or Western blotting techniques may help determine a possible mechanism for the observed effects in these experiments.

Neutrophil priming is a phenomenon associated with many inflammatory agents such as GM-CSF, TNF-α, PAF and IL-8 and is characterised by the enhancement of neutrophil immune responses on subsequent exposure of the primed neutrophils to an activating stimuli (Condliffe *et al.*, 1998; Kitchen *et al.*, 1996; Leino *et al.*, 1993; Partrick *et al.*, 1997). Neutrophils produced modulations in activation marker expression following NO-loaded zeolite exposure that were similar to priming responses shown with other well-known priming agents (Condliffe *et al.*, 1996). Nitric oxide *per se* has not been previously recognised as a priming agent, but the NO-related species, $OONO^-$ has been shown to demonstrate priming activity similar to that observed in this study (Rohn *et al.*, 1999). The nitration of neutrophil surface proteins has been suggested to produce the majority of the priming responses observed by $OONO^-$ (Swain *et al.*, 2002) thereby promoting degranulation and the modulation of surface adhesion markers. Again, measurement of nitrated tyrosine residues and the addition of SOD to eliminate O_2^- from experimental conditions could assist in characterising these interesting observations.

In conclusion, zeolite materials have been shown to be high capacity storage materials of NO that release NO stores at biologically relevant concentrations, which have powerful anti-platelet and anti-bacterial properties. Although the NO-loaded

zeolite materials studied in this thesis require optimisation before more favourable NO release durations are achieved for development as biocompatible coatings, the experiments performed have highlighted a variety of issues which should be investigated in more detail. Furthermore, these materials have provided a unique tool with which to investigate various aspects of NO biology. Indeed, this thesis has uncovered some interesting findings regarding the involvement of NO in neutrophil activation and bacterial killing, which have not been previously reported. Increasing the understanding of the effects of NO, particularly with respect to mechanism of action, could help better harness the therapeutic value of NO donating materials and drugs and finally overcome the barriers to the successful use of these agents in the clinic.

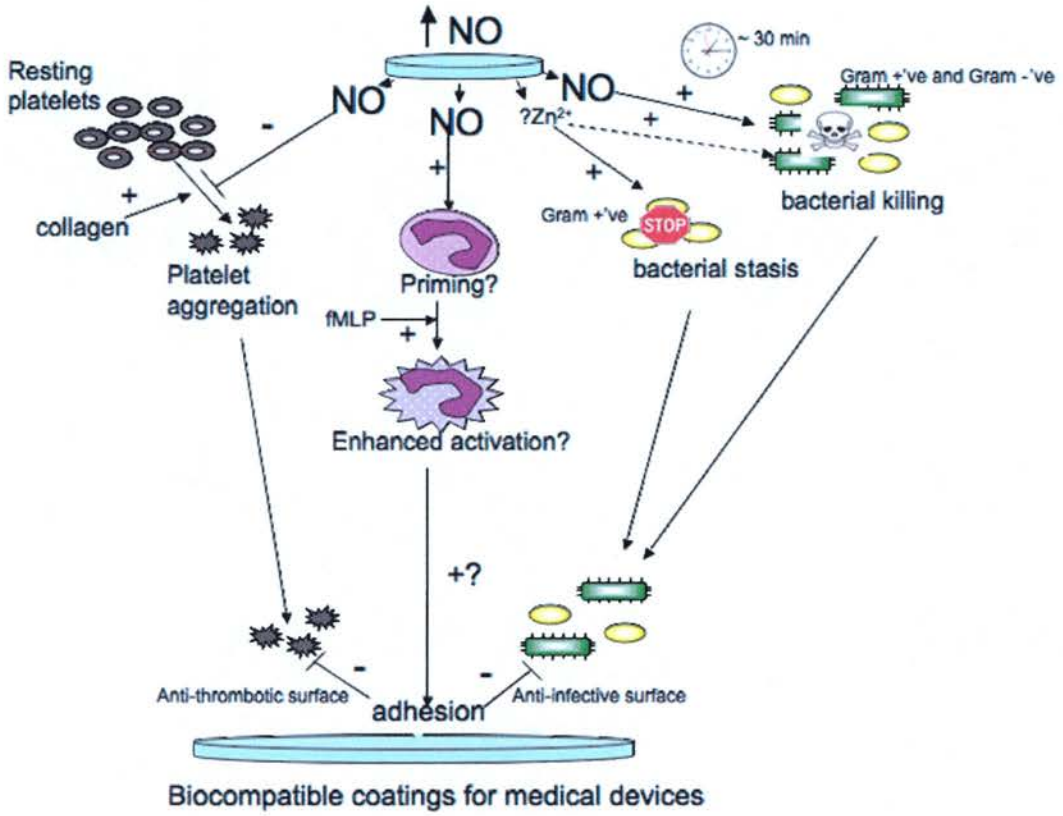

Figure 6.1. Summary diagram.

Zeolites are high capacity storage materials of NO. NO-released has been shown to inhibit platelet aggregation and adhesion (Wheatley *et al.*, 2006), have pro-inflammatory effects in human neutrophils possibly related to priming activation and have anti-bacterial properties against both Gram-positive and Gram-negative bacteria that demonstrated a dependence on both high concentrations and time of NO exposure. Zn^{2+}-exchanged zeolites may leach Zn^{2+} ions that could have cytostatic effects in Gram-positive bacteria (e.g MSSA) and may contribute to the cytotoxic properties of the zeolite against Gram-negative bacterial strain, J1386. Thus, these materials show promise in the development of anti-thrombotic and anti-infective coatings for medical devices. However, further optimisation of zeolite design is required to avoid detrimental side effects of metal leaching and high concentrations of NO.

REFERENCES

AGHATABAY, N.M., NESHAT, A., *et al.* (2007). Synthesis, characterization and antimicrobial activity of Fe(II), Zn(II), Cd(II) and Hg(II) complexes with 2,6-bis(benzimidazol-2-yl) pyridine ligand. *Eur J Med Chem*, **42,** 205-13.

AHERN, G.P., KLYACHKO, V.A., *et al.* (2002). cGMP and S-nitrosylation: two routes for modulation of neuronal excitability by NO. *Trends Neurosci*, **25,** 510-7.

AHN, K.Y., MOHAUPT, M.G., *et al.* (1994). In situ hybridization localization of mRNA encoding inducible nitric oxide synthase in rat kidney. *Am J Physiol*, **267,** F748-57.

ALBINA, J.E. & REICHNER, J.S. (1998). Role of nitric oxide in mediation of macrophage cytotoxicity and apoptosis. *Cancer Metastasis Rev*, **17,** 39-53.

AMADEU, T.P., SEABRA, A.B., *et al.* (2007). S-nitrosoglutathione-containing hydrogel accelerates rat cutaneous wound repair. *J Eur Acad Dermatol Venereol*, **21,** 629-37.

ANDERSSON, K.E. & HOLMQUIST, F. (1994). Regulation of tone in penile cavernous smooth muscle. Established concepts and new findings. *World J Urol*, **12,** 249-61.

ANNICH, G.M., MEINHARDT, J.P., *et al.* (2000). Reduced platelet activation and thrombosis in extracorporeal circuits coated with nitric oxide release polymers. *Critical care medicine*, **28,** 915-20.

ASCENZI, P., BOCEDI, A., *et al.* (2003). The anti-parasitic effects of nitric oxide. *IUBMB Life*, **55,** 573-8.

ASSREUY, J., CUNHA, F.Q., *et al.* (1994). Production of nitric oxide and superoxide by activated macrophages and killing of Leishmania major. *Eur J Immunol*, **24,** 672-6.

BABU, R., ZHANG, J., *et al.* (2006). Antimicrobial activities of silver used as a polymerization catalyst for a wound-healing matrix. *Biomaterials*, **27,** 4304-14.

BALLIGAND, J.L. & CANNON, P.J. (1997). Nitric oxide synthases and cardiac muscle. Autocrine and paracrine influences. *Arterioscler Thromb Vasc Biol*, **17,** 1846-58.

BALLIGAND, J.L., KELLY, R.A., *et al.* (1993). Control of cardiac muscle cell function by an endogenous nitric oxide signaling system. *Proc Natl Acad Sci U S A*, **90,** 347-51.

BALLIGAND, J.L., UNGUREANU-LONGROIS, D., *et al.* (1994). Cytokine-inducible nitric oxide synthase (iNOS) expression in cardiac myocytes. Characterization and regulation of iNOS expression and detection of iNOS activity in single cardiac myocytes in vitro. *J Biol Chem*, **269,** 27580-8.

BARTOSZ, G. (1996). Peroxynitrite: mediator of the toxic action of nitric oxide. *Acta Biochim Pol*, **43,** 645-59.

BASS, D.A., MCPHAIL, L.C., *et al.* (1988). Selective priming of rate and duration of the respiratory burst of neutrophils by 1,2-diacyl and 1-O-alkyl-2-acyl diglycerides. Possible relation to effects on protein kinase C. *J Biol Chem*, **263,** 19610-7.

BAULDRY, S.A., BASS, D.A., *et al.* (1991). Tumor necrosis factor alpha priming of phospholipase D in human neutrophils. Correlation between phosphatidic acid production and superoxide generation. *J Biol Chem*, **266,** 4173-9.

BEAVO, J.A., CONTI, M., *et al.* (1994). Multiple cyclic nucleotide phosphodiesterases. *Mol Pharmacol*, **46,** 399-405.

BECHERT, T., BOSWALD, M., *et al.* (1999). The Erlanger silver catheter: in vitro results for antimicrobial activity. *Infection*, **27 Suppl 1,** S24-9.

BECKMAN, J.S. & KOPPENOL, W.H. (1996). Nitric oxide, superoxide, and peroxynitrite: the good, the bad, and ugly. *Am J Physiol*, **271,** C1424-37.

BELLAMY, T.C., WOOD, J., *et al.* (2002). On the activation of soluble guanylyl cyclase by nitric oxide. *Proc Natl Acad Sci U S A*, **99,** 507-10.

BENJAMIM, C.F., SILVA, J.S., *et al.* (2002). Inhibition of leukocyte rolling by nitric oxide during sepsis leads to reduced migration of active microbicidal neutrophils. *Infect Immun*, **70,** 3602-10.

BENNETT, M.R. (1997). Non-adrenergic non-cholinergic (NANC) transmission to smooth muscle: 35 years on. *Prog Neurobiol*, **52,** 159-95.

BERDEAUX, A. (1993). Nitric oxide: an ubiquitous messenger. *Fundam Clin Pharmacol*, **7,** 401-11.

BERGIN, S.M. & WRAIGHT, P. (2006). Silver based wound dressings and topical agents for treating diabetic foot ulcers. *Cochrane Database Syst Rev*, CD005082.

BHARDWAJ, R., PAGE, C.P., *et al.* (1988). Endothelium-derived relaxing factor inhibits platelet aggregation in human whole blood in vitro and in the rat in vivo. *Eur J Pharmacol*, **157,** 83-91.

BISSETT, L. (2005). Reducing the risk of catheter-related urinary tract infection. *Nurs Times*, **101,** 64-5, 67.

BOERRIGTER, G. & BURNETT, J.C., JR. (2007). Nitric oxide-independent stimulation of soluble guanylate cyclase with BAY 41-2272 in cardiovascular disease. *Cardiovasc Drug Rev*, **25,** 30-45.

BOGDAN, C. (1997). Of microbes, macrophages and nitric oxide. *Behring Inst Mitt*, 58-72.

BOGER, R.H., BODE-BOGER, S.M., *et al.* (1998). Asymmetric dimethylarginine (ADMA): a novel risk factor for endothelial dysfunction: its role in hypercholesterolemia. *Circulation*, **98,** 1842-7.

BOGER, R.H. & RON, E.S. (2005). L-Arginine improves vascular function by overcoming deleterious effects of ADMA, a novel cardiovascular risk factor. *Altern Med Rev*, **10,** 14-23.

BOHL, K.S. & WEST, J.L. (2000). Nitric oxide-generating polymers reduce platelet adhesion and smooth muscle cell proliferation. *Biomaterials*, **21,** 2273-8.

BOLANN, B.J., RAHIL-KHAZEN, R., *et al.* (2007). Evaluation of methods for trace-element determination with emphasis on their usability in the clinical routine laboratory. *Scand J Clin Lab Invest*, **67,** 353-66.

BOLOTINA, V.M., NAJIBI, S., *et al.* (1994). Nitric oxide directly activates calcium-dependent potassium channels in vascular smooth muscle. *Nature*, **368,** 850-3.

BONTHU, S., HEISTAD, D.D., *et al.* (1997). Atherosclerosis, vascular remodeling, and impairment of endothelium-dependent relaxation in genetically altered hyperlipidemic mice. *Arterioscler Thromb Vasc Biol*, **17,** 2333-40.

BORANIC, M. (2000). [What a physician should know about zeolites]. *Lijec Vjesn*, **122,** 292-8.

BRADLEY, K.K., BUXTON, I.L., *et al.* (1998). Nitric oxide relaxes human myometrium by a cGMP-independent mechanism. *Am J Physiol*, **275,** C1668-73.

BRANDONISIO, O., PANARO, M.A., *et al.* (2001). Nitric oxide production by Leishmania-infected macrophages and modulation by cytokines and prostaglandins. *Parassitologia*, **43 Suppl 1,** 1-6.

BREDT, D.S., GLATT, C.E., *et al.* (1991a). Nitric oxide synthase protein and mRNA are discretely localized in neuronal populations of the mammalian CNS together with NADPH diaphorase. *Neuron*, **7,** 615-24.

BREDT, D.S., HWANG, P.M., *et al.* (1991b). Cloned and expressed nitric oxide synthase structurally resembles cytochrome P-450 reductase. *Nature*, **351,** 714-8.

BREDT, D.S., HWANG, P.M., *et al.* (1990). Localization of nitric oxide synthase indicating a neural role for nitric oxide. *Nature*, **347,** 768-70.

BROWN, G.C. (1999). Nitric oxide and mitochondrial respiration. *Biochim Biophys Acta*, **1411,** 351-69.

BROWN, G.C., FOXWELL, N., *et al.* (1998). Transcellular regulation of cell respiration by nitric oxide generated by activated macrophages. *FEBS Lett*, **439,** 321-4.

BRUNE, B., MESSMER, U.K., *et al.* (1995). The role of nitric oxide in cell injury. *Toxicol Lett*, **82-83,** 233-7.

BRUNE, B., SANDAU, K., *et al.* (1998a). Apoptotic cell death and nitric oxide: activating and antagonistic transducing pathways. *Biochemistry (Mosc)*, **63,** 817-25.

BRUNE, B., VON KNETHEN, A., *et al.* (1998b). Nitric oxide and its role in apoptosis. *Eur J Pharmacol*, **351,** 261-72.

BRUNE, B., ZHOU, J., *et al.* (2003). Nitric oxide, oxidative stress, and apoptosis. *Kidney Int Suppl*, S22-4.

BUERGLER, J.M., TIO, F.O., *et al.* (2000). Use of nitric-oxide-eluting polymer-coated coronary stents for prevention of restenosis in pigs. *Coron Artery Dis*, **11,** 351-7.

BUGA, G.M., GRISCAVAGE, J.M., *et al.* (1993). Negative feedback regulation of endothelial cell function by nitric oxide. *Circ Res*, **73,** 808-12.

BURROW, J.W., KOCH, J.A., *et al.* (2007). Nitric oxide donors selectively reduce the expression of matrix metalloproteinases-8 and -9 by human diabetic skin fibroblasts. *J Surg Res*, **140,** 90-8.

BUSSE, R., LUCKHOFF, A., *et al.* (1987). Endothelium-derived relaxant factor inhibits platelet activation. *Naunyn Schmiedebergs Arch Pharmacol*, **336,** 566-71.

BUTLER, A.R., FLITNEY, F.W., *et al.* (1995). NO, nitrosonium ions, nitroxide ions, nitrosothiols and iron-nitrosyls in biology: a chemist's perspective. *Trends Pharmacol Sci*, **16,** 18-22.

BUTT, E., ABEL, K., *et al.* (1994). cAMP- and cGMP-dependent protein kinase phosphorylation sites of the focal adhesion vasodilator-stimulated phosphoprotein (VASP) in vitro and in intact human platelets. *J Biol Chem*, **269,** 14509-17.

CARRIER, G.O., FUCHS, L.C., *et al.* (1997). Nitrovasodilators relax mesenteric microvessels by cGMP-induced stimulation of Ca-activated K channels. *Am J Physiol*, **273,** H76-84.

CARRIGAN, S.O., PINK, D.B., *et al.* (2007). Neutrophil transepithelial migration in response to the chemoattractant fMLP but not C5a is phospholipase D-dependent and related to the use of CD11b/CD18. *J Leukoc Biol.*

CARVAJAL, J.A., GERMAIN, A.M., *et al.* (2000). Molecular mechanism of cGMP-mediated smooth muscle relaxation. *J Cell Physiol*, **184,** 409-20.

CHAKRAPANI, H., SHOWALTER, B.M., *et al.* (2007a). Nitric oxide prodrugs: diazeniumdiolate anions of hindered secondary amines. *Org Lett*, **9,** 4551-4.

CHAKRAPANI, H., WILDE, T.C., *et al.* (2007b). Synthesis, nitric oxide release, and anti-leukemic activity of glutathione-activated nitric oxide prodrugs: Structural analogues of PABA/NO, an anti-cancer lead compound. *Bioorg Med Chem.*

CHAUX, A., RUAN, X.M., *et al.* (1998). Perivascular delivery of a nitric oxide donor inhibits neointimal hyperplasia in vein grafts implanted in the arterial circulation. *J Thorac Cardiovasc Surg*, **115,** 604-12; discussion 612-4.

CHEN, Z., ZHANG, J., *et al.* (2002). Identification of the enzymatic mechanism of nitroglycerin bioactivation. *Proc Natl Acad Sci U S A*, **99,** 8306-11.

CHENG-LAI, A. & FRISHMAN, W.H. (2004). Sirolimus-eluting coronary stents: novel devices for the management of coronary artery disease. *Am J Ther*, **11,** 218-28.

CHITKARA, K., HOGREFE, K., *et al.* (2006). Eptifibatide-eluting stent as an antiproliferative and antithrombotic agent: in vitro evaluation. *J Invasive Cardiol*, **18,** 417-22.

CHOATE, J.K., DANSON, E.J., *et al.* (2001). Peripheral vagal control of heart rate is impaired in neuronal NOS knockout mice. *Am J Physiol Heart Circ Physiol*, **281,** H2310-7.

CLATTERBUCK, R.E., GAILLOUD, P., *et al.* (2005). Controlled release of a nitric oxide donor for the prevention of delayed cerebral vasospasm following experimental subarachnoid hemorrhage in nonhuman primates. *Journal of neurosurgery*, **103,** 745-51.

COBAN, A.Y., BAYRAMOGLU, G., *et al.* (2003). [Antibacterial effect of nitric oxide]. *Mikrobiyol Bul*, **37,** 151-5.

COBB, J.P. (2001). Nitric oxide synthase inhibition as therapy for sepsis: a decade of promise. *Surg Infect (Larchmt)*, **2,** 93-100; discussion 100-1.

COENYE, T., PEETERS, E., *et al.* (2007). Biofilm formation by Propionibacterium acnes is associated with increased resistance to antimicrobial agents and increased production of putative virulence factors. *Res Microbiol*, **158,** 386-92.

CONDLIFFE, A.M., CHILVERS, E.R., *et al.* (1996). Priming differentially regulates neutrophil adhesion molecule expression/function. *Immunology*, **89,** 105-11.

CONDLIFFE, A.M., HAWKINS, P.T., *et al.* (1998). Priming of human neutrophil superoxide generation by tumour necrosis factor-alpha is signalled by enhanced phosphatidylinositol 3,4,5-trisphosphate but not inositol 1,4,5-trisphosphate accumulation. *FEBS Lett*, **439,** 147-51.

CONNELLY, L., MADHANI, M., *et al.* (2005). Resistance to endotoxic shock in endothelial nitric-oxide synthase (eNOS) knock-out mice: a pro-inflammatory role for eNOS-derived no in vivo. *J Biol Chem*, **280,** 10040-6.

CONSIGNY, P.M. (2000). Endothelial cell seeding on prosthetic surfaces. *J Long Term Eff Med Implants*, **10,** 79-95.

COOKE, J.P. (1998). Is atherosclerosis an arginine deficiency disease? *J Investig Med*, **46,** 377-80.

CORBIN, J.D., FRANCIS, S.H., *et al.* (2002). Phosphodiesterase type 5 as a pharmacologic target in erectile dysfunction. *Urology*, **60,** 4-11.

COSENTINO, F. & LUSCHER, T.F. (1998). Endothelial dysfunction in diabetes mellitus. *Journal of cardiovascular pharmacology*, **32 Suppl 3,** S54-61.

CRANE, M.S., OLLOSSON, R., *et al.* (2002). Novel role for low molecular weight plasma thiols in nitric oxide-mediated control of platelet function. *J Biol Chem*, **277,** 46858-63.

CRANE, M.S., ROSSI, A.G., *et al.* (2005). A potential role for extracellular nitric oxide generation in cGMP-independent inhibition of human platelet aggregation: biochemical and pharmacological considerations. *Br J Pharmacol*, **144,** 849-59.

CUZZOCREA, S. (2006). Role of nitric oxide and reactive oxygen species in arthritis. *Current pharmaceutical design*, **12,** 3551-70.

DAHL, T.A., MIDDEN, W.R., *et al.* (1989). Comparison of killing of gram-negative and gram-positive bacteria by pure singlet oxygen. *J Bacteriol*, **171,** 2188-94.

DAVIES, K.M., WINK, D.A., *et al.* (2001). Chemistry of the diazeniumdiolates. 2. Kinetics and mechanism of dissociation to nitric oxide in aqueous solution. *J Am Chem Soc*, **123,** 5473-81.

DE GROOTE, M.A., GRANGER, D., *et al.* (1995). Genetic and redox determinants of nitric oxide cytotoxicity in a Salmonella typhimurium model. *Proc Natl Acad Sci U S A*, **92,** 6399-403.

DE NICOLA, L., MINUTOLO, R., *et al.* (1997). Enhancement of nitric oxide synthesis by L-arginine supplementation in renal disease: is it good or bad? *Miner Electrolyte Metab*, **23,** 144-50.

DIBROV, P., DZIOBA, J., *et al.* (2002). Chemiosmotic mechanism of antimicrobial activity of Ag(+) in Vibrio cholerae. *Antimicrob Agents Chemother*, **46,** 2668-70.

DO, Y.S., KAO, E.Y., *et al.* (2004). In-stent restenosis limitation with stent-based controlled-release nitric oxide: initial results in rabbits. *Radiology*, **230,** 377-82.

DOBMEIER, K.P. & SCHOENFISCH, M.H. (2004). Antibacterial properties of nitric oxide-releasing sol-gel microarrays. *Biomacromolecules*, **5,** 2493-5.

DOGGRELL, S.A. (2005). Clinical potential of nitric oxide-independent soluble guanylate cyclase activators. *Curr Opin Investig Drugs*, **6,** 874-8.

DOH, H., SHIN, C.Y., *et al.* (2002). Mechanism of erectogenic effect of the selective phosphodiesterase type 5 inhibitor, DA-8159. *Arch Pharm Res*, **25,** 873-8.

DOWSETT, C. (2004). The use of silver-based dressings in wound care. *Nurs Stand*, **19,** 56-60.

DOYLE, D.J., BYRICK, R., *et al.* (2002). Silica zeolite scavenging of exhaled isoflurane: a preliminary report. *Can J Anaesth*, **49,** 799-804.

DRISCOLL, K.E., CARTER, J.M., *et al.* (1997). Cytokines and particle-induced inflammatory cell recruitment. *Environ Health Perspect*, **105 Suppl 5,** 1159-64.

DUAN, X. & LEWIS, R.S. (2002). Improved haemocompatibility of cysteine-modified polymers via endogenous nitric oxide. *Biomaterials*, **23,** 1197-203.

DUSTING, G.J., FENNESSY, P., *et al.* (1998). Nitric oxide in atherosclerosis: vascular protector or villain? *Clin Exp Pharmacol Physiol Suppl*, **25,** S34-41.

DYER, A., MORGAN, S., *et al.* (2000). The use of zeolites as slow release anthelmintic carriers. *J Helminthol*, **74,** 137-41.

EISERICH, J.P., PATEL, R.P., *et al.* (1998). Pathophysiology of nitric oxide and related species: free radical reactions and modification of biomolecules. *Molecular aspects of medicine*, **19,** 221-357.

ERIKSSON, E.E., XIE, X., *et al.* (2001). Direct viewing of atherosclerosis in vivo: plaque invasion by leukocytes is initiated by the endothelial selectins. *Faseb J*, **15,** 1149-57.

FANG, F.C. (1997). Perspectives series: host/pathogen interactions. Mechanisms of nitric oxide-related antimicrobial activity. *J Clin Invest*, **99,** 2818-25.

FARACI, F.M., SIGMUND, C.D., *et al.* (1998). Responses of carotid artery in mice deficient in expression of the gene for endothelial NO synthase. *Am J Physiol*, **274,** H564-70.

FAURSCHOU, M. & BORREGAARD, N. (2003). Neutrophil granules and secretory vesicles in inflammation. *Microbes Infect*, **5,** 1317-27.

FEELISCH, M. & KELM, M. (1991). Biotransformation of organic nitrates to nitric oxide by vascular smooth muscle and endothelial cells. *Biochem Biophys Res Commun*, **180,** 286-93.

FEELISCH, M., KOTSONIS, P., *et al.* (1999). The soluble guanylyl cyclase inhibitor 1H-[1,2,4]oxadiazolo[4,3,-a] quinoxalin-1-one is a nonselective heme protein inhibitor of nitric oxide synthase and other cytochrome P-450 enzymes involved in nitric oxide donor bioactivation. *Mol Pharmacol*, **56,** 243-53.

FEELISCH, M., NOACK, E., *et al.* (1988). Explanation of the discrepancy between the degree of organic nitrate decomposition, nitrite formation and guanylate cyclase stimulation. *Eur Heart J*, **9 Suppl A,** 57-62.

FEELISCH, M., OSTROWSKI, J., *et al.* (1989). On the mechanism of NO release from sydnonimines. *J Cardiovasc Pharmacol*, **14 Suppl 11,** S13-22.

FEELISCH, M., SCHONAFINGER, K., *et al.* (1992). Thiol-mediated generation of nitric oxide accounts for the vasodilator action of furoxans. *Biochem Pharmacol*, **44,** 1149-57.

FERNANDES, P.D. & ASSREUY, J. (1997). Role of nitric oxide and superoxide in Giardia lamblia killing. *Braz J Med Biol Res*, **30,** 93-9.

FITZHUGH, A.L., ANADU, N.O., *et al.* (2002). Qualitative thin-layer and high-performance liquid chromatographic analysis of 1-substituted diazen-1-ium-1,2-diolates on aminopropyl-bonded silica gel. *Anal Biochem*, **301,** 97-102.

FLESER, P.S., NUTHAKKI, V.K., *et al.* (2004). Nitric oxide-releasing biopolymers inhibit thrombus formation in a sheep model of arteriovenous bridge grafts. *J Vasc Surg*, **40,** 803-11.

FORMAN, H.J. & TORRES, M. (2002). Reactive oxygen species and cell signaling: respiratory burst in macrophage signaling. *Am J Respir Crit Care Med*, **166,** S4-8.

FORSTERMANN, U., POLLOCK, J.S., *et al.* (1991a). Calmodulin-dependent endothelium-derived relaxing factor/nitric oxide synthase activity is present in the particulate and cytosolic fractions of bovine aortic endothelial cells. *Proc Natl Acad Sci U S A*, **88,** 1788-92.

FORSTERMANN, U., SCHMIDT, H.H., *et al.* (1991b). Isoforms of nitric oxide synthase. Characterization and purification from different cell types. *Biochem Pharmacol*, **42,** 1849-57.

FREEDMAN, J.E. & KEANEY, J.F., JR. (1999). Nitric oxide and superoxide detection in human platelets. *Methods Enzymol*, **301,** 61-70.

FREEDMAN, J.E. & LOSCALZO, J. (2003). Nitric oxide and its relationship to thrombotic disorders. *J Thromb Haemost*, **1,** 1183-8.

FREEDMAN, J.E., LOSCALZO, J., *et al.* (1997). Nitric oxide released from activated platelets inhibits platelet recruitment. *J Clin Invest*, **100,** 350-6.

FREEDMAN, J.E., TING, B., *et al.* (1998). Impaired platelet production of nitric oxide predicts presence of acute coronary syndromes. *Circulation*, **98,** 1481-6.

FRENETTE, P.S. & WAGNER, D.D. (1997). Insights into selectin function from knockout mice. *Thromb Haemost*, **78,** 60-4.

FRIEDERICH, J.A. & BUTTERWORTH, J.F.T. (1995). Sodium nitroprusside: twenty years and counting. *Anesth Analg*, **81,** 152-62.

FROST, M.C. & MEYERHOFF, M.E. (2005). Synthesis, characterization, and controlled nitric oxide release from S-nitrosothiol-derivatized fumed silica polymer filler particles. *Journal of biomedical materials research*, **72,** 409-19.

FROST, M.C., REYNOLDS, M.M., *et al.* (2005). Polymers incorporating nitric oxide releasing/generating substances for improved biocompatibility of blood-contacting medical devices. *Biomaterials*, **26,** 1685-93.

FURCHGOTT, R.F., CARVALHO, M.H., *et al.* (1987). Evidence for endothelium-dependent vasodilation of resistance vessels by acetylcholine. *Blood Vessels*, **24,** 145-9.

FURCHGOTT, R.F. & ZAWADZKI, J.V. (1980). The obligatory role of endothelial cells in the relaxation of arterial smooth muscle by acetylcholine. *Nature*, **288,** 373-6.

GAPPA-FAHLENKAMP, H., DUAN, X., *et al.* (2004). Analysis of immobilized L-cysteine on polymers. *Journal of biomedical materials research*, **71,** 519-27.

GAPPA-FAHLENKAMP, H. & LEWIS, R.S. (2005). Improved hemocompatibility of poly(ethylene terephthalate) modified with various thiol-containing groups. *Biomaterials*, **26,** 3479-85.

GARBERS, D.L. (1990). The guanylyl cyclase receptor family. *New Biol*, **2,** 499-504.

GARTHWAITE, J., SOUTHAM, E., *et al.* (1995). Potent and selective inhibition of nitric oxide-sensitive guanylyl cyclase by 1H-[1,2,4]oxadiazolo[4,3-a]quinoxalin-1-one. *Mol Pharmacol*, **48,** 184-8.

GHAFFARI, A., JALILI, R., *et al.* (2007). Efficacy of gaseous nitric oxide in the treatment of skin and soft tissue infections. *Wound Repair Regen*, **15,** 368-77.

GIBB, B.J. & GARTHWAITE, J. (2001). Subunits of the nitric oxide receptor, soluble guanylyl cyclase, expressed in rat brain. *Eur J Neurosci*, **13,** 539-44.

GIUGLIANO, D., CERIELLO, A., *et al.* (1996). Oxidative stress and diabetic vascular complications. *Diabetes Care*, **19,** 257-67.

GOLDMANN, D.A. (1991). The role of barrier precautions in infection control. *J Hosp Infect*, **18 Suppl A,** 515-23.

GOMEZ-GARCIA, M.A., PITCHON, V., *et al.* (2005). Pollution by nitrogen oxides: an approach to NO(x) abatement by using sorbing catalytic materials. *Environ Int*, **31,** 445-67.

GOMPERTZ, S. & STOCKLEY, R.A. (2000). Inflammation--role of the neutrophil and the eosinophil. *Semin Respir Infect*, **15,** 14-23.

GOODWIN, D.C., GUNTHER, M.R., *et al.* (1998). Nitric oxide trapping of tyrosyl radicals generated during prostaglandin endoperoxide synthase turnover. Detection of the radical derivative of tyrosine 385. *J Biol Chem*, **273,** 8903-9.

GORDGE, M.P., HOTHERSALL, J.S., *et al.* (1998). Evidence for a cyclic GMP-independent mechanism in the anti-platelet action of S-nitrosoglutathione. *Br J Pharmacol*, **124,** 141-8.

GRANGER, D.N. & KUBES, P. (1994). The microcirculation and inflammation: modulation of leukocyte-endothelial cell adhesion. *J Leukoc Biol*, **55,** 662-75.

GROZDANOVIC, Z., BRUNING, G., *et al.* (1994). Nitric oxide--a novel autonomic neurotransmitter. *Acta Anat (Basel)*, **150,** 16-24.

GRYGLEWSKI, R.J., PALMER, R.M., *et al.* (1986). Superoxide anion is involved in the breakdown of endothelium-derived vascular relaxing factor. *Nature*, **320,** 454-6.

GRYGLEWSKI, R.J., ZEMBOWICZ, A., *et al.* (1992). Modulation of the pharmacological actions of nitrovasodilators by methylene blue and pyocyanin. *Br J Pharmacol*, **106,** 838-45.

GUERRA, R., JR., BROTHERTON, A.F., *et al.* (1989). Mechanisms of abnormal endothelium-dependent vascular relaxation in atherosclerosis: implications for altered autocrine and paracrine functions of EDRF. *Blood Vessels*, **26,** 300-14.

GUMUSEL, B., ORHAN, D., *et al.* (2001). The role of nitric oxide in mediating nonadrenergic, noncholinergic relaxation in rat pulmonary artery. *Nitric Oxide*, **5,** 296-301.

GUPTA, S., MCARTHUR, C., *et al.* (1994). Stimulation of vascular Na(+)-K(+)-ATPase activity by nitric oxide: a cGMP-independent effect. *Am J Physiol*, **266,** H2146-51.

GURBEL, P.A., DICHIARA, J., *et al.* (2007). Antiplatelet therapy after implantation of drug-eluting stents: duration, resistance, alternatives, and management of surgical patients. *Am J Cardiol*, **100,** 18M-25M.

GURDEEP, S., HARVINDER, S., *et al.* (2006). Intranasal use of QuickClot in a patient with uncontrollable epistaxis. *Med J Malaysia*, **61,** 112-3.

GUZIK, T.J., KORBUT, R., *et al.* (2003). Nitric oxide and superoxide in inflammation and immune regulation. *J Physiol Pharmacol*, **54,** 469-87.

HAFEZI-MOGHADAM, A., THOMAS, K.L., *et al.* (2001). L-selectin shedding regulates leukocyte recruitment. *J Exp Med*, **193,** 863-72.

HALBRUGGE, M., FRIEDRICH, C., *et al.* (1990). Stoichiometric and reversible phosphorylation of a 46-kDa protein in human platelets in response to cGMP- and cAMP-elevating vasodilators. *J Biol Chem*, **265,** 3088-93.

HALLIWELL, B., ZHAO, K., *et al.* (1999). Nitric oxide and peroxynitrite. The ugly, the uglier and the not so good: a personal view of recent controversies. *Free Radic Res*, **31,** 651-69.

HAMON, M., LECLUSE, E., *et al.* (1998). Pharmacological approaches to the prevention of restenosis after coronary angioplasty. *Drugs Aging*, **13,** 291-301.

HARE, J.M. (2003). Nitric oxide and excitation-contraction coupling. *J Mol Cell Cardiol*, **35,** 719-29.

HARRISON, J.J., CERI, H., *et al.* (2007). Metal Ions May Suppress or Enhance Cellular Differentiation in Candida albicans and Candida tropicalis Biofilms. *Appl Environ Microbiol*, **73,** 4940-9.

HASEGAWA, T., BANDO, A., *et al.* (2004). Enzymatic and nonenzymatic formation of reactive oxygen species from 6-anilino-5,8-quinolinequinone. *Biochim Biophys Acta*, **1670,** 19-27.

HASLETT, C. (1997). Granulocyte apoptosis and inflammatory disease. *Br Med Bull*, **53,** 669-83.

HASLETT, C. (1999). Granulocyte apoptosis and its role in the resolution and control of lung inflammation. *Am J Respir Crit Care Med*, **160,** S5-11.

HASLETT, C., SAVILL, J.S., *et al.* (1994). Granulocyte apoptosis and the control of inflammation. *Philos Trans R Soc Lond B Biol Sci*, **345,** 327-33.

HETRICK, E.M. & SCHOENFISCH, M.H. (2007). Antibacterial nitric oxide-releasing xerogels: cell viability and parallel plate flow cell adhesion studies. *Biomaterials*, **28,** 1948-56.

HOBBS, A.J. (1997). Soluble guanylate cyclase: the forgotten sibling. *Trends Pharmacol Sci*, **18,** 484-91.

HOBBS, A.J., GLADWIN, M.T., *et al.* (2002). Haemoglobin: NO transporter, NO inactivator or NOne of the above? *Trends Pharmacol Sci*, **23,** 406-11.

HOEHN, T., HUEBNER, J., *et al.* (1998). Effect of therapeutic concentrations of nitric oxide on bacterial growth in vitro. *Crit Care Med*, **26,** 1857-62.

HOGAN, J.C., LEWIS, M.J., *et al.* (1988). In vivo EDRF activity influences platelet function. *British journal of pharmacology*, **94,** 1020-2.

HOGG, N., DARLEY-USMAR, V.M., *et al.* (1992). Production of hydroxyl radicals from the simultaneous generation of superoxide and nitric oxide. *Biochem J*, **281 (Pt 2),** 419-24.

HOLMES, D.R., JR. (2001). In-stent restenosis. *Rev Cardiovasc Med*, **2,** 115-9.

HOLT, K.B. & BARD, A.J. (2005). Interaction of silver(I) ions with the respiratory chain of Escherichia coli: an electrochemical and scanning electrochemical microscopy study of the antimicrobial mechanism of micromolar Ag+. *Biochemistry*, **44,** 13214-23.

HOMER, K.L. & WANSTALL, J.C. (2002). Inhibition of rat platelet aggregation by the diazeniumdiolate nitric oxide donor MAHMA NONOate. *Br J Pharmacol*, **137,** 1071-81.

HOPPER, R.A. & GARTHWAITE, J. (2006). Tonic and phasic nitric oxide signals in hippocampal long-term potentiation. *J Neurosci*, **26,** 11513-21.

HORSTRUP, K., JABLONKA, B., *et al.* (1994). Phosphorylation of focal adhesion vasodilator-stimulated phosphoprotein at Ser157 in intact human platelets correlates with fibrinogen receptor inhibition. *Eur J Biochem*, **225,** 21-7.

HOU, D., NARCISO, H., *et al.* (2005). Stent-based nitric oxide delivery reducing neointimal proliferation in a porcine carotid overstretch injury model. *Cardiovascular and interventional radiology*, **28,** 60-5.

HSU, Y.C., HSIAO, M., *et al.* (2007). Exogenous nitric oxide stimulated collagen type I expression and TGF-beta1 production in keloid fibroblasts by a cGMP-dependent manner. *Nitric Oxide*, **16,** 258-65.

HTAY, T. & LIU, M.W. (2005). Drug-eluting stent: a review and update. *Vasc Health Risk Manag*, **1,** 263-76.

HUANG, W.C., WANN, S.R., *et al.* (2004). Catheter-associated urinary tract infections in intensive care units can be reduced by prompting physicians to remove unnecessary catheters. *Infect Control Hosp Epidemiol*, **25,** 974-8.

HUANG, Z., HUANG, P.L., *et al.* (1996). Enlarged infarcts in endothelial nitric oxide synthase knockout mice are attenuated by nitro-L-arginine. *J Cereb Blood Flow Metab*, **16,** 981-7.

HUGHES, B.J., HOLLERS, J.C., *et al.* (1992). Recruitment of CD11b/CD18 to the neutrophil surface and adherence-dependent cell locomotion. *J Clin Invest*, **90,** 1687-96.

HUI, K.S., CHAO, C.Y., *et al.* (2005). Removal of mixed heavy metal ions in wastewater by zeolite 4A and residual products from recycled coal fly ash. *J Hazard Mater*, **127,** 89-101.

HUIE, R.E. & PADMAJA, S. (1993). The reaction of no with superoxide. *Free Radic Res Commun*, **18,** 195-9.

HUSSAIN, A.S., BOZINOVSKI, J., *et al.* (1997). Inhibition of the action of nitric oxide prodrugs by pyocyanin: mechanistic studies. *Can J Physiol Pharmacol*, **75,** 398-406.

IGNARRO, L.J. (1987). Contributions to a quest. *Nature*, **330,** 526.

IGNARRO, L.J., BUGA, G.M., *et al.* (1987a). Endothelium-derived relaxing factor produced and released from artery and vein is nitric oxide. *Proc Natl Acad Sci U S A*, **84,** 9265-9.

IGNARRO, L.J., BYRNS, R.E., *et al.* (1987b). Endothelium-derived relaxing factor from pulmonary artery and vein possesses pharmacologic and chemical properties identical to those of nitric oxide radical. *Circ Res*, **61,** 866-79.

IGNARRO, L.J., BYRNS, R.E., *et al.* (1987c). Mechanisms of endothelium-dependent vascular smooth muscle relaxation elicited by bradykinin and VIP. *Am J Physiol*, **253,** H1074-82.

IGNARRO, L.J., BYRNS, R.E., *et al.* (1988). Pharmacological evidence that endothelium-derived relaxing factor is nitric oxide: use of pyrogallol and superoxide dismutase to study endothelium-dependent and nitric oxide-elicited vascular smooth muscle relaxation. *J Pharmacol Exp Ther*, **244,** 181-9.

ISCHIROPOULOS, H. (1998). Biological tyrosine nitration: a pathophysiological function of nitric oxide and reactive oxygen species. *Arch Biochem Biophys*, **356,** 1-11.

IVKOVIC, S., DEUTSCH, U., *et al.* (2004). Dietary supplementation with the tribomechanically activated zeolite clinoptilolite in immunodeficiency: effects on the immune system. *Adv Ther*, **21,** 135-47.

IWASE, H., ROBIN, E., *et al.* (2007). Nitric oxide during ischemia attenuates oxidant stress and cell death during ischemia and reperfusion in cardiomyocytes. *Free Radic Biol Med*, **43,** 590-9.

JANCHEN, J., BRUCKNER, J.B., *et al.* (1998). Adsorption of desflurane from the scavenging system during high-flow and minimal-flow anaesthesia by zeolites. *Eur J Anaesthesiol*, **15,** 324-9.

JARCHAU, T., HAUSLER, C., *et al.* (1994). Cloning, expression, and in situ localization of rat intestinal cGMP-dependent protein kinase II. *Proc Natl Acad Sci U S A*, **91,** 9426-30.

JARVIS, W.R., SCHLOSSER, J., *et al.* (2007). National prevalence of methicillin-resistant Staphylococcus aureus in inpatients at US health care facilities, 2006. *Am J Infect Control*, **35,** 631-7.

JESAITIS, A.J. & ALLEN, R.A. (1988). Activation of the neutrophil respiratory burst by chemoattractants: regulation of the N-formyl peptide receptor in the plasma membrane. *J Bioenerg Biomembr*, **20,** 679-707.

JIA, L., BONAVENTURA, C., *et al.* (1996). S-nitrosohaemoglobin: a dynamic activity of blood involved in vascular control. *Nature*, **380,** 221-6.

JONES, S.P., GIROD, W.G., *et al.* (1999). Myocardial ischemia-reperfusion injury is exacerbated in absence of endothelial cell nitric oxide synthase. *Am J Physiol*, **276,** H1567-73.

JOURD'HEUIL, D., HALLEN, K., *et al.* (2000). Dynamic state of S-nitrosothiols in human plasma and whole blood. *Free Radic Biol Med*, **28,** 409-17.

JUN, H.W., TAITE, L.J., *et al.* (2005). Nitric oxide-producing polyurethanes. *Biomacromolecules*, **6,** 838-44.

KADOTA, K., YUI, Y., *et al.* (1991). A new relaxing factor in supernatant of incubated rat peritoneal neutrophils. *Am J Physiol*, **260,** H967-72.

KAMAT, J.P. (2006). Peroxynitrite: a potent oxidizing and nitrating agent. *Indian J Exp Biol*, **44,** 436-47.

KAPOSZTA, Z., CLIFTON, A., *et al.* (2002). S-nitrosoglutathione reduces asymptomatic embolization after carotid angioplasty. *Circulation*, **106,** 3057-62.

KARCHMER, T.B., GIANNETTA, E.T., *et al.* (2000). A randomized crossover study of silver-coated urinary catheters in hospitalized patients. *Arch Intern Med*, **160,** 3294-8.

KARUPIAH, G. & HARRIS, N. (1995). Inhibition of viral replication by nitric oxide and its reversal by ferrous sulfate and tricarboxylic acid cycle metabolites. *J Exp Med*, **181,** 2171-9.

KAUL, S., CERCEK, B., *et al.* (2000). Polymeric-based perivascular delivery of a nitric oxide donor inhibits intimal thickening after balloon denudation arterial injury: role of nuclear factor-kappaB. *Journal of the American College of Cardiology*, **35,** 493-501.

KEEFER, L.K. (2005). Nitric oxide (NO)- and nitroxyl (HNO)-generating diazeniumdiolates (NONOates): emerging commercial opportunities. *Current topics in medicinal chemistry*, **5,** 625-36.

KEEFER, L.K. (2003). Progress toward clinical application of the nitric oxide-releasing diazeniumdiolates. *Annu Rev Pharmacol Toxicol*, **43,** 585-607.

KEEFER, L.K., FLIPPEN-ANDERSON, J.L., *et al.* (2001). Chemistry of the diazeniumdiolates. I. Structural and spectral characteristics of the [N(O)NO]- functional group. *Nitric Oxide*, **5,** 377-94.

KELLEY, T.J. & DRUMM, M.L. (1998). Inducible nitric oxide synthase expression is reduced in cystic fibrosis murine and human airway epithelial cells. *J Clin Invest*, **102,** 1200-7.

KENNEDY, S., PRESTON, A.A., *et al.* (2004). Correlation of changes in nitric oxide synthase, superoxide dismutase and nitrotyrosine with endothelial regeneration and neointimal hyperplasia in the balloon-injured rabbit subclavian artery. *Coron Artery Dis*, **15,** 337-46.

KENNEDY, S., WADSWORTH, R.M., *et al.* (2003). Effect of antiproliferative agents on vascular function in normal and in vitro balloon-injured porcine coronary arteries. *European journal of pharmacology*, **481,** 101-7.

KERR, J.F., WYLLIE, A.H., *et al.* (1972). Apoptosis: a basic biological phenomenon with wide-ranging implications in tissue kinetics. *Br J Cancer*, **26,** 239-57.

KHARITONOV, V.G., SHARMA, V.S., *et al.* (1997). Kinetics of nitric oxide dissociation from five- and six-coordinate nitrosyl hemes and heme proteins, including soluble guanylate cyclase. *Biochemistry*, **36,** 6814-8.

KHATSENKO, O.G., GROSS, S.S., *et al.* (1993). Nitric oxide is a mediator of the decrease in cytochrome P450-dependent metabolism caused by immunostimulants. *Proc Natl Acad Sci U S A*, **90,** 11147-51.

KIELSTEIN, J.T., FROLICH, J.C., *et al.* (2001). ADMA (asymmetric dimethylarginine): an atherosclerotic disease mediating agent in patients with renal disease? *Nephrol Dial Transplant*, **16,** 1742-5.

KIM, D., RYBALKIN, S.D., *et al.* (2001). Upregulation of phosphodiesterase 1A1 expression is associated with the development of nitrate tolerance. *Circulation*, **104,** 2338-43.

KING, R.C., LAUBACH, V.E., *et al.* (1998). Preservation with 8-bromo-cyclic GMP improves pulmonary function after prolonged ischemia. *Ann Thorac Surg*, **66,** 1732-8.

KITCHEN, E., ROSSI, A.G., *et al.* (1996). Demonstration of reversible priming of human neutrophils using platelet-activating factor. *Blood*, **88,** 4330-7.

KITSIS, E. & WEISSMANN, G. (1991). The role of the neutrophil in rheumatoid arthritis. *Clin Orthop Relat Res*, 63-72.

KNOWLES, J.W., REDDICK, R.L., *et al.* (2000). Enhanced atherosclerosis and kidney dysfunction in eNOS(-/-)Apoe(-/-) mice are ameliorated by enalapril treatment. *J Clin Invest*, **105,** 451-8.

KOESLING, D. (1999). Studying the structure and regulation of soluble guanylyl cyclase. *Methods*, **19,** 485-93.

KOESLING, D., RUSSWURM, M., *et al.* (2004). Nitric oxide-sensitive guanylyl cyclase: structure and regulation. *Neurochem Int*, **45,** 813-9.

KOJDA, G. & HARRISON, D. (1999). Interactions between NO and reactive oxygen species: pathophysiological importance in atherosclerosis, hypertension, diabetes and heart failure. *Cardiovasc Res*, **43,** 562-71.

KOMALAVILAS, P. & LINCOLN, T.M. (1994). Phosphorylation of the inositol 1,4,5-trisphosphate receptor by cyclic GMP-dependent protein kinase. *J Biol Chem*, **269,** 8701-7.

KOPPENOL, W.H., MORENO, J.J., *et al.* (1992). Peroxynitrite, a cloaked oxidant formed by nitric oxide and superoxide. *Chem Res Toxicol*, **5,** 834-42.

KOSAKA, H., UOZUMI, M., *et al.* (1989). The interaction between nitrogen oxides and hemoglobin and endothelium-derived relaxing factor. *Free Radic Biol Med*, **7,** 653-8.

KOSONEN, O., KANKAANRANTA, H., *et al.* (1999). Nitric oxide-releasing compounds inhibit neutrophil adhesion to endothelial cells. *Eur J Pharmacol*, **382,** 111-7.

KUBES, P., KANWAR, S., *et al.* (1993). Nitric oxide synthesis inhibition induces leukocyte adhesion via superoxide and mast cells. *Faseb J*, **7,** 1293-9.

KUBES, P., SUZUKI, M., *et al.* (1991). Nitric oxide: an endogenous modulator of leukocyte adhesion. *Proc Natl Acad Sci U S A*, **88,** 4651-5.

KUMAR, R. & MUNSTEDT, H. (2005). Silver ion release from antimicrobial polyamide/silver composites. *Biomaterials*, **26,** 2081-8.

KUTHE, A., MONTORSI, F., *et al.* (2002). Phosphodiesterase inhibitors for the treatment of erectile dysfunction. *Curr Opin Investig Drugs*, **3,** 1489-95.

KUTHE, A., WIEDENROTH, A., *et al.* (2001). Expression of different phosphodiesterase genes in human cavernous smooth muscle. *J Urol*, **165,** 280-3.

LEE, P.C., SALYAPONGSE, A.N., *et al.* (1999). Impaired wound healing and angiogenesis in eNOS-deficient mice. *Am J Physiol*, **277,** H1600-8.

LEE, T.J. (2000). Nitric oxide and the cerebral vascular function. *Journal of biomedical science*, **7,** 16-26.

LEINO, L., NUUTILA, J., *et al.* (1993). Human recombinant GM-CSF selectively primes receptor mediated respiratory burst of neutrophils in vitro. *Immunol Lett*, **38,** 26-31.

LEOPOLD, J.A. & LOSCALZO, J. (2003). Organic nitrate tolerance and endothelial dysfunction: role of folate therapy. *Minerva Cardioangiol*, **51,** 349-59.

LI, H. & FORSTERMANN, U. (2000). Nitric oxide in the pathogenesis of vascular disease. *J Pathol*, **190,** 244-54.

LI, Y. & YANG, R.T. (2006). Hydrogen storage in low silica type X zeolites. *J Phys Chem B*, **110,** 17175-81.

LIEDBERG, H. & LUNDEBERG, T. (1990). Silver alloy coated catheters reduce catheter-associated bacteriuria. *Br J Urol*, **65,** 379-81.

LINCOLN, T.M. & CORNWELL, T.L. (1993). Intracellular cyclic GMP receptor proteins. *Faseb J*, **7,** 328-38.

LLORENS, S. & NAVA, E. (2003). Cardiovascular diseases and the nitric oxide pathway. *Current vascular pharmacology*, **1,** 335-46.

LODISE, T.P., JR. & MCKINNON, P.S. (2007). Burden of methicillin-resistant Staphylococcus aureus: focus on clinical and economic outcomes. *Pharmacotherapy*, **27,** 1001-12.

LOSCALZO, J. (2003). Oxidant stress: a key determinant of atherothrombosis. *Biochem Soc Trans*, **31,** 1059-61.

LUNDEBERG, T. (1986). Prevention of catheter-associated urinary-tract infections by use of silver-impregnated catheters. *Lancet*, **2,** 1031.

LUO, J.D. & CHEN, A.F. (2005). Nitric oxide: a newly discovered function on wound healing. *Acta Pharmacol Sin*, **26,** 259-64.

LUSCHER, T.F. (1994). The endothelium in hypertension: bystander, target or mediator? *J Hypertens Suppl*, **12,** S105-16.

LUSCHER, T.F., STEFFEL, J., *et al.* (2007). Drug-eluting stent and coronary thrombosis: biological mechanisms and clinical implications. *Circulation*, **115,** 1051-8.

MA, X.L., WEYRICH, A.S., *et al.* (1993). Diminished basal nitric oxide release after myocardial ischemia and reperfusion promotes neutrophil adherence to coronary endothelium. *Circ Res*, **72,** 403-12.

MACDONALD, P.S., READ, M.A., *et al.* (1988). Synergistic inhibition of platelet aggregation by endothelium-derived relaxing factor and prostacyclin. *Thromb Res*, **49,** 437-49.

MACMICKING, J., XIE, Q.W., *et al.* (1997). Nitric oxide and macrophage function. *Annu Rev Immunol*, **15,** 323-50.

MACMICKING, J.D., NATHAN, C., *et al.* (1995). Altered responses to bacterial infection and endotoxic shock in mice lacking inducible nitric oxide synthase. *Cell*, **81,** 641-50.

MAKI, D.G. & TAMBYAH, P.A. (2001). Engineering out the risk for infection with urinary catheters. *Emerg Infect Dis*, **7,** 342-7.

MANNICK, J.B., MIAO, X.Q., *et al.* (1997). Nitric oxide inhibits Fas-induced apoptosis. *J Biol Chem*, **272,** 24125-8.

MARAGOS, C.M., MORLEY, D., *et al.* (1991). Complexes of .NO with nucleophiles as agents for the controlled biological release of nitric oxide. Vasorelaxant effects. *J Med Chem*, **34,** 3242-7.

MARCZIN, N., RYAN, U.S., *et al.* (1992). Methylene blue inhibits nitrovasodilator- and endothelium-derived relaxing factor-induced cyclic GMP accumulation in cultured pulmonary arterial smooth muscle cells via generation of superoxide anion. *J Pharmacol Exp Ther*, **263,** 170-9.

MARSDEN, P.A., SCHAPPERT, K.T., *et al.* (1992). Molecular cloning and characterization of human endothelial nitric oxide synthase. *FEBS Lett*, **307,** 287-93.

MARSHALL, J.C., MALAM, Z., *et al.* (2007). Modulating neutrophil apoptosis. *Novartis Found Symp*, **280,** 53-66; discussion 67-72, 160-4.

MARTELLI, A., RAPPOSELLI, S., *et al.* (2006). NO-releasing hybrids of cardiovascular drugs. *Curr Med Chem*, **13,** 609-25.

MARTIN, W., VILLANI, G.M., *et al.* (1985). Selective blockade of endothelium-dependent and glyceryl trinitrate-induced relaxation by hemoglobin and by methylene blue in the rabbit aorta. *J Pharmacol Exp Ther*, **232,** 708-16.

MASHIMO, H. & GOYAL, R.K. (1999). Lessons from genetically engineered animal models. IV. Nitric oxide synthase gene knockout mice. *Am J Physiol*, **277,** G745-50.

MASTERS, K.S., LEIBOVICH, S.J., *et al.* (2002). Effects of nitric oxide releasing poly(vinyl alcohol) hydrogel dressings on dermal wound healing in diabetic mice. *Wound Repair Regen*, **10,** 286-94.

MCGUIRE, J.J., ANDERSON, D.J., *et al.* (1998). Inhibition of NADPH-cytochrome P450 reductase and glyceryl trinitrate biotransformation by diphenyleneiodonium sulfate. *Biochem Pharmacol*, **56,** 881-93.

MCMANUS, J., HURTADO, T., *et al.* (2007). A case series describing thermal injury resulting from zeolite use for hemorrhage control in combat operations. *Prehosp Emerg Care*, **11,** 67-71.

MCMULLIN, B.B., CHITTOCK, D.R., *et al.* (2005). The antimicrobial effect of nitric oxide on the bacteria that cause nosocomial pneumonia in mechanically ventilated patients in the intensive care unit. *Respir Care*, **50,** 1451-6.

MEGSON, I.L., GREIG, I.R., *et al.* (1997). Prolonged effect of a novel S-nitrosated glyco-amino acid in endothelium-denuded rat femoral arteries: potential as a slow release nitric oxide donor drug. *Br J Pharmacol*, **122,** 1617-24.

MEGSON, I.L., MORTON, S., *et al.* (1999). N-Substituted analogues of S-nitroso-N-acetyl-D,L-penicillamine: chemical stability and prolonged nitric oxide mediated vasodilatation in isolated rat femoral arteries. *Br J Pharmacol*, **126,** 639-48.

MEGSON, I.L. & WEBB, D.J. (2002). Nitric oxide donor drugs: current status and future trends. *Expert Opin Investig Drugs*, **11,** 587-601.

MENG, Q.H., SPRINGALL, D.R., *et al.* (1998). Lack of inducible nitric oxide synthase in bronchial epithelium: a possible mechanism of susceptibility to infection in cystic fibrosis. *J Pathol*, **184,** 323-31.

MILLER, F.J., JR., GUTTERMAN, D.D., *et al.* (1998). Superoxide production in vascular smooth muscle contributes to oxidative stress and impaired relaxation in atherosclerosis. *Circ Res*, **82,** 1298-305.

MILLER, M.R., HANSPAL, I.S., *et al.* (2003). A novel S-nitrosothiol causes prolonged and selective inhibition of platelet adhesion at sites of vascular injury. *Cardiovasc Res*, **57,** 853-60.

MILLER, M.R., OKUBO, K., *et al.* (2004). Extracellular nitric oxide release mediates soluble guanylate cyclase-independent vasodilator action of spermine NONOate: comparison with other nitric oxide donors in isolated rat femoral arteries. *J Cardiovasc Pharmacol*, **43,** 440-51.

MONCADA, S. & HIGGS, E.A. (2006). The discovery of nitric oxide and its role in vascular biology. *British journal of pharmacology*, **147 Suppl 1,** S193-201.

MONCADA, S. & PALMER, R.M. (1991). Biosynthesis and actions of nitric oxide. *Semin Perinatol*, **15,** 16-9.

MONCADA, S., PALMER, R.M., *et al.* (1988). The discovery of nitric oxide as the endogenous nitrovasodilator. *Hypertension*, **12,** 365-72.

MORELAND, R.B., GOLDSTEIN, I., *et al.* (1998). Sildenafil, a novel inhibitor of phosphodiesterase type 5 in human corpus cavernosum smooth muscle cells. *Life Sci*, **62,** PL 309-18.

MOWERY, K.A., SCHOENFISCH, M.H., *et al.* (2000). Preparation and characterization of hydrophobic polymeric films that are thromboresistant via nitric oxide release. *Biomaterials*, **21,** 9-21.

MU, L., FENG, S.S., *et al.* (2000). Study of synthesis and cardiovascular activity of some furoxan derivatives as potential NO-donors. *Chem Pharm Bull (Tokyo)*, **48,** 808-16.

MUMPTON, F.A. (1999). La roca magica: uses of natural zeolites in agriculture and industry. *Proc Natl Acad Sci U S A*, **96,** 3463-70.

MUNZEL, T., DAIBER, A., *et al.* (2005). Explaining the phenomenon of nitrate tolerance. *Circ Res*, **97,** 618-28.

NABLO, B.J., CHEN, T.Y., *et al.* (2001). Sol-gel derived nitric-oxide releasing materials that reduce bacterial adhesion. *J Am Chem Soc*, **123,** 9712-3.

NABLO, B.J., PRICHARD, H.L., *et al.* (2005a). Inhibition of implant-associated infections via nitric oxide release. *Biomaterials*, **26,** 6984-90.

NABLO, B.J., ROTHROCK, A.R., *et al.* (2005b). Nitric oxide-releasing sol-gels as antibacterial coatings for orthopedic implants. *Biomaterials*, **26,** 917-24.

NABLO, B.J. & SCHOENFISCH, M.H. (2003). Antibacterial properties of nitric oxide-releasing sol-gels. *J Biomed Mater Res A*, **67,** 1276-83.

NABLO, B.J. & SCHOENFISCH, M.H. (2005). In vitro cytotoxicity of nitric oxide-releasing sol-gel derived materials. *Biomaterials*, **26,** 4405-15.

NABLO, B.J. & SCHOENFISCH, M.H. (2004). Poly(vinyl chloride)-coated sol-gels for studying the effects of nitric oxide release on bacterial adhesion. *Biomacromolecules*, **5,** 2034-41.

NAKAZAWA, H., FUKUYAMA, N., *et al.* (2000). Nitrotyrosine formation and its role in various pathological conditions. *Free Radic Res*, **33,** 771-84.

NAPOLI, C. (2002). Nitric oxide and atherosclerotic lesion progression: an overview. *J Card Surg*, **17,** 355-62.

NARA, M., DHULIPALA, P.D., *et al.* (2000). Guanylyl cyclase stimulatory coupling to K(Ca) channels. *Am J Physiol Cell Physiol*, **279,** C1938-45.

NICOTERA, P., BONFOCO, E., *et al.* (1995). Mechanisms for nitric oxide-induced cell death: involvement of apoptosis. *Adv Neuroimmunol*, **5,** 411-20.

NISHIDA, K., HARRISON, D.G., *et al.* (1992). Molecular cloning and characterization of the constitutive bovine aortic endothelial cell nitric oxide synthase. *J Clin Invest*, **90,** 2092-6.

NOACK, E. & FEELISCH, M. (1989). Molecular aspects underlying the vasodilator action of molsidomine. *J Cardiovasc Pharmacol*, **14 Suppl 11,** S1-5.

NOHL, H., KOZLOV, A.V., *et al.* (2003). Cell respiration and formation of reactive oxygen species: facts and artefacts. *Biochem Soc Trans*, **31,** 1308-11.

O'NEILL, E., POZZI, C., *et al.* (2007). Association between methicillin susceptibility and biofilm regulation in Staphylococcus aureus isolates from device-related infections. *J Clin Microbiol*, **45,** 1379-88.

OH, B.K. & MEYERHOFF, M.E. (2004). Catalytic generation of nitric oxide from nitrite at the interface of polymeric films doped with lipophilic CuII-

complex: a potential route to the preparation of thromboresistant coatings. *Biomaterials*, **25,** 283-93.

OH, B.K. & MEYERHOFF, M.E. (2003). Spontaneous catalytic generation of nitric oxide from S-nitrosothiols at the surface of polymer films doped with lipophilic copperII complex. *Journal of the American Chemical Society*, **125,** 9552-3.

OH, B.K., ROBBINS, M.E., *et al.* (2005). Miniaturized glucose biosensor modified with a nitric oxide-releasing xerogel microarray. *Biosens Bioelectron*, **21,** 749-57.

OKAYAMA, N., COE, L., *et al.* (1999). Exogenous nitric oxide increases neutrophil adhesion to cultured human endothelial monolayers through a protein kinase G dependent mechanism. *Inflammation*, **23,** 37-50.

OKAYAMA, N., COE, L., *et al.* (1998). Intracellular mechanisms of nitric oxide plus hydrogen peroxide-mediated neutrophil adherence to cultured human endothelial cells. *Inflamm Res*, **47,** 428-33.

PACHER, P., BECKMAN, J.S., *et al.* (2007). Nitric oxide and peroxynitrite in health and disease. *Physiol Rev*, **87,** 315-424.

PALMER, R.M., ASHTON, D.S., *et al.* (1988). Vascular endothelial cells synthesize nitric oxide from L-arginine. *Nature*, **333,** 664-6.

PALMER, R.M., FERRIGE, A.G., *et al.* (1987). Nitric oxide release accounts for the biological activity of endothelium-derived relaxing factor. *Nature*, **327,** 524-6.

PAPAPETROPOULOS, A., GO, C.Y., *et al.* (1996). Mechanisms of tolerance to sodium nitroprusside in rat cultured aortic smooth muscle cells. *Br J Pharmacol*, **117,** 147-55.

PARTRICK, D.A., MOORE, E.E., *et al.* (1997). Lipid mediators up-regulate CD11b and prime for concordant superoxide and elastase release in human neutrophils. *J Trauma*, **43,** 297-302; discussion 302-3.

PARZUCHOWSKI, P.G., FROST, M.C., *et al.* (2002). Synthesis and characterization of polymethacrylate-based nitric oxide donors. *Journal of the American Chemical Society*, **124,** 12182-91.

PATEL, J.D., KRUPKA, T., *et al.* (2007). iNOS-mediated generation of reactive oxygen and nitrogen species by biomaterial-adherent neutrophils. *Journal of biomedical materials research*, **80,** 381-90.

PAVELIC, K., HADZIJA, M., *et al.* (2001). Natural zeolite clinoptilolite: new adjuvant in anticancer therapy. *J Mol Med*, **78,** 708-20.

PEARCE, B.J. & MCKINSEY, J.F. (2003). Current status of intravascular stents as delivery devices to prevent restenosis. *Vasc Endovascular Surg*, **37,** 231-7; discussion 237.

PERNOLLET, M.G., LANTOINE, F., *et al.* (1996). Nitric oxide inhibits ATP-dependent Ca2+ uptake into platelet membrane vesicles. *Biochem Biophys Res Commun*, **222,** 780-5.

PETROVIC, D. & PETERLIN, B. (2005). Genetic markers of restenosis after coronary angioplasty and after stent implantation. *Med Sci Monit*, **11,** RA127-35.

PITTET, D., DHARAN, S., *et al.* (1999). Bacterial contamination of the hands of hospital staff during routine patient care. *Arch Intern Med*, **159,** 821-6.

PLANE, F., HURRELL, A., *et al.* (1996). Evidence that potassium channels make a major contribution to SIN-1-evoked relaxation of rat isolated mesenteric artery. *Br J Pharmacol*, **119,** 1557-62.

PLUMRIDGE, R.J. & GOLLEDGE, C.L. (1996). Treatment of urinary tract infection. Clinical and economic considerations. *Pharmacoeconomics*, **9,** 295-306.

POHLER, D., BUTT, E., *et al.* (1995). Expression, purification, and characterization of the cGMP-dependent protein kinases I beta and II using the baculovirus system. *FEBS Lett*, **374,** 419-25.

POLLOCK, J.S., FORSTERMANN, U., *et al.* (1991). Purification and characterization of particulate endothelium-derived relaxing factor synthase from cultured and native bovine aortic endothelial cells. *Proc Natl Acad Sci U S A*, **88,** 10480-4.

PULFER, S.K., OTT, D., *et al.* (1997). Incorporation of nitric oxide-releasing crosslinked polyethyleneimine microspheres into vascular grafts. *Journal of biomedical materials research*, **37,** 182-9.

QUIE, P.G. (1980). The phagocytic system in host defense. *Scand J Infect Dis Suppl*, **Suppl 24,** 30-2.

RADI, R. (2004). Nitric oxide, oxidants, and protein tyrosine nitration. *Proc Natl Acad Sci U S A*, **101,** 4003-8.

RADOMSKI, M.W. (1995). Nitric oxide: biological mediator, modulator and effector. *Ann Med*, **27,** 321-9.

RADOMSKI, M.W., PALMER, R.M., *et al.* (1987a). Comparative pharmacology of endothelium-derived relaxing factor, nitric oxide and prostacyclin in platelets. *British journal of pharmacology*, **92,** 181-7.

RADOMSKI, M.W., PALMER, R.M., *et al.* (1987b). Endogenous nitric oxide inhibits human platelet adhesion to vascular endothelium. *Lancet*, **2,** 1057-8.

RADOMSKI, M.W., PALMER, R.M., *et al.* (1987c). The anti-aggregating properties of vascular endothelium: interactions between prostacyclin and nitric oxide. *British journal of pharmacology*, **92,** 639-46.

RADOMSKI, M.W., PALMER, R.M., *et al.* (1987d). The role of nitric oxide and cGMP in platelet adhesion to vascular endothelium. *Biochem Biophys Res Commun*, **148,** 1482-9.

RAND, M.J. (1992). Nitrergic transmission: nitric oxide as a mediator of non-adrenergic, non-cholinergic neuro-effector transmission. *Clin Exp Pharmacol Physiol*, **19,** 147-69.

RASSAF, T., KLEINBONGARD, P., *et al.* (2005). Circulating NO pool in humans. *Kidney Blood Press Res*, **28,** 341-8.

RATCLIFFE, A. (2000). Tissue engineering of vascular grafts. *Matrix Biol*, **19,** 353-7.

RAUEN, U., LI, T., *et al.* (2007). Inhibitory and enhancing effects of NO on H(2)O(2) toxicity: dependence on the concentrations of NO and H(2)O(2). *Free Radic Res*, **41,** 402-12.

REGLI, L., ZECCHINA, A., *et al.* (2005). Hydrogen storage in Chabazite zeolite frameworks. *Phys Chem Chem Phys*, **7,** 3197-203.

REINHARD, M., GIEHL, K., *et al.* (1995). The proline-rich focal adhesion and microfilament protein VASP is a ligand for profilins. *Embo J*, **14,** 1583-9.

REINHARD, M., JARCHAU, T., *et al.* (2001). Actin-based motility: stop and go with Ena/VASP proteins. *Trends Biochem Sci*, **26,** 243-9.

REMENTERIA, A., GARCIA-TOBALINA, R., *et al.* (1995). Nitric oxide-dependent killing of Candida albicans by murine peritoneal cells during an experimental infection. *FEMS Immunol Med Microbiol*, **11,** 157-62.

RENGASAMY, A. & JOHNS, R.A. (1993). Inhibition of nitric oxide synthase by a superoxide generating system. *J Pharmacol Exp Ther*, **267,** 1024-7.

REYNOLDS, M.M., FROST, M.C., *et al.* (2004). Nitric oxide-releasing hydrophobic polymers: preparation, characterization, and potential biomedical applications. *Free radical biology & medicine*, **37,** 926-36.

REYNOLDS, M.M., HRABIE, J.A., *et al.* (2006). Nitric oxide releasing polyurethanes with covalently linked diazeniumdiolated secondary amines. *Biomacromolecules*, **7,** 987-94.

RICE, K.C. & BAYLES, K.W. (2003). Death's toolbox: examining the molecular components of bacterial programmed cell death. *Mol Microbiol*, **50,** 729-38.

ROBBINS, M.E., HOPPER, E.D., *et al.* (2004). Synthesis and characterization of nitric oxide-releasing sol-gel microarrays. *Langmuir*, **20,** 10296-302.

ROCHELLE, L.G., KRUSZYNA, H., *et al.* (1994). Bioactivation of nitroprusside by porcine endothelial cells. *Toxicol Appl Pharmacol*, **128,** 123-8.

ROGERS, C., PARIKH, S., *et al.* (1996). Endogenous cell seeding. Remnant endothelium after stenting enhances vascular repair. *Circulation*, **94,** 2909-14.

ROHN, T.T., NELSON, L.K., *et al.* (1999). Priming of human neutrophils by peroxynitrite: potential role in enhancement of the local inflammatory response. *J Leukoc Biol*, **65,** 59-70.

ROSI, N.L., ECKERT, J., *et al.* (2003). Hydrogen storage in microporous metal-organic frameworks. *Science*, **300,** 1127-9.

ROSSELET, A., FEIHL, F., *et al.* (1998). Selective iNOS inhibition is superior to norepinephrine in the treatment of rat endotoxic shock. *Am J Respir Crit Care Med*, **157,** 162-70.

ROSSI, A.G., SAWATZKY, D.A., *et al.* (2006). Cyclin-dependent kinase inhibitors enhance the resolution of inflammation by promoting inflammatory cell apoptosis. *Nat Med*, **12,** 1056-64.

RUDOLF, T., BOHLMANN, W., *et al.* (2002). Adsorption and desorption behavior of NO on H-ZSM-5, Na-ZSM-5, and Na-A as studied by EPR. *J Magn Reson*, **155,** 45-56.

RUPP, M.E., FITZGERALD, T., *et al.* (2004). Effect of silver-coated urinary catheters: efficacy, cost-effectiveness, and antimicrobial resistance. *Am J Infect Control*, **32,** 445-50.

RUSSELL, K.J., MCREDMOND, J., *et al.* (1998). Neutrophil adhesion molecule surface expression and responsiveness in cystic fibrosis. *Am J Respir Crit Care Med*, **157,** 756-61.

SAITO, Y., NAKAGAWA, C., *et al.* (2001). Adrenomedullin suppresses fMLP-induced upregulation of CD11b of human neutrophils. *Inflammation*, **25,** 197-201.

SALERNO, L., SORRENTI, V., *et al.* (2002). Progress in the development of selective nitric oxide synthase (NOS) inhibitors. *Curr Pharm Des*, **8,** 177-200.

SANDAU, K., PFEILSCHIFTER, J., *et al.* (1997). The balance between nitric oxide and superoxide determines apoptotic and necrotic death of rat mesangial cells. *J Immunol*, **158,** 4938-46.

SANDAU, K.B., CALLSEN, D., *et al.* (1999). Protection against nitric oxide-induced apoptosis in rat mesangial cells demands mitogen-activated protein kinases and reduced glutathione. *Mol Pharmacol*, **56,** 744-51.

SANDERS, K.M. & WARD, S.M. (1992). Nitric oxide as a mediator of nonadrenergic noncholinergic neurotransmission. *Am J Physiol*, **262,** G379-92.

SARKAR, K., SHARMA, S.K., *et al.* (2006). Coronary artery restenosis: vascular biology and emerging therapeutic strategies. *Expert review of cardiovascular therapy*, **4,** 543-56.

SARMIENTO-GONZALEZ, A., MARCHANTE-GAYON, J.M., *et al.* (2005). ICP-MS multielemental determination of metals potentially released from dental implants and articular prostheses in human biological fluids. *Anal Bioanal Chem*, **382,** 1001-9.

SAVILL, J. (1997). Apoptosis in resolution of inflammation. *J Leukoc Biol*, **61,** 375-80.

SAVILL, J. & HASLETT, C. (1995). Granulocyte clearance by apoptosis in the resolution of inflammation. *Semin Cell Biol*, **6,** 385-93.

SCHAFFER, M., BONGARTZ, M., *et al.* (2007). Nitric oxide restores impaired healing in normoglycaemic diabetic rats. *J Wound Care*, **16,** 311-6.

SCHECHTER, A.N. & GLADWIN, M.T. (2003). Hemoglobin and the paracrine and endocrine functions of nitric oxide. *N Engl J Med*, **348,** 1483-5.

SCHMIDT, H.H., LOHMANN, S.M., *et al.* (1993). The nitric oxide and cGMP signal transduction system: regulation and mechanism of action. *Biochim Biophys Acta*, **1178,** 153-75.

SCHMIDT, H.H., POLLOCK, J.S., *et al.* (1992a). Ca2+/calmodulin-regulated nitric oxide synthases. *Cell Calcium*, **13,** 427-34.

SCHMIDT, H.H., SMITH, R.M., *et al.* (1992b). Ca2+/calmodulin-dependent NO synthase type I: a biopteroflavoprotein with Ca2+/calmodulin-independent diaphorase and reductase activities. *Biochemistry*, **31,** 3243-9.

SCHOENFISCH, M.H., MOWERY, K.A., *et al.* (2000). Improving the thromboresistivity of chemical sensors via nitric oxide release: fabrication and in vivo evaluation of NO-releasing oxygen-sensing catheters. *Analytical chemistry*, **72,** 1119-26.

SCHOENFISCH, M.H., ZHANG, H., *et al.* (2002). Nitric oxide-releasing fluorescence-based oxygen sensing polymeric films. *Analytical chemistry*, **74,** 5937-41.

SCHRAMMEL, A., BEHRENDS, S., *et al.* (1996). Characterization of 1H-[1,2,4]oxadiazolo[4,3-a]quinoxalin-1-one as a heme-site inhibitor of nitric oxide-sensitive guanylyl cyclase. *Mol Pharmacol*, **50,** 1-5.

SEABRA, A.B., DA ROCHA, L.L., *et al.* (2005). Solid films of blended poly(vinyl alcohol)/poly(vinyl pyrrolidone) for topical S-nitrosoglutathione and nitric oxide release. *Journal of pharmaceutical sciences*, **94,** 994-1003.

SELVATICI, R., FALZARANO, S., *et al.* (2006). Signal transduction pathways triggered by selective formylpeptide analogues in human neutrophils. *Eur J Pharmacol*, **534,** 1-11.

SEYMOUR, C. (2006). Audit of catheter-associated UTI using silver alloy-coated Foley catheters. *Br J Nurs*, **15,** 598-603.

SHABANI, M., PULFER, S.K., *et al.* (1996). Enhancement of wound repair with a topically applied nitric oxide-releasing polymer. *Wound Repair Regen*, **4,** 353-62.

SHAW, C.A., TAYLOR, E.L., *et al.* (2005). Nitric oxide and the resolution of inflammation: implications for atherosclerosis. *Mem Inst Oswaldo Cruz*, **100 Suppl 1,** 67-71.

SHENG, H., SCHMIDT, H.H., *et al.* (1992). Characterization and localization of nitric oxide synthase in non-adrenergic non-cholinergic nerves from bovine retractor penis muscles. *Br J Pharmacol*, **106,** 768-73.

SHIN, J.H., MARXER, S.M., *et al.* (2004). Nitric oxide-releasing sol-gel particle/polyurethane glucose biosensors. *Analytical chemistry*, **76,** 4543-9.

SHIN, J.H. & SCHOENFISCH, M.H. (2006). Improving the biocompatibility of in vivo sensors via nitric oxide release. *The Analyst*, **131,** 609-15.

SHISHIDO, S.M. & DE OLIVEIRA, M.G. (2000). Polyethylene glycol matrix reduces the rates of photochemical and thermal release of nitric oxide from S-nitroso-N-acetylcysteine. *Photochem Photobiol*, **71,** 273-80.

SHISHIDO, S.M., SEABRA, A.B., *et al.* (2003). Thermal and photochemical nitric oxide release from S-nitrosothiols incorporated in Pluronic F127 gel: potential uses for local and controlled nitric oxide release. *Biomaterials*, **24,** 3543-53.

SIES, H. & DE GROOT, H. (1992). Role of reactive oxygen species in cell toxicity. *Toxicol Lett*, **64-65 Spec No,** 547-51.

SILVA, S.Y., RUEDA, L.C., *et al.* (2007). Double blind, randomized, placebo controlled clinical trial for the treatment of diabetic foot ulcers, using a nitric oxide releasing patch: PATHON. *Trials*, **8,** 26.

SILVER, S. (1996). Bacterial resistances to toxic metal ions--a review. *Gene*, **179,** 9-19.

SIMON, W.C., ANDERSON, D.J., *et al.* (1996). Inhibition of the pharmacological actions of glyceryl trinitrate after the electroporetic delivery of a glutathione S-transferase inhibitor. *J Pharmacol Exp Ther*, **279,** 1535-40.

SLAWSON, R.M., VAN DYKE, M.I., *et al.* (1992). Germanium and silver resistance, accumulation, and toxicity in microorganisms. *Plasmid*, **27,** 72-9.

SMITH, D.J., CHAKRAVARTHY, D., *et al.* (1996). Nitric oxide-releasing polymers containing the [N(O)NO]- group. *Journal of medicinal chemistry*, **39,** 1148-56.

SMOLENSKI, A., BURKHARDT, A.M., *et al.* (1998). Functional analysis of cGMP-dependent protein kinases I and II as mediators of NO/cGMP effects. *Naunyn Schmiedebergs Arch Pharmacol*, **358,** 134-9.

SODERBERG, T.A., SUNZEL, B., *et al.* (1990). Antibacterial effect of zinc oxide in vitro. *Scand J Plast Reconstr Surg Hand Surg*, **24,** 193-7.

SODERLING, S.H. & BEAVO, J.A. (2000). Regulation of cAMP and cGMP signaling: new phosphodiesterases and new functions. *Curr Opin Cell Biol*, **12,** 174-9.

SOGO, N., MAGID, K.S., *et al.* (2000a). Inhibition of human platelet aggregation by nitric oxide donor drugs: relative contribution of cGMP-independent mechanisms. *Biochem Biophys Res Commun*, **279,** 412-9.

SOGO, N., WILKINSON, I.B., *et al.* (2000b). A novel S-nitrosothiol (RIG200) causes prolonged relaxation in dorsal hand veins with damaged endothelium. *Clin Pharmacol Ther*, **68,** 75-81.

SOUZA, H.P., LIU, X., *et al.* (2002). Quantitation of superoxide generation and substrate utilization by vascular NAD(P)H oxidase. *Am J Physiol Heart Circ Physiol*, **282,** H466-74.

SPARROW, J.R. (1994). Inducible nitric oxide synthase in the central nervous system. *J Mol Neurosci*, **5,** 219-29.

STABILE, E., ESCOLAR, E., *et al.* (2004). Marked malapposition and aneurysm formation after sirolimus-eluting coronary stent implantation. *Circulation*, **110,** e47-8.

STALLMEYER, B., ANHOLD, M., *et al.* (2002). Regulation of eNOS in normal and diabetes-impaired skin repair: implications for tissue regeneration. *Nitric Oxide*, **6,** 168-77.

STALLMEYER, B., KAMPFER, H., *et al.* (1999). The function of nitric oxide in wound repair: inhibition of inducible nitric oxide-synthase severely impairs wound reepithelialization. *J Invest Dermatol*, **113,** 1090-8.

STAMLER, J.S., JARAKI, O., *et al.* (1992a). Nitric oxide circulates in mammalian plasma primarily as an S-nitroso adduct of serum albumin. *Proc Natl Acad Sci U S A*, **89,** 7674-7.

STAMLER, J.S., SIMON, D.I., *et al.* (1992b). S-nitrosylation of tissue-type plasminogen activator confers vasodilatory and antiplatelet properties on the enzyme. *Proc Natl Acad Sci U S A*, **89,** 8087-91.

STAMLER, J.S., SIMON, D.I., *et al.* (1992c). S-nitrosylation of proteins with nitric oxide: synthesis and characterization of biologically active compounds. *Proc Natl Acad Sci U S A*, **89,** 444-8.

STONE, J.R. & MARLETTA, M.A. (1995). The ferrous heme of soluble guanylate cyclase: formation of hexacoordinate complexes with carbon monoxide and nitrosomethane. *Biochemistry*, **34,** 16397-403.

SULTANA, A., LOENDERS, R., *et al.* (2000). DeNOx of Exhaust Gas from Lean-Burn Engines through Reversible Adsorption of N(2)O(3) in Alkali Metal Cation Exchanged Faujasite-Type Zeolites This work was sponsored by the European Community (Brite Euram III projects BE-95-2127 "SNR Technique" and BE-97-4493 "SORPTEC") and the Belgium

government (IUAP-PAI program). *Angew Chem Int Ed Engl*, **39,** 2934-2937.

SWAIN, S.D., ROHN, T.T., *et al.* (2002). Neutrophil priming in host defense: role of oxidants as priming agents. *Antioxid Redox Signal*, **4,** 69-83.

SZABO, C. (2003). Multiple pathways of peroxynitrite cytotoxicity. *Toxicol Lett*, **140-141,** 105-12.

TAKIMOTO, Y., AOYAMA, T., *et al.* (2000). Differential expression of three types of nitric oxide synthase in both infarcted and non-infarcted left ventricles after myocardial infarction in the rat. *Int J Cardiol*, **76,** 135-45.

TANUS-SANTOS, J.E., DESAI, M., *et al.* (2002). Effects of endothelial nitric oxide synthase gene polymorphisms on platelet function, nitric oxide release, and interactions with estradiol. *Pharmacogenetics*, **12,** 407-13.

TAYLOR, E.L., MEGSON, I.L., *et al.* (2003). Nitric oxide: a key regulator of myeloid inflammatory cell apoptosis. *Cell Death Differ*, **10,** 418-30.

TAYLOR, E.L., ROSSI, A.G., *et al.* (2004). GEA 3162 decomposes to co-generate nitric oxide and superoxide and induces apoptosis in human neutrophils via a peroxynitrite-dependent mechanism. *Br J Pharmacol*, **143,** 179-85.

TEDDER, T.F., STEEBER, D.A., *et al.* (1995). L-selectin-deficient mice have impaired leukocyte recruitment into inflammatory sites. *J Exp Med*, **181,** 2259-64.

TEJEDO, J., BERNABE, J.C., *et al.* (1999). NO induces a cGMP-independent release of cytochrome c from mitochondria which precedes caspase 3 activation in insulin producing RINm5F cells. *FEBS Lett*, **459,** 238-43.

TENG, C.M., WU, C.C., *et al.* (1997). YC-1, a nitric oxide-independent activator of soluble guanylate cyclase, inhibits platelet-rich thrombosis in mice. *Eur J Pharmacol*, **320,** 161-6.

TERADA, L.S., WILLINGHAM, I.R., *et al.* (1991). Generation of superoxide anion by brain endothelial cell xanthine oxidase. *J Cell Physiol*, **148,** 191-6.

THANIGARAJ, S., WOLLMUTH, J.R., *et al.* (2006). From randomized trials to routine clinical practice: an evidence-based approach for the use of drug-eluting stents. *Coron Artery Dis*, **17,** 673-9.

THIEMERMANN, C. (1997). Nitric oxide and septic shock. *Gen Pharmacol*, **29,** 159-66.

THOM, S.R., OHNISHI, S.T., *et al.* (1994). Nitric oxide released by platelets inhibits neutrophil B2 integrin function following acute carbon monoxide poisoning. *Toxicol Appl Pharmacol*, **128,** 105-10.

THOMAS, D.D., RIDNOUR, L.A., *et al.* (2006). Superoxide fluxes limit nitric oxide-induced signaling. *J Biol Chem*, **281,** 25984-93.

TODA, N., AYAJIKI, K., *et al.* (2005). Nitric oxide and penile erectile function. *Pharmacology & therapeutics*, **106,** 233-66.

TREPAKOVA, E.S., COHEN, R.A., *et al.* (1999). Nitric oxide inhibits capacitative cation influx in human platelets by promoting sarcoplasmic/endoplasmic reticulum Ca2+-ATPase-dependent refilling of Ca2+ stores. *Circ Res*, **84,** 201-9.

TURNBULL, C.M., CENA, C., *et al.* (2006a). Mechanism of action of novel NO-releasing furoxan derivatives of aspirin in human platelets. *Br J Pharmacol*, **148,** 517-26.

TURNBULL, C.M., ROSSI, A.G., *et al.* (2006b). Therapeutic effects of nitric oxide-aspirin hybrid drugs. *Expert Opin Ther Targets*, **10,** 911-22.

UCKERT, S., KUTHE, A., *et al.* (2001). Phosphodiesterase isoenzymes as pharmacological targets in the treatment of male erectile dysfunction. *World J Urol*, **19,** 14-22.

VAN GELDRE, L.A. & LEFEBVRE, R.A. (2004). Interaction of NO and VIP in gastrointestinal smooth muscle relaxation. *Curr Pharm Des*, **10,** 2483-97.

VAN OOSTROM, A.J., VAN WIJK, J.P., *et al.* (2004). Increased expression of activation markers on monocytes and neutrophils in type 2 diabetes. *Neth J Med*, **62,** 320-5.

VANE, J.R., ANGGARD, E.E., *et al.* (1990). Regulatory functions of the vascular endothelium. *N Engl J Med*, **323,** 27-36.

VASQUEZ-VIVAR, J., HOGG, N., *et al.* (1999). Tetrahydrobiopterin-dependent inhibition of superoxide generation from neuronal nitric oxide synthase. *J Biol Chem*, **274,** 26736-42.

VASQUEZ-VIVAR, J. & KALYANARAMAN, B. (2000). Generation of superoxide from nitric oxide synthase. *FEBS Lett*, **481,** 305-6.

VASQUEZ-VIVAR, J., KALYANARAMAN, B., *et al.* (2003). The role of tetrahydrobiopterin in superoxide generation from eNOS: enzymology and physiological implications. *Free Radic Res*, **37,** 121-7.

VASQUEZ-VIVAR, J., KALYANARAMAN, B., *et al.* (1998). Superoxide generation by endothelial nitric oxide synthase: the influence of cofactors. *Proc Natl Acad Sci U S A*, **95,** 9220-5.

VASQUEZ-VIVAR, J., MARTASEK, P., *et al.* (2002). The ratio between tetrahydrobiopterin and oxidized tetrahydrobiopterin analogues controls superoxide release from endothelial nitric oxide synthase: an EPR spin trapping study. *Biochem J*, **362,** 733-9.

VAZQUEZ-TORRES, A., JONES-CARSON, J., *et al.* (1996). Peroxynitrite contributes to the candidacidal activity of nitric oxide-producing macrophages. *Infect Immun*, **64,** 3127-33.

VELAZQUEZ, C., PRAVEEN RAO, P.N., *et al.* (2005). Novel nonsteroidal antiinflammatory drugs possessing a nitric oxide donor diazen-1-ium-1,2-diolate moiety: design, synthesis, biological evaluation, and nitric oxide release studies. *J Med Chem*, **48,** 4061-7.

VERMEERSCH, P., NONG, Z., *et al.* (2001). L-arginine administration reduces neointima formation after stent injury in rats by a nitric oxide-mediated mechanism. *Arterioscler Thromb Vasc Biol*, **21,** 1604-9.

VIRAG, L., SZABO, E., *et al.* (2003). Peroxynitrite-induced cytotoxicity: mechanism and opportunities for intervention. *Toxicol Lett*, **140-141,** 113-24.

VIRMANI, R., KOLODGIE, F.D., *et al.* (2004). Drug-eluting stents: are they really safe? *Am Heart Hosp J*, **2,** 85-8.

VON ANDRIAN, U.H. & ARFORS, K.E. (1993). Neutrophil-endothelial cell interactions in vivo: a chain of events characterized by distinct molecular mechanisms. *Agents Actions Suppl*, **41,** 153-64.

WANG, T.T., LI, K., *et al.* (2006). [Roles of vasodilator-stimulated phosphoprotein in the regulation of cytoskeleton]. *Sheng Li Ke Xue Jin Zhan*, **37,** 27-30.

WANIKIAT, P., WOODWARD, D.F., *et al.* (1997). Investigation of the role of nitric oxide and cyclic GMP in both the activation and inhibition of human neutrophils. *Br J Pharmacol*, **122,** 1135-45.

WANSTALL, J.C., HOMER, K.L., *et al.* (2005). Evidence for, and importance of, cGMP-independent mechanisms with NO and NO donors on blood vessels and platelets. *Curr Vasc Pharmacol*, **3,** 41-53.

WARD, C., CHILVERS, E.R., *et al.* (1999a). NF-kappaB activation is a critical regulator of human granulocyte apoptosis in vitro. *J Biol Chem*, **274,** 4309-18.

WARD, C., DRANSFIELD, I., *et al.* (1999b). Pharmacological manipulation of granulocyte apoptosis: potential therapeutic targets. *Trends Pharmacol Sci*, **20,** 503-9.

WARD, C., WONG, T.H., *et al.* (2000). Induction of human neutrophil apoptosis by nitric oxide donors: evidence for a caspase-dependent, cyclic-GMP-independent, mechanism. *Biochem Pharmacol*, **59,** 305-14.

WARREN, J.B., LOI, R., *et al.* (1990). Nitric oxide is inactivated by the bacterial pigment pyocyanin. *Biochem J*, **266,** 921-3.

WARREN, J.W. (2001). Catheter-associated urinary tract infections. *Int J Antimicrob Agents*, **17,** 299-303.

WEDEL, B., HARTENECK, C., *et al.* (1995). Functional domains of soluble guanylyl cyclase. *J Biol Chem*, **270,** 24871-5.

WELLS, T.N., SCULLY, P., *et al.* (1995). Mechanism of irreversible inactivation of phosphomannose isomerases by silver ions and flamazine. *Biochemistry*, **34,** 7896-903.

WENNMALM, A. (1994). Endothelial nitric oxide and cardiovascular disease. *J Intern Med*, **235,** 317-27.

WHEATLEY, P.S., BUTLER, A.R., *et al.* (2006). NO-releasing zeolites and their antithrombotic properties. *J Am Chem Soc*, **128,** 502-9.

WILCOX, D.E., KRUSZYNA, H., *et al.* (1990). Effect of cyanide on the reaction of nitroprusside with hemoglobin: relevance to cyanide interference with the biological activity of nitroprusside. *Chem Res Toxicol*, **3,** 71-6.

WINK, D.A., COOK, J.A., *et al.* (1995). Nitric oxide (NO) protects against cellular damage by reactive oxygen species. *Toxicol Lett*, **82-83,** 221-6.

WINK, D.A., GRISHAM, M.B., *et al.* (1996a). Direct and indirect effects of nitric oxide in chemical reactions relevant to biology. *Methods Enzymol*, **268,** 12-31.

WINK, D.A., HANBAUER, I., *et al.* (1996b). Chemical biology of nitric oxide: regulation and protective and toxic mechanisms. *Curr Top Cell Regul*, **34,** 159-87.

WINK, D.A., HANBAUER, I., *et al.* (1993a). Nitric oxide protects against cellular damage and cytotoxicity from reactive oxygen species. *Proc Natl Acad Sci U S A*, **90,** 9813-7.

WINK, D.A., MIRANDA, K.M., *et al.* (2001). Cytotoxicity related to oxidative and nitrosative stress by nitric oxide. *Exp Biol Med (Maywood)*, **226,** 621-3.

WINK, D.A., OSAWA, Y., *et al.* (1993b). Inhibition of cytochromes P450 by nitric oxide and a nitric oxide-releasing agent. *Arch Biochem Biophys*, **300,** 115-23.

WINK, D.A., VODOVOTZ, Y., *et al.* (1998a). The role of nitric oxide chemistry in cancer treatment. *Biochemistry (Mosc)*, **63,** 802-9.

WINK, D.A., VODOVOTZ, Y., *et al.* (1998b). The multifaceted roles of nitric oxide in cancer. *Carcinogenesis*, **19,** 711-21.

WITTMANN, S., ROTHE, G., *et al.* (2004). Cytokine upregulation of surface antigens correlates to the priming of the neutrophil oxidative burst response. *Cytometry A*, **57,** 53-62.

WOLIN, M.S., CHERRY, P.D., *et al.* (1990). Methylene blue inhibits vasodilation of skeletal muscle arterioles to acetylcholine and nitric oxide via the extracellular generation of superoxide anion. *J Pharmacol Exp Ther*, **254,** 872-6.

WONG, S.H. & LORD, J.M. (2004). Factors underlying chronic inflammation in rheumatoid arthritis. *Arch Immunol Ther Exp (Warsz)*, **52,** 379-88.

WRIGHT, J.K., KALNS, J., *et al.* (2004). Thermal injury resulting from application of a granular mineral hemostatic agent. *J Trauma*, **57,** 224-30.

WU, G. & MEININGER, C.J. (2000). Arginine nutrition and cardiovascular function. *J Nutr*, **130,** 2626-9.

WYLLIE, A.H., KERR, J.F., *et al.* (1980). Cell death: the significance of apoptosis. *Int Rev Cytol*, **68,** 251-306.

YOON, J.H., WU, C.J., *et al.* (2002). Local delivery of nitric oxide from an eluting stent to inhibit neointimal thickening in a porcine coronary injury model. *Yonsei Med J*, **43,** 242-51.

YOSHIOKA, Y., YAMAMURO, A., *et al.* (2006). Nitric oxide/cGMP signaling pathway protects RAW264 cells against nitric oxide-induced apoptosis by inhibiting the activation of p38 mitogen-activated protein kinase. *J Pharmacol Sci*, **101,** 126-34.

YOU, L., COX, R.S., 3RD, *et al.* (2004). Programmed population control by cell-cell communication and regulated killing. *Nature*, **428,** 868-71.

YOUNG, J.J. (2007). Neointimal formation following drug-eluting stents: physiology, timeline, and the influence of drug delivery systems. *Rev Cardiovasc Med*, **8 Suppl 1,** S3-S10.

YUI, Y., HATTORI, R., *et al.* (1991a). Purification of nitric oxide synthase from rat macrophages. *J Biol Chem*, **266,** 12544-7.

YUI, Y., HATTORI, R., *et al.* (1991b). Calmodulin-independent nitric oxide synthase from rat polymorphonuclear neutrophils. *J Biol Chem*, **266,** 3369-71.

ZAKI, M.H., AKUTA, T., *et al.* (2005). Nitric oxide-induced nitrative stress involved in microbial pathogenesis. *J Pharmacol Sci*, **98,** 117-29.

ZANZINGER, J. (1999). Role of nitric oxide in the neural control of cardiovascular function. *Cardiovascular research*, **43,** 639-49.

ZHANG, H., ANNICH, G.M., *et al.* (2002). Nitric oxide releasing silicone rubbers with improved blood compatibility: preparation, characterization, and in vivo evaluation. *Biomaterials*, **23,** 1485-94.

ZHANG, H., ANNICH, G.M., *et al.* (2003). Nitric oxide-releasing fumed silica particles: synthesis, characterization, and biomedical application. *Journal of the American Chemical Society*, **125,** 5015-24.

ZHANG, L., YU, L., *et al.* (1998). Generation of superoxide anion by succinate-cytochrome c reductase from bovine heart mitochondria. *J Biol Chem*, **273,** 33972-6.

ZHANG, L.M., CASTRESANA, M.R., *et al.* (1993). Tolerance to sodium nitroprusside. Studies in cultured porcine vascular smooth muscle cells. *Anesthesiology*, **79,** 1094-103.

ZHANG, Y. & HOGG, N. (2004). The mechanism of transmembrane S-nitrosothiol transport. *Proc Natl Acad Sci U S A*, **101,** 7891-6.

ZHAO, Y., BRANDISH, P.E., *et al.* (2000). Inhibition of soluble guanylate cyclase by ODQ. *Biochemistry*, **39,** 10848-54.

ZHOU, Z. & MEYERHOFF, M.E. (2005). Polymethacrylate-based nitric oxide donors with pendant N-diazeniumdiolated alkyldiamine moieties: synthesis, characterization, and preparation of nitric oxide releasing polymeric coatings. *Biomacromolecules*, **6,** 780-9.

ZHU, H., KA, B., *et al.* (2007). Nitric oxide accelerates the recovery from burn wounds. *World J Surg*, **31,** 624-31.

ZHU, L., GUNN, C., *et al.* (1992). Bactericidal activity of peroxynitrite. *Arch Biochem Biophys*, **298,** 452-7.

APPENDIX

NITRIC OXIDE-LOADED Co^{2+} AND Zn^{2+}-EXCHANGED ZEOLITES HAVE POWERFUL ANTI-AGGREGATORY PROPERTIES IN HUMAN PLATELETS

Sarah Fox*, Paul S. Wheatley†, Russell E. Morris†, Anthony R. Butler†, Adriano G. Rossi*, (Ian L. Megson*). *Queen's Medical Research Institute, University of Edinburgh, EH16 4TJ; †School of Chemistry, University of St Andrews, KY16 9ST.

Endothelium derived nitric oxide (NO) is a potent inhibitor of platelet activation (Radomski *et al* 1987). Polymers incorporating NO donating substances (e.g. diazeniumdiolates) have shown potential as antithrombotic surface coatings (Frost *et al* 2005), but have limited NO capacities. Zeolites are nanoporous solids that might offer an alternative to polymer-based antithrombotic coatings because they can act as high capacity storage materials for gases, including NO. The chemical characteristics of zeolites are easily manipulated by altering the specific cation, the porosity of the zeolite and the binding material in which it is embedded. In this study, we investigated the NO release properties of Zn^{2+} and Co^{2+} cation-exchanged zeolites in human plasma, and determined the extent and duration of their antiplatelet activity.

NO-loaded Zn^{2+} and Co^{2+}-exchanged zeolites of various compositions (10%-75%) in polytetrafluoroethylene binder (PTFE; pressed into 3 mm dia. discs) were found to generate substantial NO for ~60 min upon immersion in platelet-rich plasma (PRP; 1 ml, 37°C; n=6). The NO-release profile was dependent on both the exchanged cation (Zn^{2+} or Co^{2+}) and the composition of zeolite:PTFE binder (see Fig. 1).

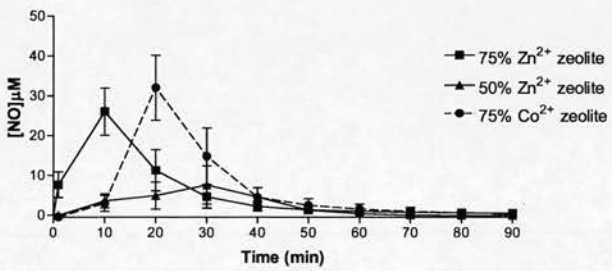

Fig. 1: NO generation from Zn^{2+} and Co^{2+}-exchanged zeolites (50-75%: PTFE) in PRP.

Turbidometric platelet aggregometry was used to determine the ability of NO-loaded zeolites to inhibit collagen induced platelet aggregation in PRP *in vitro*. Discs (3 mm dia.) containing NO-loaded Zn^{2+} and Co^{2+} ion-exchanged zeolites (10-75% in PTFE binder) were suspended in PRP (500 µl; 37°C; 1-80 min) before stimulation with collagen (2.5µl.ml^{-1}). Zn^{2+} exchanged zeolite (≥50%) and Co^{2+} exchanged zeolite (75% only) significantly inhibited platelet aggregation throughout the incubation period (80 min; $p<0.01$; n=6-8); NO-free counterparts failed to alter platelet aggregation over the same period, indicating the essential role of NO in the effect.

Our results suggest that Co^{2+} and Zn^{2+}-exchanged zeolites are high capacity storage materials of NO with powerful antiplatelet activity *in vitro*. The NO release profiles and antiplatelet effects were dependent on the specific cation exchanged and on the relative proportion of zeolite:PTFE binder. These zeolites will act as prototypes for the development of zeolites with optimal NO release capacities lasting for considerably longer durations.

Frost M.C. *et al* (2005) *Biomaterials* **26**, 1685 -1693
Radomski *et al* (1987) *The Lancet* **330** (8567), 1057-1058

J|A|C|S
ARTICLES
Published on Web 12/20/2005

NO-Releasing Zeolites and Their Antithrombotic Properties

Paul S. Wheatley,[†] Anthony R. Butler,[‡] Michael S. Crane,[§] Sarah Fox,[§] Bo Xiao,[†] Adriano G Rossi,[||] Ian L. Megson,[§] and Russell E. Morris*,[†]

Contribution from the School of Chemistry, University of St. Andrews, Purdie Building, St. Andrews KY16 9ST, U.K., Bute Medical School, University of St. Andrews, St. Andrews KY16 9TS, U.K., and Centre for Cardiovascular Science and MRC Centre for Inflammation Research, University of Edinburgh, Queen's Medical Research Institute, 47 Little France Crescent, Edinburgh EH16 4TJ, U.K.

Received January 19, 2005; E-mail: rem1@st-and.ac.uk

Abstract: Transition metal-exchanged zeolite-A adsorbs and stores nitric oxide in relatively high capacity (up to 1 mmol of NO/g of zeolite). The stored NO is released on contact with an aqueous environment under biologically relevant conditions of temperature and pH. The release of the NO can be tuned by altering the chemical composition of the zeolite, by controlling the amount of water contacting the zeolite, and by blending the zeolite with different polymers. The high capacity of zeolite for NO makes it extremely attractive for use in biological and medical applications, and our experiments indicate that the NO released from Co-exchanged zeolite-A inhibits platelet aggregation and adhesion of human platelets in vitro.

Introduction

Nitric oxide (NO) is a crucial biological agent in the cardiovascular, nervous, and immune systems.[1] NO synthesized by endothelial cells that line blood vessels mediates a number of vital functions, including vasodilatation[2,3] and inhibition of platelet[4] and inflammatory cell[5,6] activation and adhesion. In addition, NO is an important neurotransmitter and neuromodulator in the peripheral and central nervous systems,[7] and its synthesis in high concentrations contributes to the cytotoxic effects of inflammatory cells on invading pathogens.[8]

The delivery of exogenous NO is an attractive therapy for a number of ailments, but the range and diversity of its effects make target specificity a major concern, which has held back the development of some NO applications. To overcome this problem requires the development of materials that can store significant quantities of NO and then deliver it to specific sites in the body. There is currently particular interest in using NO delivery materials to prevent life-threatening complications associated with thrombosis formation at the surface of medical devices such as stents and catheters.[9]

A number of materials have been proposed as delivery agents for exogenous NO. Perhaps the chemically most advanced are those based on polymers or silica functionalized with secondary amines, which, on reaction with NO, form ionic diazenium diolates that can be used to increase the thromboresistivity of polymers.[9,10,11] Two molecules of NO react with each amine (giving rise to the trivial name NONOate) and are released on contact with moisture at an appropriate pH. Other methods of release have also been explored, including the light-activated release of NO from metal-containing polymers.[12]

A specific potential use for NO-releasing materials in the cardiovascular arena centers on the prevention of thrombosis on artificial surfaces that come into contact with blood, particularly in relation to procedures that require extracorporeal circuits, like bypass and renal replacement therapy, catheter implantations, or stents that are used in interventional cardiology to improve the patency of partially blocked arteries.[9] Current best practice to prevent thrombosis in these situations involves the administration of heparin, other anticoagulants, or antiplatelet agents to the patient, with the inherent risk of hemorrhagic[13,14]

[†] School of Chemistry, University of St. Andrews.
[‡] Bute Medical School, University of St. Andrews.
[§] Centre for Cardiovascular Science, Queen's Medical Research Institute.
[||] MRC Centre for Inflammation Research, Queen's Medical Research Institute.

(1) Moncada, S.; Palmer, R. M. J.; Higgs, E. A. *Pharmacol. Rev.* **1991**, *43*, 109.
(2) Furchgott, R. F.; Zawadzki, J. V. *Nature* **1980**, *288*, 373.
(3) Palmer, R. M. J.; Ferrige, A. G.; Moncada, S. *Nature* **1987** *327*, 524.
(4) Radomski, M. W.; Palmer, R. M. J.; Moncada, S. *Lancet* **1987**, *2*, 1057.
(5) Bath, P. M. W.; Hassall, D. G.; Gladwin, A. M.; Palmer, R. M. J.; Martin, J. F. *Arterioscler. Thromb.* **1991**, *11*, 254.
(6) Kubes, P.; Suzuki, M.; Granger, D. N. *Proc. Natl Acad. Sci. U.S.A.* **1991**, *87*, 5193.
(7) Garthwaite, J. *Trends Neurosci.* **1991**, *14*, 60.
(8) Nathan, C. F.; Hibbs, J. B. *Curr. Opin. Immunol.* **1991** *3*, 65.
(9) Keefer, L. K. *Nat. Mater.* **2003**, *2*, 357.
(10) (a) Parzuchowski, P. G.; Frost, M. C.; Meyerhoff, M. E. *J. Am. Chem. Soc.* **2002**, *124*, 12182. (b) Lee, Y.; Oh, B. K.; Meyerhoff, M. E. *Anal. Chem.* **2004**, *76*, 536. (c) Zhang, H. P.; Annich, G. M.; Miskulin, J.; Stankiewicz, K.; Osterholzer, K.; Merz, S. I.; Bartlett, R. H.; Meyerhoff, M. E. *J. Am. Chem. Soc.* **2003**, *125*, 5015. (d) Frost, M. C.; Rudich, S. M.; Zhang, H. P.; Maraschio, M. A.; Meyerhoff, M. E. *Anal. Chem.* **2002**, *74*, 5942. (e) Zhang, H. P.; Annich; G. M.; Miskulin, J.; Osterholzer, K.; Merz, S. I.; Bartlett, R. H.; Meyerhoff, M. E. *Biomaterials* **2002**, *23*, 1485.
(11) (a) Mowery, K. A.; Schoenfisch, M. H.; Saavedra, J. E.; Keefer, L. K.; Meyerhoff, M. E. *Biomaterials* **2000**, *21*, 9. (b) Mowery, K. A.; Schoenfisch, M. H.; Baliga, N.; Wahr, J. A.; Meyerhoff, M. E. *Electroanalysis* **1999**, *11* 681. (c) Espadas-Torre, C.; Oklejas, V.; Mowery, K.; Meyerhoff, M. E. *J. Am. Chem. Soc.* **1997**, *119*, 2321.
(12) (a) Mitchell-Koch, J. T.; Reed, T. M.; Borovik, A. S. *Angew. Chem.* **2004**, *43*, 2806 (b) Padden, K. M.; Krebs, J. F.; MacBeth, C. E.; Scarrow, R. C.; Borovik, A. S *J. Am. Chem. Soc.* **2001**, *123*, 1072.
(13) Sundlof, D. W.; Rerkpattanapitat, P.; Wongpraparut, N.; Pathi, P.; Kotler, M. N.; Jacobs, L. E.; Ledley G. S.; Yazdanfar, S. *Am. J. Cardiol.* **1999**, *83*, 1569.

10.1021/ja0503579 CCC: $33.50

or paradoxical thrombotic[15] complications. Stent coatings that release antithrombotic,[16] antiinflammatory,[17] and antimitogenic[18] agents to reduce in-stent thrombosis or restenosis have had some success, but NO might be expected to have all of these effects if delivered at the appropriate rate for a sufficient duration. Other potential uses of these types of solids, as shown by a number of different biological effects, include antibacterial coatings[19] and wound-healing promotors.[20]

Zeolites have well-known applications in ion exchange, gas adsorption, and catalysis (including $DeNO_x$, the removal of nitrogen oxides from exhaust gases[21,22]), and they are of increasing interest as hosts for nanotechnology applications.[23] New zeolites[24] and new methods for zeolite preparation[25,26] continue to attract attention as catalysts, but their use in medicine is limited to nontoxic medical diagnosis tools and clotting enhancers.[23] Zeolites have also been studied as microporous storage media for gases such as hydrogen.[27]

A great deal is known about the interaction of NO with zeolites, particularly from catalytic and separation studies. Pressure swing adsorption experiments indicate that there are two types of adsorbed NO in zeolites, commonly called reversibly and irreversibly adsorbed NO.[28−30] As its name suggests, reversibly adsorbed NO is a weakly held, predominantly physisorbed species. In contrast, irreversibly adsorbed NO is relatively strongly held and is not spontaneously released from the zeolite even at very low pressures. Irreversible NO is primarily chemisorbed, as has been shown by single-crystal X-ray diffraction[31] and IR spectroscopy[32] and supported by recent modeling experiments,[33] where the NO interacts with the extraframework cations in zeolites through the nitrogen atom to form either mononitrosyl or dinitrosyl complexes. Irreversible adsorption of this kind is a good method of storing a gas in a material as it is not lost too easily. However, suitable methods of initiating delivery of the gas must be found before the materials can be utilized in applications. Here we show how a suitable nucleophile (water) can be used to displace the "irreversibly" adsorbed NO from ion-exchanged zeolite-A at biologically relevant temperatures. The release of NO can be customized by altering the chemical composition of the zeolite. Experiments with human platelets confirm that NO released from a zeolite is sufficient to abolish platelet activation and adhesion in vitro, pointing to potential applications in coating surgically implanted catheters that are ordinarily regarded to be prothrombogenic. The tuneable nature of NO release from cation-exchanged zeolites extends the potential applications to tubing and instruments used in procedures such as bypass surgery and renal replacement therapy.

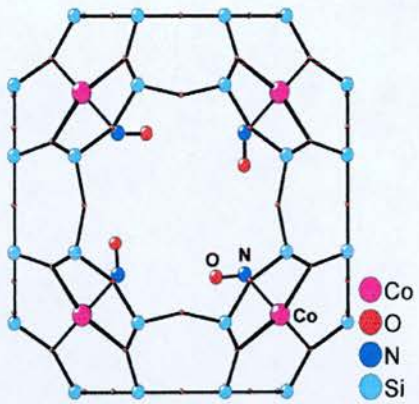

Figure 1. Structure of the cobalt−NO complex in zeolite-A as revealed by single-crystal X-ray diffraction (data taken from ref 31). The cobalt is bound to three oxygen atoms of a six-ring unit in the zeolite framework and bonds to the nitrogen of a bent mononitrosyl ligand. Oxygen atoms of the zeolite framework are shown smaller than the NO oxygen for clarity.

Zeolite-A (given the three letter framework code LTA[34]) is manufactured in >1 M tonne amounts annually for use as a detergent builder and water softener. Zeolite-A[35,36] consists of alternating SiO_4 and AlO_4 tetrahedra that share corners to produce the open framework depicted in Figure 1, with exchangeable extraframework cations residing in the channels. Zeolite-A is a poor $DeNO_x$ catalyst but is used in a number of adsorption applications. It is therefore an ideal choice of zeolite for studies of NO storage. Also, it has a well-known affinity for water, often being used by organic chemists to dry solvents.

Figure 2 shows the adsorption and desorption isotherms for NO on Co-exchanged zeolite-A and illustrates the natural affinity of the zeolite for NO, as even at low pressures the majority of the gas remains bound inside the zeolite (i.e. is irreversibly adsorbed). The hysteretic nature of the adsoption/desorption isotherm means that the zeolite can be used to hold NO at pressures below those needed to load NO onto the material. This is ideal for the storage of significant amounts of NO. Similar hysteretic adsorption has recently been seen for hydrogen storage in other types of nanoporous material.[37] The maximum amount of NO adsorbed by cobalt-exchanged zeolite-A is approximately 1.7 mmol/g of zeolite, although reduction of the NO pressure leads to loss of the reversibly adsorbed

(14) Bennett, C. L.; Connors, J. M.; Carwile, J. M.; Moake, J. L.; Bell, W. R.; Tarantolo, S. R.; McCarthy, L. J.; Sarode, R.; Hatfield, A. J.; Feldman, M. D.; Davidson, C. J.; Tsai, H. M. *N. Engl. J. Med.* **2000**, *342*, 1773.
(15) Chong, B. H. *J Thromb Haemostas* **2003**, *1*, 1471.
(16) Aggarwal, R. K.; Martin, W. A.; Azrin, M. A.; Ezekowitz, M. D.; de Bono, D. P.; Gershlick, A. H. *Circulation* **1996**, *94*, 1510.
(17) Strecker, E. P.; Gabelmann, A.; Boos I.; Lucas C.; Xu, Z. Y.; Haberstroh, J.; Freudenberg, N.; Stricker, H.; Langer, M.; Betz, E. *Cardiovasc. Intervent. Radiol.* **1998**, *21*, 487.
(18) Colombo, A.; Drzewiecki, J.; Banning, A.; Grube, E.; Hauptmann, K.; Silber, S.; Dudek, D.; Fort, S.; Schiele, F.; Zmudka, K.; Guagliumi, G.; Russell, M. E. *Circulation* **2003**, *108*, 788.
(19) Nablo, B. J., Chen, T.-Y.; Schoenfisch, M. H. *J. Am. Chem. Soc.* **2001**, *123*, 9712.
(20) Shabani, M.; Pulfer, S. K.; Bulgrin, J. P.; Smith, D. J. *Wound Rep. Regen.* **1996**, *4*, 353.
(21) Yahiro, H.; Iwamoto, M. *Appl. Catal., A* **2001**, *222*, 163.
(22) Pontikakis, G. N.; Koltsakis, G. C.; Stamatelos, A. M.; Noirot, R.; Agliany, Y.; Colas, H.; Versaevel, P.; Bourgeois, C. *Top. Catal.* **2001**, *16*, 329.
(23) Davis, M. E. *Nature* **2002**, *417*, 813.
(24) Corma, A.; Diaz-Cabanas, M.; Martinez-Triguero, J.; Rey, F.; Rius, J. *Nature* **2002**, *418*, 514.
(25) Lee, H.; Zones, S. I.; Davis, M. E. *Nature* **2003**, *425*, 385.
(26) Cooper, E. R.; Andrews, C. D.; Wheatley, P. S.; Webb, P. B.; Wormald, P.; Morris, R. E. *Nature* **2004**, *430*, 1012.
(27) Langmi, H. W.; Walton, A.; Al-Mamouri, M. M.; Johnson, S. R.; Book, D.; Speight, J. D.; Edwards, P. P.; Gameson, I.; Anderson, P. A.; Harris, I. R. *J. Alloys Compd.* **2003**, *356*, 710.
(28) Arai, H.; Machida, M. *Catal. Today* **1994**, *22*, 97.
(29) Zhang, W. X.; Yahiro, H.; Mizuno, N.; Izumi, J.; Iwamoto, M. *Langmuir* **1993**, *9*, 2337.
(30) Zhang, W. X.; Yahiro, H.; Iwamoto, M. *J. Chem. Soc., Faraday Trans.* **1995**, *91*, 767.
(31) Cruz, W. V.; Leung, P. C. W.; Seff, K. *Inorg. Chem.* **1979**, *18*, 1692.
(32) Lunsford, J. H.; Hutta, P. J.; Lin, M. J.; Windhorst, K. A. *Inorg. Chem.* **1978**, *17*, 606.
(33) Henao, J. D.; Cordoba, L. F.; Montes de Correa, C. *J. Mol. Catal., A* **2004**, *207*, 195.
(34) For more information on the nomenclature of zeolites, including details of the framework topologies, visit the International Zeolite association website www.iza-online.org.
(35) Pluth, J. J.; Smith, J. V. *J. Am. Chem. Soc.* **1980**, *102*, 4704.
(36) Cheetham, A. K.; Eddy, M. M.; Jefferson, D. A.; Thomas, J. M. *Nature* **1982**, *299*, 24.
(37) Zhao, X.; Xiao, B.; Fletcher, A. J.; Thomas, K. M.; Bradshaw, D.; Rosseinsky, M. J. *Science* **2004**, *306*, 1012.

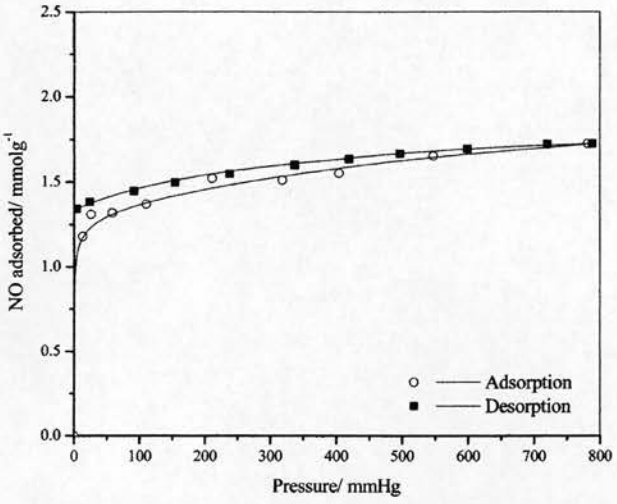

Figure 2. Adsorption/desorption isotherm of nitric oxide on Co-exchanged zeolite-A. The irreversible nature of the adsorption of the majority of NO on the zeolite is indicated by the hysteresis.

(weakly physisorbed NO) leading to a maximum storage capacity of ~1.2−1.3 mmol/g. The only remaining problem is then how to release (deliver) the NO from the zeolite when required. Fortunately, zeolites also interact strongly with water, and our hypothesis was that exposure to moisture would result in replacement of the NO by water in the zeolite, leaving the gaseous NO to diffuse out of the zeolite. Our aim in this study was to synthesize metal-containing zeolites that store NO and release it in biologically relevant amounts on contact with water. We envisaged that the rate of NO release could be modified by altering the chemical composition of the material for a range of different medical and biological applications in which exogenous NO might be beneficial.

Results and Discussion

Samples of zeolite-A were synthesized according to the procedure given in ref 38. The transition exposed to dry NO and stored in sealed vials under argon at room temperature ready for use.

Zeolites are well-known as extremely good drying agents and interact strongly with water, and this has led to their use in numerous applications, including as a method of rapidly absorbing water from blood to aid in clotting after serious wounding.[39] It is not surprising then that the NO is released very quickly when contacted by water in a physiological solution. Unfortunately, it is difficult to quantify the release rate of NO in this fashion accurately because the powder zeolite tends not to disperse well in the liquid, with much remaining floating on the surface. An alternative, and much more repeatable, method is to flow a wet gas (of controlled relative humidity) through the sample at a steady rate and measure the NO concentration of the gas using chemiluminescence measurements. The NO release profiles of NO-loaded cobalt exchanged zeolite-A expressed as a total concentration of NO in the gas stream versus time (a) and a cumulative total amount of NO

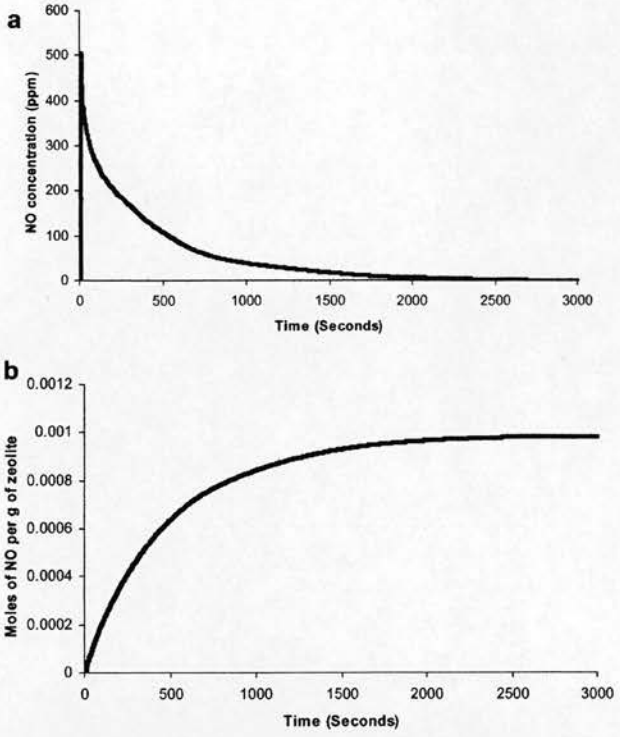

Figure 3. Two NO-release profiles for NO-loaded Co-exchanged zeolite-A: (a) NO concentration (ppm) in the gas stream passing through the chemiluminescence detector versus time; (b) total mount of NO released by the material with time (per g of zeolite). The conditions for this experiment were 31 mg of zeolite and a flow rate of 200 mL/min of wet argon at a relative humidity of 11%.

released/g of zeolite (b) are shown in Figure 3. In this case the flow rate of gas used was 200 mL/min and the relative humidity of the gas was 11%. The total amount of NO released is approximately 1 mmol of NO/g of zeolite. The duration of NO release approaches 2500 s with a half-life ($t_{1/2}$, the time it takes for half the NO to be released) of ~340 s. The total amount of NO released is also very consistent between different samples as long as care is taken to ensure that the chemical composition of the zeolite and its dehydration properties are the same. The average amount of NO released from 130 separate measurements on different samples was 1.02 mmol of NO/g with a standard deviation of 0.05. Storage of the NO-loaded zeolites under a dry atmosphere also has no effect on the total NO released by the materials. Samples of NO-loaded cobalt-exchanged zeolite-A were stored under argon in sealed ampules for up to 16 weeks. The quantification of the NO released by these samples is shown in Figure 4, with each measurement repeated at least 16 times on different samples. There is no drop off in total NO released indicating that under dry conditions cobalt-exchanged zeolite-A is a stable NO storage material with a gas storage capacity similar to that of the best NO-storing polymers reported and significantly higher than most.[10,11]

The amount of moisture present in the gas flow is also important in controlling the release of the NO. Increasing the relative humidity (while keeping the flow rate constant) to 22% increases the rate of NO release ($t_{1/2}$ = 208 s), while an almost dry gas (relative humidity 1.5%) increases the $t_{1/2}$ to more than 3000 s. It should be remembered though that there are two

(38) Robson, H.; Lillerud, K. P. *Verified Syntheses of Zeolitic Materials*, 2nd revised ed.; International Zeolite Association: Amsterdam, Netherlands, 2001; www.iza-synthesis.org.
(39) Wright, F. L.; Hua, H. T.; Velhamos, G.; Thoman, D.; Demitriades, D.; Rhee, P. M. *J. Trauma Inj. Inf. Crit. Care* **2004**, *56*, 205.

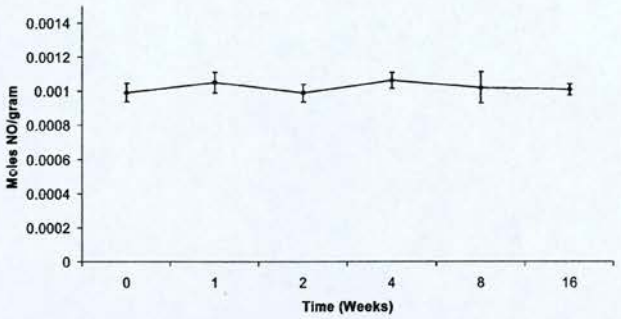

Figure 4. Storage stability experiments showing the total amount of NO released by a cobalt-exchanged zeolite-A after storage under dry conditions for different amounts of time. The results are the average of at least 16 different measurements for each storage period, and the error bars indicate the standard deviations of the measurements.

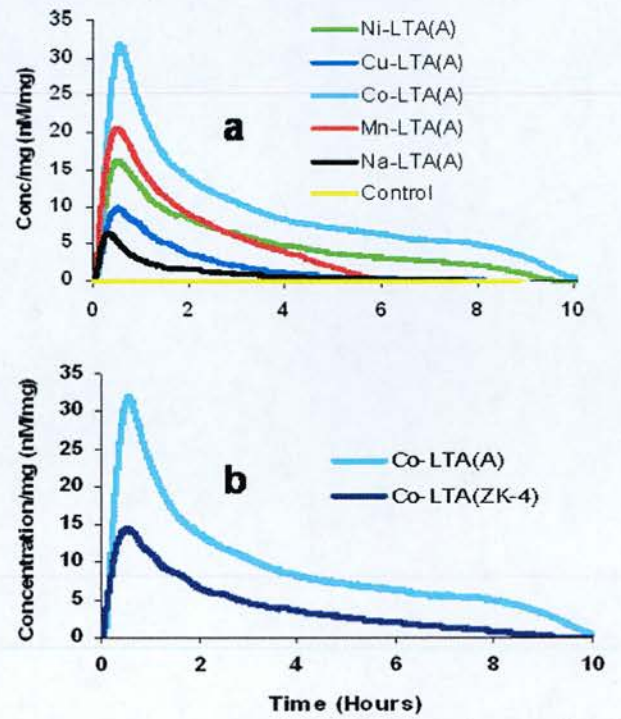

Figure 5. NO-release profiles of NO-loaded metal-exchanged zeolite-A. Top: Effect of metal ion on NO release. The control is a Co^{2+}-exchanged zeolite that has not been exposed to NO. The electrode response results have been normalized to give the concentration of NO in solution/mg of zeolite material. Bottom: Dependence of NO release on Co^{2+} exchange level. Co−zeolite-A (Co−LTA(A)) contains 19.8 wt % cobalt, while Co−zeolite-ZK4 (Co−LTA(ZK4)) contains 9.0 wt % cobalt. All zeolite samples were from the same synthesis batch to minimize particle size differences in the materials.

components to the storage of NO and that any physisorbed NO will be released even in completely dry conditions.

An alternative way to measure the release of NO from the zeolites involves contacting the zeolite with a moist gas that is subsequently bubbled through a liquid phase (phosphate buffered saline, pH 7.4 at 25 °C). The amount of NO dissolved in the solution is then measured electrochemically. This allows the flow rate to be reduced down to 5 mL/min showing that even in moisture-saturated argon the release of the NO now takes place much more slowly and lasts up to 10 h (Figure 5). Again this is consistent with the reduced flux of water on the sample from the much reduced flow rate. Figure 5 also shows the NO release profiles measured electrochemically for a number of other transition metal-exchanged zeolite-A samples in contact with an argon flow that has been saturated with water vapor. The order of how much NO is released for each metal agrees well with the NO adsorption properties of transition metal zeolites in pressure swing adsorption studies.[28,29] Co-exchanged zeolites released the most NO while the original sodium form of the zeolite released least NO. At first glance the Cu-exchanged zeolite-A results seem anomalously low, especially since Cu−zeolites are well-known deNO_x catalysts and that Cu-exchanged zeolites do adsorb significant quantities of NO.[28,29] This is because the zeolite is overexchanged, with more Cu^{2+} ions in the channels than is strictly necessary for charge balance reasons. Many of the "extra" Cu^{2+} ions are probably present as hydroxide species and so reduce the availability of the metal ions for NO coordination.

The amount of NO released by the zeolite depends not only on which transition metal is present but also on how much of the metal is there. Zeolite-ZK4 is a variant of zeolite-A that has the same framework structure and so has the same framework code (LTA). However, there are fewer exchangeable cations in zeolite-ZK4 as there is less aluminum in the framework than in zeolite-A. This means that there are fewer metal cation sites in the channels of the structure to bind NO. It is clear from Figure 5b that Co-exchanged zeolite-A releases more NO than Co-exchanged zeolite ZK4, consistent with the reduced level of cobalt in the ZK4 structure. Interestingly, Co-exchanged zeolite-A samples are self-indicating; when initially dried they are a bright blue, and when loaded with NO they are a gray/blue but change to pink as the NO is displaced by water. These color changes emphasize the importance of the metal−NO interactions in the storage of the gas and the replacement of these by metal−water interactions on delivery of the NO.

Bioactivity. The need for improvements in the biocompatibility of materials is a very important target. This is particularly true for blood-contacting solids that are used in vascular grafts and in extracorporeal tubing used in coronary bypass surgery and kidney dialysis. Life-threatening complications can occur if thrombosis formation (platelet aggregation and adhesion together with coagulation) is induced by artificial materials that are in contact with blood. Thrombus formation in healthy circulatory systems is inhibited in a number of ways, including the production of small quantities (approximately 1 pmol min^{-1} mm^{-2}; see ref 9) of NO by the endothelial cells that line the blood vessels and also by platelets. A potentially important strategy for reducing postoperative complications is to make medical devices out of an NO-releasing material, thereby mimicking the antithrombotic action of the endothelial cells.

To overcome the problem of the nondispersion of zeolite powders in the liquid phase, samples of zeolite were prepared as pressed disks with small amounts of polymers as binders. The Co-exchanged zeolite samples, in 75:25 or 50:50 wt % mixtures with powdered poly(tetrafluoroethylene) (PTFE) or poly(dimethylsiloxane) (PDMS), were prepared as pressed disks and subsequently dehydrated and loaded with NO in the same way as the powdered samples. Pressed disks made from only zeolites are slightly brittle; some material breaks off easily under stirring, and so the polymer is there primarily to add mechanical stability to the disks. However, this process clearly affects the NO release properties of the materials. Figure 6 shows that on

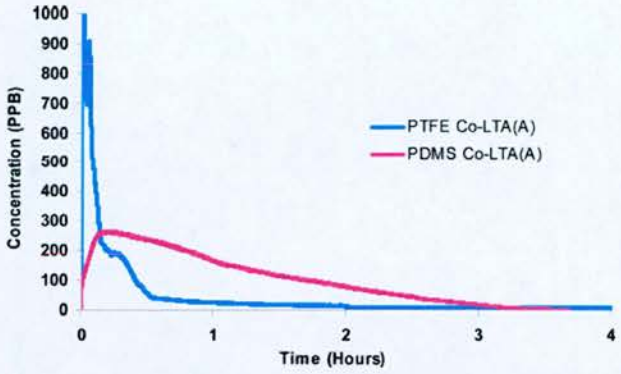

Figure 6. Chemiluminescence response to NO (in ppb) from two disks of cobalt-exchanged zeolite-A (8.5 mg) mixed with PTFE and PDMS (8.5 mg, respectively) immersed in water.

exposure to liquid water (25 °C) the release of NO is slowed considerably as compared to the powdered zeolite, with $t_{1/2}$ of 509 s for the PTFE disk and a $t_{1/2}$ of 3076 s for the PDMS disk. In addition, the total amount of NO released is very much reduced compared to the free zeolite powders (1.4×10^{-5} and 2.4×10^{-5} mol of NO/g of zeolite for PTFE and PDMS, respectively). This is not at all surprising given that the preparation of the disk will affect the accessibility of the zeolite to the NO considerably. However, given the small quantities of NO required for biological action this is not a major drawback in terms of testing the materials for their antithrombotic behavior. Clearly the nature of polymer used in any formulation can have a significant affect on the rates of release and is another method of tuning the release rate to match any potential application. Figure 7c shows that the electrochemically measured released profile of the Co−zeolite-A/PTFE disk is very similar to that seen in plasma. The NO-loaded disks were stored under an inert atmosphere in a manner similar to that described above for the powdered zeolite samples. The disks were stored for up to several weeks before being used in further experiments.

Zeolite/PTFE disks were suspended by a stainless steel wire holder below the surface of platelet-rich plasma (PRP) in the cuvette of a four-channel platelet aggregometer (Chronolog, Labmedics, Stockport, U.K.) at 37 °C. After a short induction period (1 min), platelet aggregation was initiated using the thromboxane A_2 analogue, U46619 (8 μM) and then measured as a change in turbidity (light transmission) of PRP against a platelet poor plasma (PPP) reference. The results (Figure 7) show that a NO-loaded Co-exchanged zeolite-A/PTFE sample completely inhibits platelet aggregation. Addition of the NO scavenger, oxyhemoglobin (40 μM), prevents the inhibitory effect, confirming the central role for NO in the inhibitory process and excluding the possibility that the effects of the NO−zeolite were merely cytotoxic. Furthermore, a Co-exchanged zeolite/PTFE sample that has not been loaded with NO failed to inhibit U46619-mediated aggregation. Parallel experiments

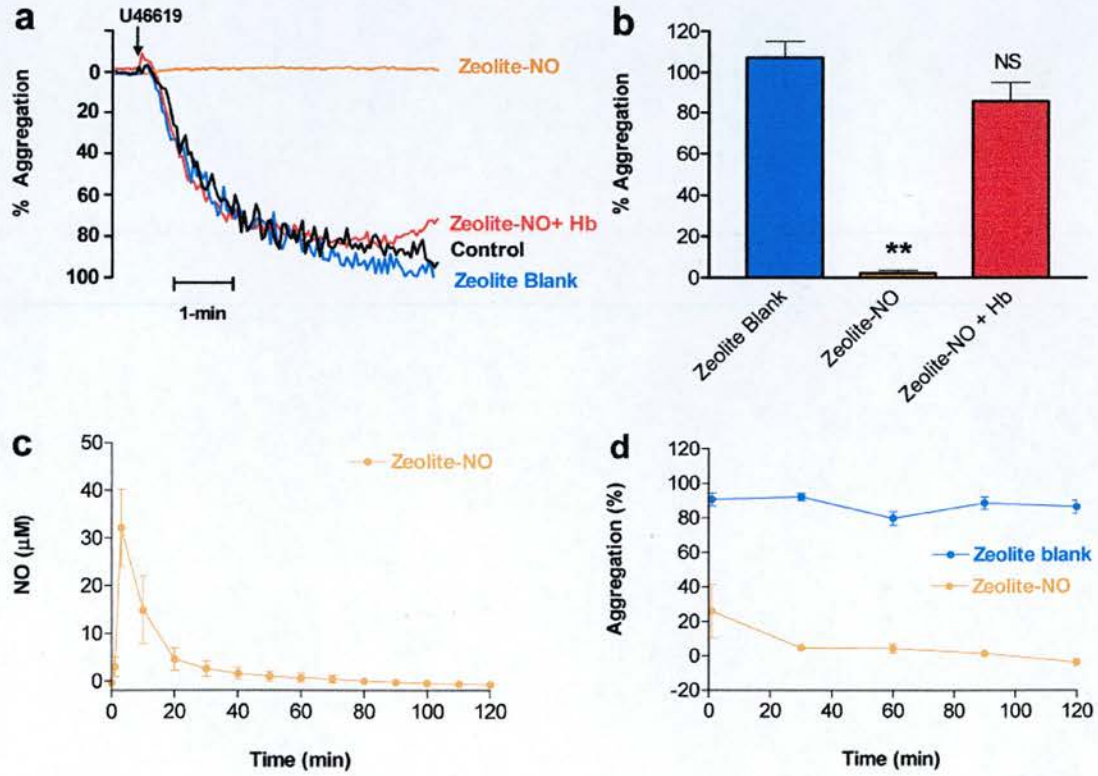

Figure 7. Effect of NO-loaded Co−zeolite-A and the NO-free Co−zeolite A (both 75% in PTFE) on platelet aggregation in response to U46619 (8 μM): (a) aggregation recordings from a single experiment in the presence and absence of the NO scavenger, oxyhemoglobin (Hb; 40 μM); (b) mean ± standard error of the mean (SEM) data for aggregation under different conditions, expressed as % of platelet aggregation in the absence of zeolite [$^{**}P < 0.01$, Dunn's multiple comparison test after nonparametric Kruskal Wallis comparison for samples with different variances; NS = not significant ($n = 6$)]; (c) electrochemically detected NO generation profile from NO-loaded Co−zeolite (75% in PTFE) suspended in PRP ($n = 5$); (d) time−course of the inhibitory effect of NO-loaded Co−zeolite A and the NO-free counterpart (both 75% in PTFE) on agonist-induced platelet aggregation at timed intervals after immersion of the zeolite in PRP ($n = 6$; $P < 0.001$, 2-factor ANOVA).

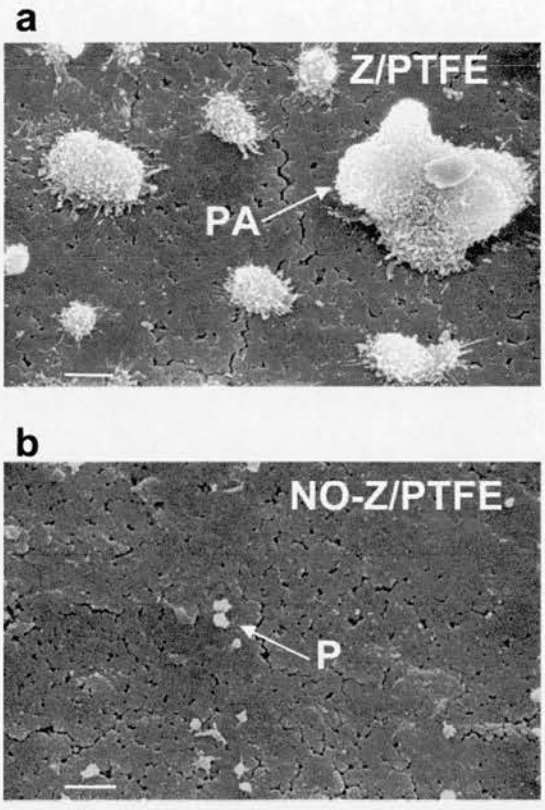

Figure 8. Scanning electron micrographs of the surface of (a) untreated Co−zeolite-A/PTFE disks (Z/PTFE) and of (b) NO-loaded Co−zeolite-A/PTFE disks. (a) shows large platelet aggregants (PA) on the surface on the surface of the untreated zeolite/PTFE disk, while (b) shows only a few, isolated platelets (P) on the surface of the NO-treated zeolite−PTFE disk. The scale bar is 10 μm.

were conducted to determine the concentration of NO generated by 75% NO-loaded zeolite disks in PTFE suspended in PRP (Figure 7c). The profile of release is similar to that shown in Figure 6, suggesting that plasma components have little impact on the water-mediated release of NO from this compound. In addition, a time−course study for the effect of equivalent disks on platelet aggregation (Figure 7d) indicate a prolonged inhibitory effect throughout the 2 h period of study, which is not shared by the NO-free counterpart. However, it is worth noting that an element of the persistent inhibition is likely to be mediated via formation of a durable NO store in plasma[40] rather than necessarily through the persistent delivery of NO directly from the zeolite. Indeed, it is clear that the zeolite/PTFE NO release profile is not ideal for maintaining a protracted antithrombotic effect, as the NO release is exhausted after ~30 min (Figures 6 and 7c). The release profile for the zeolite/PDMS disks (Figure 6) shows a considerably lower peak NO concentration and a considerable prolonged release profile. This indicates that it may be possible to tune the release profile for a protracted thrombotic effect.

Platelet aggregants (PA; Figure 8a) on the surface of the zeolite/PTFE (Z/PTFE) were visualized using scanning electron microscopy, which conclusively demonstrates the extent to which platelet aggregation and adhesion is inhibited at the surface of NO-treated zeolite/PTFE (NO−Z/PTFE; Figure 8b), on which only a small number of isolated platelets (P) can be seen.

The toxicology of zeolites has been extensively studied, and the frameworks themselves are regarded as benign materials. Zeolite-A, because of its wide range of uses in detergent powders, has been particularly well studied in terms of its potential toxicity. There are no reported adverse effects on the body from zeolite frameworks, except possible pulmonary problems caused by breathing small particles of zeolite dust.[41] Unlike zeolites for detergent applications, the zeolites reported in this paper contain transition metal ions, and the toxicity of these ions must also be taken into account. While zeolites have been proposed as materials for the inhibition of transition metal ion permeation in the skin[42] and to inhibit the toxicity of gadolinium in orally ingested MRI contrast agents,[43] long-term contact with blood will undoubtedly lead to some leaching of metal ions. As long as this leaching does not lead to excessive increases in local concentrations above normal in vivo values, then there will be no adverse effects, but this must be studied in greater detail.

Concluding Remarks

Gas storage by porous materials is currently an important topic but tends to concentrate on the storage of gases for energy applications.[44] We have demonstrated that zeolites have great potential as NO storage and release materials for biological and medical applications. Their preparation and loading with NO is relatively facile, the release of NO occurs by simple reaction with water, and the amount of NO released can be tailored by altering both the type and number of metal cations in the structures. Taking into consideration the other advantages of zeolites, such as their low cost and nontoxicity, these materials clearly have great potential as NO storage materials. We have also demonstrated that NO-releasing zeolites inhibit platelet aggregation and adhesion in plasma, a potentially important application of such solids in the prevention of thrombus formation. This work overturns the conventional idea that zeolites can be used only to destroy NO and adds a new delivery system to the armament of researchers developing NO-based therapies. The multiple roles for NO at different concentrations means that the potential for NO-release materials extends far beyond the confines of reduced thrombogenicity of prosthetic grafts, catheters, and extracorporeal blood conduits; it could also encompass other medical uses including antimicrobial adjuncts to prevent infection, for example, in chronically implanted catheters and in wound dressings for enhanced angiogenesis.

Experimental Section

Synthesis of Zeolites. Zeolites Linde type A and ZK-4 possessing the LTA framework topology were synthesized as previously published.[38]

Linde Type A. Sodium hydroxide (2.892 g) was dissolved in distilled water (320 mL) and divided equally into two nalgene bottles. To half

(40) Crane, M. C.; Olloson, R.; Moore, K.; Rossi, A. G.; Megson, I. L. *J. Biol. Chem.* **2002**, *277*, 46858.

(41) Thomas, J. A.; Ballantyne, B. *J. Am. Coll. Toxicol.* **1992**, *1*, *1* 259.
(42) Kassai, Z.; Bauerova, K.; Koprda, V.; Bujnova, A. *Biologia* **2000**, *55*, 55.
(43) Young, S. W.; Qing, F.; Rubin, D.; Balkus, K. J.; Engel, J. S.; Lang, J.; Dow, W. C.; Mutch, J. D.; Miller, R. A. *J. Magn. Reson. Imag.* **1995**, *5*, 499.
(44) Eddaoudi, M.; Kim, J.; Rosi, N.; Vodak, D.; Wachter, J.; O'Keefe, M.; Yaghi, O. M. *Science* **2002**, *295*, 469.

Table 1. Elemental Analysis (%) of Metal-Exchanged Zeolites with Metals Reported Relative to Al Content

metal	sample a	sample b
	Zeolite-A, Formula $Na_aM_bSi_{96}Al_{96}O_{384}$	
Co	0	48
Ni	10	43
Cu	0	96[a]
Mn	8	44
	Zeolite-ZK4, Formula $Na_aM_bSi_{114}Al_{78}O_{384}$	
Co	36	21

[a] This sample is ~100% overexchanged.

was added sodium aluminate (33.032 g), into the other half was added sodium metasilicate (61.92 g), and both portions were stirred until dissolved. Then the silicate solution was transferred quickly into the aluminate solution and mixed until homogeneous. This was sealed in a nalgene bottle (500 mL) and heated at 99 °C for 4 h. This was allowed to cool to room temperature, filtered, washed with distilled water until the filtrate is below pH 9, and dried at 100 °C overnight.

ZK-4. Sodium hydroxide solution (3 g, 50 wt %) and sodium aluminate (10.75 g) were added to distilled water (145 mL) and stirred until dissolved. Tetramethylammonium hydroxide solution (25 wt %, 146 g) and silica sol (38 g, AS-30) were stirred for approximately 30 min. Solutions were combined, mixed thoroughly, sealed in a nalgene bottle, and incubated at 25 °C for 24 h. This was then heated at 100 °C for 30 h, cooled to room temperature, filtered, washed with distilled water (1 L), and dried at 100 °C overnight. The zeolites were calcined in flowing oxygen at 600 °C (maintained for 600 min) with a heating rate of 10 °C min^{-1} to remove organic content.

Powder X-ray diffraction data were collected on a STOE STADIP diffractometer operating on monochromated Cu $K\alpha_1$ radiation. Powder data were collected in Debye−Scherrer geometry using 0.5 mm quartz capillaries over a period of 12 h to determine purity of the synthesized phases.

Ion Exchange of Zeolites. Metal ion-exchanged zeolites were prepared as follows. Typically, the zeolite (5 g) was placed in a 0.05 M solution of the metal acetate (400 mL, distilled water) and stirred for 24 h. The products were recovered by filtration, washed with distilled water (400 mL), and dried at 100 °C overnight. Elemental analysis was carried out to determine the amount of metal ions exchanged by an Agilent 7500 Series ICP-MS spectrometer (Table 1).

NO Adsorption/Desorption Isotherms. The adsorption/desorption of nitric oxide gas in microporous materials was measured using a gravimetric adsorption system. A CI instruments microbalance was thermally stabilized to eliminate the effect from external environment. The microbalance has a sensitivity of 0.1 μg and reproducibility of 0.01% of the load. The pressure of adsorption system was monitored by two BOC Edwards Active gauges in the ranges of 1×10^{-8}−1×10^{-2} and 1×10^{-4}−1×10^{3} mbar, respectively. The sample (~130 mg) was initially outgassed at 573 K under 1×10^{-4} mbar, until no further weight loss was observed. The sample temperature was then decreased to 298 K and kept constant by a circulation water bath with temperature accuracy ±0.02 K. The counterbalance temperature was kept the same as that of the sample to minimize the influence of temperature difference on weight readings, and the sample temperature was monitored using a K type of thermocouple, located close to sample bucket (<5 mm). The variation in sample temperature was minimal (<0.1 K) throughout the experiment. NO gas was introduced into the system until the desired pressure was achieved, and the mass uptake of the sample was measured as a function of time until the adsorption equilibrium was achieved. In this manner an adsorption isotherm was collected by incrementally increasing the pressure and noting the mass gain of the sample at equilibrium. Desorption of nitric oxide gas adsorbed in the samples was performed by gradually decreasing the system pressure to a desired value (until 2×10^{-2} mbar).

NO Loading and Release Experiments. The ion-exchanged zeolite (~0.3 g) was dehydrated for 2 h at 300 °C in vacuo (0.5 mmHg). This was cooled to room temperature and exposed to approximately 2 atm of dry NO (99.5%, Air Liquid) for 30 min, evacuated, and exposed to dry argon. Evacuation and exposure to argon occurred three times.

Quantification of NO Release by Chemiluminescence. NO measurements were performed using a Sievers NOA 280i chemiluminescence NO analyzer. The instrument was calibrated by passing air through a zero filter (Sievers, <1 ppb NO) and 89.48 ppm NO gas (Air Products, balance nitrogen). The flow rate was set to 200 mL/min with a cell pressure of 8.5 Torr and an oxygen pressure of 6.1 psig. To measure NO release from zeolite powders, nitrogen gas of known humidity was passed over the powders, the resultant gas was directed into the analyzer, and the concentration of NO in ppm or ppb was recorded.

To measure the release of NO from pressed disks, the samples were sealed in a glass vial with a septum through which the gas was sampled. Nitrogen was supplied to the vial at a rate to maintain atmospheric pressure inside the vial. Distilled water (0.5 mL) was injected to initiate NO release.

Quantification of NO Release Using Electrochemical Methods. A flow of argon (saturated with water vapor, 5 mL min^{-1}) was passed over a known amount of the NO-loaded zeolite. The gas was then bubbled through phosphate-buffered saline solution (pH 7.4, 10 mL) in which a previously calibrated NO electrode (World Precision Instruments, ISO-NO Mark II) was immersed. The concentration of NO was measured over the course of several hours. All experiments were repeated three times and gave reproducible results. A similar technique was used for measurement of NO in PRP samples (1 mL), except the cuvette was incubated in the platelet aggregometer (37 °C) and was constantly stirred (100 rpm). These experiments were repeated 6 times, and results are illustrated as mean ± se of mean.

Storage Experiments. Vials of NO-loaded Co−LTA were evacuated immediately after loading with NO, and the atmosphere was replaced by dry argon. The flasks were then stored for up to 16 weeks, and the measurements of NO release were repeated at regular intervals.

Platelet Aggregation. The zeolite was ground with PTFE in the desired ratio (75% zeolite/25% PTFE). The mixture was then pressed into disks (5 mm diameter, ~20 mg) under 2 tons for 30 s. The disks were then dehydrated and loaded with NO as described for the powder samples.

Venous blood was drawn from the antecubital fossa of six healthy volunteers (aged 20−40 years) into citrated tubes (0.38% final concentration). Volunteers had not taken any medication known to affect platelet aggregation within the last 10 days. Platelet-rich plasma (PRP) was obtained from whole blood by centrifugation (350*g*; 20 min; room temperature). Platelet-poor plasma (PPP) was obtained by further centrifugation of PRP (1200*g*; 5 min; room temperature).

Zeolite/PTFE disks were suspended in stainless steel wire holders below the surface of the PRP in the aggregometer cuvette, ensuring that they did not interfere with the light beam or the mechanical stirring (1000 rpm). After variation of incubation periods (1−120 min), platelet aggregation was initiated by addition of U46619 (8 μM). Aggregation was measured as a change in turbidity (light transmission) of PRP against a PPP blank.

Electron Microscopy. Parallel aggregation experiments were conducted on separate samples prior to gentle washing of the zeolite/PTFE disks in phosphate buffered saline, fixing in 3% glutaraldehyde and osmium tetroxide, dehydration in graded acetone, and critical point drying with carbon dioxide. The surface of the disks was examined using a Phillips 505 scanning electron microscope following gold−palladium alloy sputter coating (SC500 sputter coater, Emscope Laboratories).

Acknowledgment. P.S.W. and R.E.M. thank the Leverhulme Trust for support, and R.E.M. thanks the Royal Society for the Provision of a University Research Fellowship. M.S.C. is supported by a British Heart Foundation Fellowship (FS/2001060), and S.F. and B.X. are supported by an EPSRC project grant (GR/T09712/01). We thank Mr. S. Mitchell for his help with the electron microscopy.

JA0503579

J|A|C|S
ARTICLES
Published on Web 01/06/2007

High-Capacity Hydrogen and Nitric Oxide Adsorption and Storage in a Metal−Organic Framework

Bo Xiao,[†] Paul S. Wheatley,[†] Xuebo Zhao,[‡] Ashleigh J. Fletcher,[‡] Sarah Fox,[||] Adriano G. Rossi,[||] Ian L. Megson,[§] S. Bordiga,[⊥] L. Regli,[⊥] K. Mark Thomas,*[,‡] and Russell E. Morris*[,†]

Contribution from the EaStChem School of Chemistry, University of St. Andrews, Purdie Building, St. Andrews KY16 9ST, United Kingdom, Northern Carbon Research Laboratories, School of Natural Sciences, Bedson Building, University of Newcastle upon Tyne, Newcastle upon Tyne NE1 7RU, United Kingdom, Free Radical Research Facility, UHI Millennium Institute, Inverness IV2 3BL, United Kingdom, Queen's Medical Research Institute, University of Edinburgh, 47 Little France Crescent, Edinburgh EH16 4TJ, United Kingdom, Dipartimento di Chimica IFM and NIS Centre of Excellence, Univeristà di Torino, Via P. Giuria 7, I-10125 Torino, Italy

Received August 22, 2006; E-mail: mark.thomas@newcastle.ac.uk; rem1@st-and.ac.uk

Abstract: Gas adsorption experiments have been carried out on a copper benzene tricarboxylate metal−organic framework material, HKUST-1. Hydrogen adsorption at 1 and 10 bar (both 77 K) gives an adsorption capacity of 11.16 mmol H_2 per g of HKUST-1 (22.7 mg g^{-1}, 2.27 wt %) at 1 bar and 18 mmol per g (36.28 mg g^{-1}, 3.6 wt %) at 10 bar. Adsorption of D_2 at 1 bar (77 K) is between 1.09 (at 1 bar) and 1.20(at <100 mbar) times the H_2 values depending on the pressure, agreeing with the theoretical expectations. Gravimetric adsorption measurements of NO on HKUST-1 at 196 K (1 bar) gives a large adsorption capacity of ~9 mmol g^{-1}, which is significantly greater than any other adsorption capacity reported on a porous solid. At 298 K the adsorption capacity at 1 bar is just over 3 mmol g^{-1}. Infra red experiments show that the NO binds to the empty copper metal sites in HKUST-1. Chemiluminescence and platelet aggregometry experiments indicate that the amount of NO recovered on exposure of the resulting complex to water is enough to be biologically active, completely inhibiting platelet aggregation in platelet rich plasma.

Introduction

Porous materials of many different kinds[1] continue to be at the forefront of attempts to develop many emerging technologies; in particular, gas adsorption properties of porous materials are currently receiving great interest in many areas of science. Potential uses of these solids range from separations of mixtures to gas storage media for energy,[2] environmental,[3] and biological applications.[4] Metal−organic frameworks (MOFs), with their extremely high surface areas and porosity and their varied chemical compositions, are good candidates for high adsorption capacities of various gases. HKUST-1 is a copper benzene tricarboxylate porous material first reported by Williams and co-workers[5] and subsequently studied by numerous research groups. Perhaps the most interesting feature of this material is the presence of a metal site in the walls of the material that, after dehydration, is potentially available to act as a site where coordination to a gas molecule can take place.

Hydrogen adsorption and storage is of great interest as a method of providing the gas as a fuel for zero-emission energy production. The approaches currently being adopted for the design of hydrogen storage materials are based on many different types of material, ranging from metal hydrides[6] and carbon nanotubes and nanohorns[7] to gas clathrates,[8] although all have significant problems attached to them. Nanoporous materials, with their inherently large internal pore volumes and

[†] University of St. Andrews.
[‡] University of Newcastle upon Tyne.
[§] Free Radical Research Facility, UHI Millennium Institute.
[||] University of Edinburgh.
[⊥] Univeristà di Torino.

(1) (a) Davis, M. E. *Nature* **2002**, *417*, 813. (b) Corma, A.; Diaz-Cabanas, M.; Jorda, J. L.; Martinez, C.; Moliner, M. *Nature* **2006**, *443*, 842. (c) Cooper, E. R.; Andrews, C. D.; Wheatley, P. S.; Webb, P. B.; Wormald, P.; Morris, R. E. *Nature* **2004**, *430*, 1012.
(2) (a) Eddaoudi, M.; Kim, J.; Rosi, N.; Vodak, D.; Wachter, J.; O'Keefe, M.; Yaghi, O. M. *Science* **2002**, *295*, 469. (b) Rosi, N. L.; Eckert, J.; Eddaoudi, M.; Vodak, D.; Kim, J.; O'Keefe, M.; Yaghi, O. M. *Science* **2003**, *300*, 1127. (c) Zhao, X.; Xiao, B.; Fletcher, A. J.; Thomas, K. M.; Bradshaw, D.; Rosseinsky, M. J. *Science* **2004**, *306*, 1012. (d) Ferey, G.; Mellot-Draznieks, C.; Serre, C.; Millange, F.; Dutour, J.; Surble, S.; Margiolaki, I. *Science* **2005**, *309*, 2040.
(3) Millward, A. R.; Yaghi, O. M. *J. Am. Chem. Soc.* **2005**, *127*, 17998.
(4) Wheatley, P. S.; Butler, A. R.; Crane, M. S.; Fox, S.; Xiao, B.; Rossi, A. G.; Megson, I. L.; Morris, R. E. *J. Am. Chem. Soc.* **2006**, *128*, 502.
(5) Chui, S. S. Y.; Lo, S. M. F.; Charmant, J. P. H.; Orpen, A. G.; Williams, I. D. *Science* **1999**, *283*, 1148.
(6) (a) Schlapbach, L.; Züttel, A.; *Nature* **2001**, *414*, 353. (b) Bogdanovic, B.; Felderhoff, M.; Pommerin, A.; Schuth, T.; Spielkamp, N. *Adv. Mater.* **2006**, *18*, 1998.
(7) (a) Dillon, A. C.; Jones, K. M.; Bekkedahl, T. A.; Kiang, C. H.; Bethune, D. S.; Heben, M. J. *Nature* **1997**, *386*, 377. (b) Zhou, Y.; Feng, K.; Sun, Y.; Zhou, L. *Chem. Phys. Lett.* **2003**, *380*, 526. (c) Shiraishi, M.; Takenobu, T.; Kataura, H.; Ata, M. *Appl. Phys.* **2004**, *A78*, 947. (d) H. Kanoh, H.; Yudasaka, M.; Iijima, S.; Kaneko, K. *J. Am. Chem. Soc.* **2005**, *127*, 7511.
(8) Lee, H.; Lee, J. W.; Kim, D. Y.; Park, J.; Seo, Y. T.; Zeng, H.; Moudrakovski, I. L.; Ratcliffe, C. I.; Ripmeester, J. A. *Nature* **2005**, *434*, 743.

10.1021/ja066098k CCC: $37.00

surface areas are obvious candidates for high-capacity storage materials. MOFs have great promise in this area, and HKUST-1 has been shown to be capable of adsorbing significant amounts of hydrogen at 77 K. There are, however, significant questions still to be answered. From the literature it is clear that, while hydrogen adsorption capacity is still usually below the levels required for commercial application, high-capacity materials are being prepared. The relatively weak interaction between the hydrogen molecule and the walls of porous solids means that this adsorption is only significant at low temperatures, which might further limit the possible applications.

High nitric oxide (NO) adsorption is of great interest for environmental applications in gas separation and NO*x* traps for lean burn engines. NO is also an extremely important molecule in biology, and NO-storing solids have potential applications as antithrombosis materials.[9] NO is a crucial biological agent in the cardiovascular, nervous, and immune systems.[10] NO synthesized by endothelial cells that line blood vessels mediates a number of vital functions, including vasodilation[11,12] and inhibition of platelet[13] and inflammatory cell[14,15] activation and adhesion. In addition, NO is an important neurotransmitter and neuromodulator in the peripheral and central nervous systems,[16] and its synthesis in high concentrations contributes to the cytotoxic effects of inflammatory cells on invading pathogens.[17]

The delivery of exogenous NO is an attractive therapy for a number of ailments, but the range and diversity of its effects make target specificity a major concern, which has held back the development of some NO applications. To overcome this problem requires the development of materials that can store significant quantities of NO and then deliver it to specific sites in the body. There is currently particular interest in using NO delivery materials to prevent life-threatening complications associated with thrombosis formation at the surface of medical devices such as stents and catheters.[9]

A number of materials have been proposed as delivery agents for exogenous NO. Perhaps the chemically most advanced are those based on polymers or silica functionalized with secondary amines, which, on reaction with NO, form ionic diazeniumdiolates that can be used to increase the thromboresistivity of polymers.[9,18,19] Two molecules of NO react with each amine (giving rise to the trivial name NONOate) and are released on contact with moisture at an appropriate pH. Other methods of release have also been explored, including the light-activated release of nitric oxide from metal containing polymers.[20] More recently zeolites, nanoporous inorganic framework materials normally associated with the destruction of NO in deNOx catalysis, have also been shown to be high-storage capacity materials for NO, with maximum adsorption capacities of around 1 mmol g^{-1} at 298 K.[4]

A specific potential use for NO-releasing materials in the cardiovascular arena centers on the prevention of thrombosis on artificial surfaces that come into contact with blood, particularly in relation to procedures that require extracorporeal circuits, such as bypass and renal replacement therapy, catheter implantations, or stents that are used in interventional cardiology to improve the patency of partially blocked arteries.[9] Current best practice to prevent thrombosis in these situations involves the administration of heparin, other anticoagulants, or antiplatelet agents to the patient, with the inherent risk of hemeorrhagic[21,22] or paradoxical thrombotic[23] complications. Stent coatings that release antithrombotic,[2424] antiinflammatory,[25] and antimitogenic[26] agents to reduce in-stent thrombosis or restenosis have met with some success, but NO might be expected to have all of these effects if delivered at the appropriate rate for a sufficient duration. Other potential uses of these types of solid, as shown by a number of different biological effects, include antibacterial coatings[27] and wound-healing promoters.[28]

Here we report the full characterization of the porous nature of HKUST-1 using N_2 and CO_2 adsorption together with a demonstration of high H_2 and D_2 adsorption. We also show that HKUST-1 adsorbs significantly more NO than any other porous solid yet reported and that it releases enough NO on contact with a physiological solution (platelet-rich plasma) to fully inhibit platelet aggregation.

Results and Discussion

Hydrogen Adsorption Studies. HKUST-1 was synthesized according to the method reported by Williams and co-workers.[5] The powder X-ray diffraction pattern indicated that there were none of the impurities reported in the initial publications. Nitrogen (77 K) and carbon dioxide (195 K) adsorption studies were used to characterize the pore volume in the material, giving values of 0.684 and 0.703 $cm^3\ g^{-1}$, respectively. Pore volumes of HKUST-1 obtained from N_2 adsorption have been reported as 0.33 $cm^3\ g^{-1}$ by Chui et al.[5] and 0.4 $cm^3\ g^{-1}$ in Lee's paper;[29]

(9) Keefer, L. K. *Nat. Mater.* **2003**, *2*, 357.
(10) Moncada, S.; Palmer, R. M. J.; Higgs, E. A. *Pharmacol. Rev.* **1991**, *43*, 109.
(11) Furchgott, R. F.; Zawadzki, J. V. *Nature* **1980**, *288*, 373.
(12) Palmer, R. M. J.; Ferrige, A. G.; Moncada, S. *Nature* **1987**, *327*, 524.
(13) Radomski, M. W.; Palmer, R. M. J.; Moncada, S. *Lancet* **1987**, *2*, 1057.
(14) Bath, P. M. W.; Hassall, D. G.; Gladwin, A. M.; Palmer, R. M. J.; Martin, J. F. *Arterioscler. Thromb.* **1991**, *11*, 254.
(15) Kubes, P.; Suzuki, M.; Granger, D. N. *Proc. Natl. Acad. Sci. U.S.A.* **1991**, *87*, 5193.
(16) Garthwaite, J. *Trends Neurosci.* **1991**, *14*, 60.
(17) Nathan, C. F.; Hibbs, J. B. *Curr. Opin. Immunol.* **1991**, *3*, 65.
(18) (a) Parzuchowski, P. G.; Frost, M. C.; Meyerhoff, M. E. *J. Am. Chem. Soc.* **2002**, *124*, 12182. (b) Lee, Y.; Oh, B. K.; Meyerhoff, M. E. *Anal. Chem.* **2004**, *76*, 536. (c) Zhang, H. P.; Annich, G. M.; Miskulin, J.; Stankiewicz, K.; Osterholzer, K.; Merz, S. I.; Bartlett, R. H.; Meyerhoff, M. E. *J. Am. Chem. Soc.* **2003**, *125*, 5015. (d) Frost, M. C.; Rudich, S. M.; Zhang, H. P.; Maraschio, M. A.; Meyerhoff, M. E. *Anal. Chem.* **2002**, *74*, 5942. (e) Zhang, H. P.; Annich, G. M.; Miskulin, J.; Osterholzer, K.; Merz, S. I.; Bartlett, R. H.; Meyerhoff, M. E. *Biomaterials* **2002**, *23*, 1485.
(19) (a) Mowery, K. A.; Schoenfisch, M. H.; Saavedra, J. E.; Keefer, L. K.; Meyerhoff, M. E. *Biomaterials* **2000**, *21*, 9. (b) Mowery, K. A.; Schoenfisch, M. H.; Baliga, N.; Wahr, J. A.; Meyerhoff, M. E. *Electroanalysis* **1999**, *11* 681. (c) Espadas-Torre, C.; Oklejas, V.; Mowery, K.; Meyerhoff, M. E. *J. Am. Chem. Soc.* **1997**, *119*, 2321.
(20) (a) Mitchell-Koch, J. T.; Reed, T. M.; Borovik, A. S. *Angew. Chem.* **2004**, *43*, 2806. (b) Padden, K. M.; Krebs, J. F.; MacBeth, C. E.; Scarrow, R. C.; Borovik, A. S *J. Am. Chem. Soc.* **2001**, *123*, 1072.
(21) Sundlof, D. W.; Rerkpattanapitat, P.; Wongpraparut, N.; Pathi, P.; Kotler, M. N.; Jacobs, L. E.; Ledley, G. S.; Yazdanfar, S. *Am. J. Cardiol.* **1999**, *83*, 1569.
(22) Bennett, C. L.; Connors, J. M.; Carwile, J. M.; Moake, J. L.; Bell, W. R.; Tarantolo, S. R.; McCarthy, L. J.; Sarode, R.; Hatfield, A. J.; Feldman, M. D.; Davidson, C. J.; Tsai, H. M. *N. Engl. J. Med.* **2000**, *342*, 1773.
(23) Chong, B. H. *J. Thromb. Haemostasis* **2003**, *1*, 1471.
(24) Aggarwal, R. K.; Martin, W. A.; Azrin, M. A.; Ezekowitz, M. D.; de Bono, D. P.; Gershlick, A. H. *Circulation* **1996**, *94*, 1510.
(25) Strecker, E. P.; Gabelmann, A.; Boos, I.; Lucas, C.; Xu, Z. Y.; Haberstroh, J.; Freudenberg, N.; Stricker, H.; Langer, M.; Betz, E. *Cardiovasc. Intervent. Radiol.* **1998**, *21*, 487.
(26) Colombo, A.; Drzewiecki, J.; Banning, A.; Grube, E.; Hauptmann, K.; Silber, S.; Dudek, D.; Fort, S.; Schiele, F.; Zmudka, K.; Guagliumi, G.; Russell, M. E. *Circulation* **2003**, *108*, 788.
(27) Nablo, B. J., Chen, T.-Y.; Schoenfisch, M. H. *J. Am. Chem. Soc.* **2001**, *123*, 9712.
(28) Shabani, M.; Pulfer, S. K.; Bulgrin, J. P.; Smith, D. J. *Wound Rep. Regen.* **1996**, *4*, 353.
(29) Lee, J.-Y.; Li, J.; Jagiello, J. *J. Solid State. Chem.* **2005**, *178*, 2527.

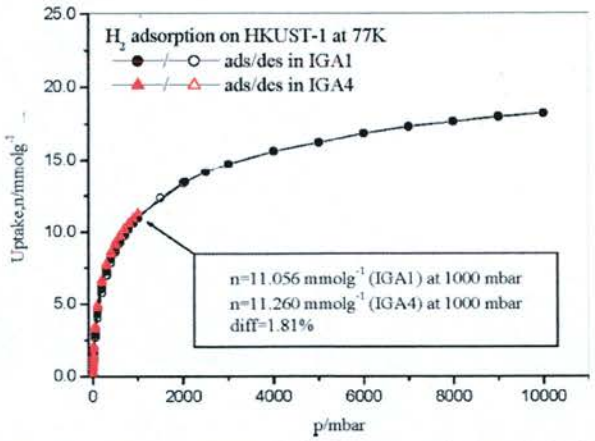

Figure 1. Adsorption and desorption isotherms (77 K) for H_2 on HKUST-1 to 1 bar (red triangles) and to 10 bar (black circles). The repeatability is <2% at 1 bar. IGA1 and IGA4 are different instruments for high- and low-pressure measurements respectively.

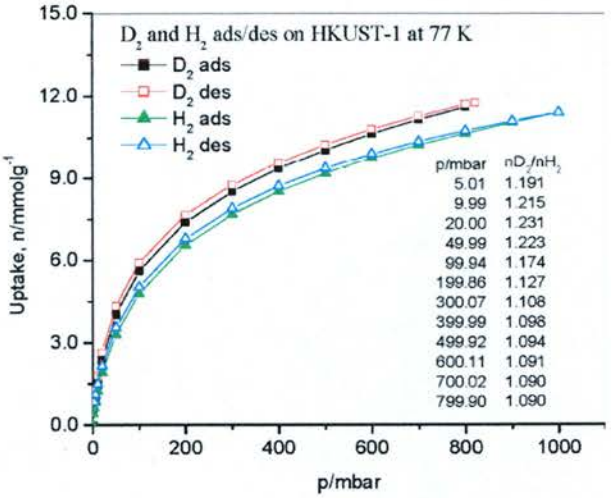

Figure 2. H_2 and D_2 adsorption desorption isotherms (77 K to 1 bar) on HKUST-1. The D_2/H_2 ratio of adsorption at 800 mbar is 1.09.

Rowsell et al.[31] reported a value of 0.75 $cm^3\ g^{-1}$. The calculated crystallographic pore volume obtained from PLATON is ~0.72 $cm^3\ g^{-1}$.

Highly crystalline materials such as HKUST-1 should have very repeatable pore structures and adsorption properties, but reports of hydrogen adsorption properties of HKUST-1 vary quite substantially. Lee et al.[29] and Prestipino et al.[30] both report a H_2 uptake of ~6 mmol g^{-1} (~12.5 mg g^{-1}, ~1.25 wt %), while Yaghi and co-workers report 12.4 mmol g^{-1} (25 mg g^{-1}, 2.5 wt %)[31] in one paper and nearer 7.9 mmol g^{-1} (16 mg g^{-1}, 1.6 wt %)[32] in another (all measurements 77 K and 1 bar. Note that the result from ref 32 is based on interpolation of a high-pressure isotherm). The issues with regard to repeatability of nitrogen adsorption measurements for HKUST-1 may be attributed to (1) sample purity and (2) sample activation. The presence of amorphous or nonporous impurity phases must be eliminated. Activation involves removal of any guest molecules that are contained within the pores of the material, either through thermal or chemical means (or through a combination of the two). The stage where the template has been completely removed by evacuation to give the porous structure has to be established carefully. Good agreement between pore volumes obtained from crystallographic studies and gas adsorption is necessary to confirm the purity of the material. In the case of H_2 adsorption measurements, there are additional considerations since the experimental system must be ultraclean and it is necessary to purify even ultrahigh-purity hydrogen before the measurements.

Several hydrogen adsorption experiments were repeated using samples of HKUST-1 from different batches and different adsorption instruments and to pressures of 1 and 10 bar (77 K). We have carefully characterized the buoyancy corrections needed, and the repeatability of the results gives us great confidence that the sample- and instrument-dependent factors have been controlled (See Supporting Information).

Gravimetric measurements at 1 bar indicate an average H_2 adsorption capacity of ~11.16 mmol g^{-1} of HKUST-1 (22.7 mg g^{-1}, 2.27 wt %, Figure 1) comparable to the highest results reported by Yaghi and co-workers.[31] The isotherm is repeatable to within 1.8% on different instruments and using different samples of HKUST-1. At higher pressure (10 bar) the adsorption capacity increases up to approximately 18 mmol per g (36.28 mg g^{-1}, 3.6 wt % Figure 1). Yaghi and co-workers[32] reported the adsorption isotherms up to 80 bar as only 16.17 mmol g^{-1} (32.6 mg g^{-1}, 3.26 wt %). D_2 adsorption on HKUST-1 at 77 K up to 1 bar (Figure 2) shows a slight increase in adsorption capacity (from 1.09 to 1.20 times the H_2 values depending on the pressure). This is consistent with adsorption studies on porous carbons[33] and zeolites[34] and is due to quantum mechanical effects. The density of the adsorbed hydrogen calculated from the maximum amount adsorbed determined using the Langmuir equation and the N_2 pore volume was ~0.057 g cm^{-3}. This value is similar to densities for porous carbons and lower than 0.0708 g cm^{-3} for liquid H_2 at 20.2 K.[35]

These results show that the maximum adsorption capacity of HKUST-1 for hydrogen at 77 K was 11.16 mmol g^{-1}, or approximately 2.27 wt % at 1 bar rising to approximately 18 mmol g^{-1} at 10 bar. None of the samples we measured showed the lower adsorption capacities reported by Lee et al. and Prestipino et al.

Nitric Oxide Adsorption Studies

Nitric oxide adsorption is important for a number of applications, with particular potential for impact in the medical and biological areas. Materials based on organic[19] and metal-containing polymers,[21] and zeolites[4] have all been proposed as NO adsorbents. The adsorption capacity of these materials ranges from quite low values in the μmol NO per g range[21] up to approximately 1 to 1.5 mmol NO per g of material.[4,19] Although adsorption capacity is not the only consideration in

(30) Prestipino, C.; Regli, L.; Vitillo, J. G.; Bonino, F.; Damin, A.; Lamberti, C.; Zecchina, A.; Solari, P. L.; Kongshaug, K. O.; Bordiga, S. *Chem. Mater.* **2006**, *18*, 1337.
(31) Rowsell, J. L. C.; Yaghi, O. M. *J. Am. Chem. Soc.* **2006**, *128*, 1304.
(32) Wong-Foy, A. G.; Matzger, A. J.; Yaghi, O. M. *J. Am. Chem. Soc.* **2006**, *128*, 3494.
(33) (a) Zhao, X. B.; Xiao, B.; Fletcher, A. J.; Thomas, K. M. *J. Phys. Chem. B* **2005**, *109*, 8880. (b) Zhao, X. B.; Villar-Rodil, S.; Fletcher, A. J.; Thomas, K. M. *J. Phys. Chem. B* **2006**, *110*, 9947.
(34) Stephanie-Victoire, F.; Goulay, A. M.; de Lara, E. C. *Langmuir* **1998**, *14*, 7255.
(35) *CRC Handbook of Chemistry and Physics*, 74th ed.; CRC Press: Boca Ratan, Florida, 1993.

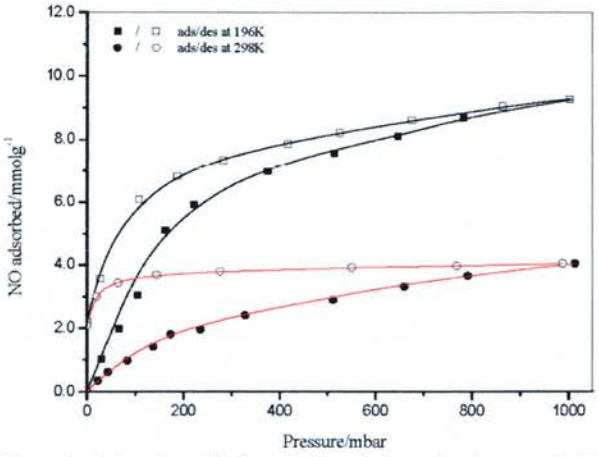

Figure 3. Adsorption (filled symbols) and desorption (open symbols) isotherms at 196 K (squares) and 298 K (circles) for nitric oxide on HKUST-1.

determining the effectiveness of a material, it is advantageous to maximize the adsorption capacity of a material to increase the reservoir of stored gas. NO is physisorbed in the pores and also coordinates with the metal sites present in HKUST-1. Gravimetric adsorption measurements on HKUST-1 at 196 K (1 bar) gives a large adsorption capacity of ~9 mmol g^{-1}, which is significantly greater than any other adsorption capacity reported on a porous solid. At 298 K the adsorption capacity at 1 bar is just over 3 mmol g^{-1}. These values are high, bearing in mind that the NO critical temperature and pressure are 180.1 K and 64.83 bar. There is significant isotherm hysteresis at both temperatures, indicative of the strong irreversible adsorption of some of the NO molecules on the open copper sites that line the walls of the pores in dehydrated HKUST-1. At both temperatures, there is about 2.21 mmol g^{-1} that is not desorbed when the pressure of NO is reduced to almost zero. This corresponds to ~1 NO per dicopper(II) tetracarboxylate building block for HKUST-1. The results indicate that HKUST-1 is potentially a very good storage material for NO, with a very high capacity compared to those of zeolites and organic polymers.

IR studies

The dehydrated form of HKUST-1 has accessible copper sites in the walls of the framework itself. Given the well-known tendency of NO to form metal coordination complexes, it seems likely that the hysteresis seen in the adsorption−desorption isotherms of NO on HKUST-1 (Figure 3) is due to trapping of the gas on the metal. Infrared spectroscopy is the technique of choice for probing such bond formation in these solids.

Figure 4 reports the effect NO interaction at room temperature on HKUST-1 monitored by IR spectroscopy. The IR spectrum of a dehydrated HKUST-1 sample is reported in red. The two sharp bands at 1912 and 1886 cm^{-1} are due to overtones and combination modes of framework vibrations, while the 1750−1200 cm^{-1} region is dominated by very intense bands due to asymmetric and symmetric modes of carboxylate (Raman doublet at 1550 and 1460 cm^{-1}), bands due to benzene ring stretching modes and C−H bending vibrations.[36]

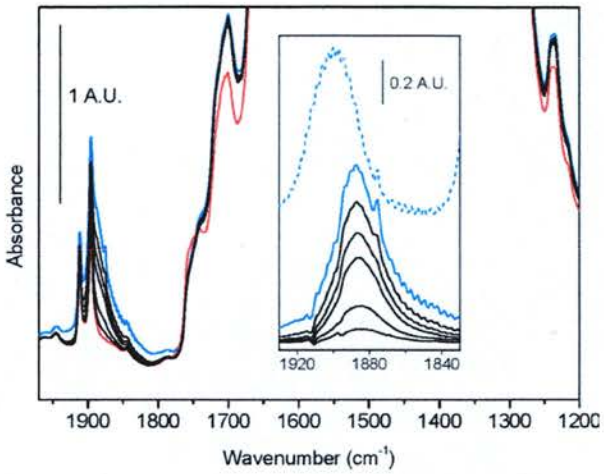

Figure 4. Interaction with NO monitored by IR spectroscopy. Red curve: HKUST-1 outagassed at 180 °C. Blue curve: effect of 30 Torr of NO. Black curves: effect of increasing pumping, residual pressure 10^{-3} Torr. (Inset) Background-subtracted spectra in the region of NO stretching (same color code). In the upper part of the inset (blue dashed curve) the spectrum of NO adsorbed at room temperature on a Cu−ZSM-5 zeolite is reported for comparison.

Upon contact with 30 Torr of NO, (blue curve) the growth of a new component at 1887 cm^{-1} is clearly visible, testifying to the formation of a Cu(II)···NO adduct. In the meantime some further changes are observed in the framework modes of HKUST-1, suggesting that the material responds to the NO adsorption. In particular, we observe the erosion of a shoulder at 1755 cm^{-1}, the parallel growth of a component at 1735 cm^{-1} (isosbestic point at 1745 cm^{-1}), and the intensity increase of the bands at 1700 and at 1237 cm^{-1}. The effect of progressive outgassing is reported with black curves. The last spectrum is obtained after outgassing for 15 min at room temperature in dynamic vacuo with a residual partial pressure of 10^{-3} Torr.

The spectroscopic features of NO adsorbed on Cu(II) species are better illustrated in the inset of Figure 4 (same color code) where difference spectra are reported. The Cu(II)···NO adduct is characterized by a band at 1887 cm^{-1} that decreases in intensity without substantial shifts. A $\Delta\nu(NO) = +11$ cm^{-1} with respect to νNO in the gas phase ($\nu^0_{N-O} = 1876$ cm^{-1}) is close to what has been obtained in case of Cu(II)···(NO) complex in copper-exchanged zeolites and similar systems,[37−39] where a band in the range 1910−1880 cm^{-1} has been observed. For sake of comparison the spectrum obtained at room temperature on a Cu(ZSM-5) is reported as dashed blue curve in the inset of Figure 4.[38]

Spectroscopic data on copper nitrosylic complexes have been obtained by Zhou et al.[40] They have studied the formation of Cu(NO), $[Cu(NO)]^+$, and $[Cu(NO)]^-$ in neon matrices,[40,41] finding a strong similarity between the spectroscopic features of $[Cu(NO)]^+$ species (1907.8 cm^{-1}) and that obtained in the case of Cu(II)-exchanged zeolites. In particular, it has been observed that the N−O stretching frequency reported for Cu-

(36) Prestipino, C.; Regli, L.; Vitillo, J. G.; Bonino, F.; Damin, A.; Lamberti, C.; Zecchina, A.; Solari, P. L.; Kongshaug, K. O.; Bordiga, S. *Chem. Mater.* **2006**, *18*, 1337.

(37) Bordiga, S.; Pazè, C.; Berlier, G.; Scarano, D.; Spoto, G.; Zecchina, A. *Catal. Today* **2001**, *70*, 91.

(38) Lamberti, C.; Bordiga, S.; Salvalaggio, M.; Spoto, G.; Zecchina, A.; Geobaldo, F.; Vlaic, G.; Bellatreccia, M. *J. Phys. Chem. B* **1997**, *101*, 344.

(39) Llabrés i Xamena, F. X.; Fisicaro, P.; Berlier, G.; Zecchina, A.; Turnes Palomino, G.; Prestipino, C.; Bordiga, S.; Giamello, E.; Lamberti, C. *J. Phys. Chem. B* **2003**, *107*, 7036.

(40) Zhou, M.; Andrews, L. *J. Phys. Chem. A* **2000**, *104*, 2618.

(41) Andrews, L.; Citra A. *Chem. Rev.* **2002**, *102*, 885.

(II)−NO/zeolite is near 1900 cm^{-1}, a value very close to that observed for $[Cu(NO)]^+$, which suggests a +1.0 net charge on the Cu(NO) center for this formal Cu(II)−NO/zeolite species. The $Cu(NO)^+$ complex has been described in an ab initio study by Thomas et al.[42] who calculated a binding energy of 91 kJ/mol.

A strong interaction energy and the fact that ν(NO) in the Cu(II)···NO adduct appears only slightly shifted from that of the molecule in the gas phase can be explained by considering that the observed frequency is the final result of competitive effects: (i) the polarization effect and σ donation that give an upward shift and (ii) the π back-donation that gives the opposite effect. The fact that the ν(NO) in the Cu(II)···NO adduct formed in HKUST-1 is at lower frequency than that observed in Cu−ZSM-5 suggests that in this case the back-donation is more effective. This fact is in agreement with the qualitative observation that the stability of the Cu(II)···NO adducts formed in Cu−ZSM-5 is lower (complete reversibility at room temperature) than that found in HKUST-1. A dedicated study to obtain more quantitative data about the stability of the complex Cu(II)···NO formed in HKUST-1 is in progress.

Quantification of NO Release

Of course, to make use of a material as a gas storage medium does not just entail being able to adsorb large quantities of the gas but to be able to control the release of the gas at the time and at the rate required for the particular application. The optimum rate of release of NO differs, depending on the exact nature of the target application. For example, for antithrombotic applications the rate of release of NO required should approximate the rate released by the endothelial cells that line the blood vessels in mammals. This rate is quite slow, relating to around 1 pmol min^{-1} mm^{-2}.[9] On the other hand it seems that the antibacterial effects of NO require greater flux of the gas. In our work on zeolites we have shown that exposure of the NO-loaded material to a nucleophile such as water triggers release of the NO. The standard method of measuring NO release from a powdered solid is to expose the material to a flow of wet gas at a controlled relative humidity and measure the NO in the outlet stream using the intensity of chemiluminescence on reaction of NO with ozone. Such experiments carried out on NO-loaded HKUST-1 (Figure 5) indicate that NO is released on contact with water vapor in a manner similar to that seen previously for zeolites. However, the total amount of NO released is 2 orders of magnitude less (2 μmol NO per g of HKUST-1) than the amount initially adsorbed. This is not necessarily a detrimental property as biological applications can require only a very low flux of NO, and we show below that this release of NO is sufficient to completely inhibit platelet aggregation in biological experiments. The total amount of NO released is also significantly less than that seen for zeolites or NONOate polymers but is comparable to the amount of NO released by metal-containing polymers.

Bioactivity of NO-Loaded HKUST-1

The need for improvements in the biocompatibility of materials is a very important target. This is particularly true for blood-contacting solids that are used in vascular grafts and in extracorporeal tubing used in coronary bypass surgery and kidney dialysis. Life-threatening complications can occur if thrombosis formation (platelet aggregation and adhesion) is induced by artificial materials that are in contact with blood. Thrombus formation in healthy circulatory systems is inhibited in a number of ways, including the production of small quantities (approximately 1 pmol min^{-1} mm^{-2}; see reference 9) of NO by the endothelial cells that line the blood vessels and also by platelets. A potentially important strategy for reducing postoperative complications is to make medical devices out of a NO-releasing material, thereby mimicking the antithrombotic action of the endothelial cells.

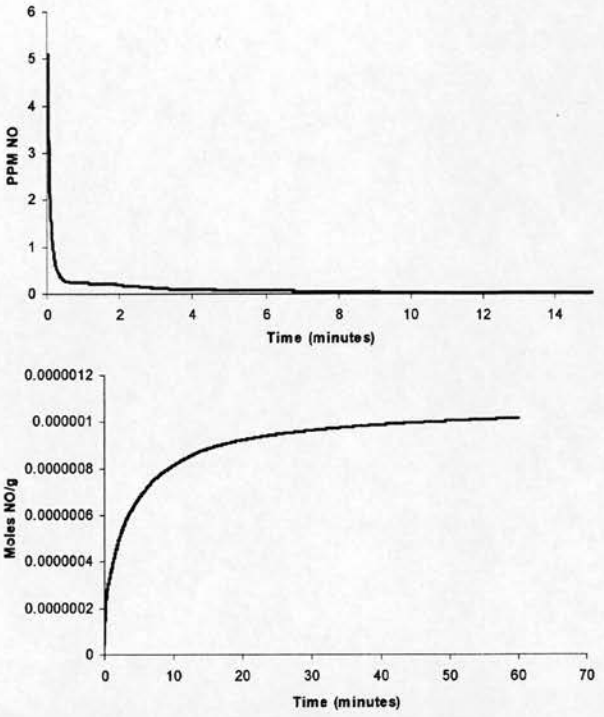

Figure 5. NO release profile for NO-loaded HKUST-1 (top) and the cumulative NO released per g of HKUST-1 (bottom).

To overcome the problem of the nondispersion of powders in the liquid-phase, samples of HKUST-1 were prepared as pressed disks with small amounts of poly(tetrafluoroethylene) (PTFE) polymer as a binder. The NO-loaded disks were stored under an inert atmosphere for up to several weeks before being used in further experiments.

The HKUST-1/PTFE disks were suspended by a stainless steel wire holder below the surface of platelet-rich plasma (PRP) in the cuvette of a four-channel platelet aggregometer (Chronolog, Labmedics, Stockport, UK) at 37 °C. After a short induction period (1 min), platelet aggregation was initiated using the pro-aggregatory agent, collagen (2.5 μg mL^{-1}), and then measured as a change in turbidity (light transmission) of PRP against a platelet-poor plasma (PPP) reference. Figure 6 shows that a NO-loaded HKUST-1/PTFE sample completely inhibits platelet aggregation. Addition of the NO-scavenger, oxyhemoglobin (40 μM), prevents the inhibitory effect, confirming the central role for NO in the inhibitory process and excluding the possibility that the effects of the NO−HKUST-1 were merely cytotoxic. Furthermore, a control consisting of only HKUST-1

(42) Thomas, J. L. C.; Bauschlicher, C. W., Jr.; Hall, M. B. *J. Phys. Chem. A* **1997**, *101*, 8530.
(43) *Lange's Handbook of Chemistry*, 15th ed.; McGraw-Hill: New York, 1999.

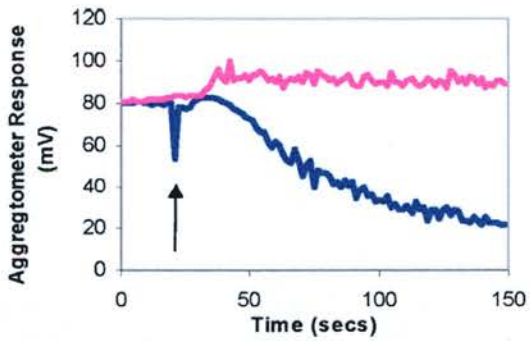

Figure 6. Platelet aggregation experiments show that this material inhibits platelet aggregation completely. (Pink = NO-HKUST-1. Blue = control.) On initiation of aggregation (by addition of collagen marked by the arrow) the aggregometer response for the control (blue) indicates that the platelets have aggregated and fallen out of suspension. However, there is no such response for the NO-loaded HKUST-1 sample (pink). This indicates that the amount of NO released by the HKUST-1 is sufficient to completely inhibit platelet aggregation in this experiment.

without NO failed to inhibit aggregation, ruling out any effect from the material itself. For short term applications NO-loaded HKUST-1 seems very promising for antithrombotic applications in that it releases NO at a suitable rate. Unfortunately, however, its stability in biological solutions is limited. Even after a few hours exposure to platelet-rich plasma, the solution itself began to go green, indicating dissolution of the copper from the framework material. Clearly this is an issue as the toxicological implications of excess coppers ions in, for example, human blood may be enough to prevent application of such materials. Further work in this area is ongoing.

Concluding Remarks

Metal−organic frameworks, such as HKUST-1, are clearly of interest because of their very high adsorption capacities. The hydrogen adsorption measurements are entirely consistent with other gas adsorption measurements and the crystallographic studies. The relatively weak interaction of hydrogen with the walls of a porous solid means that adsorption is restricted to low temperatures. In addition, other gases may well adsorb more strongly than hydrogen, leading to problems unless the hydrogen is ultrapure. This may be exacerbated in materials such as HKUST-1 where there are open metal sites that will interact strongly with other gases or water. However, for adsorption of gases such as NO that do interact strongly with metals, this may be an advantage. In biological applications, the relatively poor stability of MOFs in physiological solutions, and their rather unstudied toxicology, mean that their undoubted promise needs further development before applications can be found. Having said that, however, it is clear that HKUST-1 is a very high-capacity adsorption material. Both hydrogen and nitric oxide adsorb in high quantities on HKUST-1, confirming their applicability as potential gas storage materials for energy, environmental, and biological applications.

Experimental Section

Synthesis of HKUST-1. In a typical synthesis, 3.0 mmol of $Cu(NO_3)_2{\cdot}3H_2O$ (0.716 g) and 2.0 mmol of benzene 1,3,5-tricarboxylic acid (0.421 g) were mixed with 12 mL of EtOH/H_2O (50:50) solution in a Teflon-lined autoclave. The mixture was stirred for 30 min at ambient temperature prior to heating in an oven preheated at 383 K, followed by heating at 383 K for 24 h. After crystallization the autoclave was naturally cooled down to room temperature. The yield was sonicated for 5−10 min in a solution of EtOH/H_2O (50:50). Large, turquoise-blue crystals were isolated by Büchner filtration and dried in air for 1 day.

Gas Adsorption/Desorption Measurements. Gases. Ultrapure hydrogen (H_2 99.9999%, H_2O < 500 ppb, N_2 < 200 ppb, O_2 < 100 ppb, CO + CO_2 < 50 ppb, total hydrocarbons <50 ppb) hydrogen was supplied by Air Products Ltd. Deuterium (99.98% D_2), nitrogen (99.9995%), and carbon dioxide (99.999%) were supplied by BOC Ltd.

H_2/D_2 Purification. Hydrogen and deuterium were purified using a two-stage process involving adsorption on a zeolite (calcium alumino silicate (1/16 in. pellets)), at 298 K to remove any water vapor present, and activated carbon (G212, particle size 6 × 12 mesh) at 195 K to remove hydrocarbons and other gas impurities.[33] The impurities were adsorbed under these conditions, while little or no hydrogen or deuterium was adsorbed at 195 K. Both adsorbents were degassed at 700 K prior to use.

Adsorption Studies for H_2, D_2, N_2, and CO_2. The adsorption/desorption characteristics of H_2, D_2, N_2, and CO_2 were studied using a Hiden Isochema Gravimetric Analyzer, which is an ultraclean, ultrahigh-vacuum system with a diaphragm and turbo pumping system. The microbalance had a long-term stability of ±1 μg with a weighing resolution of 0.2 μg. The sample was degassed at 453 K under ultrahigh vacuum (10^{-10} bar) until no further weight loss occurred prior to H_2 and D_2 adsorption. The approach to equilibrium was measured in real time using a computer algorithm. The pressure was monitored by three pressure transducers with ranges 0−0.2, 0−10, and 0−100 kPa and maintained at the set point by active computer control of inlet/outlet valves throughout the duration of the adsorption kinetic experiments. The accuracy of the set-point pressure regulation was ±0.02% of the range used. Both the sample and counterweight sides of the balance were cooled to 77 K for the H_2 and D_2 adsorption/desorption experiments in order to minimize buoyancy corrections and thermal transpiration effects. A detailed buoyancy correction was carried out on the basis of experimental measurements of the system buoyancy and the helium density of HKUST-1.

The major problem with studying H_2 and D_2 adsorption and desorption is the adsorption of impurities from both the adsorptive gas used and within the UHV system.[33] The measurement protocols used in this study were validated by the complete desorption of H_2 with little or no isotherm hysteresis. More detailed validation of the protocols has been presented previously.[33]

NO Adsorption/Desorption Measurements. The adsorption/desorption of NO gas in HKUST-1 was measured using a gravimetric adsorption system. A CI instruments microbalance was thermally stabilized to eliminate the effect from external environment. The microbalance has a sensitivity of 0.1 μg and reproducibility of 0.01% of the load. The pressure of the adsorption system was monitored by two BOC Edwards Active gauges in the ranges of 1×10^{-8}−1×10^{-2} and 1×10^{-4}−1×10^{3} mbar, respectively. The sample (~130 mg) was initially outgassed at 573 K under 1×10^{-4} mbar, until no further weight loss was observed. The sample temperature was then decreased to 298 K and kept constant by a circulation water bath with temperature accuracy ±0.02 K. The counterbalance temperature was kept the same as that of the sample to minimize the influence of temperature difference on weight readings, and the sample temperature was monitored using a K type of thermocouple, located close to the sample bucket (<5 mm). The variation in sample temperature was minimal (<0.1 K) throughout the experiment. Nitric oxide gas was introduced into the adsorption system until the desired pressure was achieved, and the mass uptake of the sample was measured as a function of time until the adsorption equilibrium was achieved. In this manner an adsorption isotherm was collected by incrementally increasing the pressure and noting the mass gain of the sample after equilibrium was reached. The desorption of nitric oxide gas adsorbed in the samples was performed by gradually decreasing the system pressure to a desired value (until 2×10^{-2} mbar).

Saturated Vapor Pressures. Hydrogen, deuterium, and nitric oxide were used above their critical temperatures. The saturated vapor pressures for carbon dioxide and nitrogen were calculated using the following equation[44]

$$\log_{10} p = A - \frac{B}{T + C} \quad (1)$$

where p is the saturated vapor pressure (Torr), T is the temperature in degrees Celsius and A, B, and C are constants defined by the adsorbate: carbon dioxide (77−303 K): $A = 7.810237$, $B = 995.7048$, $C = 293.4754$; nitrogen (75−373 K): $A = 6{\cdot}49457$, $B = 255{\cdot}68$, $C = 266{\cdot}550$.

IR Studies. IR spectra were collected, at 2 cm^{-1} resolution, on a Bruker IFS 66 FTIR instrument equipped with a cryogenic MCT detector in transmission mode on a self-supported pellet. Suitable measurements cells were used allowing in situ thermal treatments at 180 °C in high vacuo and NO dosage at room temperature.

Quanitifaction of NO Release by Chemiluminescence. Nitric oxide measurements were performed using a Sievers NOA 280i chemiluminescence Nitric Oxide Analyzer. The instrument was calibrated by passing air through a zero filter (Sievers, <1 ppb NO) and 89.48 ppm NO gas (Air Products, balance nitrogen). The flow rate was set to 200 mL/min with a cell pressure of 8.5 Torr and an oxygen pressure of 6.1 psig. To measure NO release from HKUST powders, nitrogen gas of known humidity was passed over the powders, the resultant gas was directed into the analyzer, and the concentration of NO in ppm or ppb was recorded.

Platelet Aggregation. The sample of HKUST-1 was ground with PTFE in the desired ratio (75% zeolite/25% PTFE). The mixture was then pressed into disks (5 mm diameter, ~20 mg) under 2 tons for 30 s. The disks were then dehydrated and loaded with nitric oxide as described for the powder samples.

Venous blood was drawn from the antecubital fossa of a healthy volunteer into citrated tubes (0.38% final concentration). The volunteer had not taken any medication known to affect platelet aggregation within the last 10 days. Platelet-rich plasma (PRP) was obtained from whole blood by centrifugation (350*g*; 20 min; room temperature). Platelet-poor plasma (PPP) was obtained by further centrifugation of PRP (1200*g*; 5 min; room temperature).

The HKUST-1/PTFE disks were suspended in a stainless steel wire holder below the surface of the PRP in the aggregometer cuvette, ensuring that they did not interfere with the light beam or the mechanical stirring (1000 rpm). After a short incubation period (1 min), platelet aggregation was initiated by addition of agonist collagen (2.5 μg/mL). Aggregation was measured as a change in turbidity (light transmission) of PRP against a PPP blank.

Acknowledgment. P.S.W. and R.E.M. thank the Leverhulme Trust for support and R.E.M. thanks the Royal Society for the Provision of a University Research Fellowship. We also thank the E.P.S.R.C for support. The friendly and stimulating discussion with Carlo Lamberti and Adriano Zecchina (University of Torino) is gratefully acknowledged.

Supporting Information Available: Experimental details. This material is available free of charge via the Internet at http://pubs.acs.org.

JA066098K